

SCS-CN-INSPIRED RAINFALL-RUNOFF, SEDIMENT YIELD, AND ENVIRONMENTAL FLOW MODELLING

Ph.D. THESIS

by

SHAILENDRA KUMAR KUMRE



**DEPARTMENT OF WATER RESOURCES DEVELOPMENT & MANAGEMENT
INDIAN INSTITUTE OF TECHNOLOGY ROORKEE
ROORKEE - 247 667 (INDIA)
MAY, 2019**



SCS-CN-INSPIRED RAINFALL-RUNOFF, SEDIMENT YIELD, AND ENVIRONMENTAL FLOW MODELLING

A THESIS

*Submitted in partial fulfilment of the
requirements for the award of the degree*

of

DOCTOR OF PHILOSOPHY

in

WATER RESOURCES DEVELOPMENT AND MANAGEMENT

by

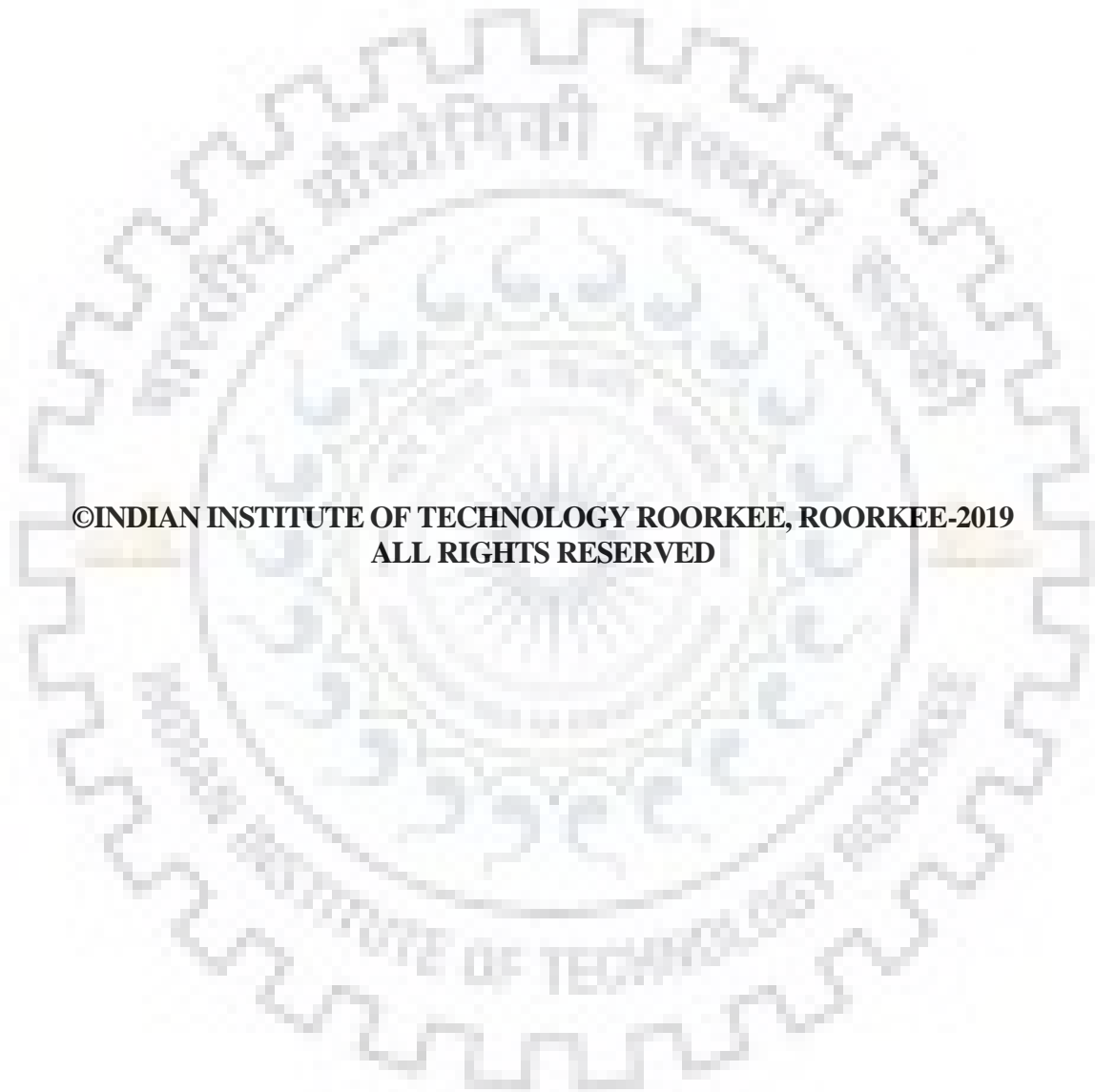
SHAILENDRA KUMAR KUMRE



**DEPARTMENT OF WATER RESOURCES DEVELOPMENT & MANAGEMENT
INDIAN INSTITUTE OF TECHNOLOGY ROORKEE
ROORKEE - 247 667 (INDIA)
MAY, 2019**







**©INDIAN INSTITUTE OF TECHNOLOGY ROORKEE, ROORKEE-2019
ALL RIGHTS RESERVED**



INDIAN INSTITUTE OF TECHNOLOGY ROORKEE

CANDIDATE'S DECLARATION

I hereby certify that the work which is being presented in the thesis entitled “**SCS-CN-INSPIRED RAINFALL-RUNOFF, SEDIMENT YIELD, AND ENVIRONMENTAL FLOW MODELLING**” in partial fulfilment of the requirement for the award of the Degree of Doctor of Philosophy and submitted in the Department of Water Resources Development and Management of the Indian Institute of Technology Roorkee, Roorkee is an authentic record of my own work carried out during a period from July, 2013 to May, 2019 under the supervision of Dr. S. K. Mishra, Professor and Dr. Ashish Pandey, Associate Professor, Department of Water Resources Development and Management, Indian Institute of Technology Roorkee, Roorkee.

The matter presented in this thesis has not been submitted by me for the award of any other degree of this or any other Institute.

(**SHAIENDRA KUMAR KUMRE**)

This is to certify that the above statement made by the candidate is correct to the best of my knowledge.

(Dr. Ashish Pandey)
Supervisor

(Dr. S. K. Mishra)
Supervisor

The Ph. D. Viva-Voce Examination of **Mr. Shailendra Kumar Kumre**, Research Scholar, has been held on _____

Chairman, SRC

Signature of External Examiner

This is to certify that the student has made all the corrections in the thesis.

Signature of Supervisor (s)

Head of the Department

Date:



ABSTRACT

Water is not only vital for life but also a natural resource of paramount importance for well-being of the society on the earth, essentially required for growth, sustainability of ecosystem, and prosperity of nation. For sustainability of the ecosystem, water management is required and it can be used for improved watershed models to address the management issues more effectively. It is well known that the watershed models are used to analyze the quantity and quality of stream flow, erosion and sediment yield, reservoir system operations, groundwater development and protection, surface water and groundwater conjunctive use management, water distribution systems, irrigation water use, and a range of such water resources management activities.

The component processes of hydrologic cycle over a watershed, viz., precipitation, evapotranspiration, detention, interception, infiltration, percolation, interflow, base flow, overland flow, and runoff etc., depend on climatic and catchment characteristics which vary both spatially and temporally. Thus, for reliable predictions of the runoff and sediment yield from land surface into streams and rivers, it is very important to understand rainfall-runoff-sediment relationship for making reliable estimates of runoff and sediment yield from a watershed. Simultaneously, the hydrological models used should also be parametrically efficient for the available data of watershed.

The SCS-CN method has been used by a number of researchers for runoff estimation worldwide since its inception in 1956. As a result, it has been a subject of intense and extensive exploration for its formation, rationality, applicability and extendibility, physical significance, and so on. Beside others, the method still inherits a major structural inconsistency associated with S-CN mapping, where S = potential maximum retention and CN = curve number, and results into abnormality in description of watershed behavior, i.e., complacent, standard, and violent, and runoff estimation based on the existing SCS-CN method. Thus, there is a need to revisit the S-CN mapping relationship for improvement and, in turn, improved SCS-CN methodology.

Suspended sediment is another hydrologic variable of severe environmental concern. Its transport in river systems is of paramount importance for ecologists and water and land- managers. The presence of sediment in water greatly influences the design and operation of hydraulic structures, like canals, diversions and dams. Therefore, its accurate assessment can be of potential use in future water resources management policies. This assessment is nonlinear and quite involved in

nature and depends on a number of factors such as flow, precipitation, topography and soil and land use characteristics of the watershed.

A number of models of varied complexity are available to model soil erosion and sediment yield. The Universal Soil Loss Equation (USLE) is the most popular model for soil erosion. Since sediment yield depends on surface runoff, the erosion models are often coupled with rainfall-runoff models, such as the existing SCS-CN methodology, and thus, there exists a scope for further improvements.

The present study was thus taken up with the following specific objectives:

- To develop an improved SCS-CN model based on the proportional equality revised for the first order linear hypothesis and Horton infiltration concepts for runoff estimation.
- To propose CN-P mapping relation based on the physical description of CN for describing the watersheds behavior realistically.
- To propose improved conceptual sediment yield models based on coupling of Universal Soil Loss equation (USLE) and modified SCS-CN method.
- Prediction of environmental flow condition using runoff curve number.

To accomplish the above tasks of more accurate runoff and sediment yield estimation, SCS-CN methodology was revisited in perspective of its various component processes. The proportional equality of this methodology, which is in core of the CN-concept was modified by replacement of the parameter potential maximum retention (S) by $S_0 e^{-\alpha P}$, where S_0 is the initial (or absolute maximum potential retention) and α is the decay parameter. It was founded on the concept that S is in correspondence with P (or $P_e = P - I_a$), which is variable whereas S_0 being absolute is not variable, and therefore, a better substitute for being a parameter. This modified version is validated using the rainfall and runoff data from Hawkins (1993), Strange (1882), and Tehri catchment (Uttarakhand, India); the last two belong to southern and northern parts of India, respectively. The proposed modification to the application approach of the SCS-CN methodology (i.e. Model 3) is more rational and has the efficacy to describe the watershed behavior more rationally/scientifically and resolve the issue of CN decaying with increasing rainfall (P). Besides, the methodology is found to be consistent when applied to all three datasets. The performance was evaluated using NSE, RMSE and Bias error criteria. Though the proposed methodology generally performed as well as the existing one in runoff estimation, it described realistically the physical behavior of the three types of watersheds, viz. complacent, standard,

and violent, and the increasing (in contrast to the established decreasing) trend of runoff coefficient with rainfall..

While revisiting the above SCS-CN methodology, it was also investigated for the S-CN mapping. It was revealed that the parameter Curve Number (CN) actually represents the runoff potential for a given amount of rainfall, which at present is considered as 1 inch (= 254 mm). Therefore, in real-world applications, when the rainfall varies or is different from given rainfall amount, it is necessary to revise the Curve Number (CN) as CNP, which corresponds to the actual amount of rainfall P. This major structural modification in the existing S-CN mapping relationship was proposed to solve abnormality in watersheds behavior, i.e. complacent, standard, and violent, as described by Hawkins (1993). The proposed modification effectively resolves the abnormalities and supports the general notion that the runoff coefficient (C) (or CN, another form of C) increases with increasing P. This modification also describes the CNP-P relationship and, in turn, the behavior of three watersheds for growing rainfall. The results show that the pre-derived CNP-P relationship for a watershed can be an improved alternative for runoff prediction using SCS-CN methodology. These relationships were also derived for Strange and Tehri catchment data and results showed that both the models performed well on these data sets. The study revealed that proposed modification also showed an enhanced model performance based on NSE, RMSE and Bias error criteria.

To meet the third objective, the applicability of USLE-coupled SCS-CN models was examined for computing total sediment yield from a storm event using the rainfall-runoff-sediment yield data observed from 09 experimental watersheds (plot size 12×3 m²) of different land uses, soils, and slopes. The sediment rating curves drawn between the observed sediment and observed runoff for the plots of different slopes showed increasing trend of sediment yield (mass) with runoff and slope for all land uses, viz., maize, finger millet, and fallow land. The rate of increase in sediment yield with runoff was sharper for greater slopes, and vice versa. Both existing and proposed SCS-CN models were tested using observed sediment and runoff data (Chapter 4). The proposed sediment yield models (PS1 with $\lambda = 0.0$ and PS3 with varying λ) performed much better than the existing models (S1 with $\lambda = 0.0$ and S3 with varying λ), and significantly better than S2 with $\lambda = 0.2$ when applied to both years 2016 and 2017 data. The higher slope plots generated higher sediment yield and runoff, and vice versa. The sediment yield models were ranked for performance as: PS3>PS1>PS2. The runoff models PR3 with varying λ and PR1 with $\lambda = 0$ performed approximately similar and model PR2 with $\lambda = 0.2$ performed poorer than any other proposed models.

For the accomplishment of the last objective, a relation of percentage of average annual flow (%AAF) with CN has been explored and its application has been demonstrated on seventeen catchments located in different river basins of India. These catchments include nine catchments from Godavari basin (viz. Ashti, Bimini, Bhatpalli, Satrapur, Jagadapur, Nandgaon, Ramakona Hivra, P.G. Penganga), two catchments of Mahi basin (Chakaliya and Dhariwad), four catchments of Mahanadi basin (viz. Baronda, Basantpur, Ghatora, Rampur), one catchment of Brahmani-Baitarini basin (i.e. Jenepur) and one catchment of narmada basin (i.e. Kogaon) falling in sub-tropical, and sub-humid climatic regions of India have been used. The coefficient of determination of more than 0.6 for most catchments shows the existence of an excellent relationship between CN and %AAF (used to describe EF condition). Hence, the environmental flow condition of these catchments may be determined using CN for known catchment characteristic.



ACKNOWLEDGEMENT

I wish to express my deep sense of gratitude to my supervisors Dr. S. K. Mishra, Professor and Dr. Ashish Pandey, Associate Professor, Department of Water Resources Development and Management, Indian Institute of Technology Roorkee, for their invaluable guidance, thought provoking discussions and untiring efforts throughout the course of this work. Their timely help, encouragement, constructive criticism, and painstaking efforts made it possible to present the work carried out by me in the form of this thesis.

I am thankful to Prof. Ajit Kumar Chaturvedi (Director, IIT Roorkee), Prof. M. L. Kansal (Head, Department of Water Resources Development and Management, IIT Roorkee), Prof. Deepak Khare (Chairman, DRC; Internal Member and Chairman of SRC), Dr. Sumit Sen (Department of Hydrology & External Member of SRC), and Dr. P. K. Singh (Scientist C, National Institute of Hydrology, Roorkee) for providing support, constructive suggestions and boosting moral during the study period.

I thankfully acknowledge the moral and technical support received from my friends, Dr. P. Patil, Dr. S. K. Himanshu, Prof. A. K. Gautam, Dr. Kumar Amrit, Dr. S. S. Palmate, Dr. B. K. Pandey, Dr. B. Yadav, Mr. A. Chandrakar, Mr. A. Lal, Mr. Radha Krishan, Mr. V. Jadhao, Mr. Deen Dayal, Miss P. Gunjan, Mr. S. Swain, Mr. I. Sharma, Mr. G. Singh, Mr. S. Gupta and Mr. S. Giri. It will be unjust on my part to bind in words the spirits of unparalleled sacrifices made by my parents, Shri Shrilal Kumre and Smt. Shahaja Bai Kumre for their blessings. I also feel obliged to my family members who has always supported me spiritually throughout writing this thesis and my life in general.

I thankfully acknowledge the financial support received by the Government of India through MHRD fellowship during the period of study. I also acknowledge the extended financial support provided by IIT Roorkee for completion this work and attending the EGU Conference-2019. I would like to thank the Ministry of Water Resources, River Development and Ganga Rejuvenation, Government of India, for providing financial support through Research Project entitled 'Experimental Verification of SCS Runoff Curve Numbers for Selected Soils and Land Uses' (MOW-627-WRD).

Further, my humble thanks are due to all those who in any manner, directly or indirectly, put a helping hand in every bit of completion of this research work.

(Shailendra Kumar Kumre)



TABLE OF CONTENTS

ABSTRACT	i
ACKNOWLEDGEMENT	v
TABLE OF CONTENTS	vii
LIST OF FIGURES	xi
LIST OF TABLES	xvii
LIST OF ABBREVIATIONS AND SYMBOLS	xix
1. INTRODUCTION	1-6
1.1 GENERAL	1
1.2 RAINFALL RUNOFF MODELLING	2
1.3 SEDIMENT YIELD MODELLING	2
1.4 ENVIRONMENTAL FLOW	3
1.5 OBJECTIVES OF THE STUDY	4
1.6 ORGANIZATION OF THESIS	5
2. REVIEW LITERATURE	7-36
2.1 GENERAL	7
2.2 STRUCTURAL AND ANALYTICAL FOUNDATION OF SCS-CN METHOD	8
2.2.1 CN Estimation Methods	10
2.2.2 Asymptotic Approach	11
2.2.3 Slope Considerations in CN Estimation	12
2.2.4 Diagnosis of Ia-S Relationship	13
2.2.5 Soil Moisture Accounting (SMA) Procedure	15
2.2.6 SCS-CN Method derived from Entropy Theory	16
2.2.7 SCS-CN Based Advanced Applications	17
2.3 SCS-CN BASED HYDROLOGIC SIMULATION MODELS	18
2.3.1 SMA Based Williams and LaSeur (1976) Model	18
2.3.2 Hawkins ET-CN Model	19
2.3.3 Versatile SCS-CN (VSCS-CN) Model	19
2.3.4 Michel SCS-CN Model	19
2.3.5 Sahu et al. SCS-CN Model	20
2.3.6 Sahu-Mishra-Eldho Model	20
2.3.7 Geetha SCS-CN Model	21
2.3.8 SCS-CN Based ASMA Model	21
2.3.9 SCS-CN Based PET-IWR Models	21

2.3.10 MMSCS-CN Model	22
2.3.11 Parsimonious SCS-CN Model	22
2.3.12 Enhanced SMA based SCS-CN Model	22
2.4 SEDIMENT YIELD MODELLING	22
2.4.1 Factors affecting Erosion and Sediment Yield	23
2.5 SCS-CN BASED EROSION AND SEDIMENT YIELD MODELS	25
2.5.1 USLE Coupled SCS-CN Based Sediment Yield Model	25
2.5.2 SCS-CN based Conceptual Sediment Graph Model	26
2.5.3 SCS-CN Based SLR Time Distributed Sediment Yield Model	27
2.5.4 RUSLE Coupled SCS-CN Based Sediment Yield Model	28
2.6 ENVIRONMENTAL FLOW REQUIREMENT	28
2.7 ASSESSMENT OF ENVIRONMENTAL FLOW	30
2.7.1 Hydrologic methods	30
2.7.2 Hydrological drought Indices	31
2.7.3 Habitat simulation methods	31
2.7.4 Holistic methods	31
2.8 RESEARCH GAPS	34
3. STUDY AREA AND DATA COLLECTION	37-52
3.1 DESCRIPTION OF WATERSHEDS AND DATA COLLECTION	37
3.1.1 West Donaldson Creek Watershed	37
3.1.2 Coweeta watershed	37
3.1.3 Berea watershed	38
3.1.4 Strange tabular data	38
3.1.5 Tehri Watershed	39
3.2 EXPERIMENTAL PLOTS/WATERSHEDS	40
3.2.1 Experimentations with Artificial Rainfall	42
3.1 DATA USED FOR ENVIRONMENTAL FLOW MODELLING	43
3.3.1 Study Catchments of Mahanadi Basin	43
3.3.1 Study Catchments of Mahi Basin	45
3.3.1 Study Catchments of Godavari Basin	47
3.3.1 Study Catchments of Brahmani-Baitarini Basin	50
3.3.1 Study Catchments of Narmada Basin	51
4. MODIFIED SCS-CN-BASED METHODOLOGY	53-76
4.1 INTRODUCTION	53

4.2 METHMATIONAL FORMULATION	55
4.2.1 SCS-CN Methodology	55
4.3 PROPOSED SCS-CN METHODOLOGY	56
4.4 RESULTS AND DISCUSSION	66
4.4.1 Performance Evaluation Criteria	58
4.4.2 Hawkins data (1993)	59
4.4.3 Strange and Tehri data	60
4.5 ADVANTAGES AND LIMITATIONS OF THE PROPOSED MODEL	76
4.6 SUMMARY AND CONCLUSIONS	76
5. INVESTIGATION OF S-CN MAPPING	77-101
5.1 INTRODUCTION	77
5.2 SIGNIFICANCE OF S-CN MAPPING	78
5.2.1 Mathematical Formulation	78
5.2.2 Significance of λ	80
5.3 DESCRIPTION OF WATERSHED BEHAVIOUR	81
5.3.1 S-CN mapping based Description of Watershed Behaviour	83
5.3.2 Runoff Calculation Approaches Based on Existing and Modified S-CN Mappings	87
5.3.3 Description of Watershed Behaviour based on Strange and Tehri Watershed Data	87
5.3.3.1 Existing Relationships based on Strange Table	87
5.3.3.2 Based on the existing S-CN mapping	88
5.3.3.3 Based on the proposed S-CN mapping	90
5.4 DISCUSION OF RESULTS	93
5.4.1 Hawkins Data	93
5.4.2 Strange and Tehri data	93
5.5 SUMMARY AND CONCLUSIONS	102
6. SCS-CN-BASED SEDIMENT YIELD MODELING	103-150
6.1 INTRODUCTION	103
6.2 METHODOLOGY	104
6.2.1 Universal Soil Loss Equation	104
6.2.2 Computation of Sediment Yield	105
6.3 FORMULATION OF SEDIMENT YIELD MODEL	106

6.3.1 Hypothesis: $C = Sr$	106
6.3.2 Hypothesis: A - S Relationship	107
6.3.3 Hypothesis: $DR = C$	108
6.3.4 Coupling of the SCS-CN Method with USLE	108
6.4 PROPOSED SEDIMENT YIELD MODEL	109
6.5 APPLICATION	109
6.5.1 Data Used	109
6.5.2 Model Formulations and Parameter estimation	109
6.6 RESULTS AND DISCUSSION	111
6.6.1 Development of Sediment Yield - Runoff Relationship	111
6.6.2 Model Calibration and Verification	112
6.6.3 Data observed from artificial rains	114
6.6.3.1 Sediment Yield - Runoff Relationship	114
6.6.3.2 Calibration and Verification of SCS-CN Inspired models	114
6.7 SUMMARY AND CONCLUSIONS	150
7. RELATION BETWEEN SCS-CN AND TENNANT METHOD	150-170
7.1 INTRODUCTION	150
7.2 METHODOLOGY	156
7.2.1 Tennant method	156
7.2.2 SCS-CN method	156
7.3 ANALYSIS AND DISCUSSION OF RESULTS	157
7.4 7.5 SUMMARY AND CONCLUSIONS	168
8. SUMMARY AND CONCLUSIONS	171-175
8.1 CONCLUSIONS	173
8.2 MAJOR RESEARCH CONTRIBUTIONS	174
8.3 LIMITATION OF THE STUDY	174
8.4 FUTURE SCOPE OF WORK	174
REFERENCES	177-206
APPENDIX	207-226
LIST OF PUBLICATIONS	227

LIST OF FIGURES

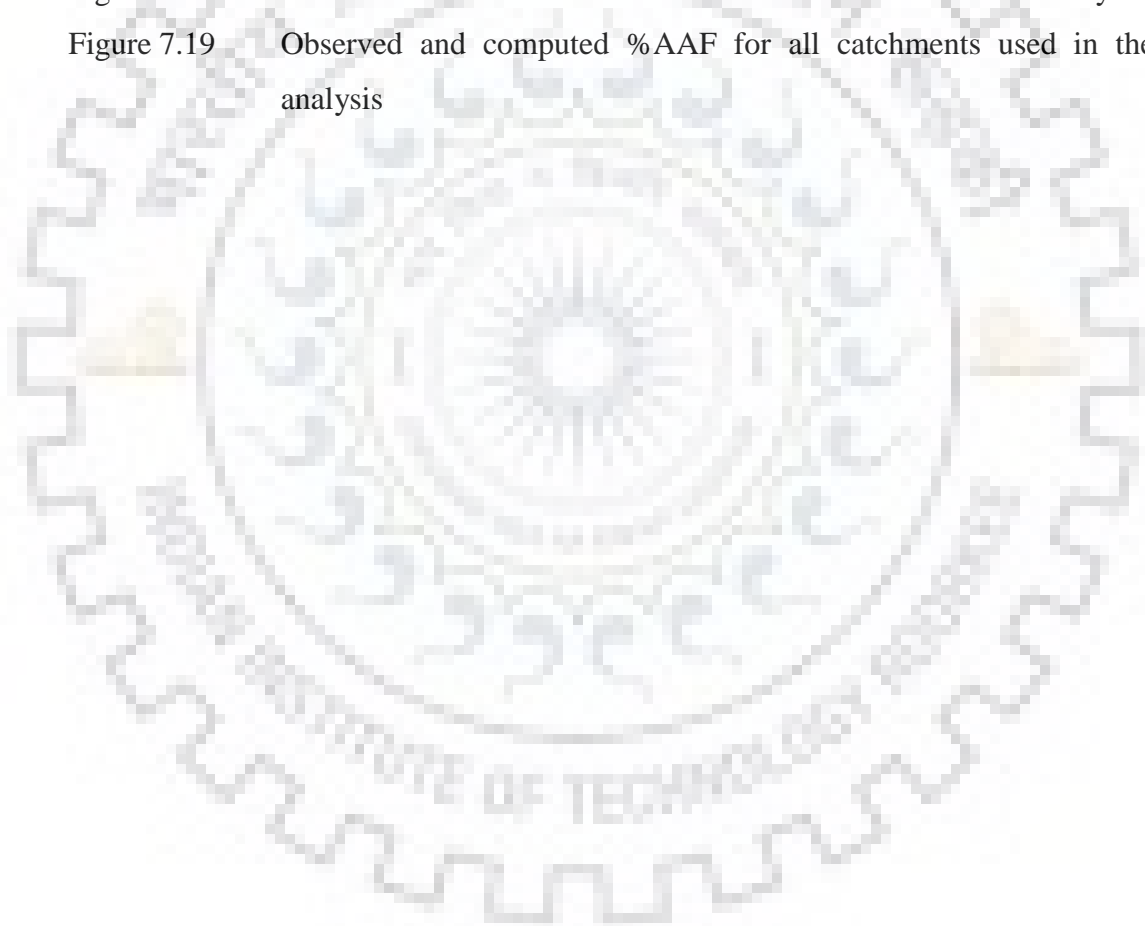
Figure No.	Description	Page No.
Figure 2.1	Variation of initial abstraction coefficient λ with runoff factor C and non-dimensional initial abstraction I_a^* . (Source: Mishra and Singh, 2003)	14
Figure 3.1	Location map of Tehri watershed	40
Figure 3.2	Location map of experimental area.	41
Figure 3.3	Experimental setup and running experiment	43
Figure 3.4	Drainage network of the study catchments of Mahanadi basin	45
Figure 3.5	Drainage network of Chakaliya watershed	46
Figure 3.6	Drainage network of Dhariawad watershed	47
Figure 3.7	Drainage network of the study catchments of Godavari basin	50
Figure 3.8	Drainage network of Jenapur watershed	51
Figure 3.9	Drainage network of Kogaon watershed	52
Figure 4.1	CN, CNp versus P fitting of the three datasets.	58
Figure 4.2a	Evaluation of Models 1-4 by comparing the computed runoff (mm) with the observed runoff (mm) of Violent watershed (Hawkins, 1993).	64
Figure 4.2b	Evaluation of Models 1-4 by comparing the computed runoff (mm) with the observed runoff (mm) of Standard watershed (Hawkins, 1993).	65
Figure 4.2c	Evaluation of Models 1-4 by comparing the computed runoff (mm) with the observed runoff (mm) of Complacent watershed (Hawkins, 1993).	66
Figure 4.3	C-CNo relationship for Model 3 ($\alpha = 0.01$).	67
Figure 4.4	Variation of CN with P (mm) for three types of watersheds for Model 3 with $\alpha = 0.01$.	67
Figure 4.5a	Evaluation of Models 1-4 by comparing the computed runoff (mm) with the observed runoff (mm) of Good watershed (Strange, 1892).	68

Figure 4.5b	Evaluation of Models 1-4 by comparing the computed runoff (mm) with the observed runoff (mm) of Average watershed (Strange, 1892).	69
Figure 4.5c	Evaluation of Models 1-4 by comparing the computed runoff (mm) with the observed runoff (mm) of Bad watershed (Strange, 1892).	70
Figure 4.6a	Evaluation of Models 1-4 by comparing the computed runoff (mm) with the observed runoff (mm) of Good watershed (Tehri watershed).	71
Figure 4.6b	Evaluation of Models 1-4 by comparing the computed runoff (mm) with the observed runoff (mm) of Average watershed (Tehri watershed).	72
Figure 4.6c	Evaluation of Models 1-4 by comparing the computed runoff (mm) with the observed runoff (mm) of Bad watershed (Tehri watershed).	73
Figure 4.7	C-CNo relationship for Model 3 ($\alpha = 0.0001$) for Strange data and Tehri watershed.	74
Figure 4.8	Variation of CNo with P (mm) for Strange data and Tehri data for Model 3 with $\alpha = 0.0001$. Note: Tehri data for $P < 45$ mm excluded.	75
Figure 5.1	Variation of runoff factor C with curve number CN and precipitation P (inch). 1 inch = 25.4 mm.	80
Figure 5.2	Depiction of watershed behaviour in terms of CN-C-P relationship.	84
Figure 5.3a	CN (or CN ₁₀) versus P fitting of the three datasets.	86
Figure 5.3b	CN _p versus P fitting of the three datasets.	86
Figure 5.4a	Plot of Strange data in the existing CN perspective. Third parameter = C (= Q/P).	89
Figure 5.4b	CN and CN _p versus P relations for Strange's datasets. Note: Strange data best fitted with CN using 2 period moving average.	91
Figure 5.5a	Plot of Tehri watershed data in the existing CN perspective.	93
Figure 5.5b	CN and CN _p versus P relations for Tehri watershed datasets.	93
Figure 5.6	Evaluation of Models 1-2 by comparing the computed runoff (mm) with the observed runoff (mm) of (a) Violent, (b) Standard and (c) Complacent watershed (Hawkins, 1993).	97
Figure 5.7	Evaluation of Models 1-2 by comparing the computed runoff (mm) with the observed runoff (mm) of (a) Good, (b) Average and (c) Bad watershed (Strange, 1992).	98

Figure 5.8	Evaluation of Models 1-2 by comparing the computed runoff (mm) with the observed runoff (mm) of (a) Good, (b) Average and (c) Bad watershed (Tehri Watershed).	100
Figure 5.9	C-CNp relationship (Model-2 consisting of Eqs. 4.2b, 4.4 (Chapter 4) and 5.3) description of watershed behaviour (Hawkins, 1993).	100
Figure 5.10	C-CNp relationship (Model-2 consisting of Eqs. 4.2b, 4.4 (Chapter 4) and 5.3) for description of watershed behaviour (Strange data and Tehri watershed).	101
Figure 6.1	Schematic diagram showing soil-water-air	106
Figure 6.2	Sediment rating curve of different slope of maize	128
Figure 6.3	Sediment rating curve of different slope of finger millet.	128
Figure 6.4	Sediment rating curve of different slope of fallow land	129
Figure 6.5	Sediment rating curve of different land use on 8% slope.	129
Figure 6.6	Sediment rating curve of different land use on 12% slope	130
Figure 6.7	Sediment rating curve of different land use on 16% slope.	130
Figure 6.8	Nash Sutcliffe Efficiency of existing and proposed Rainfall-Sediment Yield models (S1 and PS1)	131
Figure 6.9	Nash Sutcliffe Efficiency of existing and proposed Rainfall-Sediment Yield models (S2 and PS2).	131
Figure 6.10	Nash Sutcliffe Efficiency of existing and proposed Rainfall-Sediment Yield models (S3 and PS3).	132
Figure 6.11	Relationship between CN values derived from rainfall-sediment yield and rainfall-runoff models (Model 1).	133
Figure 6.12	Relationship between CN values derived from rainfall-sediment yield and rainfall-runoff models (Model 2).	134
Figure 6.13	Relationship between CN values derived from rainfall-sediment yield and rainfall-runoff models (Model 3).	135
Figure 6.14	Performance of PS1 and PR1 models in application to 2016 data of different land uses/slopes. Sediment yield in kg and runoff in mm. (LPF = Line of perfect fit)	138
Figure 6.15	Performance of PS1 and PR1 models in application to 2017 data of different land uses/slopes. Sediment yield in kg and runoff in mm. (LPF = Line of perfect fit)	141

Figure 6.16	Sediment rating curve for different land uses on different slopes.	142
Figure 6.17	Sediment rating curve for different land uses on different slopes	143
Figure 6.18	Nash Sutcliffe Efficiency of existing and proposed Rainfall- Sediment Yield models	145
Figure 6.19	Relationship between CN values derived from existing and proposed rainfall-runoff models.	146
Figure 6.20	Performance of PS1 and PR1 models in application to 2017 data observed using artificial rainfall of different land uses/slopes. Sediment yield in kg and runoff in mm. (LPF = Line of perfect fit).	149
Figure 7.1(a)	%AAF versus CN values for Ghatora catchment	158
Figure 7.1(b)	Observed and computed %AAF for Ghatora catchment	158
Figure 7.2(a)	%AAF versus CN values for Jagadapur catchment	158
Figure 7.2(b)	Observed and computed %AAF for Jagadapur catchment	158
Figure 7.3(a)	%AAF versus CN values for P. G. Penganga catchment	159
Figure 7.3(b)	Observed and computed %AAF for P. G. Penganga catchment	159
Figure 7.4(a)	%AAF versus CN values for Ramakona catchment	159
Figure 7.4(b)	Observed and computed %AAF for Ramakona catchment	159
Figure 7.5(a)	%AAF versus CN values for Rampur catchment	160
Figure 7.5(b)	Observed and computed %AAF for Rampur catchment	160
Figure 7.6(a)	%AAF versus CN values for Hivra catchment	160
Figure 7.6(b)	Observed and computed %AAF for Hivra catchment	160
Figure 7.7(a)	%AAF versus CN values for Nandgaon catchment	161
Figure 7.7(b)	Observed and computed %AAF for Nandgaon catchment	161
Figure 7.8(a)	%AAF versus CN values for Chakaliya catchment	162
Figure 7.8(b)	Observed and computed %AAF for Chakaliya catchment	162
Figure 7.9(a)	%AAF versus CN values for Dhariawad catchment	162
Figure 7.9(b)	Observed and computed %AAF for Dhariawad catchment	162
Figure 7.10(a)	%AAF versus CN values for Koegon catchment	163
Figure 7.10(b)	Observed and computed %AAF for Koegon catchment	163
Figure 7.11(a)	%AAF versus CN values for Jenepur catchment	163
Figure 7.11(b)	Observed and computed %AAF for Jenepur catchment	163
Figure 7.12(a)	%AAF versus CN values for Ashti catchment	164
Figure 7.12(b)	Observed and computed %AAF for Ashti catchment	164

Figure 7.13(a)	%AAF versus CN values for Bamini catchment	164
Figure 7.13(b)	Observed and computed %AAF for Bamini catchment	164
Figure 7.14(a)	%AAF versus CN values for Baronda catchment	165
Figure 7.14(b)	Observed and computed %AAF for Baronda catchment	165
Figure 7.15(a)	%AAF versus CN values for Basantpur catchment	165
Figure 7.15(b)	Observed and computed %AAF for Basantpur catchment	165
Figure 7.16(a)	%AAF versus CN values for Bhatpalli catchment	166
Figure 7.16(b)	Observed and computed %AAF for Bhatpalli catchment	166
Figure 7.17(a)	%AAF versus CN values for Satrapur catchment	166
Figure 7.17(b)	Observed and computed %AAF for Satrapur catchment	166
Figure 7.18	%AAF versus CN values for all the catchments used in the study	167
Figure 7.19	Observed and computed %AAF for all catchments used in the analysis	168





LIST OF TABLES

Table No.	Description	Page No.
Table 2.1	CN Conversion Formulae (Source: Mishra and Singh, 2003)	11
Table 2.2	Formulation of Rainfall-Sediment Yield and Rainfall-Runoff Models (Mishra and Singh, 2006)	25
Table 2.3	Formulation of Conceptual Sediment Graph Models (Singh et al., 2008).	27
Table 2.4	Popular methods based on Tharme (2003) classification	32
Table 3.1	Strange data of total monsoon rainfall and estimated percent runoff coefficients.	38
Table 4.1	Model formulations/procedures.	61
Table 4.2	Performance evaluation of various models on Hawkins (1993) data.	62
Table 4.3	Performance evaluation of various models on Strange and Tehri Data.	63
Table 5.1	Model formulations/procedures.	94
Table 5.2	Performance evaluation of various models. $C = \text{Mean runoff} / \text{Mean rainfall}$.	95
Table 6.1	Formulation of Rainfall-Sediment Yield and Rainfall-Runoff Models.	109
Table 6.2	Model procedures of Rainfall-Sediment Yield and rainfall-Runoff models.	111
Table 6.3	Observed Runoff, Potential maximum retention (S) and Curve Number (CN) data for experimental plot (2016).	117
Table 6.4	Observed Runoff, Potential maximum retention (S) and Curve Number (CN) data for experimental plot (2016).	119
Table 6.5	Results of existing (S1 & R1) and proposed (PS1 & PR1) models.	122
Table 6.6	Results of existing (S2 & R2) and proposed (PS2 & PR2) models.	123
Table 6.7	Results of existing (S3 & R3) and proposed (PS3 & PR3) models.	124
Table 6.8	Linear [$y = m(x - c/m)$] fitting of sediment yield (kg) and runoff (mm) plots. Here, m is the slope and c is the constant and $R_0 \text{ (mm)} = c/m$ represents the threshold runoff generating sediment yield.	125
Table 6.9	Results of existing (S1 & R1) and proposed (PS1 & PR1) models.	125
Table 6.10	Results of existing (S2 & R2) and proposed (PS2 & PR2) models.	126
Table 6.11	Results of existing (S3 & R3) and proposed (PS3 & PR3) models.	126

Table 6.12	Linear [$y = m (x - c/m)$] fitting of sediment yield (kg) and runoff (mm) plots. Here, m is the slope and c is the constant and R_o (mm) = c/m represents the threshold runoff generating sediment yield.	127
Table 7.1	Summary characteristics of study catchments	154
Table 7.2	Flow conditions based on percentage of AAF for low flow season (October-March) (Tennant, 1975)	156
Table 7.3	Description of flow condition based on %AAF or CN during low flow season	168



LIST OF ABBREVIATIONS AND SYMBOLS

Abbreviation/Symbol	Description
λ	Initial abstraction coefficient
α	A decay coefficient
β	A parameter
a	A decay coefficient
%AAF	Percentage of average annual flow
A	Annual potential soil erosion
AAF	Average annual flow
ABF	Aquatic base flow
AGNPS	Agricultural Non-point Source
AGNPS	Agricultural Non-point Source Model
AMC	Antecedent moisture condition
ANSWERS	Areal Non-point Source Watershed Environment Response Simulation
b	Index related to watershed
BBM	Building block method
C	Runoff coefficient
CLS	Constrained linear simulation
CN	Runoff Curve Number (defined (wrongly) in practice for any rainfall
CN0	CN corresponding to S_o
CN10	Runoff Curve Number defined for rainfall of 10 inches (25.4 mm). Here, CN CN10.
CNP	Runoff Curve Number defined for actual rainfall of P inches
CP	Cover management factor and supporting practice factor
CREAMS	Chemicals, Runoff, and Erosion from Agricultural Management Systems
DR	Sediment delivery ratio
EF	Environmental flow
EFA	Environmental flow assessment
EFR	Environmental flow requirement
EPIC	Erosion/productivity impact calculator

ET	Evapo-transpiration
F	Cumulative infiltration
f	Infiltration rate
fc	Final infiltration rate
Fc	Static or gravitational infiltration
Fd	Dynamic portion of infiltration
FDAM	Flow duration analysis method
FDC	Flow duration curve
HEC-1	Hydrologic engineering center-1
HSC	Habitat suitability criteria
i0	Uniform rainfall intensity
Ia	Initial abstraction
ie	Rainfall intensity
IFIM	Instream flow incremental method
IHA	Indicators of Hydrologic Alterations
IUSG	Instantaneous unit sediment graph
k	Decay parameter
K	Soil erodibility factor
LS	Slope length and steepness factor
M	Antecedent moisture amount
MLTHSASMA	Modified long-term hydrologic simulation advance soil moisture accounting
MMSCS-CN	Modified Michel SCS-CN
MUSLE	Modified universal soil loss equation
NEH	National engineering handbook
NEH-4	National engineering handbook
NRCS	Natural resource conservation service
NRCS-CN	Natural resources conservation service curve number
NSE	Nash–Sutcliffe efficiency
P	Rainfall
P5	Antecedent 5-d precipitation amount
PANC	Pan coefficient
Q	Direct surface runoff

Qp	Peak runoff
R	Rainfall erosivity factor
RMSE	Root mean square error
RVA	Range of Variability Approach
S	Potential maximum retention for P10 inch (254 mm)
Sabs	Absolute maximum potential retention
SCS	Soil conservation service
SGMs	Sediment graph models
SMA	Soil moisture accounting procedure
SMA	Soil moisture accounting
SMI	Soil moisture index
SMP	Soil moisture proxies
So	Absolute maximum potential maximum retention
Sp	Potential maximum retention computed for any rainfall P
SPI	Standardized precipitation index
Sr	Degree of saturation (F/S)
SVL	Soil-vegetation-landuse
SWAT	Soil and Water Assessment Tool
SWAT	Soil and Water Assessment Tool
SWMM	Storm water management model
t	Time
USG	Unit sediment graph
USLE	Universal soil loss equation
V0	Initial soil moisture
Va	Volume of air
VSA	Variable source area
VSCS-CN	Versatile SCS-CN
Vv	Void space,
Vw	Available moisture due to 254 mm rainfall
Y	sediment yield



CHAPTER 1

INTRODUCTION

1.1 GENERAL

Water is regarded as a necessary natural resource and is vital for sustenance of life. Thus, water resources are vital for growth, sustainable development and sustainability of the ecosystem, and prosperity of the nation as well. Growth of population is one of the most serious issues at present, all around the globe (Golubeva and Biswas, 1984; Fischer and Heilig, 1997; Koutsoyiannis et al., 2009). The water resource managers, scientists, policy makers and stakeholders are well aware that the relationship between water and population is more delicate today than ever, raising pertinent concerns of water security (Postela 1992, Oki and Kanae, 2006, Vogel, 2011, Sivapalan et al., 2012, Srinivasan et al., 2012).

The researchers around the globe are attempting to improve the existing watershed models and develop new models to address these issues more effectively. The watershed models, for example, are used to analyze the quantity and quality of streamflow, erosion and sediment yield, reservoir system operations, groundwater development and protection, surface water and groundwater conjunctive use management, water distribution systems, irrigation water use, and a range of such water resources management activities (Wurbs 1998; Wu et. al., 1993; Singh and Woolhiser, 2002). While occurring over a watershed, the precipitation passes through several phases of hydrologic cycle, viz., evaporation, detention, interception, evapotranspiration, percolation, infiltration, base flow, interflow, overland flow etc., and finally becomes runoff at outlet of the watershed. These depend on the climatic (i.e. duration, frequency and intensity of rainfall) and catchment (viz. LULC, geology, topography, drainage density, drainage pattern) characteristics which vary both spatially and temporally.

Reliable predictions of runoff and sediment yield from land surface into streams and rivers are time-consuming, difficult and expensive. Therefore, it is very important to understand rainfall-runoff-sediment relationship for more realistic estimates from a watershed. At the same time, it is also emphasized that the hydrological models used for the purpose should also be parametrically efficient and identifiable from the available data of watershed (Skaugen et al., 2015).

1.2 RAINFALL RUNOFF MODELLING

In modern times with increasing socio-economic development, much attention has been given for developing the physically based rainfall-runoff models. However, the conceptual and empirical models have their own advantages (Senbeta et al., 1999; Ajmal et al., 2015). The parameter identification becomes quite complex with the over-parameterization in hydrological models and subsequently it becomes difficult to predict the rainfall-runoff process in ungauged catchments (Aggarwal et al., 2013; Skaugen et al., 2015). There are numerous rainfall-runoff models used across the globe to estimate the runoff in ungauged catchments (Singh and Woolhiser, 2002), however, among these methods, the Soil Conservation Service Curve Number (SCS-CN) (SCS, 1956, 1972) method is one of the simplest and most widely used methods for addressing aforementioned assignments.

The SCS-CN method has been the focus of discussion and debate in hydrologic literature since its inception in 1956. The method has been used by a number of researchers for runoff estimation worldwide and, in turn, has been explored for its applicability, rationality, physical significance and extendibility etc. The review of literature suggests that the SCS-CN method still inherits major structural inconsistency associated with the S-CN mapping (where S = potential maximum retention and CN = curve number) resulting into abnormality in description of watershed behavior (i.e., complacent, standard, and violent) and runoff estimation based on the existing SCS-CN method. Thus, there is a need for development of a revised S-CN mapping relationship based on a sound hydrological perception. Further, the existing SCS-CN method can be modified using the proposed S-CN mapping and improved SCS-CN method based on the revised proportional equality for variation of S with rainfall (P) as per first order linear hypothesis (Mishra and Singh, 2003) and Horton (1932) model.

1.3 SEDIMENT YIELD MODELLING

Prediction of suspended sediment transport in river systems is of the highest importance for ecologists and for land- and water-use managers (Mao and Carrillo, 2016). It is very crucial for sustainable water resources and environmental systems (Kisi, 2009; Yang et al., 2009). Suspended sediments greatly govern the design and operation of hydraulic structures, like canals, diversions and dams. Therefore, its accurate prediction could be an important index to design the future water resources management policies (Merritt et al., 2003). Prediction of suspended sediment loads is very complicated and nonlinear in nature, it depends on a number of complex factors such as flow, precipitation, topography and soil characteristics of the river basin or watershed.

Several models, varying in complexity from lumped empirical to physically based have been developed by various researchers to model the soil erosion and sediment yield (Foster and Meyer, 1972a; Nearing et al., 1989; Woolhiser et al., 1990; Govindaraju and Kavvas, 1991; Tayfur and Kavvas, 1994; Liu et. al., 1994; Kothyari et al., 1997; Tayfur, 2001 & 2002; Su et al., 2004; Kalb et al., 2004; Jain et al., 2005). A common approach to the assessment of soil erosion and sediment yield is the use of empirical equations, such as the Universal Soil Loss Equation (USLE) (Wischmeier and Smith, 1965; 1978) or its extensions viz., Modified Universal Soil Equation (MUSLE) (Williams, 1975) and Revised Universal Soil Equation (RUSLE) (Renard et al., 1991). As the sediment yield process depends on surface runoff, erosion models are coupled with the models capable of simulating the rainfall-runoff response of watershed (Leonard et al., 1987; Rode and Frede, 1997). A critical review of literature further suggests that the sediment yield models developed by Mishra et al. (2006) are based on coupling of the existing SCS-CN methodology and USLE, and thus, there exists a scope for further improvements based on the proposed modifications to the SCS-CN method for sediment yield estimation.

1.4 ENVIRONMENTAL FLOW

The most vital natural resource required for the welfare of human being and for the environment on the globe is fresh water (Gleick, 1993). There is increase in water demand globally due to the lack of water supply which is coupled with increasing population and industrialization. This leads to scarcity of fresh water resource on the earth (Wang and Lu, 2009). Water has to be sustained in rivers for conservation of natural ecosystem. River habitat, water quality, and biotic interaction are greatly affected by the large variation in quantum of flow (i.e. discharge), flow length etc. around the globe (Naiman et al., 2002; Belmar et al., 2012). Since the degrading ecosystem leads to both social and economic loss which affect the large number of poor people around the world, it is important to understand the value of the ecosystem services to maintain livelihoods in future for sustainable development (Dyson et al., 2003; Pearce et al., 2007). It is of common experience that most of the rivers around the globe are fragmented by hydrological changes, causing deterioration of aquatic ecosystem (Millennium Ecosystem Assessment, 2005; Poff et al., 1997; Postel and Richter, 2003; Revenga et al., 2005). The major challenge for the water managers to fulfill the water requirements of people without imparting any deteriorating effect on the ecological services, provided by the healthy rivers (Bunn et al., 2014; Yao et al., 2018). The rapid socioeconomic development and change in climatic conditions over the previous decades have greatly influenced global hydrologic cycle up to the extent of putting a threat to water security, wellness of aquatic ecosystem, and biodiversity of river (Vörösmarty et al., 2010; Jacobsen et

al., 2012; Van Vliet et al., 2013; Amrit et al., 2017). It is very important to understand the role of flow regulation for the sustainability of good hydro-ecosystems (Turnbull et al., 2012; Yao et al., 2018). Alternatively, minimum amount of flow in river required for sustainability of aquatic lives and conservation of the natural ecosystem is known as environmental flow (Brisbane Declaration, 2007; Mathews and Richter, 2007; Poff et al., 2009; Wang and Lu, 2009). The protection of endangered and rejuvenation of damaged river ecosystems using the idea of environmental flows are base for the management of river and catchment (Palmer et al., 2008; Mackay et al., 2014).

An increase in global water demand forced the researcher to think about the assessment of flow requirement. Various studies have been done across the globe to formulate, implement and adapt different methods of environmental flow assessment (EFA). The various methods of EFA have been often reviewed critically in a number of studies (Stalnaker and Arnette 1976; Jowett 1997; Arthington 2012; Linnansaari et al. 2012; Hatfield et al. 2013). Methods for EF assessment were initially developed to estimate instream flow needs of fish below the irrigation and hydroelectric dams on large rivers (Trihey and Stalnaker 1985; Dunbar et al. 1998; Tharme and Smakhtin 2003; Kumar et al., 2007) with aim to set the flow required during low flow season (Leathe and Nelson 1986). Presently, a large number of methods (more than 240) are being used across the world to estimate EFR to uphold the rivers in healthy condition (Tharme, 2003) during both (low and high) flow seasons. The methods for estimation of environmental flow requirement are grouped as (a) hydrological, (b) hydraulic rating, (c) habitat simulation, and (d) holistic methods.

1.5 OBJECTIVES OF THE STUDY

A critical review of the literature dealing with the applications of the SCS-CN methodology in the field of rainfall-runoff and sediment yield modeling shows possibility as well as necessity for further improvements in the SCS-CN based runoff and sediment yield models. This study is undertaken with the following specific objectives:

1. To revisit the SCS-CN methodology in perspective of its various component processes, identify its strengths and weaknesses, and explore possibilities for improvement.
2. To develop an improved SCS-CN model based on the proportional equality revised for the first order linear hypothesis and Horton infiltration concepts for runoff estimation.
3. To propose CN-P mapping relation based on the physical description of CN for describing the watersheds behavior realistically.
4. To propose improved conceptual sediment yield models based on coupling of Universal Soil Loss equation (USLE) and modified SCS-CN method.

5. Prediction of environmental flow condition using runoff curve number.

1.5 ORGANIZATION OF THESIS

The thesis is arranged in eight chapters as follows:

Chapter One: This chapter presents the problem introduction, brief description of the state-of-the-art knowledge and outline of the research objectives.

Chapter Two: This chapter presents a critical review of literature available in the field of runoff and sediment yield modeling using SCS-CN method related with this study. To accomplish this, the chapter is divided into two sections. First section deals with application of SCS-CN method for runoff modeling and the second section deals with the application of SCS-CN method for sediment yield modelling. The review of literature is critically diagnosed and finally summarized for research gaps and scope of improvements.

Chapter Three: This chapter describes the study area considered for different studies as well as the corresponding types of data used. The types of data are lumped, event rainfall-runoff data and event based sediment yield data.

Chapter Four: In this chapter, modification to the proportional equality (coupling the first order linear hypothesis (Mishra and Singh, 2003) and Horton infiltration model (Horton, 1932), an improved SCS-CN model is proposed. The proposed SCS-CN models is tested for its applicability for runoff estimation for three different watersheds behavior using Hawkin (1993), strange table and tehri watershed data sets.

Chapter Five: This chapter revisits the S-CN mapping relationship and develops its improved formulation based on realistic hydrological perceptions. Based on the improved S-CN mapping relationship, simplified CN-P formulations are developed corresponding to three types of watersheds' behavior which are equally applicable to ungauged basins for future applications. Finally, revised S-CN mapping is proposed and tested its applicability for runoff estimation for three different watersheds behavior on Hawkin (1993), strange table and tehri watershed data sets.

Chapter Six: In this chapter, improved conceptual sediment yield models based on coupling of USLE and improved SCS-CN method (chapter 4) are developed and the workability of these models is tested using event rainfall-runoff and sediment yield data of plot scale experimental units with varying slopes and land uses in Indian conditions.

Chapter Seven: This chapter explains the relationship between Tennant concept and Curve Number for the prediction of environmental flow condition during low flow season (October-June) using the data of seventeen catchments from the four different river basins (viz. Mahanadi, Godavari, Brahmani-Baitarini and Narmada) of India.

Chapter Eight: This chapter presents summary, important conclusions drawn from the study, major research contributions of the study, and scope for future research work.



This chapter deals with the structural diagnosis of the Soil Conservation Service Curve Number (SCS-CN) methodology and its application, including recent advancements in the area of rainfall-runoff and sediment yield modelling. The applications have been summarized and critically reviewed for its potential and scope for further improvements.

2.1 GENERAL

Surface runoff is the portion of precipitation that runs into surface waters as overland flow (Perlman, 2016). The amount of surface runoff is influenced by vegetation, LULC, soil properties, slope, and storm properties (duration, intensity and amount of rainfall). The runoff models help in understanding the hydrologic cycle and the influential factors (Xu, 2002). Although plethora of hydrologic models exist to estimate runoff from rainfall, thorough calibration necessities and intensive input data are the limitations in most of these models. On the other hand, the SCS-CN method fulfils the demands with less data requirements and clearly stated assumptions.

During the initial phase of development of the SCS-CN methodology during the late 1930s and 1940s, the information available from exhaustive field investigations that were carried out by various researchers including Mockus (1949), Sherman (1949), Andrews (1954), and Ogrosky (1956) was used. Mockus (1949) found that the direct runoff from ungauged watersheds was depended on landuse, antecedent rainfall, soil, amount of rainfall, date and duration of storm, and mean annual temperature. He proposed an empirical index “b” to account for all these factors collectively and developed a relationship of storm rainfall depth (P) and direct runoff (Q) as eq. 2.1 (Mishra and Singh, 1999):

$$Q = P(1 - 10^{-bP}) \quad (2.1)$$

where P and Q are in inches. The Mockus empirical P-Q rainfall-runoff relationship and Andrews’s soil-vegetation-landuse (SVL) complex were the building blocks of the existing SCS-CN method documented in Section-4, National Engineering Handbook (NEH-4) (Rallison and Miller, 1982; Hydrology, 1985). Of late, the method has been renamed as Natural Resources Conservation Service Curve Number (NRCS-CN) Method).

The SCS-CN method is a conceptual technique to estimate direct runoff volume from depth of rainfall using its parameter curve number CN (Ponce and Hawkins, 1996). The method has also been coupled with numerous commercial hydrologic software programs, viz., Agricultural Non-point Source Model (AGNPS), Areal Non-point Source Watershed Environment Response Simulation (ANSWERS), Chemicals, Runoff, and Erosion from Agricultural Management Systems (CREAMS), Constrained Linear Simulation (CLS), Hydrologic Engineering Center-1 (HEC-1), Storm Water Management Model (SWMM) and Soil and Water Assessment Tool (SWAT) (Pandey et al., 2016).

2.2 STRUCTURAL AND ANALYTICAL BACKGROUND

The structural foundation of the SCS-CN method based on the water balance equation and two hypotheses (Mishra and Singh, 2003a), are as follows:

Water Balance Equation:

$$P = I_a + F + Q \quad (2.2)$$

First Hypothesis: Proportionality equality:

$$\frac{Q}{(P - I_a)} = \frac{F}{S} \quad (2.3)$$

Second Hypothesis: I_a - S relationship:

$$I_a = \lambda S \quad (2.4)$$

where, P = total rainfall, Q = direct surface runoff, F = cumulative infiltration, I_a = initial abstraction, S = potential maximum retention, and λ = initial abstraction ratio.

Using Eqs. (2.2) and (2.3), the general form of the SCS-CN method can be derived as:

$$Q = \frac{(P - I_a)^2}{P - I_a + S} \quad ; \text{ for } P \geq I_a; \quad Q = 0; \text{ otherwise} \quad (2.5)$$

For $\lambda = 0.2$, the coupling of Eqs. (2.3) and (2.4) results in

$$Q = \frac{(P - 0.2S)^2}{P + 0.8S} \quad (2.6)$$

Eq. (2.6) is considered as a popular form of the existing SCS-CN method and is widely applied. The initial abstraction parameter λ is considered as a local/regional parameter dependent on climatic and geologic factors. Typically, λ varies in the range of (0, 0.3) (SCS, 1972; Springer et al., 1980; Cazier and Hawkins, 1984; Ramasastri and Seth, 1985; Bosznay, 1989). Hawkins et al. (2001) recommended $\lambda = 0.05$ as more appropriate for calculating runoff. Mishra and Singh (2004a) framed a basis to validate the SCS-CN method with varying λ and defined the applicability bounds for the SCS-CN method. The parameter S depends on antecedent moisture condition (AMC), hydrologic condition, land use and soil type, and can be mapped on to a dimensionless curve number CN (eq. 2.7), ranging (0, 100), as:

$$S = \frac{25400}{CN} - 254 \quad (2.7)$$

where S is in millimetres. The CN value is representative of imperviousness of the surface, and thus, varies inversely with potential maximum retention (S). A zero value of CN represents an infinite abstraction condition ($S = \infty$). On the other hand, CN value of 100 indicates an absolute impermeable condition ($S = 0$). However, both these conditions are unlikely to occur.

According to Chen(1982) and Mishra and Singh (2004a,b), the SCS-CN method is an alternative expression of the infiltration decay curve and, in practice, it can be used as one of the parametric infiltration models or modified forms thereof to formulate the standard infiltration capacity curve for a given soil–cover–moisture complex. Yu (1998) derived SCS-CN method theoretically (analytically) assuming exponential distribution for the spatial variation of infiltration capacity and the temporal variation of rainfall rate. The method has undergone rigorous review and has been recognized to perform well without impairing its simplicity. The works of Poncea and Hawkins (1996), Yu (1998), Mishra and Singh (1999; 2002a&b; 2003a&b; 2004a&b), Mishra et al. (2003a&b) and Michel et al. (2005) are noteworthy. Ponce and Hawkins (1996) and Mishra and Singh (2003a) also described the SCS-CN method as a conceptual model dependent on a single numeric parameter CN. Mishra and Singh (2002a; 2003a, b) revisited the empirical rainfall-runoff models proposed by Mockus (1949) and Horton (1938) and derived the existing SCS-CN method. In an advanced form, Mishra and Singh (2002a, 2003b) derived the existing SCS-CN method using second-order storage hypothesis, leading to its categorization as a

conceptual model. Michel et al. (2005) proposed a conceptual, coherent, and hydrologically sound SCS-CN model through soil moisture accounting (SMA) procedure in the existing SCS-CN methodology.

Mishra and Singh (2002a) described F (Eq. (2.3)) as the dynamic portion of infiltration (F_d) and distinguished it from the static or gravitational infiltration (F_c) while Mishra and Singh (2003b) derived Eq. (2.3) using the first-order linear hypothesis for the variation of S with rainfall. Further, Mishra and Singh (2003a) explained the physical significance of S using the diffusion term of the linear Fokker–Planck equation for infiltration (Philip 1974), which relates S to the storage and transmission properties of the soil.

2.2.1 CN Estimation Methods

Runoff estimation is more adversely affected due to errors in obtaining CN as compared to errors of similar magnitude in storm rainfall. (Hawkins, 1975). This depicts the relevance of accuracy required for CN estimation in SCS-CN methodology. However, despite the popularity of SCS-CN methodology, accurate estimation of CN is still a challenge for hydrologist's worldwide (Hawkins, 1978; Chen, 1982; Bonta, 1997; and Mishra and Singh, 2006). In hydrologic literature, for given rainfall-runoff records, CN can be computed by using following three methods: (i) using NEH-4 Table, (ii) ordered P and Q data (asymptotic CN estimation), and (iii) derived frequency distribution (Hjelmfelt, 1980 and Bonta, 1997). A detailed overview and diagnosis of these methods has been presented by Mishra and Singh (2003a). Still, the hydrology community doesn't advocate a single CN procedure with consensus based on rainfall runoff data (Soulis and Valiantzas, 2013). The CN parameter reflects the catchment characteristics like soil type, land use and antecedent moisture conditions (AMCs) (Ajmal et al., 2014, Ajmal et al., 2015; Epps et al., 2013; Malone et al., 2015; Váňová and Langhammer, 2011).

For any change in AMC (say from AMC_I to AMC_{III}) in a given catchment, there is an abrupt rise in CN value (i.e. from CN I to CN III), which is discontinuous in nature, and consequently, resulting in a sudden jump in computed runoff. This indirectly reflects discrete nature of CN-AMC relationship. Depending on 5-day antecedent rainfall, various relationships have been developed to convert CN_{II} to CN_I and CN_{III} (Sobhani, 1975; Hawkins et al., 1985; Neitsch et al., 2002; Mishra et al., 2008). In addition, direct conversion is possible using NEH-4 tables (SCS, 1972; McCuen, 1982; McCuen, 1989; Ponce, 1989; Singh, 1992; Woodward and Gbuerek, 1992; Mishra and Singh, 2003a). Mishra et al. (2008) compared CN conversion formulae (Table 2.1) developed by Sobhani (1975), Hawkins et al. (1985), Chow et al. (1988) and Neitsch et al. (2002)

and found that the Neitsch formulae shows poorest correspondence with NEH-4 values taken as target values. The best formulae for CN_I and CN_{III} -conversion correspond to Sobhani formula and the Hawkins formula respectively. However, in field application, Mishra et al. (2008) model performed the best of all. Out of these three methods, the Asymptotic Approach has been a topic of discussion among the hydrologists and hence a brief description of this method is also given table 2.1.

Table 2.1: CN Conversion Formulae (Source: Mishra and Singh, 2003)

Model	AMCI	AMC III
Sobhania(1975)	$CN_I = \frac{CN_{II}}{2.334 - 0.01334CN_{II}}$	$CN_{III} = \frac{CN_{II}}{0.4036 + 0.005964CN_{II}}$
Hawkins et al. (1985)	$CN_I = \frac{CN_{II}}{2.281 - 0.01281CN_{II}}$	$CN_{III} = \frac{CN_{II}}{0.427 + 0.00573CN_{II}}$
Chow et al. (1988)	$CN_I = \frac{4.2CN_{II}}{10 - 0.058CN_{II}}$	$CN_{III} = \frac{23CN_{II}}{10 + 0.13CN_{II}}$
Neitsch et al. (2002)	$CN_I = CN_{II} - \frac{20(100 - CN_{II})}{\{100 - CN_{II} + \exp[2.533 - 0.0636(100 - CN_{II})]\}}$	$CN_{III} = CN_{II} \exp\{0.0067 - 3(100 - CN_{II})\}$
Mishra et al. (2008)	$CN_I = CN_{II} - \frac{20(100 - CN_{II})}{2.274 - 0.012754CN_{II}}$	$CN_{III} = \frac{CN_{II}}{0.430 + 0.0057CN_{II}}$

2.2.2 Asymptotic Approach

This approach is based on ‘frequency matching’, which was first pointed out by Hjelmfelt (1980) in the SCS-CN model. It uses an ‘Ordered’ data, that is, P and Q data are arranged in descending order, in which a Q-value corresponding to a particular P may not necessarily represent the actual runoff due to this rainfall. The ‘Natural’ data, however, retain the actual P–Q dataset. Therefore, this approach preserves the return-period matching of rainfall and runoff. Hawkins (1993) found that a secondary relationship almost emerges between the CN and the storm rainfall depth from ordered P–Q dataset. The secondary relationship leads to the description of three types of CN-P behavior, namely, Complacent, Standard, and Violent. In the complacent behavior, the observed CN declines steadily with increasing rainfall depth, and evidences no appreciable tendency to achieve a stable value. In case of ‘standard’ behavior, the observed CN declines with increasing

storm size, as in the complacent situation, but the CNs approach and/or maintain a near-constant value with increasingly larger storms. In case of ‘violent’ behavior, the observed CNs rise suddenly and asymptotically approach an apparent constant value. Hawkins (1993) attributed this abnormality to the secondary systematic correlation between the calculated CN value and the rainfall depth.

It is well known fact that the runoff coefficient (C) and the runoff curve number (CN) are both expressions of the relative rainstorm response characteristics of watersheds (McCuen and Bondelid, 1981 and Hawkins, 1993). The runoff coefficient (C), which is the ratio of direct surface runoff (Q) to rainfall (P), increases with increasing P, and vice versa. Furthermore, for a given amount of rainfall, as C increases, CN also increases, and vice versa. Thus, both C and CN behave similarly. In other words, CN should increase with P as does C and therefore, there is a strong need for critical diagnosis of CN-P and S-CN relationships to rectify the abnormalities in the description of watersheds’ behavior.

2.2.3 Slope Considerations in CN Estimation

The standard NRCS model is used to experimentally obtain CN values for runoff estimation from the measured rainfall-runoff data for diverse geographic, soil, and land management conditions. However, the model doesn’t consider the watershed slope adjustment which is an important factor for determining movement of water within a landscape (Huang et al., 2006, Garg et al., 2013). The runoff estimation capabilities of the NRCS model can be improved by using slope-adjusted CN values. CN values obtained from the NRCS handbook (NRCS, 2004) usually correspond to a slope of 5%. (Sharpley and Williams, 1990; Huang et al., 2006; Mishra et al., 2014).

Researchers in the past have attempted to incorporate watershed slope for estimation of CN. Sharpley and Williams (1990) assumed that CN_{II} obtained from NEH-4 (SCS, 1972) corresponds to a slope of 5% and expressed the slope adjusted CN_{II} (named as $CN_{2\alpha}$) as:

$$CN_{II\alpha} = \frac{1}{3}(CN_{III} - CN_{II})(1 - 2e^{-13.86\alpha}) + CN_{II} \quad (2.8)$$

Huang et al. (2006) analysed Eq. (2.8) and found that it is suitable for limited applications, and consequently developed an improvised version for climatic and steep slope conditions existing in Loess Plateau of China (eq. 2.9)as:

$$CN_{II\alpha} = CN_{II} \left[\frac{322.79 + 15.63\alpha}{(\alpha + 323.52)} \right] \quad (2.9)$$

More recently, Ajmal et al. (2016) used a measured rainfall-runoff data from 39 mountainous watersheds in South Korea to develop an enhanced version of $CN_{II\alpha}$. The developed relationship can be expressed as:

$$CN_{II\alpha} = CN_{II} \left[\frac{1.927\alpha + 2.1327}{(\alpha + 2.1791)} \right] \quad (2.10)$$

However, the credibility of the above equation (eq. 2.10) was not validated for other areas with almost identical climatic and slope conditions. The constant α denotes watershed slope in m/m.

2.2.4 Diagnosis of I_a -S Relationship

During the initial formulation of SCS-CN model, I_a was not taken into consideration (Plummer & Woodward, 2002). However, in later stages of development, the model was incorporated as a fixed ratio of I_a to S . Since inception, the relationship $I_a = 0.2S$ has been the focus of discussion because of the larger variability (Mishra and Singh 2003a). Aron et al. (1977) suggested $\lambda \leq 0.1$ and Golding (1979) provided λ values for urban watersheds depending on CN as $\lambda = 0.075$ for $CN \leq 70$, $\lambda = 0.1$ for $70 < CN \leq 80$, and $\lambda = 0.15$ for $80 < CN \leq 90$. Hawkins et al. (2001) suggested that $\lambda = 0.05$ gives a better fit to data and recommended it to be used for runoff calculations.

Mishra and Singh (1999) suggested that the initial abstraction component accounts for the short-term losses such as interception, surface storage and infiltration before runoff begins, and therefore, λ can take any non-negative value. Mishra and Singh (2004a) developed a criterion for validity of the SCS-CN method with λ variation using the following relationships:

$$\lambda = \frac{CI_a^*}{(1 - I_a^*)(1 - I_a^* - C)} \quad (2.11a)$$

and

$$S \leq \frac{(P - Q)}{\lambda} \quad (2.11b)$$

where $I_a^* = I_a/P$; varies as $0 \leq I_a^* \leq 1$, and for $I_a^* > 1$, $C = Q/P = 0$.

Graphically, Eq. (2.11) can be depicted as shown in Fig. 2.1. It can be inferred from the figure that λ can take any non-negative value $(0, \infty)$; for a given value of I_a^* , λ increases with C and reaches ∞ as $(C+I_a^*)$ approaches 1; for a given value of C , λ increases with I_a^* ; as $I_a^* \rightarrow 0$, $\lambda \rightarrow 0$. This is attributed to the poor performance of the existing SCS-CN method on very low runoff producing (or low C values) lands, such as sandy soils and forest lands. Fig. 2.1 also shows that the existing SCS-CN method has an extensive applicability on the watersheds having C values in the approximate range of $(0.4 - 0.6)$ and the initial abstraction of the order of 10% of total rainfall. On the basis of Fig. 2.1, they defined the applicability bounds for the SCS-CN method as: $\lambda \leq 0.3$; $I_a^* \leq 0.35$ and $C \geq 0.23$.

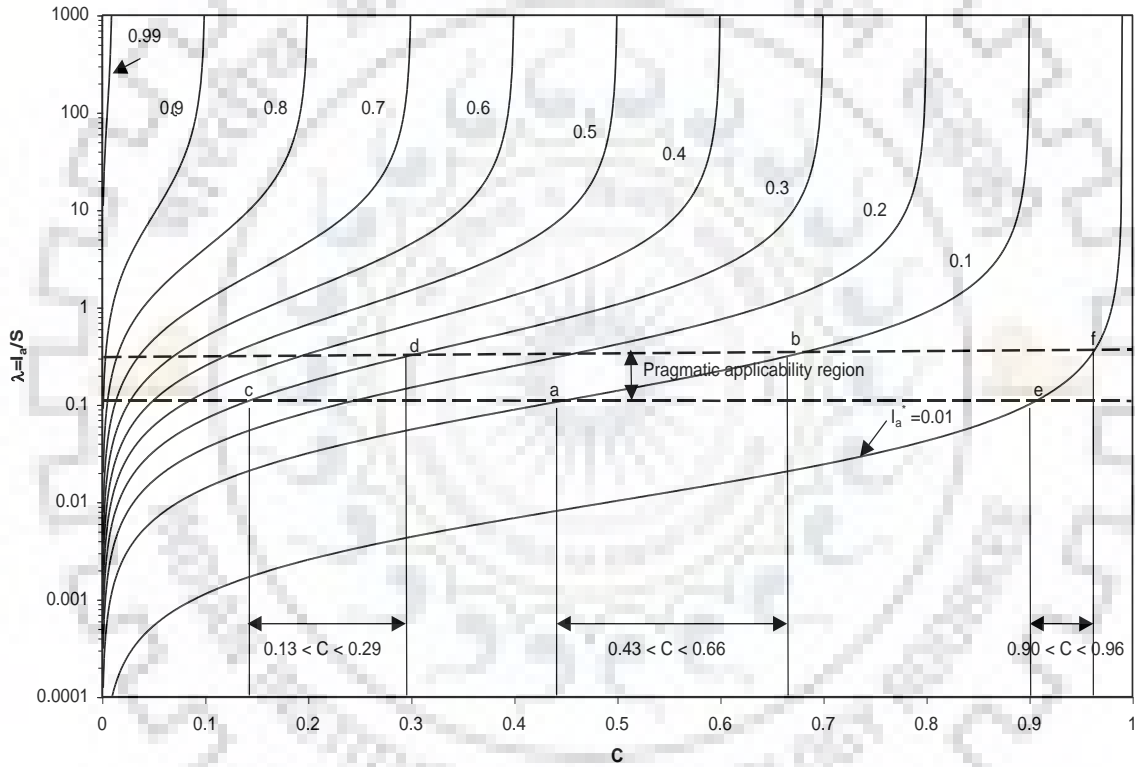


Figure 2.1: Variation of initial abstraction coefficient λ with runoff factor C and non-dimensional initial abstraction I_a^* . (Source: Mishra and Singh, 2003)

The I_a - S relationships developed by Jain et al. (2006a) and Mishra et al. (2006a) are the refinements over the existing $I_a = 0.2S$ relationship. Considering the fact that P is an indirect function of climatic/meteorological characteristics. Jain et al. (2006b) developed a more general non-linear I_a - S relation as:

$$I_a = \lambda S \left(\frac{P}{P+S} \right)^\alpha \quad (2.12)$$

where α is a constant. Eq. (2.12) reduces to $I_a = 0.2S$ for $\lambda = 0.2$ and $\alpha = 0$ and hence could be considered as a generalized form of I_a - S relationship. Based on the hypothesis that I_a largely depends on initial soil moisture M , as Mishra et al. (2006a) developed a modified non-linear I_a - S relationship:

$$I_a = \frac{\lambda S^2}{(S + M)} \quad (2.13)$$

where M is the antecedent moisture amount.

The generalized nature of Eq. 2.13 can be seen as, for $M=0$ or a completely dry condition, Eq. (2.13) reduces to Eq. (2.4), which is the basic I_a - S relationship. Therefore, it can be concluded that there is a scope of exploring these relationships (or their modification) in different hydro-climatological areas for their augmented application and versatility.

2.2.5 Soil Moisture Accounting (SMA) Procedure

Due to the event-based variation of CN values there is a need for realistic prediction of runoff from rainfall. For this purpose, a sound soil moisture accounting procedure (SMA) in combination with the CN procedure was introduced. In wet soil conditions, for realistic prediction of runoff, CN value has to be high, and vice versa. A sound SMA has to incorporate all soil moisture conditions (Mishra et al., 2004a; Mishra and Singh, 2004a; Michel et al., 2005; Kannan et al., 2008).

The SMA concept was first introduced by Williams & LaSeur (1976) to develop a continuous water yield model using the existing SCS-CN method. Fundamental to the SMA concept is the continuous variation of 'Curve Number' (CN) with soil moisture resulting in many values of CN instead of only three, i.e., CN_I , CN_{II} , CN_{III} . Later, an appreciable attempt was further made by Hawkins (1978) to account for soil moisture on continuous basis.

Later, Mishra and Singh (2004a) used the concept of soil moisture budgeting to develop a versatile SCS-CN (VSCS-CN) model on continuous basis. Its brief discussion follows (Mishra et al., 2004a):

Using the $C = S_r$ concept, where C is the runoff coefficient ($=Q/(P - I_a)$) and S_r = degree of saturation (F/S), Mishra and Singh (2002a) modified Eq. (2) for antecedent moisture M as:

$$\frac{Q}{(P - I_a)} = \frac{F + V_0}{S + V_0} \quad (2.14)$$

which upon substitution into Eq. (2.14) leads to

$$Q = \frac{(P - I_a)(P - I_a + V_0)}{(P - I_a + V_0 + S)} \quad (2.15)$$

Here V_0 is computed as:

$$V_0 = \frac{(P_5 - 0.2S_1)S_1}{P_5 + 0.8S_1} \quad (2.16)$$

where P_5 is the antecedent 5-d precipitation amount and $S_1 (= S + V_0)$ is the potential maximum retention corresponding to AMC I and V_0 is the initial moisture. Eq. (2.15) assumes the watershed to be dry 5 days before the onset of the rain storm. Based on this concept, a number of improved SCS-CN-based models (for example, Sahu et al., 2007&2010; Geetha et al., 2008; Durbude et al., 2011; Jain et al., 2012; Ajmal et al., 2015; and Singh et al., 2015) have been proposed to address the issue of quantum jump of runoff estimation with varying degree of complexities in mathematical structure and parameterization.

2.2.6 SCS-CN Method derived from Entropy Theory

Using rainfall-runoff models (Zoch, 1934, 1936; Mockus, 1949) with Horton infiltration model, and first (linear) and second (non-linear) order hypotheses, Mishra and Singh (2002a) derived the SCS-CN method. Recently, Singh (2013) derived it using the entropy theory. The probability distributions of its variables, viz., CN, F, I_a , P, Q and S are developed assuming their nature to be random. It was observed that no information regarding probability distribution of runoff is required by SCS-CN method, except following the total probability law. The expression of entropy associated with SCS-CN method is as follows:

$$H(Q) = \int_0^{P - I_a} \frac{1}{P - I_a} \ln \left[\frac{1}{P - I_a} \right] dQ = \ln(P - I_a) \quad (2.17)$$

or

$$H(Q) = \ln S - \ln F + \ln Q \quad (2.18)$$

Eq. (2.17) can also be expressed in terms of CN as:

$$H(Q) = \ln \left[P - \lambda \left(\frac{25400}{CN} - 254 \right) \right] \quad (2.19)$$

Likewise, Eq. (2.18) can be cast as

$$H(Q) = \ln \left[\left(\frac{25400}{CN} - 254 \right) \right] - \ln F + \ln Q \quad (2.20)$$

where $H(Q)$ is the Shannon (1948) entropy of Q , expressed as:

$$H(Q) = - \int_0^{P-I_a} f(Q) \ln [f(Q)] dQ \quad (2.21)$$

in which $f(Q)$ is the probability density function of Q , expressed as: $[F/QS]$. Eqs. (2.17-2.21) provide different ways to express the uncertainty or entropy linked with the SCS-CN method. The study reveals the gamma distribution to be the ‘best’ representative distribution of CN, P , Q , S , F/S and $Q/(P-I_a)$. The infiltration acts as a filter to the uncertainty in Q , which mainly depends on $(P-I_a)$. Thus, I_a and P (which depends on S or CN) should be determined with maximum possible accuracy.

2.2.7 SCS-CN Based Advanced Applications

The SCS-CN method was developed as an event-based and empirical procedure for surface runoff estimation, it has been widely applied in hydrology because of its simplicity, stability and accountability for most runoff producing catchment properties: Surface condition, land use treatment, Soil type, and AMC. Singh and Frevert (2002) edited a book titled “Mathematical Models of Small Watershed Hydrology and Applications” consisting of 22 chapters, of which at least 6 were about SCS-CN based models. This shows the versatility and robustness of SCS-CN methodology.

Apart from rainfall-runoff modeling of the ungauged watersheds, the SCS-CN method has witnessed extensive applications in hydrology, environmental engineering and watershed management, e.g. hydrograph simulation (Aron et al., 1977; Mishra and Singh, 2002a, 2004b), long-term hydrologic simulation (LTHS) (Williams & LaSeur, 1976; Hawkins, 1978; Choi et al., 2002; Mishra et al., 2004a; Mishra and Singh, 2004a; Michel et al., 2005; Sahu et al., 2007; Geetha et al. (2008); Kannan et al., 2008; Durbude et al., 2011; Sahu et al., 2010; Williams et al., 2011), urban hydrology (Pandit & Gopalakrishnan, 1996 and Singh et al., 2013), metal partitioning (Mishra et al., 2004b&c), soil moisture accounting (Mishra et al., 2004a; Michel et al., 2005; Sahu et al., 2010; Ajmal et al., 2015; Singh et al., 2015), sediment yield modeling (Mishra et al., 2006b; Tyagi et al., 2008; and Singh et al., 2008; and Bhunya et al., 2010), baseflow simulation (Coustau et al., 2012), river bank filtration and water quality (Ojha, 2012), evapotranspiration (Mishra et al., 2014) and irrigation requirement (Chakraborty et al., 2015). The versatility and popularity of the SCS-CN method has led many researchers to integrate it into new hydrological models too (Singh et al., 2010). Walter and Stephen (2005) advocated that the criticisms of SCS-CN method should be considered as an encouragement towards finding suitable approaches to resolve the current problems, rather than interpreting as “negative reflections” on its developers. Many researchers reported that the SCS-CN method underestimated the measured event outflows. Thus, many modifications of the original SCS-CN method have been presents by researches (Singh et al., 2015; walega et al. 2015, Petroselli et al., 2013; Grimaldi et al., 2013a, Grimaldi et al., 2013b; Geetha et al., 2007; Eldo et al., 2007, Sahu et al., 2010, Sahu et al., 2012; Sahu et al., 2007, Yuan et. al., 2001). This may strengthen the progressive efforts towards the advancement of SCS-CN methodology. Some of the prominent works related to integration of SCS-CN with other hydrological models are discussed briefly as follows.

2.3 SCS-CN BASED HYDROLOGIC SIMULATION MODELS

This section presents some of the crucial and ubiquitous hydrologic simulation models based on SCS-CN method. These models are specifically handy for effective water resources planning and management (Choi et al., 2002; Mishra and Singh, 2004a).

2.3.1 SMA Based Williams and LaSeur (1976) Model

The concept of Soil Moisture Accounting (SMA) was first developed by Williams & LaSeur (1976) while developing a SCS-CN based continuous model. Owing to the continuous variation of CN with respect to soil moisture, the model favored considering numerous values of CN rather

than only three (i.e. CN_I , CN_{II} , CN_{III}). Subsequently, a parameter i.e. soil moisture index (SMI) depletion was used, which forced a reconciliation between the predicted and observed average annual runoff. The sudden jump in CN during the transition phase of AMC change were eliminated by the model. The model can be used over the ungauged catchments by adjusting their curve number proportional to the ratio of CN (AMC II) and average predicted CN for the gauged catchment. Nevertheless, there are certain shortcomings of the model. The absolute potential maximum retention S_b was taken as 20 inches, which is arbitrary. Further, the soil moisture was assumed to decay with the lake evaporation unreasonably.

2.3.2 Hawkins ET-CN Model

A continuous simulation model was developed by Hawkins (1978) by linking the CN with evapotranspiration (ET). The model continuously reckons the soil moisture through volumetric concept and hence, obviates the issues of abrupt jump in CN. However, for even zero rainfall condition, $Q = 0.05S$ is computed by the model, which is not feasible and a violation of principle of mass conservation as well. Moreover, it assumes the methodology of SCS-CN to be rooted on (I_a+S) scheme, while I_a and S are separate in the existing methodology (Mishra and Singh, 2004).

2.3.3 Versatile SCS-CN (VSCS-CN) Model

A four-parameter versatile SCS-CN (VSCS-CN) model was developed by Mishra and Singh (2004a) to eliminate the complexities and inconsistencies of the existing models. The abrupt jumps in CN values are eliminated by the model whereas watershed routing procedures, ET and continuous soil moisture budgeting are specifically considered, thus being regarded as a versatile model. Numerous SMA-based models were developed after this model made provisions for structural diagnosis of the existing SCS-CN method.

Both the static and dynamic components of evapotranspiration (ET) and infiltration excess are accounted by the model in terms of absolute maximum potential retention (S_{abs}) and pan coefficient (PANC), where $S_{abs} = (S+S_a)$, and $PANC = S/ S_{abs}$. The S_a represents the threshold soil moisture $= (V_0+I_a)$. A further exploration of these models could be carried out to comprehend their formulations and assess the applicability.

2.3.4 Michel SCS-CN Model

Michelaet al. (2005) developed a modified version of SCS-CN model to consider the soil moisture accounting (SMA) procedure on continuous basis. The model was hypothesized to be valid at any instant during a storm, rather than only at the end of storm. The SMA procedure is

conceptualized on the idea that a higher runoff is generated, provided a higher level of moisture stored in the watershed. To estimate direct surface runoff, Michel SCS-CN model obviates I_a and a threshold soil moisture parameter S_a , where $S_a = (I_a + V_0)$.

2.3.5 Sahu et al. SCS-CN Model

An advanced SMA procedure based SCS-CN model was developed by Sahu et al. (2007) for continuous hydrologic simulation. The initial soil moisture (V_0) was hypothesized to be dependent on retention capacity (S), along with antecedent 5-day precipitation (P_5). This is due to the fact that the watershed with higher S retains higher moisture in comparison with the watershed with lesser S for a given P_5 . The sudden jump in runoff estimations are eliminated by the model, which is an upgradation over Michel SCS-CN model (Michel et al., 2005).

2.3.6 Sahu-Mishra-Eldho Model

Sahua et al. (2010a) developed a revised version of the SCS-CN method incorporating a continuous function for antecedent moisture in the Mishra and Singh (2002a) model, expressed as:

$$Q = \frac{(P - I_a)(P - I_a + V_0)}{(P - I_a + S_0)}; \quad \text{for } P \geq I_a; \quad Q = 0; \quad \text{otherwise} \quad (2.22)$$

where $I_a = \lambda (S_0 - V_0)$; S_0 = potential maximum retention in completely dry condition and V_0 is expressed as:

$$V_0 = \beta \left[\frac{(P_5 - \lambda S_0) S_0}{P_5 + (1 - \lambda) S_0} \right] \quad \text{for } P_5 > \lambda S_0 \quad (2.23)$$

$$= 0 \quad \text{for } P_5 \leq \lambda S_0 \quad (2.24)$$

Eqs. (2.22)-(2.24) form the SME model. The proposed SME model was a more viable alternative to the original SCS-CN method and the Mishra and Singh (2002a) model for field applications. Walega et al. (2017) modified SME approach by introducing potential retention of soil S according to the original SCS-CN method. Walega and Salata (2019) modified SME-CN model for more accurate estimation of direct runoff employing a catchment land cover for smaller map scales derived from BDOT10k.

2.3.7 Geetha SCS-CN Model

Geetha et al. (2008) conceptualized and developed a lumped model based on the SCS-CN method modified for accounting of the antecedent moisture effect for long-term hydrologic simulation. The developed model was found to be useful in continuous simulation of rainfall–runoff process and performed better than another lumped conceptual model based on variable source area (VSA) theory (Mishra et al., 2005c) on the data of five Indian watersheds. The modified SCS-CN-based lumped model considers various hydrologic components involved in runoff generation mechanisms and takes into account the temporal variation of curve number.

2.3.8 SCS-CN Based ASMA Model

Jain et al. (2012) proposed modified long-term hydrologic simulation advance soil moisture accounting (MLTHS ASMA) model by coupling the advanced soil moisture accounting (ASMA) procedure, the modified subsurface drainage flow concept, and curve number (CN)–based model for simulating daily flows. The proposed model uses the ASMA procedure both for surface and sub-surface flows.

2.3.9 SCS-CN Based PET-IWR Models

The proportionality concept ($C = S_r$ concept) of the SCS-CN method was used by Mishra et al. (2014) in the simple water balance equation to derive a power relationship between CN and mean (PET) using the usually available long-term daily rainfall-runoff data. The general form of the CN (or S) vs PET potential evapotranspiration (or evapotranspiration ET) model can be expressed as:

$$ET = \alpha S^\beta \quad (2.25)$$

where α and β are the coefficient and exponent, respectively. Because there exists an inverse relationship between S and CN [Eq. (2.7)], Eq. (2.25) suggests ET to be high for the watersheds of low CN and vice versa. This ET-CN rationale was based on the following relationship as expressed here:

$$E = I_a + \frac{(P - I_a)(E^* - I_a)}{(P - I_a + S)} \quad (2.26a)$$

$$E = E_T + E_S + E_I \quad (2.26b)$$

where E_T is the daily transpiration (moisture transferred from the soil to the atmosphere through the root-stem-leaf system of vegetation); E_S is the daily soil evaporation (moisture transferred from the soil to the atmosphere by hydraulic diffusion through the pores of the soil); E_I is the daily interception loss (water evaporated from the wet surface of the vegetation and wet surface of the soil) during rain storm; and E^* is the daily potential evapotranspiration.

2.3.10 MMSCS-CN Model

Based on soil moisture accounting procedure (SMA) and changed parameterization with improved relationships for estimation of parameters, Singh et al. (2015) developed modified Michel SCS-CN (MMSCS-CN) model for runoff computations. Simple expressions of V_0 and S_a an intrinsic parameter were provided to obviate the manual adjustments in V_0 to accommodate all the three AMCs and fixation of S_a with S .

Based on the revised SMA procedure incorporating storm duration and a physical formulation for estimating antecedent soil moisture (V_0), Shi et al. (2017) proposed a modified SCS-CN method.

2.3.11 Parsimonious SCS-CN Model

Based on in-depth structural diagnosis of the SCS-CN model and implicit inconsistencies in model parameterization, Ajmal et al. (2015) developed a parsimonious SCS-CN model based on soil moisture proxies (SMP) and proposed improved relationships for V_0 and S_a . The model is very simple in use and has only one parameter as the existing SCS-CN method.

2.3.12 Enhanced SMA based SCS-CN Model

Recently, Choi and Engel (2018) proposed a continuous SCS-CN model for estimation of long-term discontinuous storm runoff depth with a revised SMA approach, incorporating time-varied potential maximum retention, conditional initial abstraction, static infiltration, and evapotranspiration equations. Verma et al. (2018) incorporated the concept of initial soil moisture (V_0) in the SCS-CN method to avoid the sudden jumps in CN and, in turn, in computed runoff. The developed model was found to perform better than the models of Mishra and Singh (2002), Michelaet al. (2005) and Singh et al. (2015).

2.4 SEDIMENT YIELD MODELLING

Sediment yield is defined as the total sediment from the catchment deposited at the outlet point in a specific time period (ASCE, 1970). An accurate estimation of sediment yield is essential for designing of erosion control structures, evaluation of reservoir sedimentation, water quality management, and for framing of the future water resources management policies (Merritt et al., 2003). Prediction of sediment yield is very complicated and nonlinear in nature. It depends on a number of complex factors such as flow, precipitation, topography and soil characteristics of the river basin or watershed. This section briefly discusses about factors affecting erosion and sediment yield process, approaches of sediment yield modelling followed by the recent models based on the popular SCS-CN method and USLE model for this purpose. Finally, the section is summarized with remarks showing the scope of further improvements in the models developed for modelling erosion and sediment yield.

2.4.1 Factors governing Sediment Yield

The process of soil loss and sediment yield is largely affected by climatic parameters, LULC, catchment characteristics and soil properties. A brief review of these factors and their influence on sediment yield is presented below.

Climate: The sediment yield or soil erosion have always been influenced significantly by the climate. It is observed that the quantity of soil detached significantly depends on the rainfall characteristics (viz. Intensity, duration and frequency of rain events). Generally, the rain with higher intensity and shorter duration creates severe erosion. The intensity of rainfall and the raindrop action play a vital role in generating runoff and sediment yield at the outlet of a catchment. The longer duration of low intensity rainfall sometimes becomes extremely erosive due to saturation of soil with subsequent increase in runoff (Morgan, 1995). The soil erosion may be aggravated due to wind driven rainfall as wind action enhances the erosive energy of rainfall (Lal, 1976). The wind can also accelerate the overland flow velocity, thereby leading to increased detachment of soil as well as the sediment transport. The process of runoff and weathering of rocks are affected by the temperature, which consequently affects the sediment yield.

Soil Properties: Various soil properties (viz. aggregation, organic matter, texture, soil structure and tillage) which affects infiltration and stability of soil also influences water erosion and sediment yield. Soil erodibility is an important property, which is a measure of resistivity of soil to detachment as well as transportation (Wischmeier and Smith, 1978; Pandey et al., 2019). The organic content, soil structure, permeability, soil texture are the main factors which influence erodibility. As the sandy soil has very high infiltration capacity, the water rapidly infiltrates into

the soil leading to reduction in the erosion potential. The particles in clay soil are closely bound together which reduces its erodibility. If the silt content of the soil is high (i.e. 40 to 60%), it is more susceptible to erosion. Likewise, if the clay constituent of soil is 10-30 %, the soil is easily erodible (Evans, 1980). The resistance to erosion by fine particles is due to their cohesiveness, which hinders the detachment. In contrast, the resistance offered by large particles is against the transportation due to their size. The effect of soil texture on erosion was assessed by Moldenhauer and Long (1964) through rainfall simulations. For rainfall of high intensity, the relative soil erosion followed the order of: soil loss from fine sand < loam < silt < silty clay loam < silty clay. But, the order of soil erosion for low intensity rainfall was as follows: soil loss from fine sand < silt < loam < silty clay < silty clay loam. With equal water loss, the erodibility followed the order of: soil loss from loam < silt < silty clay loam < silty clay < fine sand. The effects of organic matter and soil texture on soil erodibility have been modelled in several prior works (Wischmeier and Mannering, 1969; Wischmeier et al., 1971; Alberts et al., 1980). Flaxman (1972) developed an equation for annual sediment yield taking the soil particle size into account (i.e. the portion of soil > 1 mm in diameter).

Watershed Characteristics: The sediment yield and runoff are highly affected by the watershed characteristics viz., drainage density, slope, area and shape (Jansen and Painter, 1974; Garde and Kothiyari, 1987; Himanshu et al., 2019). The potential of losing the soil will be higher on steep slopes than the gradual slope, as the amount of sediment carried will be higher in water moving with higher velocity than the water moving with lower velocity (Morgan, 1979). Zingg (1940) derived an equation for soil erosion as an exponential function of slope steepness. The area of the catchment also plays a vital role in sediment yield at the outlet. Typically, a catchment with higher areal extent generates higher sediment yield. However, the sediment delivery ratio, which is defined as the portion of eroded soil in the catchment reaching the outlet, decreases with increase in area of catchment (Schumm, 1954; Roehl, 1962; Wilson, 1973; David & Beer 1975a&b, Taylor, 1983).

Land Use/ Land Cover: The type of LULC has direct effects on runoff. Presence of vegetation cover leads to interceptions from rainfall, which weakens the erosive force of the raindrops and consequently, hinders soil erosion. Further, it assists in quick deposition of eroded soil over the catchment, thereby reducing the sediment yield at the outlet. Chow (1959) conceptualized the effects of the vegetation cover over the overland flow in terms of the roughness. Wischmeier (1975) studied the role of vegetation roots on soil loss and found that the roots bind the soil mass to enhance the erosion resistance. The widely used empirical equation for soil loss estimation, i.e. USLE, also addresses this issue by considering Cover Management Practice Factor. Meyer

et al. (1975a) studied the effects of residue on rate of soil erosion, which have been analyzed further by several researchers (Meyer et al., 1975a & 1981; Laflen and Colvin, 1981; Foster, 1982; Hussein and Laflen, 1982; Cogo et al., 1984; Dickey et al., 1985; Norton et al., 1985; Gilley et al., 1986; Brown & Foster, 1987; Franti et al., 1996).

2.5 SCS-CN BASED EROSION AND SEDIMENT YIELD MODELS

This section briefly discusses some of the recently developed models based on SCS-CN method for erosion, sedimentation and metal partitioning in hydrological and environmental engineering. As discussed previously, most of the computer based sedimentation simulation models such as AGNPS (Young et al., 1989), CREAMS (Knisel, 1980), SWRRB (Arnold et al., 1990), SWAT (Neitsch et al., 2002), EPIC (Sharpley & Williams, 1990) and GWLF (Haith and Shoemaker, 1987) use the SCS-CN method as a component model for runoff estimation. However, as a model itself, the SCS-CN method has not witnessed many applications in the field of soil erosion, sedimentation and water quality, despite some noteworthy works of Mishra et al. (2006b), Tyagi et al. (2008), Singh et al. (2008), and Bhunya et al. (2010). Garen and Moore (2005) explored the applicability of SCS-CN methodology in Water Quality Modeling and named it as “Curve Number Hydrology”, which signifies the versatility of the model itself. Therefore, the SCS-CN method has enormous potential and it is one of the “hydrological modeling technique” available to the scientific community with its broad applicability.

2.5.1 USLE Coupled SCS-CN Based Sediment Yield Model

The popular and widely used models, i.e., SCS-CN method and USLE were coupled by Mishra et al. (2006b) for modeling rain-storm generated sediment yield from a watershed. The coupling is based on three hypotheses: (i) the runoff coefficient (C) is equal to the degree of saturation (S_r); (ii) the potential maximum retention (S) can be expressed in terms of the USLE parameters, and (iii) the sediment delivery ratio (DR) is equal to the runoff coefficient (C). Table 2.2 shows the summary of the developed models for different conditions. The developed models have ample potential for application to the un-gauged watersheds.

Table 2.2.: Formulation of Rainfall-Sediment Yield and Rainfall-Runoff Models (Mishra and Singh, 2003)

Model	Rainfall-sediment yield models	Model	Rainfall-runoff models
S1	$Y = \frac{AP}{P+S}$	R1	$Q = \frac{P^2}{P+S}$

S2	$Y = \frac{A(P - 0.2S)}{P + 0.8S}$	R2	$Q = \frac{(P - 0.2S)^2}{P + 0.8S}$
S3	$Y = \frac{A(P - \lambda S)}{P + (1 - \lambda)S}$	R3	$Q = \frac{(P - \lambda S)^2}{P + (1 - \lambda)S}$
S4	$Y = \frac{A[P - \lambda S + M]}{P + (1 - \lambda)S + M}$	R4	$Q = \frac{(P - \lambda S)(P - \lambda S + M)}{P + (1 - \lambda)S + M}$
S5	$Y = \frac{A[P - 0.2S + M]}{P + 0.8S + M}$	R5	$Q = \frac{(P - 0.2S)(P - 0.2S + M)}{P + 0.8S + M}$
S6	$Y = \left[\frac{(1 - \lambda_1)[P - 0.2S + M]}{P + 0.8S + M} + \lambda_1 \right] A$	R6	$Q = \frac{(P - 0.2S)(P - 0.2S + M)}{P + 0.8S + M}$
S7	$Y = \left[\frac{(1 - \lambda_1)[P - \lambda S + M]}{P + (1 - \lambda)S + M} + \lambda_1 \right] A$	R7	$Q = \frac{(P - \lambda S)(P - \lambda S + M)}{P + (1 - \lambda)S + M}$
S8	$Y = \left\{ (1 - \lambda_1) \alpha \left[\frac{[P - 0.2S + M]}{P + 0.8S + M} \right]^\beta + \lambda_1 \right\} A$	R8	$Q = \frac{(P - 0.2S)(P - 0.2S + M)}{P + 0.8S + M}$
S9	$Y = \left\{ (1 - \lambda_1) \alpha \left[\frac{[P - \lambda S + M]}{P + (1 - \lambda)S + M} \right]^\beta + \lambda_1 \right\} A$	R9	$Q = \frac{(P - \lambda S)(P - \lambda S + M)}{P + (1 - \lambda)S + M}$

It can be observed from Table 2.2 that these models are based on the existing SCS-CN method and hence there is ample scope for their further refinements based on improved S-CN mapping and revised proportional equality (based on first order linear hypothesis and Horton method) and test the applicability of these models on the rainfall-runoff and sediment yield data of the experimental plots for which the USLE model was originally developed in USA.

Changyeol et al. (2016) tested the applicability of these models for Korean watersheds and compared their performance with the MUSLE model. They found that USLE coupled SCS-CN model performs much better than MUSLE model. Srivastava and Imtiyaz (2016) tested the SCS-CN coupled USLE model for estimating runoff and sediment yield for eleven watersheds of Damodar Valley Corporation (DVC), Jharkhand. This shows that the sediment yield models based on the coupling of SCS-CN method with USLE have large potential for erosion and sediment yield estimation.

2.5.2 SCS-CN based Conceptual Sediment Graph Model

The popular and extensively used Nash (1957) model based instantaneous unit sediment graph (IUSG), SCS-CN method, and Power law (Novotny and Olem, 1994) were coupled by Singh et al. (2008) to develop conceptual sediment graph models to get time-distributed sediment yield on storm basis. These models account for various components aggravating soil disintegration and

sediment yield. The sediment graph models (SGMs) for four different cases, depending on the number of model parameters, and these are designated as SGM₁ through SGM₄, respectively as shown in Table 2.3. For SGM₁, both the initial soil moisture V_0 and initial abstraction I_a are assumed to be zero, i.e. $V_0 = 0$ and $I_a = 0$. For SGM₂, $V_0 = 0$, but $I_a \neq 0$. For SGM₃, $V_0 \neq 0$ and $I_a = 0$. Finally, for SGM₄, $V_0 \neq 0$ and $I_a \neq 0$.

Table 2.3: Formulation of Conceptual Sediment Graph Models (Singh et al., 2008).

Sl. No.	Model	Model Expression
1:	SGM ₁	$Q_s(t) = \left[\alpha A A_w [kt / (1 + kt)]^\beta (n_s - 1)^{n_s} / t_{ps} \Gamma(n_s) [(t / t_{ps}) e^{-(t / t_{ps})}]^{n_s - 1} \right]$
2:	SGM ₂	$Q_s(t) = \left[\alpha A A_w [(kt - \lambda) / (1 + kt - \lambda)]^\beta (n_s - 1)^{n_s} / t_{ps} \Gamma(n_s) [(t / t_{ps}) e^{-(t / t_{ps})}]^{n_s - 1} \right]$
3:	SGM ₃	$Q_s(t) = \left[\alpha A A_w [(kt + V_0 / S) / (1 + kt + V_0 / S)]^\beta (n_s - 1)^{n_s} / t_{ps} \Gamma(n_s) [(t / t_{ps}) e^{-(t / t_{ps})}]^{n_s - 1} \right]$
4:	SGM ₄	$Q_s(t) = \left[\alpha A A_w [(kt - \lambda + V_0 / S) / (1 + kt - \lambda + V_0 / S)]^\beta (n_s - 1)^{n_s} / t_{ps} \Gamma(n_s) [(t / t_{ps}) e^{-(t / t_{ps})}]^{n_s - 1} \right]$

The models could be valuable in the calculation of time disseminated sediment yield and the total silt yield and can be effectively implemented for un-gauged conditions also. The models can be exceptionally valuable for figuring dynamic contamination loads in water quality modelling if it is needed to determine the peak rather than the mean sediment flow for the toxic pollutants transported with the sediment.

2.5.3 SCS-CN Based SLR Time Distributed Sediment Yield Model

A single linear reservoir (SLR) time-distributed sediment yield model was developed by Tyagi et al. (2008) utilizing the SCS-CN-based infiltration model for computation of rainfall-excess rate, and the SCS-CN-inspired proportionality concept for computation of sediment-excess. Finally, for computation of time-distributed sediment, the sediment-excess is routed to the watershed outlet using a single linear reservoir technique. Mathematically, the model is expressed (eq. 2.27) as:

$$Y_t = \frac{A_s}{P_{\Delta t}} \left[1 - \frac{S^2}{(P + S - \lambda S)^2} \right] (i - f_c) \quad (2.27)$$

where A_s is the actual potential maximum erosion of the watershed, dependent on the soil properties and storage capacity (S); $P_{\Delta t}$ is the rainfall amount during time interval Δt ; i is the rainfall intensity, and f_c is the final infiltration rate.

2.5.4 RUSLE Coupled SCS-CN Based Sediment Yield Model

Recently, Gao et al. (2012) incorporated antecedent moisture condition (AMC) in SCS-CN based runoff production and considered the direct effect of runoff on event soil loss by adopting a rainfall-runoff erosivity factor in the RUSLE model. The modified SCS-CN and RUSLE models were coupled to link rainfall-runoff-sediment yield modelling. The effects of AMC, slope gradient and initial abstraction ratio on curve number of SCS-CN, as well as those of vegetation cover on cover-management factor of RUSLE, were also considered in this study. It was found that the original SCS-CN model significantly underestimated the event runoff, especially for the rainfall events that have large 5-day antecedent precipitation whereas the modified SCS-CN model was accurate in predicting event runoff with Nash-Sutcliffe model efficiency (EF) over 0.85. The original RUSLE model overestimated low values of measured soil loss and under-predicted the high values with EF values only about 0.30. In contrast, the prediction accuracy of the modified RUSLE model improved with EF values being over 0.70. The results indicated that the AMC should be explicitly incorporated in runoff production and direct consideration of runoff should be included when predicting event soil loss. They found that the coupling the modified SCS-CN and RUSLE models has great practical importance for runoff and soil loss simulation. The RUSLE coupled SCS-CN based sediment yield model is found to perform very well.

2.6 ENVIRONMENTAL FLOW REQUIREMENT

The rivers around the globe went through changes due to engineering development, change in land use, construction of flood control, diversion and irrigation structures, and pollution causing from heavy metals. The rivers in different continents are at different stages of adjustment due to increasing industrialization and urbanization, subsequently raises the attention towards the river rehabilitation. Rehabilitation of rivers along with repairing of water quality and ecological losses are the issues of international concern, for the sustainability of ecosystem (Langhans et al., 2013; Pan et al., 2016; Paillex et al., 2017). Anthropogenic activities like regulation of river flow and removal of vegetation from riparian zone are the major factors contributing to geomorphic alteration and river degradation (Galay, 1983; Nilsson and Berggren, 2000). During last three decades, river management becomes a multi-disciplinary initiative to address the diversity of

river values and needs of the ecosystem (Piegay et al., 2008; Wohl et al., 2008; Fryirs et al., 2013). It is not only expensive and tough to stop the deterioration in riparian zone once it started, but even mild degradation can cause remarkable damage to freshwater ecosystems (Chessman et al., 2006).

The health of river ecosystem is very important for human being as it provides the vital source of water for humans (Meng et al., 2009). Cheng et al. (2018) assess the health of river ecosystem in Haihe River Basin by sampling 148 river sites during pre- and post-monsoon seasons. Their study revealed that the change in land use and socio-economic development are major factors responsible for river deterioration. In the recent past, the over exploitation of water resources coupled with increasing industrialization and urbanization caused a serious ecological imbalance around the globe (Vorosmarty, 1997; Meador et al., 2003; Paukert et al., 2011; Stamou et al., 2018). The over-exploitation such as abstraction of water from river is one of the major reasons which changes the flow regime and may impend river ecosystem (Pearce, 2012) to “artificial desiccation” (Skoulikidis et al., 2011) and extinction of fish (Vorosmarty et al., 2010; Stamou et al., 2018). In literature, the major impacts of alteration of flow regime on the amount of habitat for various species such as micro-organisms, fish and aquatic plants (Bunn and Arthington, 2002; Arthington, 2012; Stamou et al., 2018). It is well known that to uphold a minimum flow in rivers is very important for sustainability of biodiversity and ecosystem integrity (Tharme, 2003; Arthington et al., 2006; Poff et al., 2010).

The concept of environmental flow (EF) was evolved to determine the minimum amount of water required for the sustenance of ecological species (Poff and Mathews, 2013; Operacz et al., 2018). In literature, environmental flow has been defined in different ways by various researchers (Kostrzewa, 1977; Tharme, 2003; O’Keeffe, 2009; Poff and Mathews, 2013; Młynski et al., 2015; Vietzet et al., 2017). “Environmental flows describe the quantity, quality and timing of water flows required to sustain freshwater and estuarine ecosystems and the human livelihoods and well-being that depend on these ecosystems” (Brisbane Declaration, 2007). Environmental flow can also be defined as the part of natural flow that should be maintained in stream or river for the sustainability of aquatic ecosystem and species depends on these ecosystems (Tharme, 2003; Operacz et al., 2018). The main objective of environmental flow is to provide suitable physical conditions for smooth functioning of natural ecosystems within flow regulation limits (Vietzet et al., 2017). Generally, environmental flow describes the flow regime necessary to sustain estuarine and freshwater ecosystems, and livelihoods of species that depends on them (Hirji et

al., 2009; Saintilan et al., 2010; Gippel et al., 2012; Webb et al., 2012; Banks and Docker, 2013; Overton et al., 2014; Warner et al., 2014; Padikkal et al., 2019).

2.7 ASSESSMENT OF ENVIRONMENTAL FLOW

The development of methodologies for the assessment of environmental flow started quite early. Initially, the method to estimate the minimum flow appeared in USA in 1940. The methodologies for the assessment of environmental flow have been classified differently by the researchers (Stalnaker, 1990; Dunbar et al., 1998; Dyson et al., 2003; Tharme and Smakhtin, 2003; King et al., 2009). Stalnaker (1990) grouped the methods into two categories namely Standard setting and Incremental. Further, the Incremental methodologies was replaced by Empirical methods (Dunbar et al., 1998). Empirical methods are based on biological and physical data collected in the field which are used to determine a schedule of flow requirement. Dyson et al. (2003) made a distinction among Methods, Approaches and Frameworks. Methods particularly describe the specific assessments of environmental needs; the ways to derive the assessments are called as Approach; and Frameworks provides wider strategy for the assessment of environmental flow for management of natural ecosystem by using specific methods or applying a particular approach. King and Brown (2003) described the differences between the methods based on Prescriptive and Interactive approaches. The prescriptive methodology provides a single flow regime to maintain a river condition and is suitable where objectives are clear and conflicts are a minimum. The interactive methodology provides a range of flow regime linked to different river conditions and suitable where the users are many. The recent global review on methods of environmental flow assessments reveals that more than 240 methods are used widely for the estimation of environmental flow (Amrit et al., 2017).

Tharme (2003) and Tharme and Smakhtin (2003) classified the methods for environmental flow assessment in four groups. These are hydrological, hydraulic rating, habitat simulation and holistic methods. This classification is widely used for the assessment of environmental flow.

2.7.1 Hydrological Methods

In this method the streamflow (observed or simulated) data (usually 30 years or more) are used to estimate the various statistics of flow. The data may be arranged daily, weekly, 10-daily or monthly. Since the method is based on past data, it is also called as Historical flow method. Hydrologic models are commonly used to reproduce streamflow records and to simulate natural flow conditions before any anticipated changes in stream regime as a result of human activities like LULC changes or urbanization. The method involves an expert assessment, based on the

existing information of hydrology, characteristics of river and some fish species of primary interest, and of the level of flow that would maintain the stream/river ecosystem at an acceptable or desired level. The popular hydrological methods used for the assessments environmental flow are given in Table 2.4.

2.7.2 Hydraulic rating methods

The hydraulic rating methods are based on the assumption that discharge and some of the hydraulic measures of stream are related along the single river cross section as replacement for habitat factors (Tharme 2003). The influence of stream hydraulics on the distribution of benthic fauna across the river course had already been highlighted by several studies (Gore 1978; Statzner 1981; Statzner and Higler 1986). Hydraulic methods relate various hydraulic variables such as maximum depth, wetted perimeter, velocity, longitudinal connectivity, etc., based on surveyed cross sections, to discharge rates (Jowett 1989). Tharme (1996) reviewed the widely used hydraulic rating methods and associated models for hydraulic simulation used to estimate the environmental flow. These methods are simple, inexpensive and relate streamflow and ecology, considering the physical habitat conditions. The popular hydraulic rating methods used for the assessment of environmental flow are given in Table 2.4.

2.7.3 Habitat simulation methods

These methods are also known as Habitat Rating Methods, Habitat Modelling Methods or Microhabitat Methods. Generally, Habitat simulation methods are considered to be the extension of hydraulic methods. The various models in this category comprise of two components (a) hydraulic simulation, and (b) habitat simulation. The output of hydraulic simulation is used as an input for the habitat simulation programs to relate the simulated physical conditions (depth and velocity) to the conditions essential for a particular species at several stages of its life called Habitat Suitability Criteria (HSC).

So far about 60 different habitat modeling methods (or approaches) have been developed. Most of them originate from various States in USA and have only occasionally been used in other countries. However, some of them have contributed to the evolution of more complex modeling approaches such as the In-Stream Flow Incremental Methodology (IFIM) that are now widely used. Some of the popular Habitat Simulation methods used for the assessment of environmental flow are given in Table 2.4.

2.7.4 Holistic Methods

The word holistic refers to methodologies which considers whole aquatic ecosystem. The need for a holistic method was felt first in the beginning of 1990s almost at the same time in Australia and South Africa. During an International Workshop on Water Allocation for the Environment, the holistic approach was conceptualized (Brisbane, 1991) and described jointly by the scientists from the two countries (Arthington et al. 1992). Building Block Method (BBM) was the first models developed under this category while in early 1980's another holistic method developed was Instream Flow Incremental Method (IFIM). The data requirement of holistic models is very high. Some of the popular Holistic methods used for assessment of environmental flow are given in Table 2.4.

Table 2.4 Popular methods based on Tharme (2003) classification

<i>Category</i>	<i>Methods</i>
<i>Hydrological</i>	<i>Tennant method, The BC-Instream Flow Threshold, Alberta Desktop Method, Flow Duration Curve Methods, Shifting FDC Technique, Indicators of Hydrologic Alteration (IHA) and Range of Variability Approach, Sustainability Boundary Approach (SBA) and Presumptive Standards.</i>
<i>Hydraulic Rating</i>	<i>Wetted Perimeter Method, Toe-Width Method, Riffle Analysis, Adapted Ecological Hydraulic Radius Approach (AEHRA), Flow Event Method, Lotic Invertebrate for Flow Evaluation (LIFE).</i>
<i>Habitat Simulation</i>	<i>Habitat Quality Index, In-Stream Flow Incremental Methodology (IFIM), PHABSIM, MesoHABSIM, RHYHABSIM, Riverine Habitat Simulation (RHABSIM), System for Environmental Flow Analysis (SEFA), CASiMiR (Computer Assisted Simulation Model for Instream Flow Requirement).</i>
<i>Holistic</i>	<i>Building Block Methodology (BBM), Desktop Reserve Model (DRM), Downstream Response to Imposed Flow Transformation (DRIFT), Benchmarking Method, Specialist's Team-based Methods, Flow Restoration Methodology, ELOHA (Ecological Limits of Hydrologic Alteration), Savannah Process.</i>

Yin and Yang (2011) developed a coupled water diversion and reservoir operation model to maintain a balance between social and environmental flow needs. The model proposed was helpful in analyzing the tradeoffs between human and environmental water requirements, subsequently minimize the risk of water scarcities and reduces the disturbances in ecological integrity. Zhao and Chen (2011) used a hydrological model for evaluation of EF and changes in land use in Wolonghu wetland, China. The analysis indicated that environmental flows have both

direct and indirect effects on wetland ecosystem and should be linked to sustainable management of wetland. Yin and Yang (2012) studied about the correlation between environmental flow and ability of rivers to supply water. The capacity to ensure planned water supply is important factor for determining reasonable environmental flow in the regions having water scarcity. The study proposed a method to estimate the reasonable environmental flow. The applicability of the proposed approach was demonstrated on Tanghe River China. The approach proposed was found to be very useful for directing water supply and reservoir operations. Kiwango et al. (2015) carried out a case study on Wami River estuary and investigated the need of maintaining a minimum environmental flow to preserve estuaries in Tanzania. The study revealed that, the increase in sedimentation and reduction in freshwater flow caused by decrease in rainfall will affect the estuary. The assessment of environmental flow for Wami River has been done and the minimum flows which was to be maintained were recommended.

Glenn et al. (2017) studied the effectiveness of environmental flow in four rivers (Tarim in China; Colorado in Mexico; Bill Williams in U.S.; Murrumbidgee in Australia) for the restoration of riparian zones. The successful restoration of Euphrates poplar forest on river Tarim and germination of new chorts of willows on river Bill Williams have been achieved after maintaining the environmental flow for the period of 15 to 20 years. Gonza´lez-Villela et al. (2018) investigated the effects of changing climate on environmental flow in river Conchos, Mexico. The availability of water in the river was analyzed based on the frequency and magnitude of rainfall. Rainfall is related to environmental flow in assessing how much of the flow in the river has been altered due to effects of climate change or anthropogenic activities. The change in water availability was estimated for the periods of 1961-1983 and 1984-2008. The significant increase in rainfall during monsoon, with substantial reduction in minimum rainfall and in number of rainfall events have been observed.

Volchek et al. (2019) carried out a comparative study of five methods for the assessment of environmental flow in River Yaselda, Belarus. The study reveals that, the exceedance probability transfer method is quite useful and efficient. The analysis proposed that, yearly adjustment in rates of environmental flow can be done by considering the discharges in preceding year. Mishra et al. (2019) correlated the percentage of average annual flow (%AAF) of Tennat method with Standardized Precipitation Index (SPI) using the data of five catchments of Godavari basin. The proposed approach can be used for the assessment of environmental flow condition of the study catchments during the low flow season (October-June) using rainfall data only.

Amrit et al. (2019) proposed an approach for the estimation of environmental flow condition of a watershed during high flow season (July-September) based on easily available rainfall data. The applicability of the proposed approach was demonstrated on the 16 watersheds from four river basins (i.e. Mahanadi, Godavari, Brahmani-Baitarini and Tapi) of India. The method suggested is very useful for the watershed having no or sparse availability of flow data.

2.8 RESEARCH GAPS

Rainfall-runoff modelling

In this section, a pertinent review of the SCS-CN methodology dealing with its origin, structural and theoretical foundation, nature, advantages and limitations, issues pertaining to CN estimation, CN vs AMC description, I_a and S relationship, CN vs P description leading to description of watershed behavior, slope consideration in SCS-CN methodology, and SMA procedure in SCS-CN methodology, and advanced applications of methodology for runoff estimation have been presented and discussed for their merits and demerits. However, there are still some structural inconsistencies associated with the existing SCS-CN method such as the genesis of S-CN relationship and CN-P description leading to abnormalities or complications in description of watershed behavior. Therefore, it is necessary to improve the CN-P relationship such that the CN variation is consistent with that of C with P. These issues need due consideration for further rectification based on the sound hydrological perceptions.

Sediment Yield modelling

The sediment yield directly relies on the direct surface runoff, LULC and soil moisture. In this regard, a silt yield model either estimates the runoff in a lumped manner to calculate total sediment yield from a storm event or, mostly, generates the temporal rainfall-excess rate (or runoff rate) using an appropriate infiltration model to simulate temporally varying sediment rate at the catchment outlet. The SCS-CN method developed originally for rainfall-runoff modelling has not witnessed many applications in the field of soil erosion and sedimentation. A critical diagnosis of the review of literature on SCS-CN based sediment yield shows that the coupling of the USLE and RUSLE model with the SCS-CN method has significant practical utility. Therefore, it is quite obvious that the structural inconsistencies in the existing SCS-CN models may propagate through the sediment yield models based on it, thereby leading to inaccurate results of sediment yield estimation. Though it is of vital concern in hydrological applications, no previous study is found to have addressed this issue meticulously. Hence, efforts should be

made towards the rectification of these structural anomalies associated with SCS-CN method for accurate estimation of runoff and sediment yield.

Environmental Flow

The assessment of Environmental flow is very important for the survival of the healthy ecosystem. The review of literature diagnoses the methods developed for the assessment of environmental flow condition of the catchment. It is quite difficult to estimate the environmental flow condition using hydrological methods in ungauged catchments. Therefore, it is essential to develop a methodology which can be used for the assessment of EF condition of a catchment using other more easily available data, such as rainfall. Very few studies have been carried out recently to link the EF condition with the easily available rainfall data only. However, the intermediate processes undergoing between precipitation and streamflow play a major role in the hydrological cycle. These processes are significantly dependent on the surface characteristics of the catchment. Therefore, it is crucial to develop a method to establish a relationship between EF and the catchment surface characteristics, which can be instrumental for the ungauged catchments. No previous study has linked the eco-hydrological conditions (characterized by EF) with hydro-meteorological conditions of a catchment.



CHAPTER 3

STUDY AREA AND DATA COLLECTION

This chapter discusses the study area and data used to address various objectives of this research study. The present research work aims at an improved S-CN relationship to address the abnormality in watersheds behavior (i.e., complacent, standard, and violent). The accuracy of models is largely determined by the availability and quality of the hydrologic and sediment yield data used for calibration.

3.1 DESCRIPTION OF WATERSHEDS AND DATA COLLECTION

The S-CN mapping relationship has been improved and subsequently this improved relation used to propose a simplified CN-P relationship for describing the watershed behavior as complacent, standard, and violent. The study area and data used for this work are described here.

3.1.1 West Donaldson Creek Watershed

West Donaldson Creek watershed is situated in the Malheur National Forest, Oregon, draining an area of 3.9 km². This analysis uses the rainfall-runoff data from the study of Hawkins (1993). From literature, these data were collected by United State Department of Agriculture (USDA) from the Malheur National Forest watershed, Oregon during 1979 to 1984. In total 44 storm events were collected and the range of rainfall occurred in that area was between 58.42 to 1.06 mm/day. Background of data collection from the watersheds is given in Higgins et al. (1989).

3.1.2 Coweeta watershed

The Coweeta watershed is located about 80 miles southwest of Asheville, North Carolina, in the Nantahala Mountains. The data were collected by the Coweeta Hydrologic Laboratory under United State Department of Agriculture- United State Forest Services (USDA-USFS), it is in the Nantahala Mountain Range of western North Carolina, USA within the Blue Ridge Physiographic Province, near the southern end of the Appalachian Mountain chain (latitude 35°03' N, longitude 83°25'W). The watershed (drainage area = 12.1 ha) having climate humid temperate to humid sub-tropical. The average annual rainfall of the catchment is 1700 mm and its occurrence is distributed uniformly over the year. The 793 storms data were reported in literature during the period of 1945 to 1976. This data set was also used by Hawkins (1993).

3.1.3 Berea watershed

The Berea watershed in Kentucky, which is 116.1 ha (287 acres) in size, is located in hardwood forest. The data set includes 84 rainfall events greater than 23 mm (0.91 in.) during the period of 1966 to 1975. The data used in present study were taken from Hawkins (1993).

The applicability of suggested approach was tested using field data and data available in literature. The proposed models were tested on the data of (a) Strange Table, (b) 35 US based watersheds, (c) Tehri watershed India, and (d) experimental plot of Department of Water Resources Development and Management, Indian Institute of Technology Roorkee. The data of last watershed was observed under a research and development project sponsored by the Ministry of Water Resources, River Development and Ganga Rejuvenation.

3.1.4 Strange tabular data

The data of Strange Table has been taken directly from the text of Engineering Hydrology (Subramanya, 2013). The rainfall-runoff data of bordered areas of Maharashtra and Karnataka were used by Strange (1982). Strange classified three types of watershed according to magnitudes of runoff yield generated. The details of data are given in Table 3.1 and this table is also available in appendix table A6.

Table 3.1. Strange data of total monsoon rainfall and estimated percent runoff coefficients.

Total monsoon rainfall (in)	Total monsoon rainfall (mm)	Percent runoff coefficient			Total monsoon rainfall (in)	Total monsoon rainfall (mm)	Percent runoff coefficient		
		Good catchment	Average catchment	Bad catchment			Good catchment	Average catchment	Bad catchment
1.0	25.4	0.1	0.1	0.1	31.0	787.4	27.4	20.5	13.7
2.0	50.8	0.2	0.2	0.1	32.0	812.8	28.5	21.3	14.2
3.0	76.2	0.4	0.3	0.2	33.0	838.2	29.6	22.2	14.8
4.0	101.6	0.7	0.5	0.3	34.0	863.6	30.8	23.1	15.4
5.0	127.0	1.0	0.7	0.5	35.0	889.0	31.9	23.9	15.9
6.0	152.4	1.5	1.1	0.7	36.0	914.4	33.0	24.7	16.5
7.0	177.8	2.1	1.5	1.0	37.0	939.8	34.1	25.5	17.0
8.0	203.2	2.8	2.1	1.4	38.0	965.2	35.3	26.4	17.6
9.0	228.6	3.5	2.6	1.7	39.0	990.6	36.4	27.3	18.2
10.0	254.0	4.3	3.2	2.1	40.0	1016.0	37.5	28.1	18.7
11.0	279.4	5.2	3.9	2.6	41.0	1041.4	38.6	28.9	19.3
12.0	304.8	6.2	4.6	3.1	42.0	1066.8	39.8	29.8	19.9
13.0	330.2	7.2	5.4	3.6	43.0	1092.2	40.9	30.6	20.4

14.0	355.6	8.3	6.2	4.1	44.0	1117.6	42.0	31.5	21.0
15.0	381.0	9.4	7.0	4.7	45.0	1143.0	43.1	32.3	21.5
16.0	406.4	10.5	7.8	5.2	46.0	1168.4	44.3	33.2	22.1
17.0	431.8	11.6	8.7	5.8	47.0	1193.8	45.4	34.0	22.7
18.0	457.2	12.8	9.6	6.4	48.0	1219.2	46.5	34.8	23.2
19.0	482.6	13.9	10.4	6.9	49.0	1244.6	47.6	35.7	23.8
20.0	508.0	15.0	11.3	7.5	50.0	1270.0	48.8	36.6	24.4
21.0	533.4	16.1	12.0	8.0	51.0	1295.4	49.9	37.4	24.9
22.0	558.8	17.3	12.9	8.6	52.0	1320.8	51.0	38.2	25.5
23.0	584.2	18.4	13.8	9.2	53.0	1346.2	52.1	39.0	26.0
24.0	609.6	19.5	14.6	9.7	54.0	1371.6	53.3	39.9	26.6
25.0	635.0	20.6	15.4	10.3	55.0	1397.0	54.4	40.8	27.2
26.0	660.4	21.8	16.3	10.9	56.0	1422.4	55.5	41.6	27.7
27.0	685.8	22.9	17.1	11.4	57.0	1447.8	56.6	42.4	28.3
28.0	711.2	24.0	18.0	12.0	58.0	1473.2	57.8	43.3	28.9
29.0	736.6	25.1	18.8	12.5	59.0	1498.6	58.9	44.4	29.4
30.0	762.0	26.3	19.7	13.1	60.0	1524.0	60.0	45.0	30.0

3.1.5 Tehri Watershed

Tehri watershed (area = 7295 sq. km) is located in Tehri-Garhwal district of Uttarakhand State in India. It lies between 77° 22'28" and 79° 24' 57"E longitude and between 30° 17' 19" and 31° 18' 52"N latitude (Fig. 3.1). The Tehri Dam Project is located in Bhagirathi River a major tributary of River Ganga, about 80 km upstream from Rishikesh in Garhwal District of the newly formed northern State of Uttarakhand. River Bhagirathi originates from Gangotri glacier at an altitude of 7,010 meters and traverses about 200 kilometers to its confluence with Bhilganga, where Asia's second tallest Tehri Dam is walled up.

The main Tehri Dam is engineered with earth and rock material in a unique height of 261 m, making it the 8th highest in the world. In Tehri Dam, the earthen core is centrally located with flatter sloping sections and is separated from the rock material with well graded filters on both sides. Rainfall varies from 1500-2000 mm and variation of temperature is 0-36°C. topography is of mixed type. Ten daily rainfall-runoff-sediment yield data were available for the period 2003-11. These data were used for rainfall-runoff analysis. The location map of Tehri watershed is presented in Fig. 3.1.

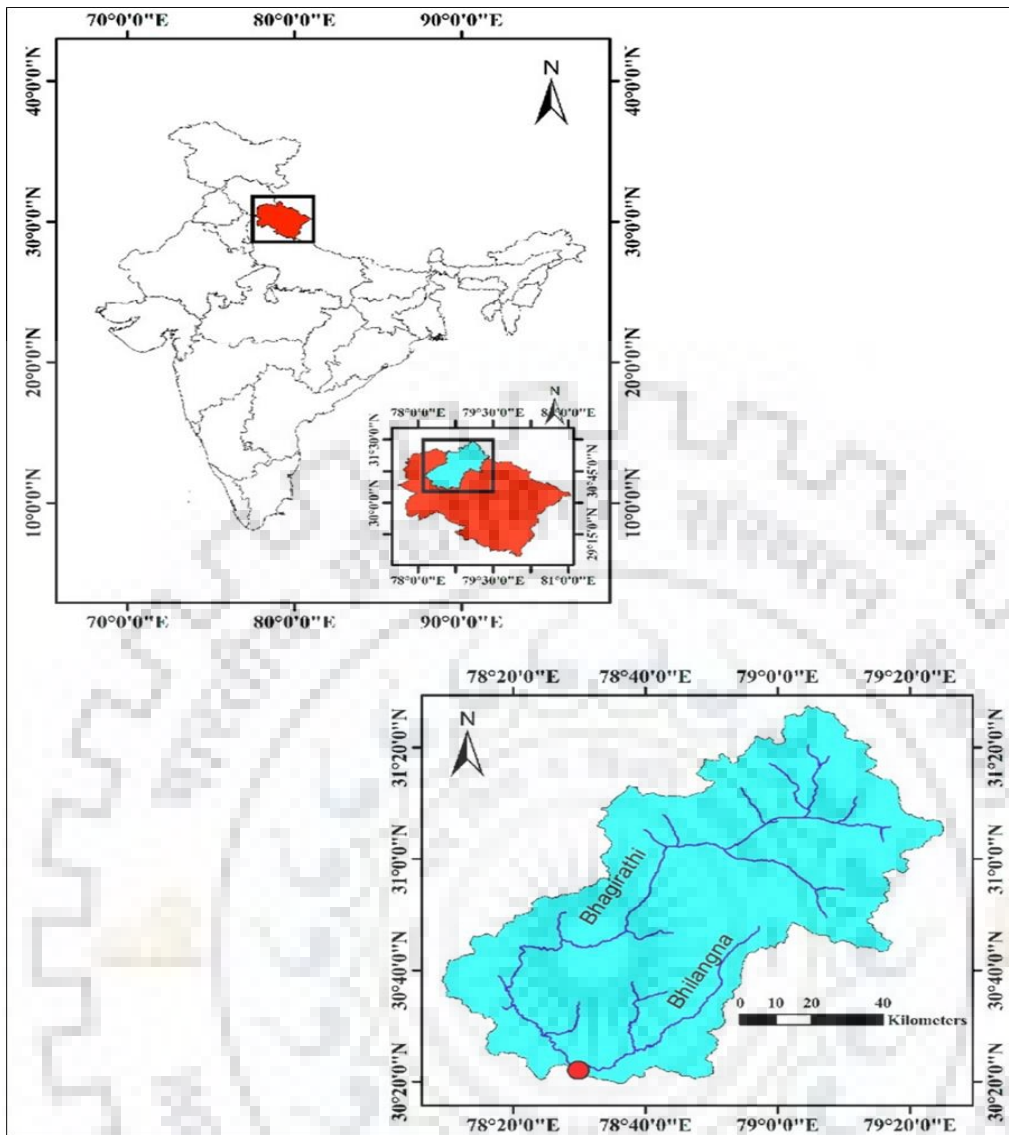


Figure 3.1: Location map of Tehri watershed

3.2 EXPERIMENTAL PLOTS/WATERSHEDS

The experimental farm is located at $29^{\circ} 50' 09''$ N and $77^{\circ} 55' 21''$ E at Toda Kalyanpur, Roorkee, district Haridwar of Uttarakhand State (India) (Fig. 3.2). The elevation of study site is about 262 m. The climate is sub-tropical humid type with three pronounced seasons, summer, monsoon and winter. Extreme variation in summer and winter temperatures can be seen in the study area. The period of summer season is late March to mid-June where the variation in maximum and minimum monthly temperatures is 45°C and 20°C , respectively. Similarly, the winter season starts from late November to February last where maximum and minimum monthly temperatures are 18°C and 10°C , respectively. The monsoon season starts from mid-June and continues till first week of September, during which about 75% of average annual rainfall (about 1100 mm) is

received. The average humidity varies from 30 - 100% and potential evapotranspiration is of the order of 1300 mm.

For data collection, the plots of size 12 m length and 3 m width having three land uses: Maize, finger millet and Fallow land and three slopes (8%, 12% and 16%) were developed. Three plots of each bed slope has been made for different land use condition. The crops maize and finger millet shown in two plots while the third is kept as fallow land for each type of the bed slope to estimate the runoff and sediment yield. Further in this study the soil sieve analysis has been done along with the estimation of infiltration capacity, bulk density, particle density and porosity of the soil were tested in departmental laboratory. The experimental work was carried out during 2016-2017. The observed rainfall, runoff, soil moisture, sieve analysis and double ring infiltrometer test data are given in appendix.

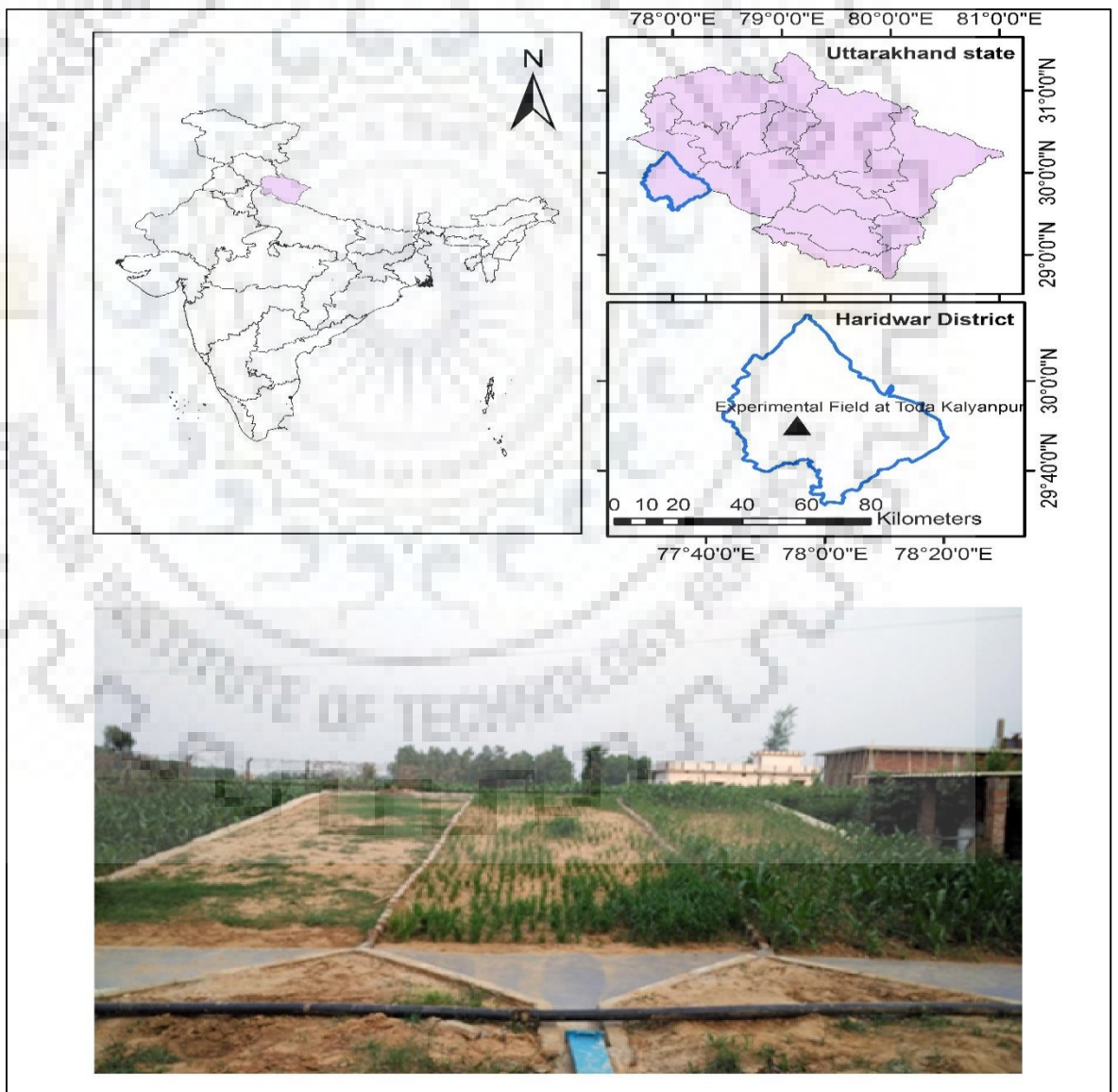


Figure 3.2. Location map of experimental area.

3.2.1 Experimentations with Artificial Rainfall

After the monsoon season, similar experiments were conducted using artificial rainfall to each plot (Fig. 3.3). Four type of nozzle were used for generation of rainfall. Nine nozzle slots were made in a 12 meter galvanized Iron pipe and distance between slots is 1.25 meter. This pipe heled 5 meter above the ground surface with help of three 7 meter rectangular cast iron pipes (pipe size 2.5 inch). A pulley system made in one end of pipe for up and down of nozzle pipe line. Nine 7 meter rectangular pipe were made to increase the frequency of experiments. Middle of each plots place three rectangular pipe were placed and hang nozzle pipe and start the experiment. Experimental setup and running experiment are shown in figure 3.4. Each experiment was performed in every plot for 20 min duration and runoff measured in collection chamber. Rainfall was measured in fallow land of each slop each experimental day with help of non-recording rain gauge and plastic jug. During each artificial rainfall experiment, the runoff collected in the tank was measured with the help of scale at the interval of each minute and final total runoff was also noted after experiment stop. For the measurement of suspended solid, the runoff sample was collected in one liter mineral water bottle and it was brought to department laboratory for oven drying and the sediment content was found out in the same procedure as conducted for natural rainfall-runoff event. The suspended solid was also found out with the help of suspended solid analyzer for each event time to time for the verification purpose. The analysis results for different land use and slope type of plots are given in Table 3.2.





Figure. 3.3: Experimental setup and running experiment

3.3 DATA USED FOR ENVIRONMENTAL FLOW MODELLING

By exploring relationship between CN, frequently used for runoff estimation, and Tennant concept, popularly used in environmental flow (EF) assessment, this study attempts to predict EF condition of a catchment using runoff curve number. Its application has been demonstrated using the data of 17 different catchments from the five river basins (Mahanadi basin, Mahi Basin, Godavari basin, Brahmani-Baitarni and Narmada basin) in India during low seasons. The description and drainage network of various study catchment are given below.

3.3.1 Study Catchments of Mahanadi Basin

Ghatora Catchment:

Arpa river, tributary of Mahanadi River, rises in the Plateau of Pendra-Lormi located in Khodri ranges near Bilaspur in Chhattisgarh, India. Traversing a length of 147 km, it flows through Balod Bazar and merges to the Seonath River near the place Thakur Deva. Its catchment (area = 3035 km²) at Ghatora (elevation = 246 m.) lies between 22^o 2' & 22^o 46' latitudes north and 81^o 36' & 82^o 26' east longitudes. The region receives average annual rainfall of 1320 mm and having sub-tropical and sub-humid climatic condition. The drainage network of the watershed is presented in Figure 3.4.

Rampur Catchment:

Jonk river, tributary of Mahanadi River, originates in Sundabeda plateau and enters Maraguda valley located in Naupada district in Odisha, India. The river flows through the Raipur district and traverse a distance of 588 km before it merges in Mahanadi at Sheorinarayan. The catchment area at Rampur (elevation=231 m) is estimated about 2920 km². The climate of the catchment is sub-humid with 1160 mm of annual rainfall. The region consists of tropical vegetation. The drainage network of the watershed is presented in Figure 3.4.

Baronda Catchment:

River Pairi is the tributary of Mahanadi River and it merges into Mahanadi near Rajim, Chhattisgarh. The drainage area of the catchment is 3225 Km². The catchment has spatial extent varies from latitude 20⁰ 00' to 20⁰ 40' N and longitude 81⁰ 40' to 82⁰ 40' E. The catchment receives annual rainfall of 1150 with sub-tropical climatic condition. Major portion of the catchment is located in Raipur district Chhattisgarh. The drainage network of the watershed is presented in Figure 3.4.

Basantpur Catchment:

The river Mahanadi rises in Pharsiya village at an elevation of 442 m above m.s.l. in Dhamtari, Chhattisgarh. Seonath, Jonk, Hasdeo, Ong, Mand and Pairi rivers are the major tributaries of Mahanadi. The river flows through a distance of 562 Km up to Basantpur gauging site (elevation = 206 m). The catchment (area = 57,780 Km²) has spatial extent varies from latitude 20⁰ 30' to 23⁰ 30' N and longitude 80⁰ 00' to 84⁰ 00' E. The catchment receives annual rainfall of 1180 with sub-tropical climatic condition. The major portion of the catchment is located in Bilaspur, Korba, Mahasmand, Raipur and Durg districts. The drainage network of the watershed is presented in Figure 3.4.

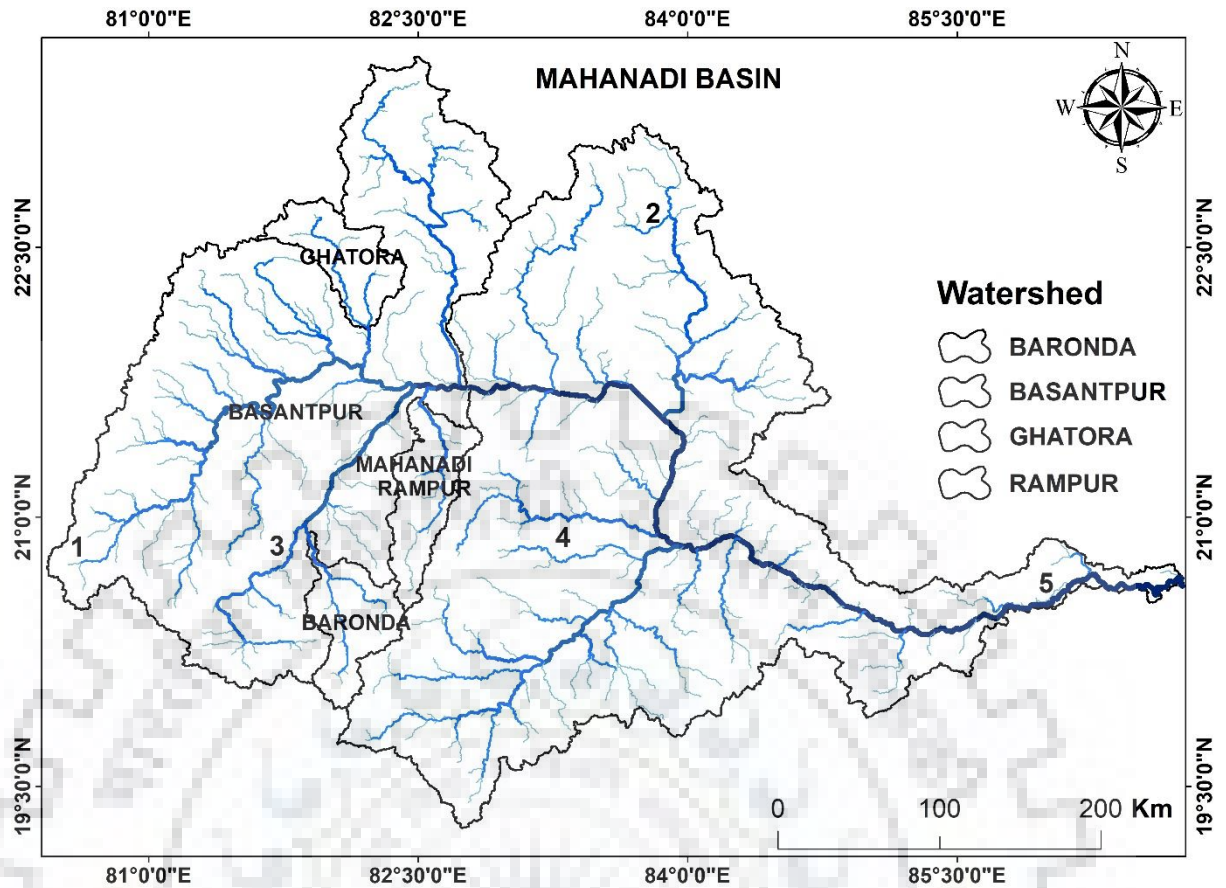


Figure 3.4 Drainage network of the study catchments of Mahanadi basin

3.3.2 Study Catchments of Mahi Basin

Chakaliya Catchment:

River Anas is tributary of Mahi river. It originates at an altitude of 450 m above mean sea level (m.s.l) near Kalmora, Madhya Pradesh. The river flows through a distance of 24 Km upto Chakaliya gauging site (elevation = 215 m) in Panchmahal district of Gujarat. The catchment (area = 3121 Km²) has spatial extent range from latitude 22^o 30' to 23^o 10' N and longitude 74^o 00' to 74^o 50' E. The major portion of catchment is located in Jhabua district of Madhya Pradesh. The region receives the average precipitation of 900 mm annually, in which 80% of precipitation occurs during monsoon. The drainage network of the watershed is presented in Figure 3.5.

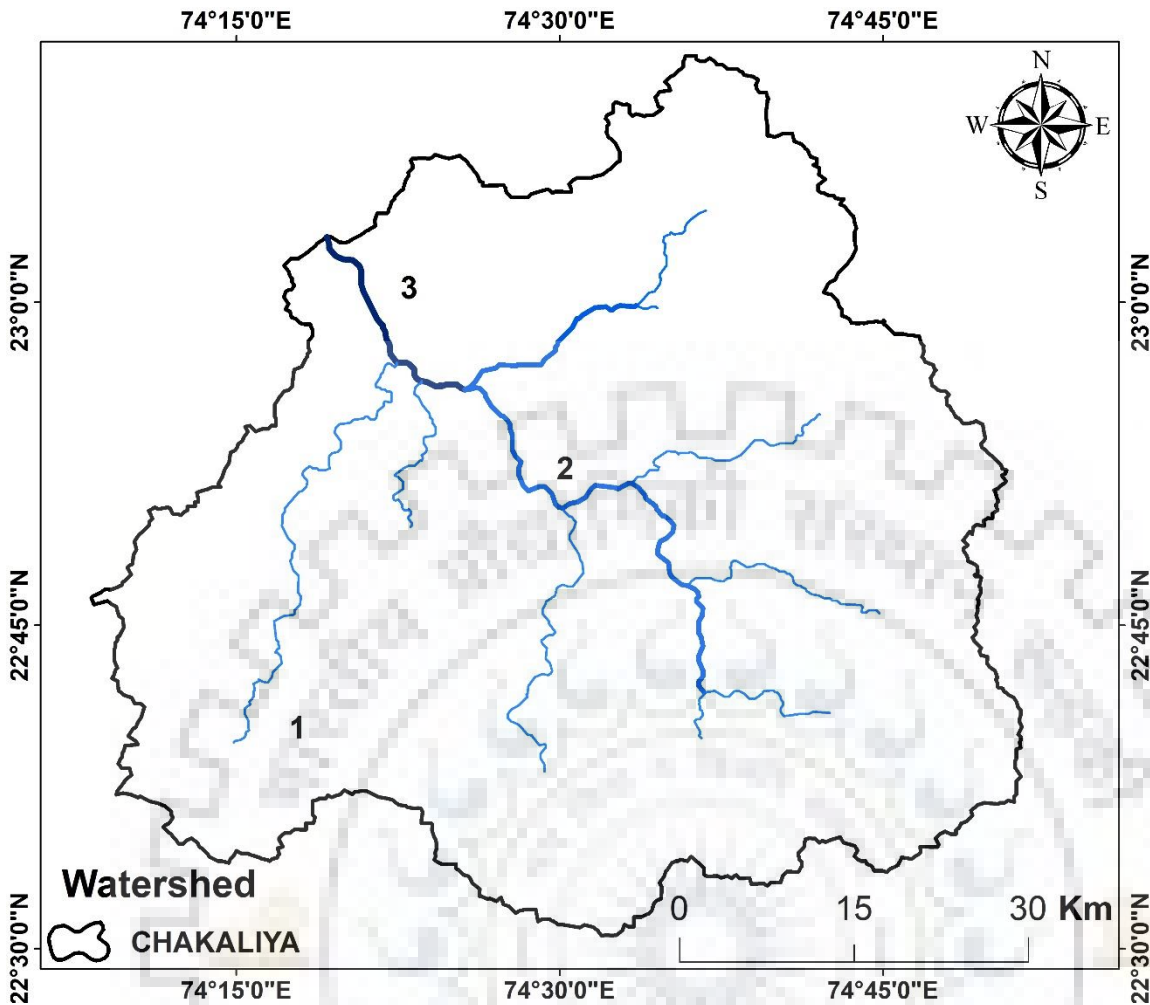


Figure 3.5 Drainage network of Chakaliya watershed

Dhariawad Catchment:

Jakhm river is the tributary of River Mahi and rises in Jakhamia village in Chittorgarh, Rajasthan. The river drains the area of 1510 Km² up to Dhariawad gauging site (elevation = 203 m). River traverse through a length of 70 Km up to Dhariawad gauging site. The catchment has spatial extent range from latitude 24⁰ 00' to 24⁰ 20' N and longitude 74⁰ 20' to 74⁰ 50' E. The region receives the average precipitation of 710 mm anually, in which 80% of precipitation occurs during monsoon. The catchment has semi-arid climatic condition. The drainage network of the watershed is presented in Figure 3.6.

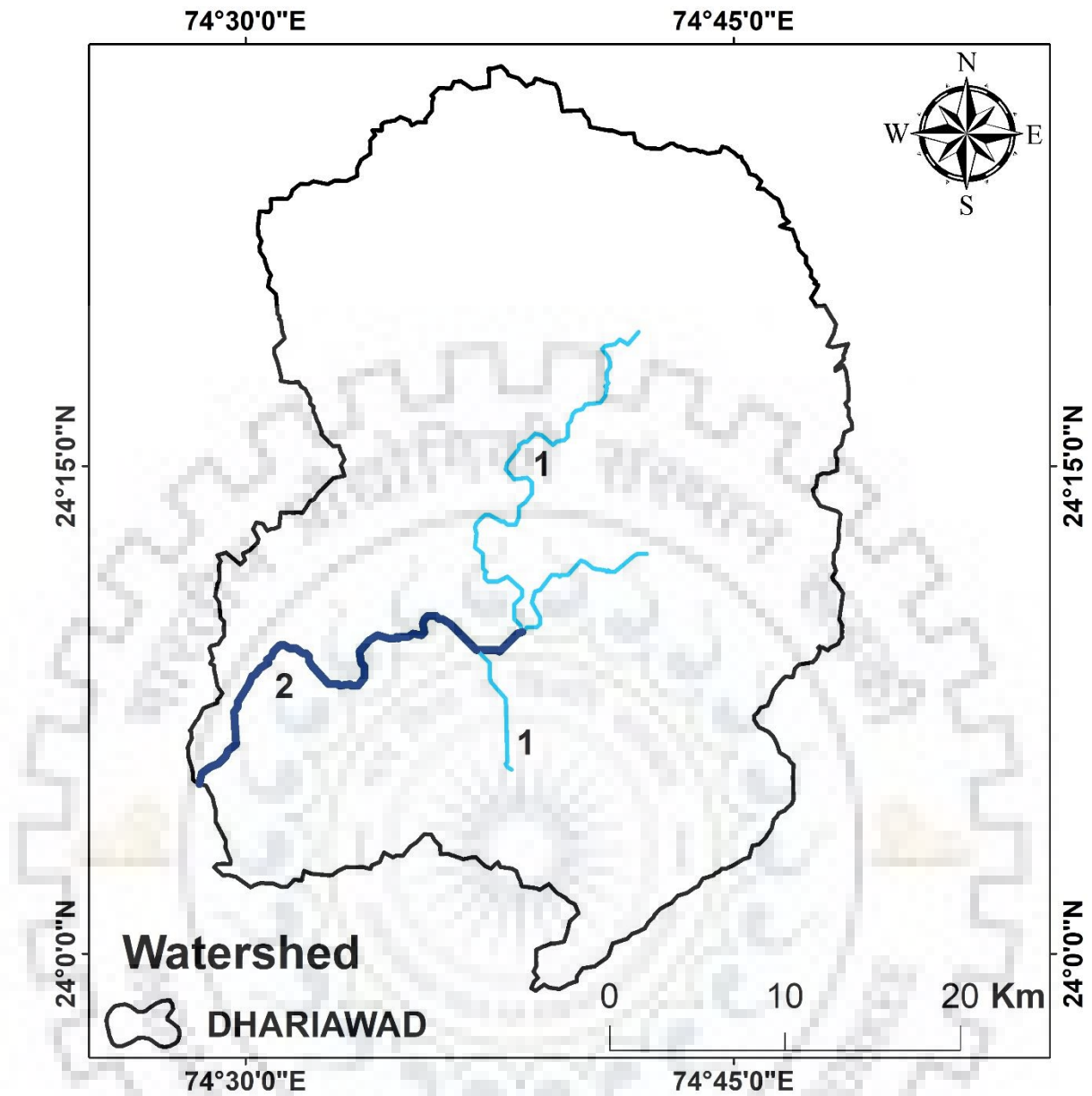


Figure 3.6 Drainage network of Dhariawad watershed

3.3.3 Study Catchments of Godavari Basin

Hivra Catchment:

It is a catchment of Wardha River, sub-tributary of Godavari River, originating in Satpura range in village khairwani (elevation = 777 m) in Madhya Pradesh. The spatial extent of catchment (area = 10240 km²) at Hivra (altitude = 230 m.) ranges from 20° 21' & 21° 52' latitudes north and 77° 25' & 78° 45' east longitudes. The catchment has tropical climatic condition with 1020 mm of annual rainfall. The drainage network of the watershed is presented in Figure 3.7.

Jagdalpur Catchment:

The river Indravathi, tributary of Godavari river, rises in Dhandakaranya range at an elevation of 914 meters located in Kalahandi district of Odisha. It traverse the length of 166 km up to Jagdalpur gauging site (elevation = 543 m) and covers the drainage area of 7380 km². The average annual precipitation of the region is 1220 mm with tropical climatic condition. The drainage network of the watershed is presented in Figure 3.7.

Nandgaon Catchment:

It is a catchment of Wunna river (sub-tributary of Godavari river) originating in Wardha, Maharashtra at 496 m above msl. The river flows through distance of 110 km up to Nandgaon gauging site (altitude =198 m). The spatial extent of catchment ranges from 21⁰ 58' & 23⁰ 05' latitudes north and 82⁰ 50' & 83⁰ 34' east longitudes, draining 4580 km² area. The catchment has tropical climatic condition, receiving average annual rainfall of 1060 mm. The drainage network of the watershed is presented in Figure 3.7

Penganga Catchment:

Penganga river, sub-tributary of Godavari river rises in Ajantha ranges in Aurangabad district of Maharashtra. It is the major river of Yavatmal district. The river covers the drainage area of 18441km² up to P.G. Bridge (elevation=198m) gauging site. The catchment has sub-tropical climate and 1015 mm of annual rainfall. The region has good cultivation of cotton and wheat. The drainage network of the watershed is presented in Figure 3.7

Ramakona Catchment:

Kanhan River (tributary of river Wainganga and sub-tributary of river Godavari), originates at 336 m above msl in Satpura range, Madhya Pradesh. The river drains 2500 km² area up to the gauging site at Ramakona. The catchment has 1080 mm of annual precipitation and tropical and subtropical wet and dry climate. The drainage network of the watershed is presented in Figure 3.7.

Satrapur Catchment:

It is catchment of the river Kanhan (tributary of river Wainganga), originates at 336 m above msl in Satpura range, Madhya Pradesh. The river drains 11100 km² area up to the gauging site at Satrapur. The catchment has 1110 mm of annual precipitation and tropical savannah climate. The drainage network of the watershed is presented in Figure 3.7

Ashti Catchment:

The river Wainganga, tributary of Pranhita river and sub-tributary of river Godavari has origination point at an altitude of 1048 m in Mundara village (Satpura range), Madhya Pradesh, India. The catchment has large spatial extent range from latitude $20^{\circ} 00'$ to $22^{\circ} 40'N$ and longitude $77^{\circ} 20'$ to $81^{\circ} 20' E$. The drainage area of the river up to discharge measurement site at Ashti (elevation=289 m) is 50,990 km². The major portion of the catchment is located Gadchiroli, Gondiya and Nagpur districts of Maharashtra. The catchment has sub-tropical climatic condition with 1110 mm of annual precipitation. The drainage network of the watershed is presented in Figure 3.7.

Bhatpalli Catchment:

It is catchment of river Peddavagu which is tributary of Pranhita river and sub-tributary of River Godavari. The catchment has an area of 3100 Km² and spatial extent range from latitude $19^{\circ} 10'$ to $19^{\circ} 40' N$ and longitude $78^{\circ} 40'$ to $79^{\circ} 30' E$. The catchment has sub-humid climatic condition with 1070 mm of annual precipitation. The major part of the catchment lies in Adilabad, Telangana. The drainage network of the watershed is presented in Figure 3.7.

Bamini Catchment

Wardha river is tributary of Pranhita river and sub tributary of Godavari river. The origination point of river is in Satpura range in village khairwani (elevation = 777 m) in Madhya Pradesh. The spatial extent of the catchment (area = 46020 Km²) varies from latitude $19^{\circ} 20'$ to $21^{\circ} 20' N$ and longitude $76^{\circ} 00'$ to $79^{\circ} 20' E$. The catchment has annual rainfall of 1000 mm with tropical climatic condition. The major portion of catchment is falls in Wardha, Yavatmal and Nagpur districts. The drainage network of the watershed is presented in Figure 3.7.

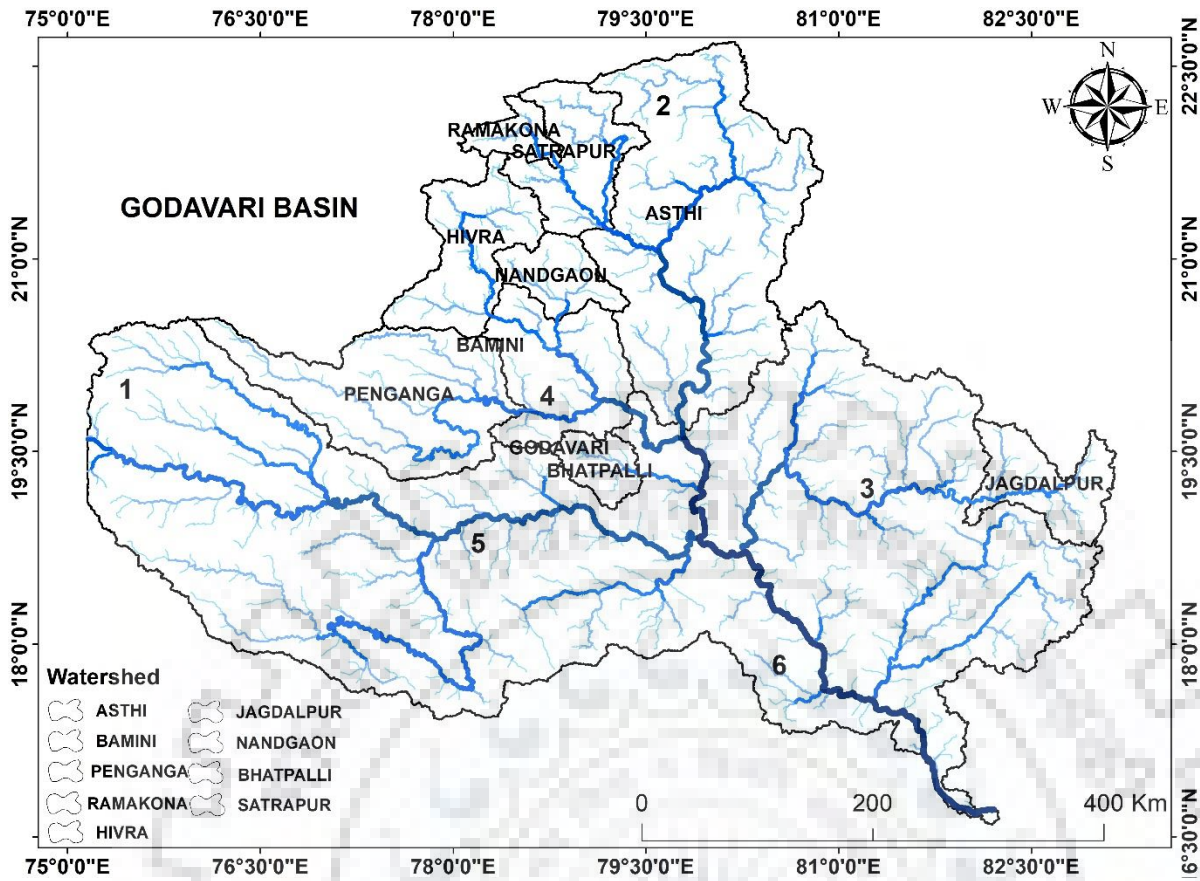


Figure 3.7 Drainage network of the study catchments of Godavari basin

3.3.4 Study Catchments of Brahmani-Baitarini Basin

Jenapur Catchment

The river Brahmani is formed by the confluence of Sankh and koel rivers and flows through the various districts of Odisha. It is the major seasonal river in Odisha. The catchment area of the river up to Jenapur gauging site is 33,955 Km². The spatial extent of the catchment varies from latitude 20⁰ 40' to 23⁰ 20' N and longitude 83⁰ 20' to 86⁰ 40' E. The catchment has annual rainfall of 1400 mm with sub-humid climatic condition. Major part of the catchment falls in Jajpur, Kendujhar and Dhenkenal districts. The drainage network of the watershed is presented in Figure 3.8.

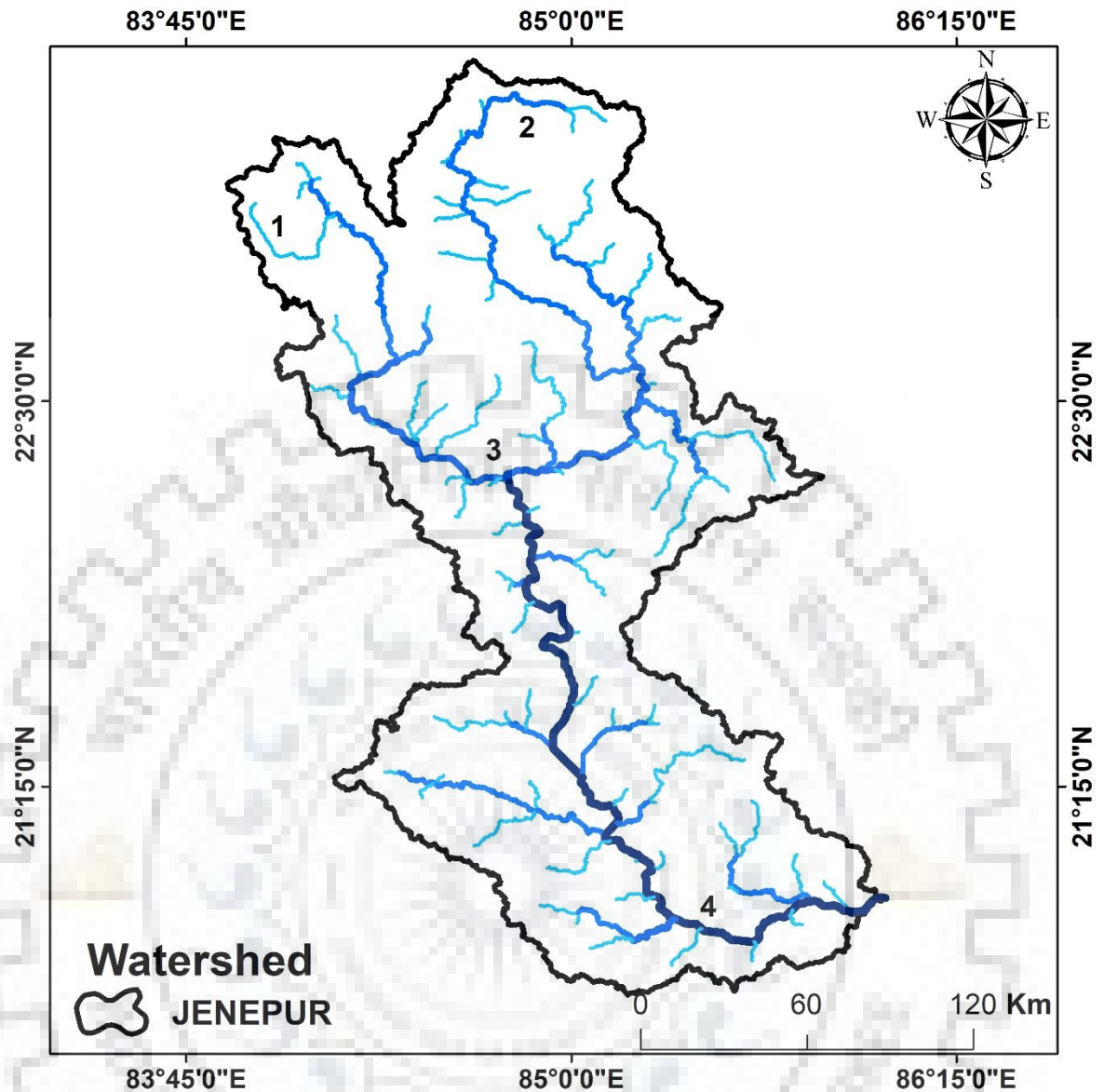


Figure 3.8 Drainage network of Jenapur watershed

3.3.5 Study Catchments of Narmada Basin

Kogaon Catchment:

Kunda river is tributary of River Narmada. The river flows through a distance of 108 Km up to Kogaon gauging site. The catchment (area = 3919 Km²) has spatial extent varies from latitude 21° 30' to 22° 10' N and longitude 75° 20' to 76° 10' E. The catchment has annual rainfall of 715 mm with semi-arid climatic condition. A larger portion of catchment falls in Khargone district Madhya Pradesh. The drainage network of the watershed is presented in Figure 3.9.

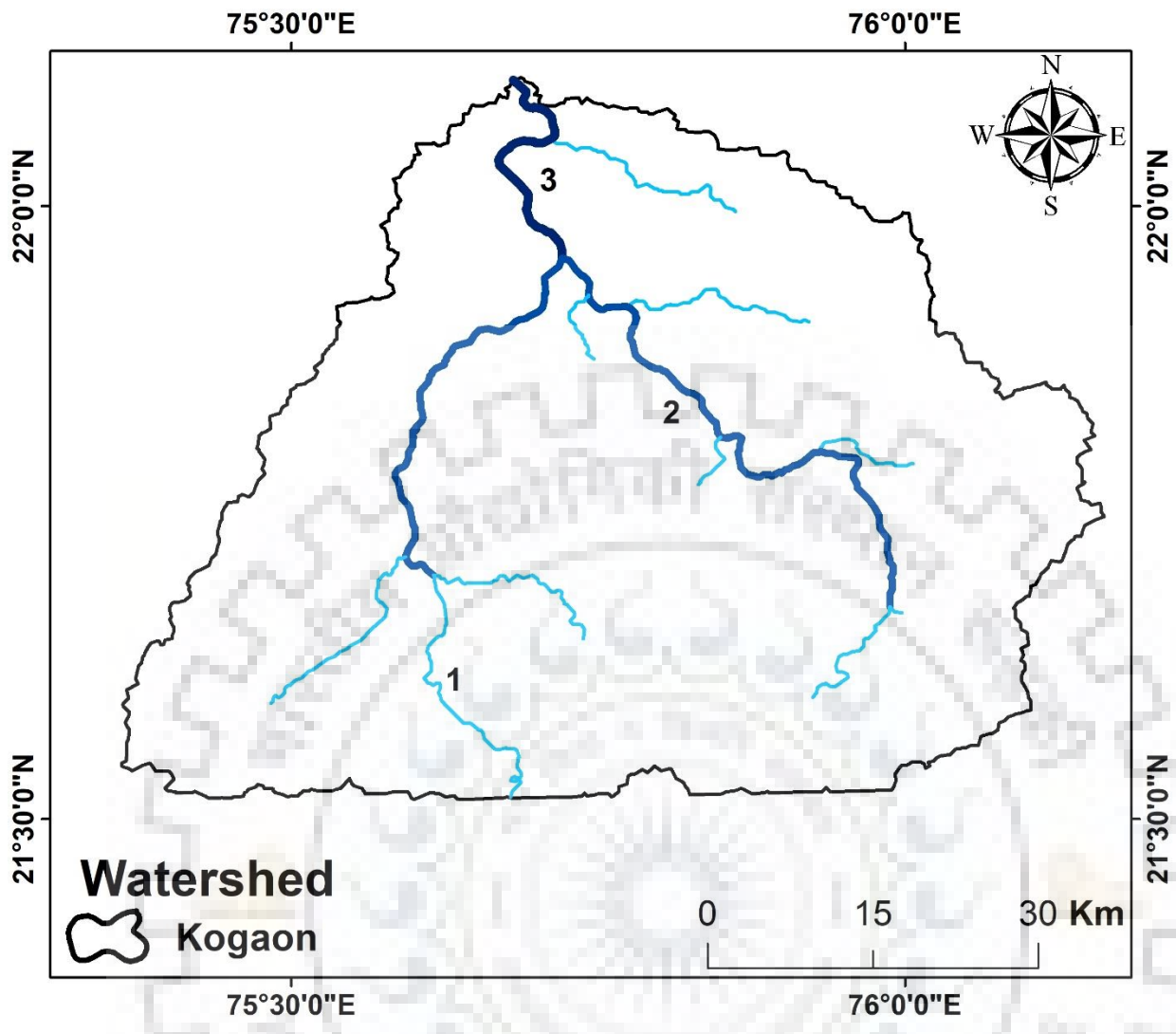


Figure 3.9 Drainage network of Kogaon watershed

4.1 INTRODUCTION

There are many components in hydrologic cycle are interconnected, in which surface runoff connects precipitation to various water. The part of precipitation that not infiltrate into the soil and flow across the land through various networks such as rivers, streams, lakes etc. is surface runoff (Perlman, 2016). The runoff varies space and time. Generally, one-third part of total precipitation falls on the earth becomes runoff, while the remaining part is either returned to the atmosphere through evapotranspiration or move into the soil through infiltration (Perlman, 2016).

The major factors over which the magnitude of surface runoff depends are rainfall characteristics (i.e. intensity, amount and duration), slope, LULC, vegetation and soil properties. The combination two mechanisms (i.e. saturation-excess and infiltration-excess) results in the generation of runoff (Yang et al., 2015). Saturation excess occurs when the soil gets fully saturated with water and thus, the surplus rainfall converts to overland flow as it can't be held in the soil (Johnson et al., 2003; Aksoy & Kavvas; 2005). Infiltration-excess occurs when the rainfall intensity exceeds the infiltration capacity so that excess water turns out to be overland flow (Yang et al., 2015).

The surface runoff estimation is very important for the evaluation of water yield potential of a catchment, planning strategies for soil and water conservation, sediment reduction, and hazards due to flooding at downstream. Although a large number of models are used to estimate the direct surface runoff from storm rainfall. The calibration and intensive data requirement in most of the models limits their application. Thus, the simple models with less input data and clearly stated assumptions should be used for management decisions (Grayson et al., 1992 and Shi et al., 2009). The SCS-CN method is widely applied to compute the direct runoff from a particular storm event for small catchments. Owing to its simplicity and lesser requirements of input data, numerous hydrological models viz., CREAMS (Knisel, 1980), AGNPS (Young et al., 1989), EPIC (Sharpley and Williams, 1990), and SWAT (Arnold et al., 1996) employ this methodology. Its wider applicability can be largely attributed to its inherited multi-facet characteristics such as convenience, simplicity, use of major runoff producing watershed properties, broad acceptability,

and remarkable foundation as well as institutional momentum for this technique within Natural Resource Conservation Service (NRCS) (Garen and Moore, 2005).

Despite widespread use of the SCS-CN methodology, accurate estimation of parameter CN has been a topic of much discussion and concern among hydrologists since its inception in 1956 (Hawkins, 1978; Hawkins, 1993; Chen, 1982; Bonta, 1997; and Mishra and Singh, 2006). These CNs are found to vary with soil type, land use/treatment classes, hydrologic soil group, hydrologic condition, and the antecedent moisture condition (AMC) as given in NEH-4 Table. According to Hawkins (1975), the errors in CN may have much more serious effects on runoff calculation than do similar levels of error in the storm rainfall P . When CNs are calculated from real storm data (a usual procedure), a secondary relationship almost always emerges between a CN and the storm rainfall depth and this variation lead to the classification of the watersheds' behavior as 'standard', 'violent,' and 'complacent' (Hawkins, 1993). In the complacent behavior, the observed CN declines steadily with increasing rainfall depth, and evidences no appreciable tendency to achieve a stable value. In case of 'standard' behavior, the observed CN declines with increasing storm size, as in the complacent situation, but the CNs approach and/or maintain a near-constant value with increasingly larger storms. In case of 'violent' behavior, the observed CNs rise suddenly and asymptotically approach an apparent constant value. Hawkins (1993) attributed this abnormality to the secondary systematic correlation between the calculated CN value and the rainfall depth.

The runoff coefficient (C) and the runoff curve number (CN) are both expressions of the relative rainstorm response characteristics of watersheds (McCuen and Bondelid, 1981 and Hawkins, 1983). It is of common experience that the runoff coefficient (C), which is the ratio of direct surface runoff (Q) to rainfall (P), increases with increasing P , and vice versa (Subramanya, 2013). Furthermore, for a given amount of rainfall, as C increases, CN also increases, and vice versa. Thus, both C and CN behave similarly. In other words, CN should increase with P as does C . Notably, while describing the behavior of watersheds as complacent or standard, it has been found that CN decreases with an increase in storm size (P) whereas the violent watersheds exhibit sudden increase in CN with an increase in P .

In the light of the above, in this chapter, an attempt has been made to rectify the contrasting behavior of the watersheds by proposing a structural modification to the S-CN mapping relationship using proportional equality (Mishra and Singh, 2003) of the SCS-CN methodology.

4.2 METHMATIONAL FORMULATION

4.2.1 SCS-CN Methodology

The SCS-CN model is based on the water balance equation and two fundamental hypotheses. The first hypothesis equates the $Q/(P - I_a)$ ratio to the F/S ratio whereas, the second hypothesis relates I_a and S . These are expressed, respectively, as:

$$P = I_a + F + Q \quad (4.1a)$$

$$\frac{Q}{(P - I_a)} = \frac{F}{S} \quad (4.1b)$$

$$I_a = \lambda S \quad (4.1c)$$

The existing SCS-CN method assumes λ equal to 0.2 for routine practical applications. However, λ may range from 0 to ∞ , as I_a accounts for interception, evaporation, surface storage and infiltration before runoff begins (Mishra and Singh, 2004).

Combining Eqs. 4.1a&b, the expressions for Q can be derived as follows:

$$Q = \frac{(P - I_a)^2}{P - I_a + S} \quad ; \quad \text{for } P > I_a, Q = 0, \text{ otherwise} \quad (4.2a)$$

Eq. 4.2a, which is Model 1 is the general form of the SCS-CN methodology. For $\lambda = 0.2$, the coupling of Eqs. 4.1c & 2a results as:

$$Q = \frac{(P - 0.2S)^2}{P + 0.8S} \quad (4.2b)$$

Eq. (4.2b), which is Model 2, is the popular form of the existing SCS-CN methodology. The relationship between I_a - S (Eq. 4.1c) has been a topic of discussion among researchers worldwide. I_a was not a part of the SCS-CN model in its initial formulation. However, as the developmental stages continued, it was included as a fixed ratio of I_a to S (Plummer & Woodward, 2002). Aron et al. (1977) suggested $\lambda \leq 0.1$ and Golding (1979) provided λ values for urban watersheds as $\lambda = 0.075$ for $CN \leq 70$, $\lambda = 0.1$ for $70 < CN \leq 80$, and $\lambda = 0.15$ for $80 < CN \leq 90$. Hawkins et al. (2001) found a value of $\lambda = 0.05$ to better fit the data and therefore be more appropriate for use in runoff calculations. Mishra & Singh (1999) suggested λ to take any non-negative value and Mishra & Singh (2004) prescribed the applicability bounds for SCS-CN method as follows: for $\lambda \leq 0.3$, $I_a/P \leq 0.35$ and $C \geq 0.23$.

Since parameter S can vary in the range of $0 \leq S \leq \infty$, it is mapped onto a dimensionless curve number (CN) varying in a more appealing range $0 \leq CN \leq 100$ as:

$$S = \frac{100}{CN} - 10 \quad (S \text{ in inch}) \quad (4.3a)$$

and

$$S = \frac{25400}{CN} - 254 \quad (S \text{ in mm}) \quad (4.3b)$$

For a given set of event rainfall-runoff data, S can be determined from Eq. 4.2b as (Hawkins, 1993):

$$S = 5(P + 2Q - \sqrt{Q(4Q + 5P)}) \quad (4.4)$$

A value of $CN = 100$ represents $S = 0$, a condition of zero potential maximum retention, i.e. a completely non-abstracting impermeable watershed. Conversely, $CN = 0$ represents a theoretical upper bound to S ($= \infty$), i.e. an infinitely abstracting watershed. However, the practical design values validated by experience lie in the range (40, 98) (Van Mullem, 1989).

4.3 PROPOSED SCS-CN METHODOLOGY

The basic proportionality of the SCS-CN methodology has been modified structurally keeping in view the decreasing trend of S (or increasing trend of CN) with P that grows with time (Mishra and Singh, 2003), as shown in Fig. 4.1. It also eliminates the CN- P inconsistency (Fig. 4.1) and also obviates the use of I_a , a term that has been of concern since the inception of SCS-CN methodology. The modified version (designated as Model 3) can be derived as follows.

Following Mishra and Singh (2003a, b), the Horton's method (Horton 1932) can be expressed mathematically to relate F and S as:

$$\frac{F}{S} = (1 - e^{-\alpha t}) \quad (4.5)$$

where, t is the rainfall duration. Also, P is assumed to grow linearly with time t .

$$P = i_e t \quad (4.6)$$

This assumption is rational and valid for computing infiltration rate in experimental tests (Mishra and Singh 2004a, b). Here,

$$\frac{P}{S} = \alpha t \quad (4.7)$$

Substituting equation (4.6) into equation (4.7) leads to

$$Q = P(1 - e^{-P/S}) \quad (4.8)$$

Equation (4.8) representing the Mockus method (Mishra and Singh, 2003) can also be derived using the first-order linear hypothesis for the variation of S with time or rainfall as:

$$\frac{dS_t}{dt} = -\alpha S_t \quad (4.9)$$

It can be solved as

$$S_t = S_o e^{-\alpha t} \quad (4.10)$$

Or

$$S_t = S_o e^{-\alpha P} = S_p = S \quad (4.11)$$

for $S_t = S_o$ (or S in equation (4.11)) at $t = 0$ or $P = 0$. Here, α is another decay coefficient different from the earlier one. This means, for a given AMC, $S = S_o$ represents the potential maximum space available for moisture retention or the maximum possible amount of infiltration.

The proportional equality hypothesis (Eq. 4.1b) is re-written and revised as follows:

$$\frac{F(P - I_a)}{Q} = S = S_o e^{-\alpha P} \quad (4.12)$$

where S_o is the initial storage space (or absolute potential maximum retention) when $P = 0$, at the start of the event). The right hand side of Eq. 4.12 is consistent with the description of Mishra and Singh (2003) that the storage space actually decreases as rainfall grows with time. Taking I_a (an extraneous term) equal to zero, Eq. 4.12 can be reformulated as:

$$Q = \frac{P^2}{P + S_o e^{-\alpha P}} \quad (4.13)$$

which is the revised model formulation designated as Model 3. Further, Eq. 4.13 can be re-arranged as: Taking $I_a = \beta P$ (Ajmal, et al., 2015) and S_o as $(S_o - \beta P)$, Eqs. 4.13 can be further approximated as:

$$Q = \frac{(1 - \beta)^2 P^2}{(1 - \beta)P + (S_o - \beta P)e^{-\alpha P}} \quad (4.14)$$

which is Model 4, another formulation of Model 3 including I_a (designated as Model 4). Here, I_a parameter $1 \leq \beta \geq 0$, the other condition can be described similarly as above.

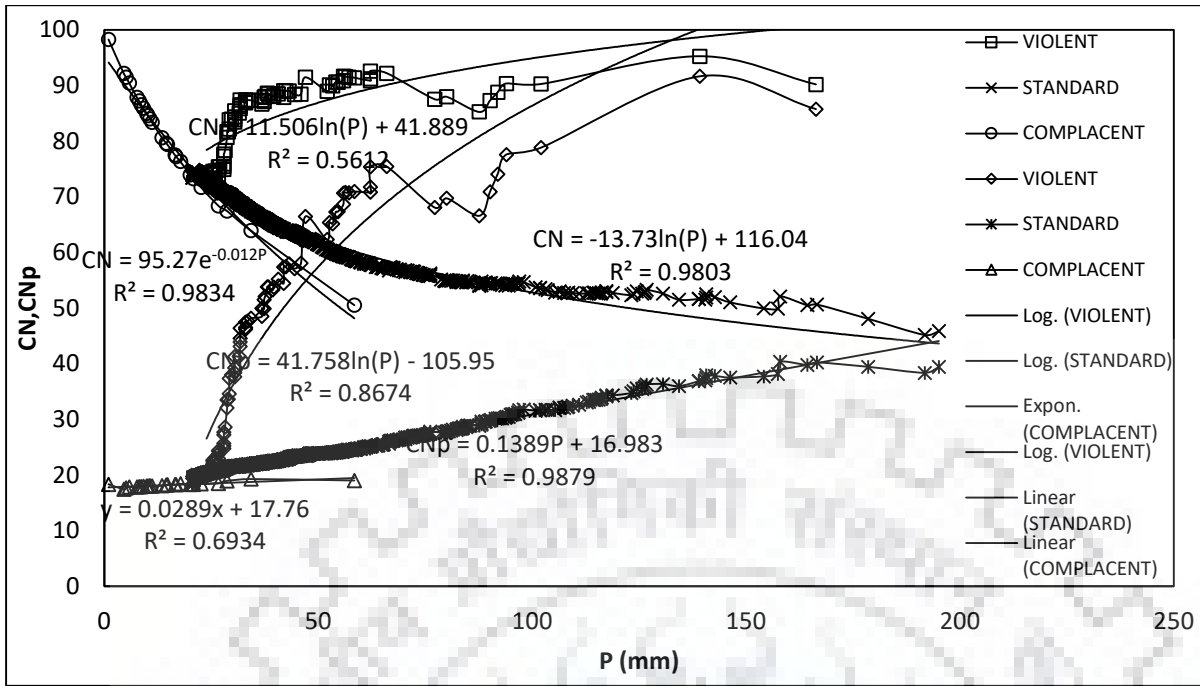


Figure 4.1 CN, CN_p versus P fitting of the three datasets.

4.4 RESULTS AND DISCUSSION

The proposed models require observed data on total rainfall, runoff of the storm events for its calibration and verification. Therefore, as discussed in Chapter 3, the data of Hawkins (1993), Strange Table data and data of Tehri watershed are used for testing of the proposed models.

4.4.1 Performance Evaluation Criteria

In total, 4 models (Table 4.1) are evaluated for performance. As seen from the table, Model 1 is the general form of the existing SCS-CN Model 2. Models 3-4 are the models proposed in this study and these are compared for performance with Models 1 and 2. For evaluating their comparative performance, Nash and Sutcliffe (1970) efficiency (NSE); root mean square error (RMSE); and bias criteria have been used. These are defined, respectively, as:

$$NSE = \left[1 - \frac{\sum_{i=1}^N (Q_{obs} - Q_{comp})_i^2}{\sum_{i=1}^N (Q_{obs} - \overline{Q_{obs}})_i^2} \right] \times 100\% \quad (4.15)$$

$$RMSE = \sqrt{\sum_{i=1}^N (Q_{obs} - Q_{comp})_i^2 / N} \quad (4.16)$$

$$Bias = (1/N) \sum_{i=1}^N (Q_{comp} - Q_{obs}) \quad (4.17)$$

where Q_{obs} is the observed storm runoff (mm), Q_{comp} is the computed runoff (mm), $\overline{Q_{obs}}$ is the average of observed runoff values in a watershed, N is the total number of rainfall-runoff events, m is the number of model parameters, i is an integer varying from 1 to N , and N is the number of events for the watershed. The value of NSE is less than or equal to 100 %. NSE = 100 % is representative of a perfect reconciliation of computed and observed values (ASCE Task Committee, 1993; Fentie et al., 2002). Similarly, NSE < 0 indicates the model predictions to be inferior as compared to the mean of the observed data (Coffey et al., 2004). Recently, McCuen et al. (2006) advocated for NSE to be an excellent criterion for comparing hydrologic models. Regarding RMSE, a higher value is indicative of poor model performance, and vice versa. A value of RMSE equal to zero exhibits a perfect fit. RMSE has the units of $[L^2]$ and is valid for linear as well as non-linear models (McCuen 2003). The negative and positive values of Bias indicate whether or not a model has under- and over-predicted the results.

4.4.2 Hawkins data (1993)

The existing as well as the modified SCS-CN models (Table 4.1) were applied to the data of the three study watersheds, i.e., West Donaldson Creek, Oregon; Coweeta watershed #2, North Carolina; and Berea watershed #6, Kentucky. The performance was evaluated in terms of NSE, RMSE and BIAS. Model 1 has two parameters, i.e., λ and CN and Model 2 has only one parameter CN.. Models 3 & 4 have parameters α , β , and CN_0 . Models 1&2 and 3&4, the parameters were optimized using Marquardt (1963) algorithm of constrained least squares (MCLS). The application results of all the six models are given in Table 4.2 and the results are also graphically shown in Figs. 4.2a-c.

As seen from Table 4.2, the violent watershed has the highest ($=0.44$) runoff coefficient (C) (derived from mean values of rainfall and runoff), the complacent the lowest ($=0.003$), and the standard in between these two ($=0.06$). Such order of runoff generating potential is described by CN (or CN_0 for S_0) values derived (for the same $P = 254$ mm) from all model applications except Model 2, that is the existing SCS-CN model. This model did not describe the consistent trend because it performed extremely poorly on complacent watershed, perhaps not applicable to such watersheds. Similarly, Model 4 shows an unacceptable reverse trend.

Model 4 performed the best of all on complacent and standard watersheds, and Model 1 on violent watershed. λ of Model 1 is seen to have ranged from 0 (for complacent watershed) to 1

(for violent watershed). Thus, λ appears to be mean C (or CN)-dependent. It is of paramount importance in field applications as a proper prescription of average C-dependent λ -value can enhance the results significantly. $\lambda = 0$ appears to be reasonable for complacent type of watersheds, largely for the reason that such watersheds exhibit very high S (or low CN) value to describe a certain value of initial abstraction ($I_a = \lambda S$). Similarly, very high λ -value (of the order of 1) is proper for violent type of watersheds as these watersheds exhibit very low S (or very high CN) values. Bias in Table 2 is presented to indicate whether a model over (positive) - or under (negative)-predicted the runoff.

Model 3 with its parameters α and S_o exhibits consistently decreasing and increasing trends with violent to standard and to complacent watersheds, respectively. In addition, Eq. 4.12 of Model 3 when plotted for a specific value of α , the resulting C-CN_o (Fig. 4.3) and CN_o-P (Fig. 4.4) relations more rationally describe the behavior of the three types of watersheds. Notably, Models 3 and 1 have performed similarly for complacent type of watersheds. It is for the reason that α -value is very low ($=1.00 \times 10^{-8}$), almost near to zero, for which Model 3 reduces to Model 1.

Thus, in order of preference Model 1 is the best for the violent and generally better for standard type of watersheds. Model 4 however outperforms for complacent type of watersheds and, in general, has performed much better for other watersheds. Thus, Model 4 is best suited for these watersheds. Here, it is noted that the values of β equal to 0.99 for complacent and 0.81 for standard watersheds indicate the predominance of I_a in runoff prediction using Model 3 and use of mean C- α relation might be better for complacent type of watersheds.

4.4.3 Strange and Tehri data

All the models generally performed extremely well on both Strange and Tehri data and their three watershed conditions. For the former, i.e. for Strange table data, λ of Model 1 ranges from 0.07 (for Bad watershed) to 0.29 (for Good watershed) and for Tehri watershed, these values are 0 to 0.34. Thus, λ appears to be mean C (or CN)-dependent. It is of paramount importance in field applications as a proper prescription of average C-dependent λ -value can enhance the results significantly. $\lambda \rightarrow 0$ appears to be reasonable for Bad type of watersheds, largely because such watersheds exhibit very high S (or low CN) value to describe a certain value of initial abstraction ($I_a = \lambda S$). Similarly, a relatively high λ -value is proper for Good type of watersheds as these watersheds exhibit very low S (or very high CN) values. Such an assertion however does not hold for Tehri data. Bias in Table 4.3 indicates whether a model over (positive) or under (negative) predicted the runoff and also shows graphically in Figs.4.5a-c & 4.6a-c.

Model 3 is a general form of Model 4, and it is also exhibited by their application results. Both the parameters α and S_0 , respectively, exhibit consistently decreasing and increasing trends with Good to Average and to Bad watersheds. In addition, Eq. 4.13 of Model 3 when plotted for a specific value of α , the resulting C-CNo (Figs. 4.7) and CNo-P (Figs. 4.8) relations more rationally describe the behavior of both the watersheds and their three watershed conditions data of Strange table data. Note, Fig. 4.8 has been used to describe three types of Tehri watershed conditions, and data segregated to represent good (or high CN or high runoff generating), and bad (or low CN or low runoff generating) watersheds; and average representing the middle.

Table 4.1 Model formulations/procedures.

Model No.	Equations	Parameter(s)	Procedure
1	4.2a, 3	λ, S (or CN from Eq. 4.3)	Optimization using Marquardt algorithm
2	4.2b, 3	S (or CN from Eq. 4.3)	
3	4.13	α, S_0 (or CNo from Eq. 4.3)	
4	4.15	α, β, S_0 (or CNo from Eq. 4.3)	

Table 4.2 Performance evaluation of various models on Hawkins (1993) data.

Sl. No.	Watershed No.	No. of events	Mean rainfall (mm)	Mean runoff (mm)	C = Mean runoff/ Mean rainfall	Model 1					Model 2			
						λ	S (CN)	NSE	RMSE	BIAS	S (CN)	NSE	RMSE	BIAS
							(mm)	(%)	(mm)	(mm)	(mm)	(%)	(mm)	(mm)
1	Violent	84	43.70	19.40	0.44	1	15 (94.42)	97.88	3.62	0.52	33.31 (88.41)	96.00	4.97	-1.42
2	Standard	793	46.26	2.80	0.06	0.04	475.97 (34.80)	98.97	0.56	0.10	223.15 (80.74)	88.75	1.84	-0.11
3	Complacent	25	15.89	0.05	0.003	0.00	9656.3 (2.56)	86.19	0.03	0.01	111.92 (96.66)	-134636	2.47	-1.61

Table 4.2 Contd.

Sl. No.	Model 3					Model 4					
	α	S ₀ (CN ₀)	NSE	RMSE	BIAS	β	α	S ₀ (CN ₀)	NSE	RMSE	BIAS
	(mm ⁻¹)	(mm)	(%)	(mm)	(mm)		(mm ⁻¹)	(mm)	(%)	(mm)	(mm)
1	0.010	99.04 (71.95)	96.27	4.79	-1.20	0.23	0.058	348.56 (42.16)	97.31	4.08	-0.71
2	0.004	1224 (17.19)	97.91	0.79	-0.28	0.81	0.011	114.46 (68.94)	99.74	0.28	0.06
3	1.00x10 ⁻⁸	9656.29 (2.48)	86.19	0.03	0.01	0.99	2.6x10 ⁻¹	38.5 (86.84)	92.47	0.02	0.009

Table 4.3 Performance evaluation of various models on Strange and Tehri Data.

Sl. No.	Watershed Type	No. of events	Mean rainfall (mm)	C = Mean runoff/ Mean rainfall	Model 1				Model 2		
					λ	S (CN)	Eff.	Bias	S (CN)	Eff.	Bias
						(mm)	(%)	(mm)	(mm)	(%)	(mm)
Strange Data											
1	Good	60	774.70	0.38	0.29	746.42 (25.39)	98.88	6.34	869.49 (22.61)	96.69	6.73
2	Average	60	774.70	0.28	0.17	1311.94 (16.22)	99.61	1.84	1240.12 (17.00)	99.49	-2.39
3	Bad	60	774.70	0.19	0.07	2666.84 (8.69)	99.92	-0.03	1737.76 (12.75)	98.11	-0.26
Tehri Watershed											
1	Good	15	40.96	0.76	0	19.87 (92.74)	96.52	-1.30	14.67 (94.52)	96.00	-1.52
2	Average	15	72.32	0.47	0	135.42 (65.22)	98.04	-1.87	87.59 (74.36)	96.17	-3.32
3	Bad	13	116.12	0.34	0.34	176.45 (59.01)	96.96	-1.84	218.58 (53.75)	96.61	-2.56
Sl. No.	Model 3				Model 4						
	α	S_0 (CN ₀)	Eff.	Bias	β	α	S_0 (CN ₀)	Eff.	Bias		
	(mm ⁻¹)	(mm)	(%)	(mm)		(mm ⁻¹)	(mm)	(%)	(mm)		
Strange Data											
1	0.00099	4620.69 (5.21)	99.99	0.89	0.00001	0.00098	4632.14 (5.20)	99.99	0.83		
2	0.00069	5300.71 (4.57)	98.98	1.18	0.00035	0.00035	1193.90 (17.54)	99.99	1.10		
3	0.00047	7176.06 (3.42)	99.97	1.10	0.61	0.00035	1222.60(17.20)	99.95	1.46		
Tehri Watershed											
1	0	19.87 (92.74)	96.52	-1.30	0.39	0.021	16455 (1.52)	99.02	-4.61		
2	0	135.42 (65.22)	98.04	-1.87	0.10	0	100.94 (71.56)	98.08	-1.59		
3	0.00389	1192.45 (17.56)	98.59	-2.44	0.04	0	17.55 (93.54)	98.08	-1.59		

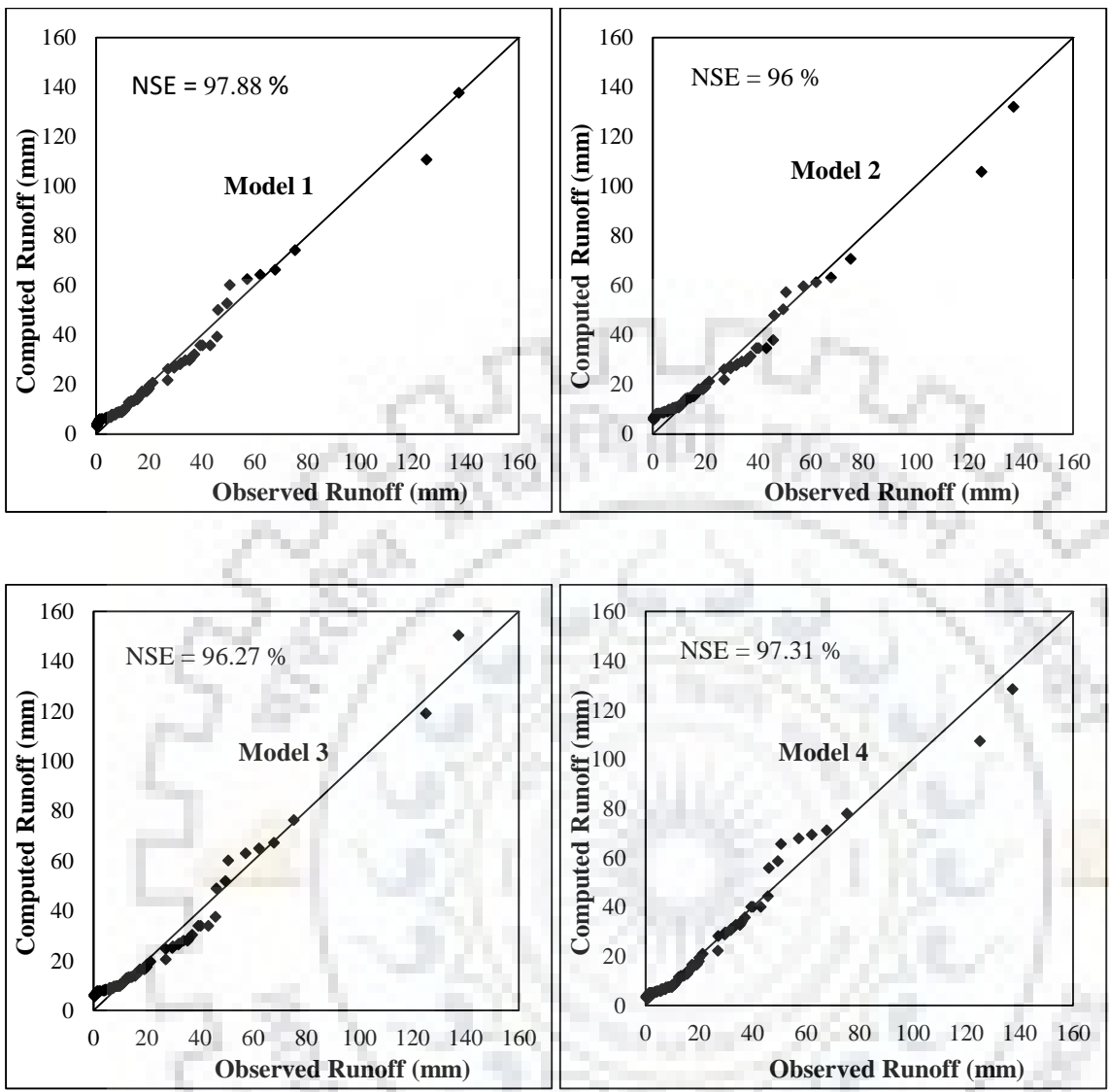


Figure 4.2a Evaluation of Models 1-4 by comparing the computed runoff (mm) with the observed runoff (mm) of Violent watershed (Hawkins, 1993).

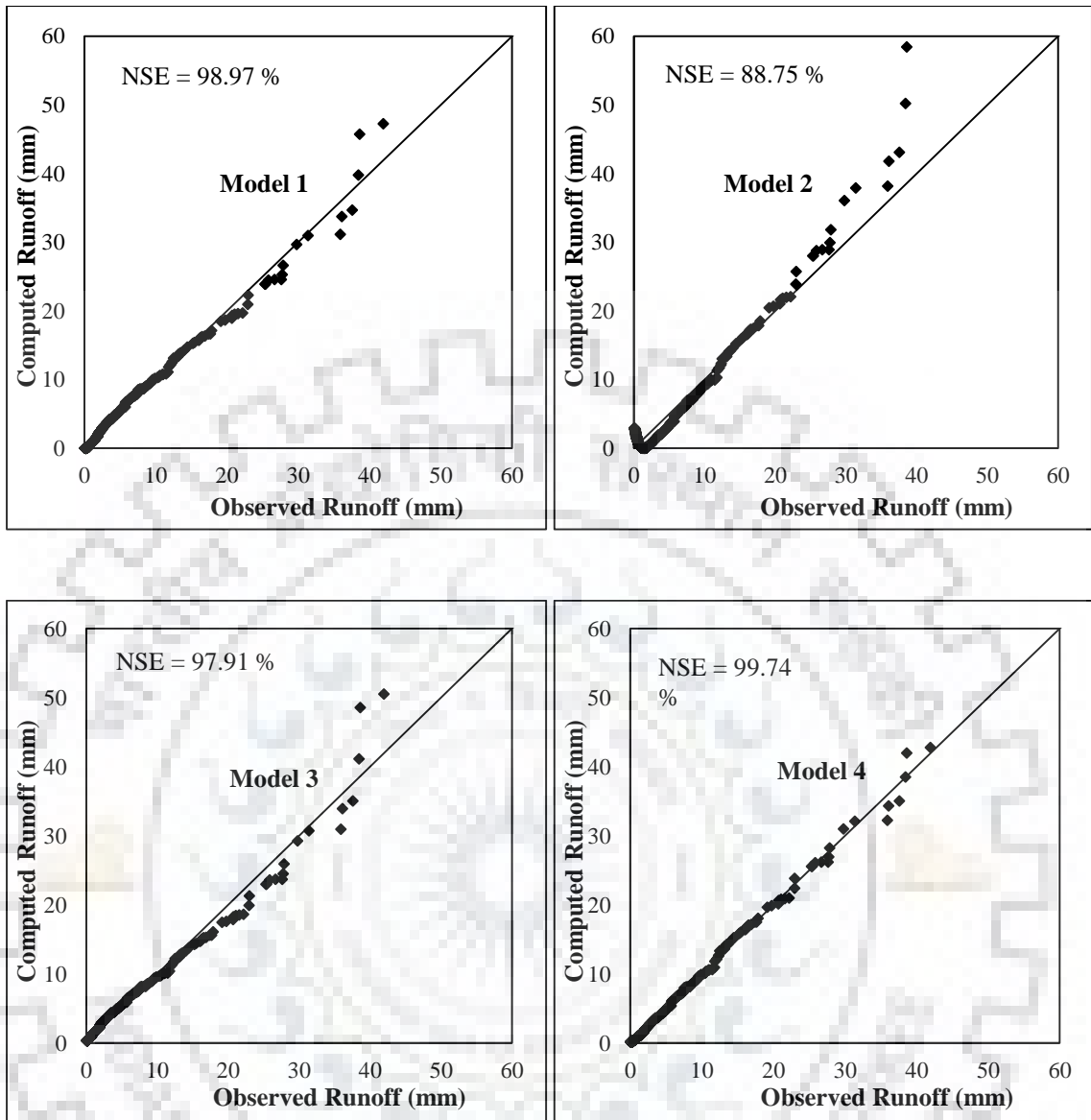


Figure 4.2b Evaluation of Models 1-4 by comparing the computed runoff (mm) with the observed runoff (mm) of Standard watershed (Hawkins, 1993).

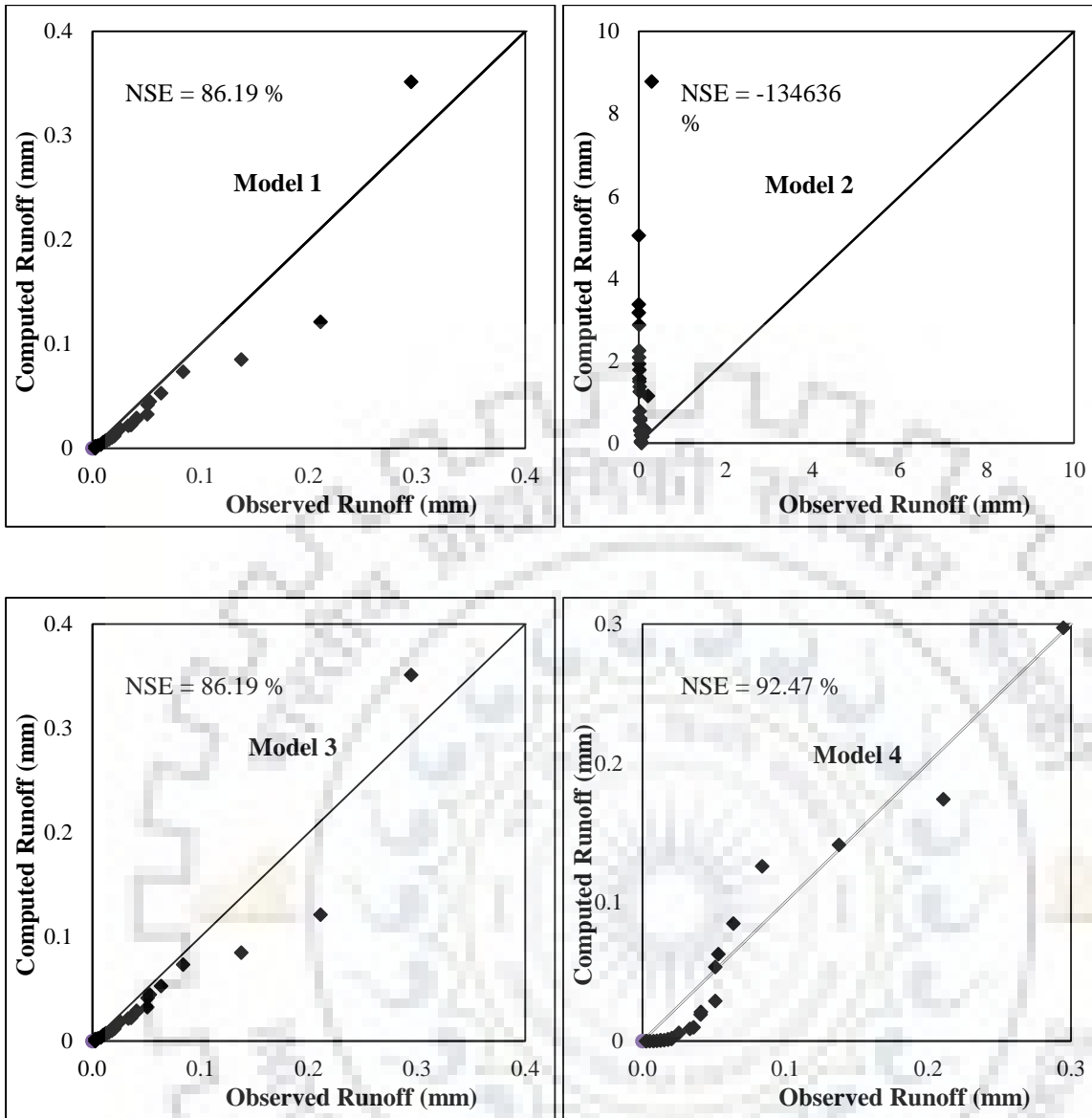


Figure 4.2c Evaluation of Models 1-4 by comparing the computed runoff (mm) with the observed runoff (mm) of Complacent watershed (Hawkins, 1993).

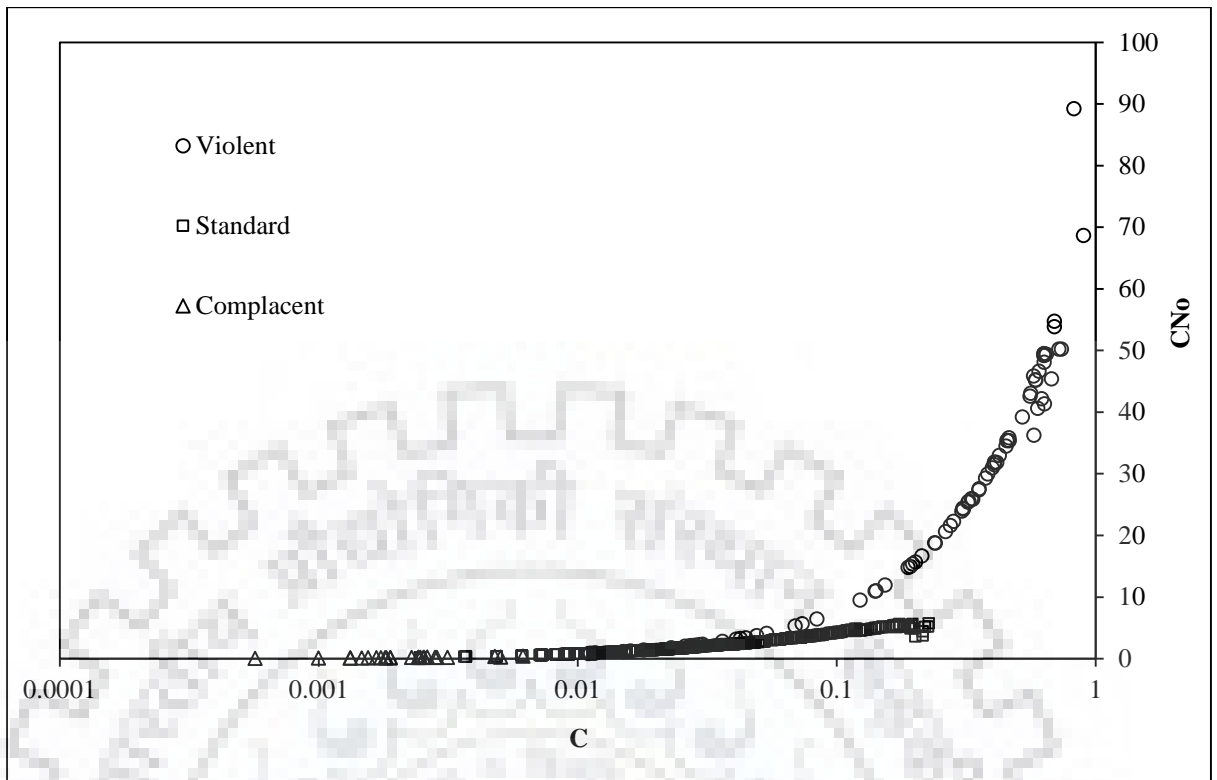


Figure 4.3 C-CNo relationship for Model 3 ($\alpha = 0.01$).

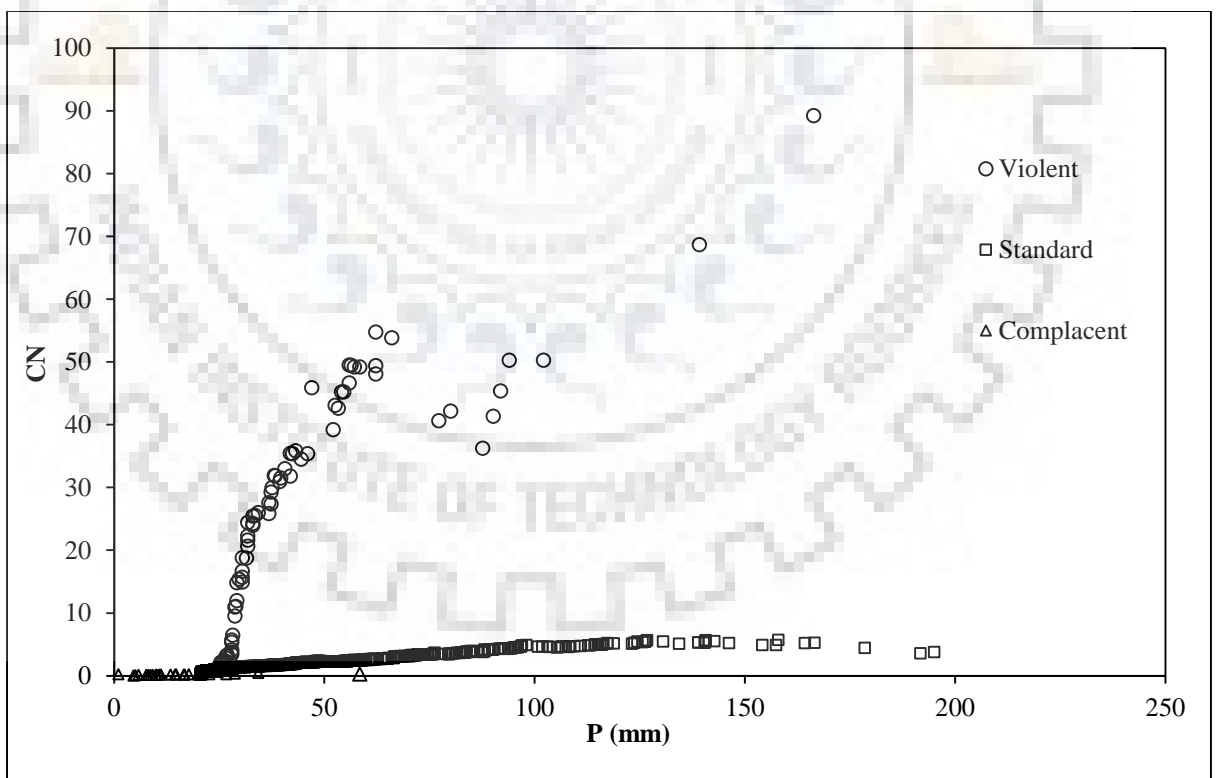


Figure 4.4 Variation of CN with P (mm) for three types of watersheds for Model 3 with $\alpha = 0.01$.

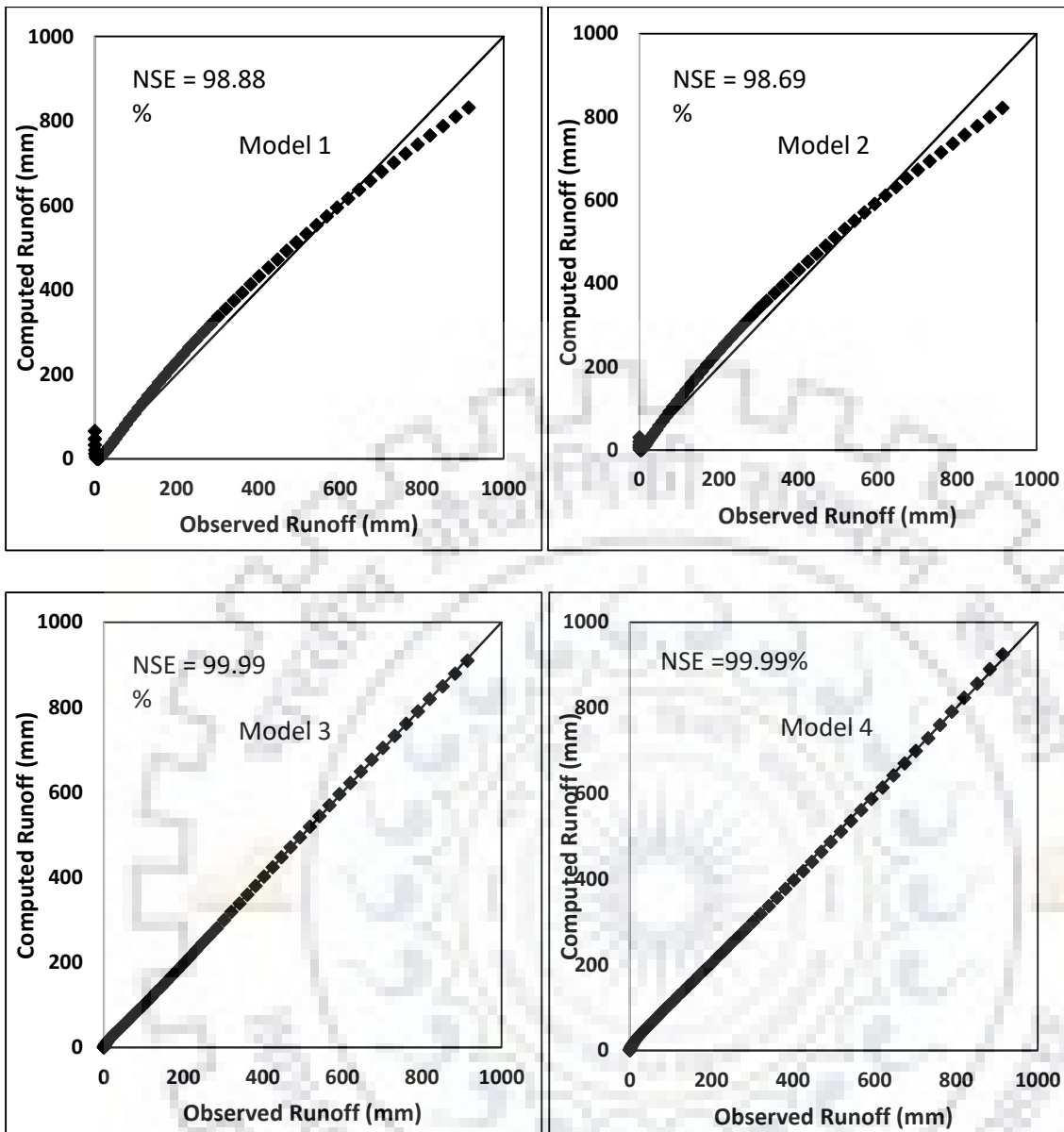


Figure 4.5a Evaluation of Models 1-4 by comparing the computed runoff (mm) with the observed runoff (mm) of Good watershed (Strange, 1892).

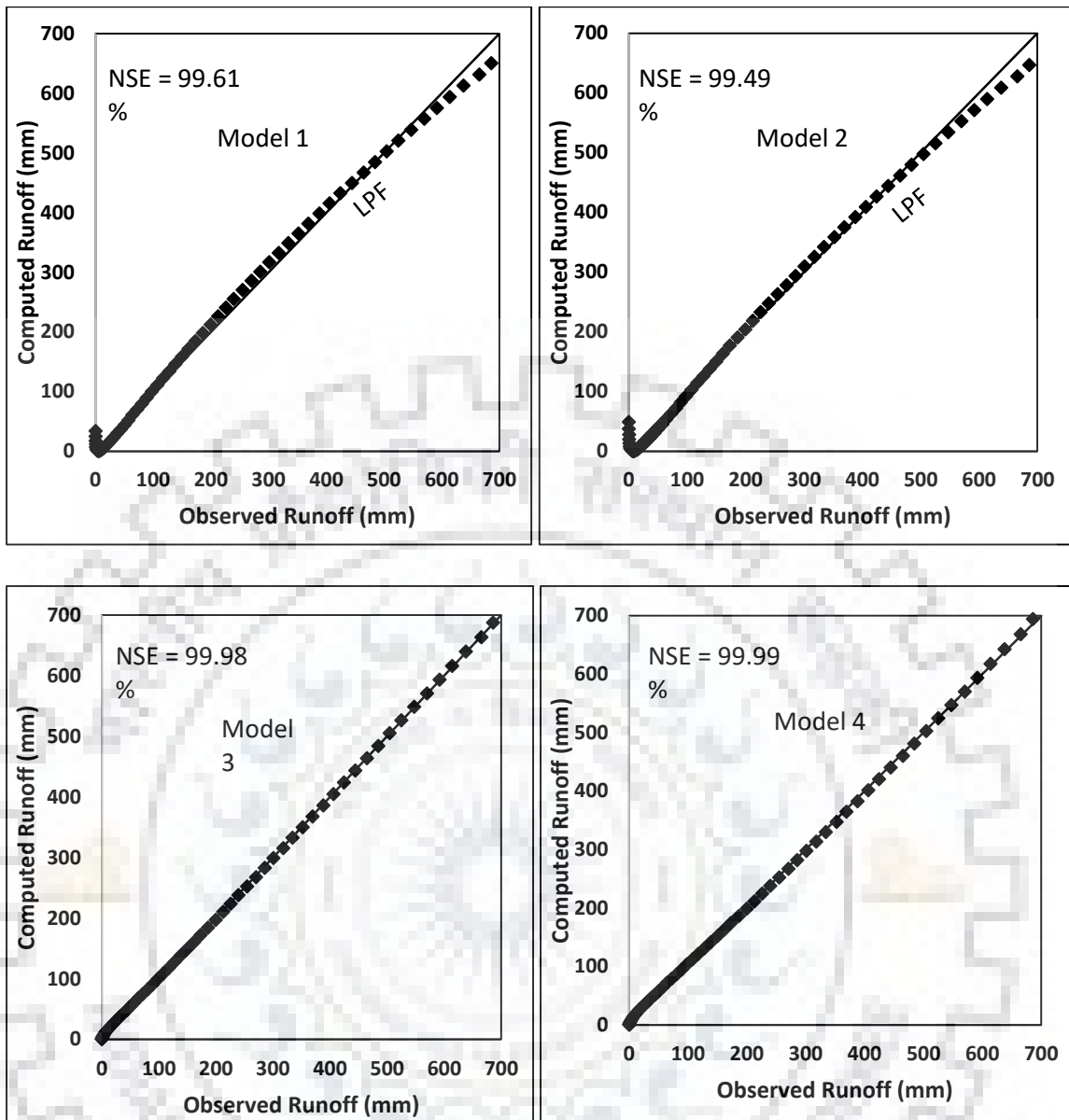


Figure 4. 5b Evaluation of Models 1-4 by comparing the computed runoff (mm) with the observed runoff (mm) of Average watershed (Strange, 1892).

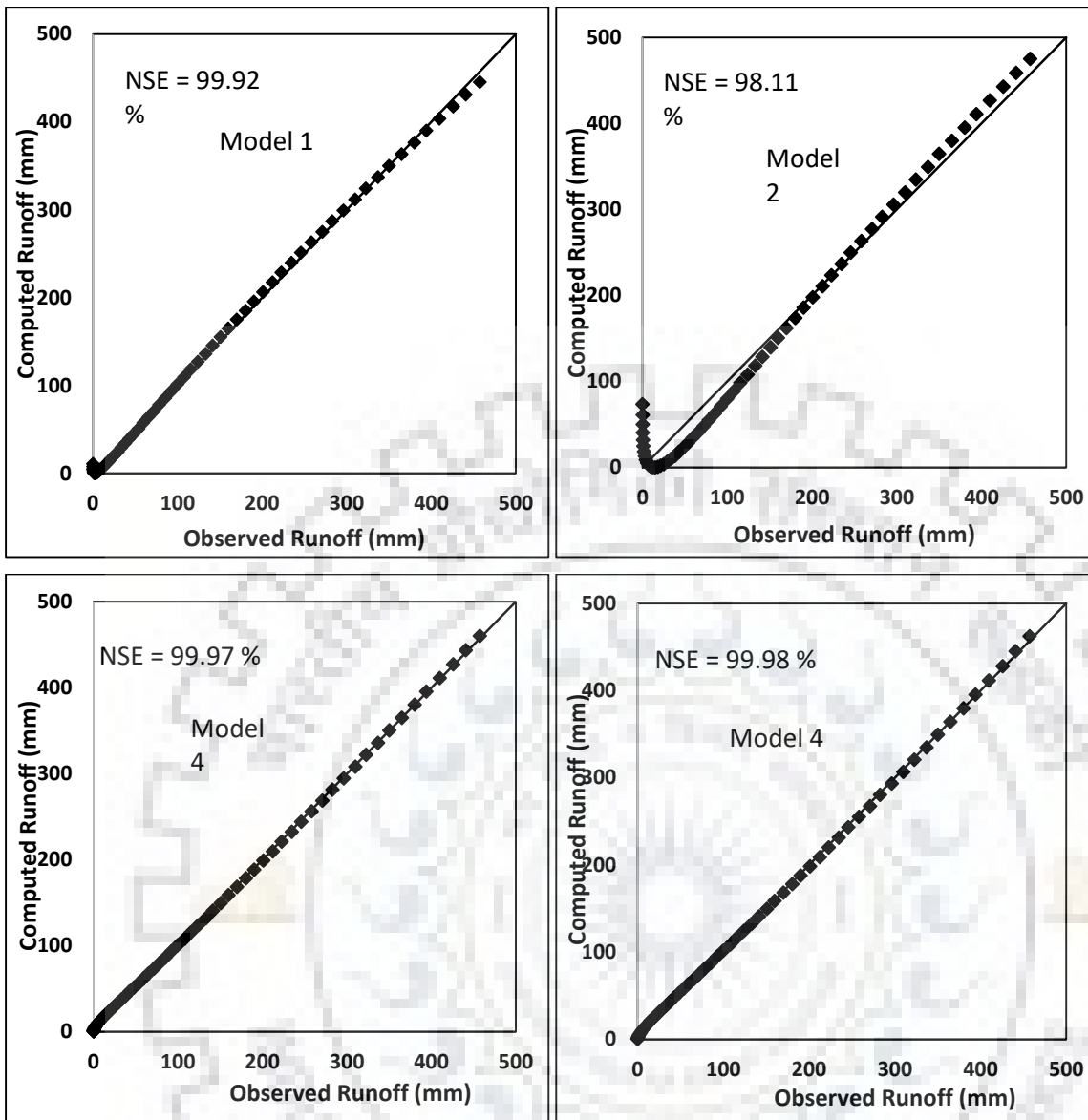


Figure 4.5c Evaluation of Models 1-4 by comparing the computed runoff (mm) with the observed runoff (mm) of Bad watershed (Strange, 1892).

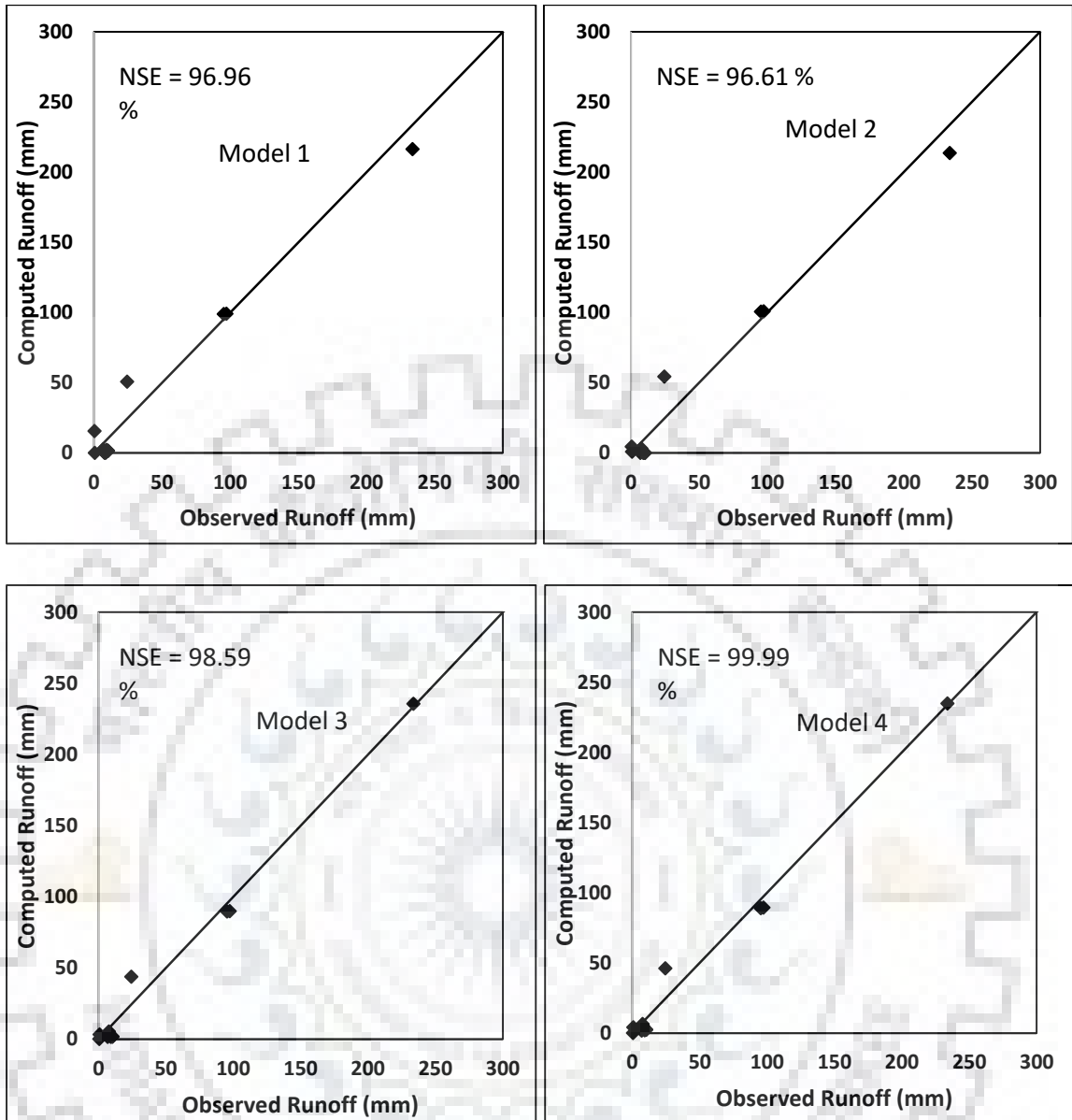


Figure 4.6a Evaluation of Models 1-4 by comparing the computed runoff (mm) with the observed runoff (mm) of Good watershed (Tehri watershed).

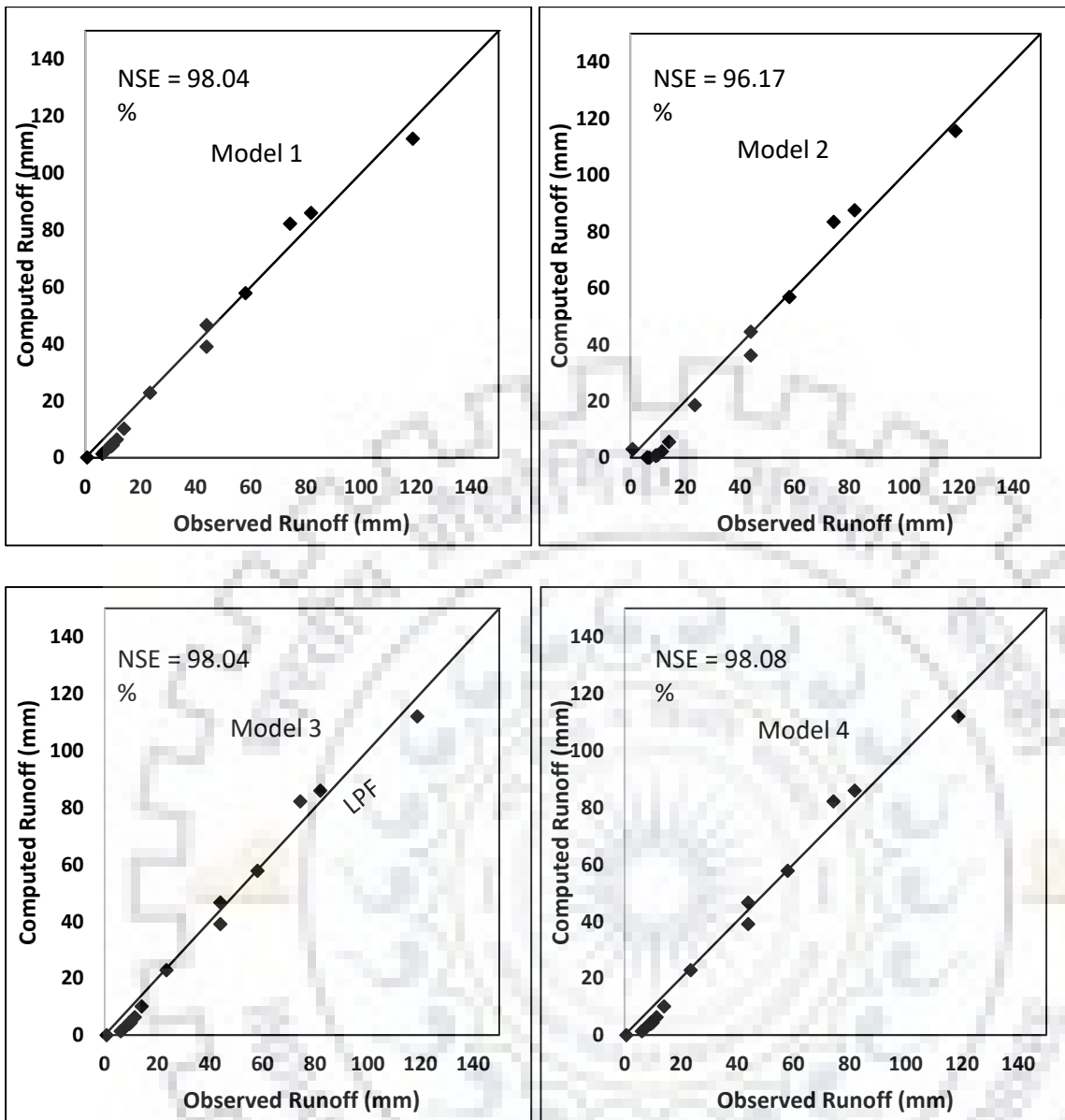


Figure 4. 6b Evaluation of Models 1-4 by comparing the computed runoff (mm) with the observed runoff (mm) of Average watershed (Tehri watershed).

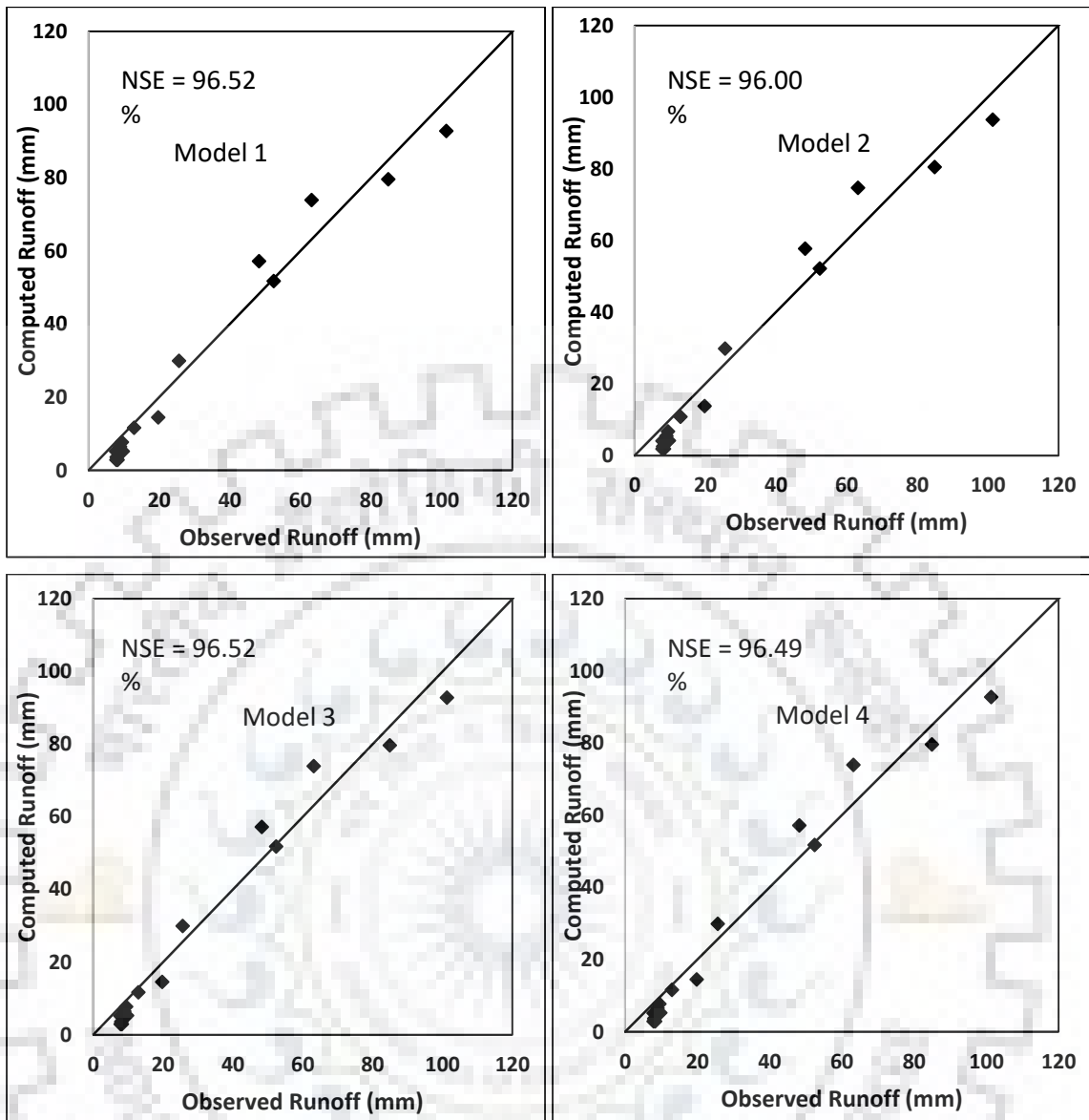
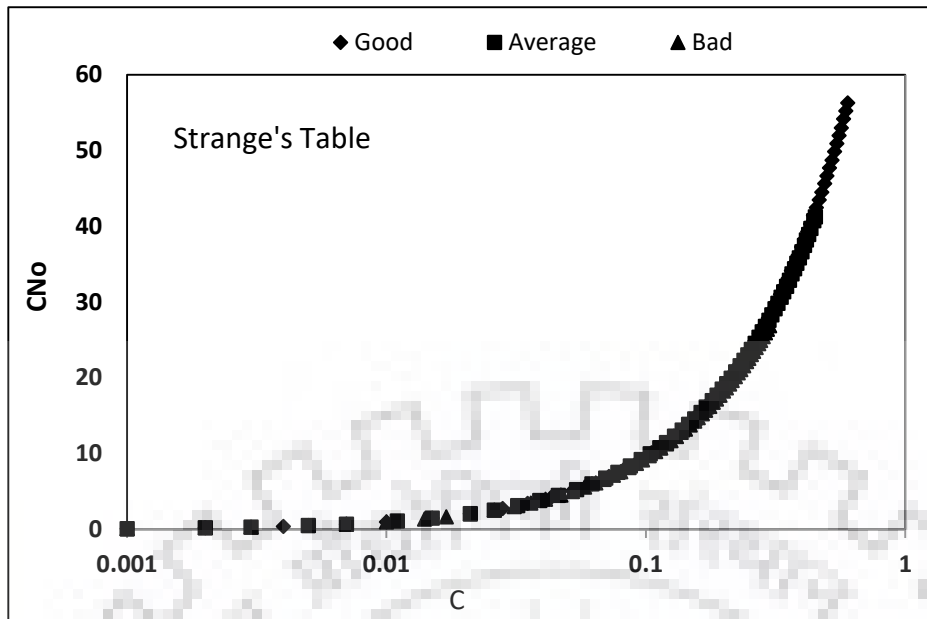
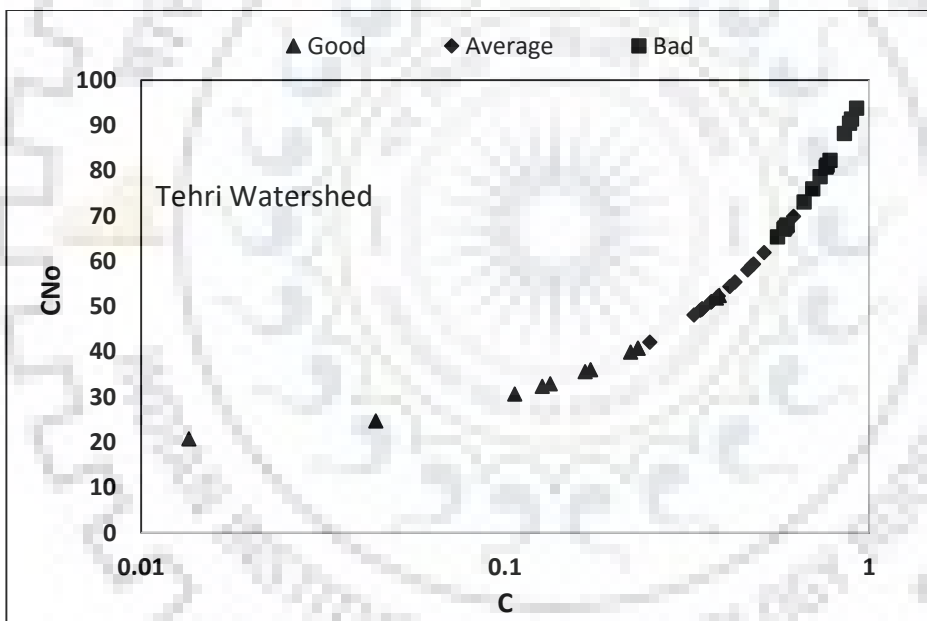


Figure 4.6c Evaluation of Models 1-4 by comparing the computed runoff (mm) with the observed runoff (mm) of Bad watershed (Tehri watershed).

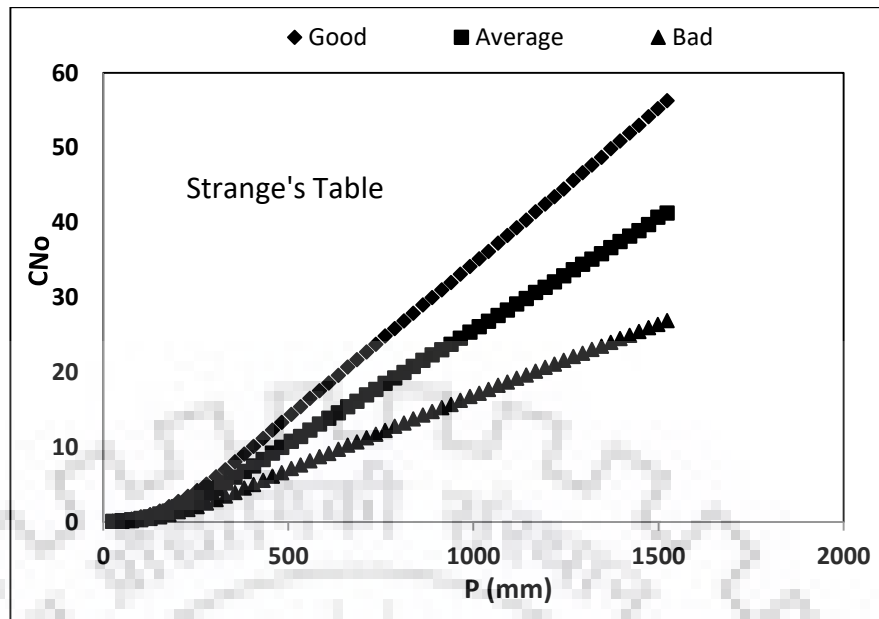


(a)

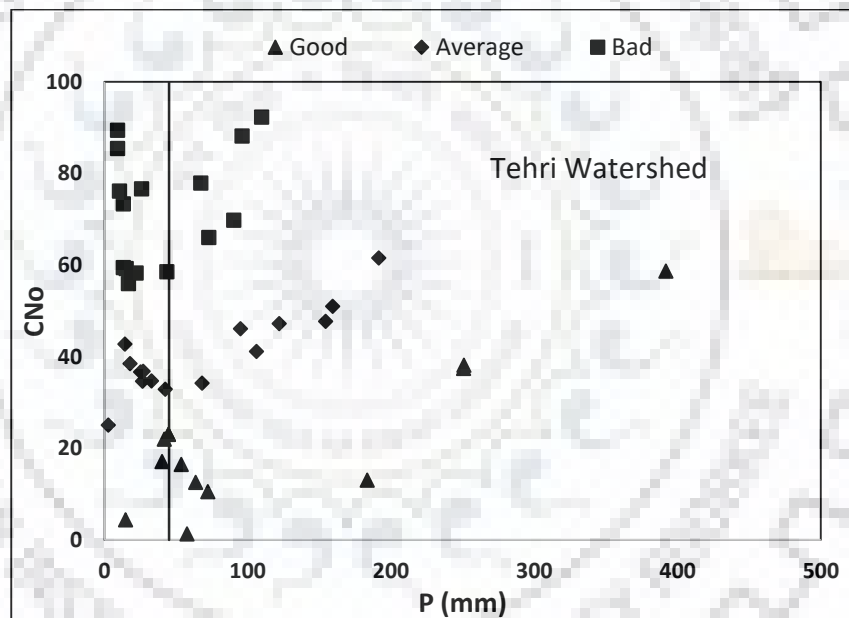


(b)

Figure 4.7 C- CN_o relationship for Model 3 ($\alpha = 0.0001$) for Strange data and Tehri watershed.



(a)



(b)

Figure 4.8 Variation of CNo with P (mm) for Strange data and Tehri data for Model 3 with $\alpha = 0.0001$. Note: Tehri data for $P < 45$ mm excluded.

4.5 ADVANTAGES AND LIMITATIONS OF THE PROPOSED MODEL

The proposed model possesses certain advantages over the existing SCS-CN method. The modification proposed to the proportional equality of SCS-CN methodology describes the realistic increasing trend of runoff coefficient C with rainfall and resolves the issue of CN decaying unrealistically with increasing rainfall (P). Secondly, CN is presented as an index of describing runoff potential of a watershed for given amount of rainfall (it is 10 inch = 254 mm at present). Moreover, the proposed variation of CN with P in real world applications has the efficacy to describe watershed behaviour. It supports the fact that runoff coefficient (C) (or CN) increases with increasing P . The proposed S_o modification assumed that the ground surface is completely dry before the start of rainfall ($S_t = S_o$).

4.6 SUMMARY AND CONCLUSIONS

This chapter presented a modified version of the popular rainfall-runoff Soil Conservation Service Curve Number (SCS-CN) methodology and its validation using rainfall-runoff data on Hawkins (1993) as well as Strange (1982) and Tehri catchment (Uttarakhand, India), belonging to southern and northern parts of India, respectively. The proposed modification to the application approach of the SCS-CN methodology (i.e. Model 3) was more rational, had the efficacy to describe the watershed behavior more scientifically and resolved the issue of CN decaying with increasing rainfall (P). Besides, the proposed methodology is found to be consistent with the expectation (increase in CN with increase in P) when applied to field datasets.

The proposed models 3 and 4 are found to be equally suitable in physically describing the behavior of the three watersheds. The proposed CN_o - P helps categorize the data representing good, average, and bad conditions of the watershed, vital for improving the model performance. Model 4 performed the best on the data of all watersheds except the Hawkins (1993) violent watershed whereas model 1 was superior to all. For $\lambda = 1$, model 1 showed a generally increasing trend with both mean C and mean P of the violent watersheds. Model 1 performed decently for standard and very poorly over the complacent watersheds as compared to model 4 on Hawkins dataset. It is interesting to note that model 4 is most suitable for standard and complacent watersheds though it contrasts the conceptualized linear direct C -CN relationship. For Tehri data, all the models showed competent results. However, model 4 was found to be the overall best performer. All the four models performed excellently on Strange (1982) data, which warrants the applicability of SCS-CN-based models to any duration rainfall values.

5.1 INTRODUCTION

The SCS-CN method is a conceptual/empirical model of hydrologic abstraction and requires basic descriptive inputs that are smoothly converted into numeric values of CN (Bonta, 1997) which reflect the runoff potential of the watershed (Mishra and Singh, 2003). As also emphasized in Chapter 4, the accurate estimation of parameter CN has been a topic of much discussion and concern among hydrologists since the inception of SCS-CN methodology. When CNs are calculated from real storm data (a usual procedure), a secondary relationship almost always emerged between CN and storm rainfall depth and this variation led to the classification of the watersheds' behavior as 'standard', 'violent,' and 'complacent' (Hawkins, 1993). In the complacent behavior, the observed CN declines steadily with increasing rainfall depth, and evidences no appreciable tendency to achieve a stable value. In case of 'standard' behavior, the observed CN declines with increasing storm size, as in the complacent situation, but the CNs approach and/or maintain a near-constant value with increasingly larger storms. In case of 'violent' behavior, the observed CNs rise suddenly and asymptotically approach an apparent constant value. Hawkins (1993) attributed this abnormality to the secondary systematic correlation between the calculated CN value and the rainfall depth.

The runoff coefficient (C) and the runoff curve number (CN) are both expressions of the relative rainstorm response characteristics of watersheds (McCuen and Bondelid, 1981 and Hawkins, 1983). It is of common experience that the runoff coefficient (C), which is the ratio of direct surface runoff (Q) to rainfall (P), increases with increasing P, and vice versa (Subramanya, 2013). Furthermore, for a given amount of rainfall, as C increases, CN also increases, and vice versa. Thus, both C and CN behave similarly. In other words, CN should increase with P as does C. Notably, while describing the behavior of watersheds as complacent or standard, it has been found that CN decreases with an increase in storm size (P) whereas the violent watersheds exhibit sudden increase in CN with an increase in P.

In this Chapter, an attempt has been made to (i) rectify the contrasting behavior of the watersheds by proposing a structural modification to the S-CN mapping relationship using proportional equality ($C = S_r$, where C = runoff coefficient and S_r = degree of saturation) (Mishra and Singh,

2003) of the SCS-CN methodology; and (ii) develop simplified CN-P relationships to compute CN for a given P for runoff estimation using SCS-CN methodology.

5.2 SIGNIFICANCE OF S-CN MAPPING

5.2.1 Mathematical Formulation

The theoretical description of popular SCS-CN methodology already discussed in Chapter 4.

The functionality of the existing models (Eqs. 4a&b, Chapter 4) depends on the S-CN mapping relation for pragmatic reasons. It is described as (Eq. 4.3b, Chapter 4):

$$S = 25400/CN - 254 \quad (5.1)$$

As discussed earlier, the inconsistent behaviour of watersheds is not due to the secondary relationship existing between CN and P, rather due to incorrect use of the S-CN mapping relationship and the description of CN.

According to Mishra and Singh (2003), CN is an index of runoff potential of a watershed corresponding to 254 mm (= 10 inches) of rainfall contrary to Hawkins' (1978) version that CN has no intrinsic meaning, except for a convenient transformation of S to establish a 0 to 100 scale. The rationale to this hypothesis is described as follows.

The linkage between CN and S can be explained using Eqs. 4.2a (Chapter 4), which can be re-written for $I_a = 0$ as:

$$\frac{F}{S} = \frac{P}{P+S} \quad (5.2)$$

It describes the variation of degree of saturation (S_r) of the watershed (Mishra and Singh, 2003) with rainfall P, leading to the derivation of S-CN mapping relation (Eq. 4.3, Chapter 4) as follows.

The ratio F/S can vary from 0 to 1. To map it on a scale of 0-100, it is necessary to multiply Eq. 5.2 by 100 leading to

$$100 \frac{F}{S} = \frac{100 P}{P+S} \quad (5.3a)$$

Defining its left-hand side as P-dependent CN (or CN_p) leads to

$$CN_p = \frac{100 P}{P+S} = \frac{100}{1+S/P} \quad (5.3b)$$

which describes the variation of CN_p with P for a given S. Assuming $P = 254$ mm (= 10 inches) leads to Eq. 4.3 (Chapter 4), which can be recast as:

$$CN_p = \frac{25400}{S + 254} = CN_{10} = CN \quad (5.4)$$

Thus,

$$CN = 100 \frac{F}{S} \text{ for } P = 254 \text{ mm or 10 inches} \quad (5.5)$$

Thus, Eq. 5.4 defines CN as the percent degree of saturation (S_r) of the watershed due to a 254 mm (=10-inch) rainfall (Mishra and Singh, 2003). It is worth noting that the direct use of CN in the proportionality hypothesis (Eq. 4.1b, Chapter 4) for computing Q is restricted because CN, by definition, corresponds to the 254 mm base rainfall amount, not to the actual amount P. Therefore, Eq. 4.2 (Chapter 4) with $I_a = 0$ should be resorted to computation of Q for a given rainfall amount P, rather than 254 mm. It can also be asserted as follows.

In terms of CN, the runoff factor C (= Q/P) can be defined from Eq. 4.2 (Chapter 4) (for $I_a = 0$) as:

$$C = \frac{1}{1 + \frac{254}{P} \left(\frac{100}{CN} - 1 \right)} \quad (5.6)$$

To describe C (or CN) physically it is necessary to explain the bracketed portion in the denominator of Eq. 5.6 in terms of the volumetric elements of the soil (Mishra and Singh, 2003) as:

$$\frac{100}{CN} - 1 = \frac{100}{100 V_w / V_v} - 1 = \frac{V_v - V_w}{V_w} = \frac{V_a}{V_w} \quad (5.7)$$

where $CN = 100 S_r = 100 V_w/V_v$, V_v is the void space, V_w is the available moisture due to 254 mm rainfall (i.e. F), and V_a is the air space available for water retention due to 254 mm rainfall, i.e. S. An actual rainfall P greater than 254 mm would result in higher V_w and, consequently, lesser V_a or, in turn, a lesser V_a/V_w ratio, and vice versa. Therefore, the bracketed term in denominator of Eq. 5.6 will need to be revised or updated (increased or reduced) in proportion to 254/P to describe the actual V_a/V_w ratio that corresponds to the actual rainfall amount P.

The actual V_a/V_w ratio computed in the denominator of Eq. 5.7 and the inverse of the resulting sum of the denominator yields the actual S_r that corresponds to P, which equals C to form the proportional equality, $C = S_r$. Alternatively, the implication of such an assertion is that for CN to represent a watershed characteristic, S/P should form a basic parameter of the SCS-CN model while deriving CN from rainfall-runoff data, rather than S alone. To summarize in brief, $100C = 100 Q/P = 100 P/(P+S) = 100 F/S = CN_p$; $CN_p = CN$ for $P = 254$ mm (or 10 inches). The variation

of C or CN with P (Eq. 5.7) can be shown in Fig. 5.1. It can be seen that $C = CN/100$ for $P = 10$ inches, primarily due to usage of $S = 1000/CN - 10$ while describing CN . The use of $S = 100P/CN - P$ will yield $CN = 100 C$ for all P values. Thus, C and CN are variation of each other. Since field data exhibit C to depend on P (Subramanya, 2013), CN will also depend on P .

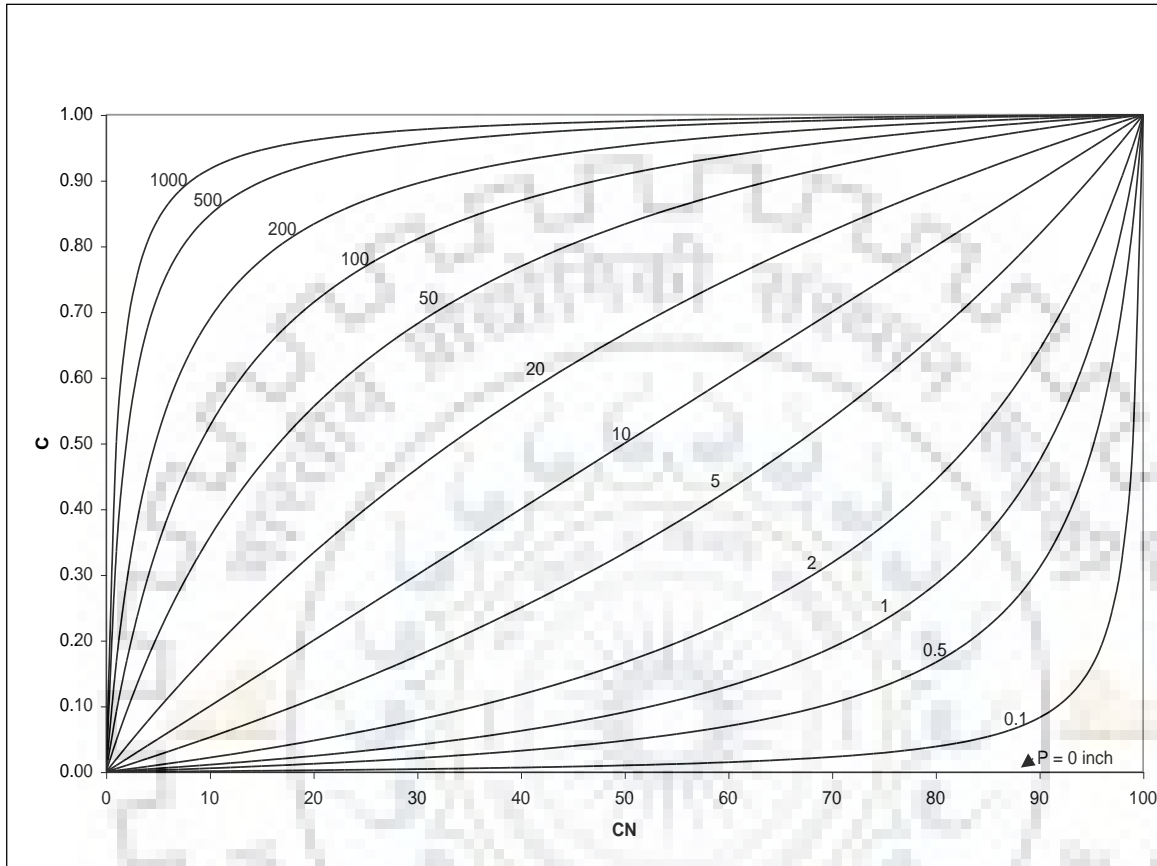


Figure 5.1. Variation of runoff factor C with curve number CN and precipitation P (inch). 1 inch = 25.4 mm.

5.2.2 Significance of λ

λ represents the ratio of initial abstraction (I_a) to parameter S . Since I_a included climate-dependent evaporation, soil-dependent initial infiltration, surface feature (land use)-dependent surface detention, and vegetal (land cover) interception, and all these affect the surface runoff potential described by CN (or S), and therefore, it is logical to describe it as a function (or fraction or multiple) of S (or CN). S , in turn, is mapped on to CN , and therefore, it is not out of order to foresee the dependency of λ on CN (or C) that varies with P (Hawkins, 1993).

Because of larger variability, $I_a = 0.2S$ relationship has been the focus of discussion in literature and modification since its inception. Aron et al. (1977) suggested $\lambda \leq 0.1$ and Golding (1979) provided λ values for urban watersheds depending on CN as $\lambda = 0.075$ for $CN \leq 70$, $\lambda = 0.1$ for

$70 < CN \leq 80$, and $\lambda = 0.15$ for $80 < CN \leq 90$. Ponce & Hawkins (1996) suggested that the fixing of λ as 0.2 might not be the most appropriate number, and that it should be interpreted as a regional parameter. Hawkins et al. (2001) found a value of $\lambda = 0.05$ to better fit the data and therefore be more appropriate for use in runoff calculations.

Mishra & Singh (1999) suggested that λ can take any non-negative value. Mishra & Singh (2004b) developed criterion for the applicability of SCS-CN method based on runoff coefficient (C) and λ variation. They defined the applicability bounds for the SCS-CN method as for $\lambda \leq 0.3, I_a/P \leq 0.35$ and $C \geq 0.23$. Since P relies on climate/meteorological characteristics of the region, Jain et al. (2006b) proposed a more general non-linear I_a -S-P relation, and Mishra et al. (2006) used I_a -S-M relationship based on the hypothesis that I_a largely depends on the initial soil moisture (M). Thus, there exists a sufficient scope for improvement.

5.3 DESCRIPTION OF WATERSHED BEHAVIOUR

Three different conditions can be visualised from Fig. 5.1 (i) For $P = 10$ inches $C = CN/100$ and if C increases or decreases because of any reason, CN also behaves similarly, and therefore, it is easy to infer that both C and CN are synonymous in working as far as runoff production is of concern and it hold for any other rainfall value; (ii) for a given $P < 10$ inches, the initial growth of CN with C is much faster than that in later part, in which the growth of C with CN is much faster. Such a P-dependent C (or CN) abnormal behaviour is largely attributed to the use of S (inch) = $1000/CN - 10$.

The watershed behaviour can also be described physically as:

- For a given P (= 10 inches, say) as C increases, CN also increases. This condition can be realized when the watershed characteristics change, for example, from agriculture to urban.
- For a given CN, C increases as P increases. Since field data exhibit C to increase with P, CN should also increase with P and thus the condition of constant CN is not realizable.
- For a given C, CN increases with decreasing P, and vice versa. This condition is also hard to realize for the simple reason that C is forced to remain constant with changing P, which actually can't, and therefore, CN is forced to exhibit a decreasing trend with increasing P for enabling C to remain at a fixed value in Eq. 5.6. This abnormal condition/behaviour can be further explained as below.

Re-writing Eq. 4.4 (Chapter 4) in terms of C and P, it can be shown that S (or S_P) is a function of both C and P. It is of common experience that C increases with P and S (or S_P) is directly

proportional to P (Eq. 4.4, Chapter 4). Thus, S (or S_P) will increase with increasing P, and vice versa, and, from Eq. 4.3 (Chapter 4), CN is inversely related to S (or S_P). It leads to infer that CN is inversely related to P. Such an unrealistic behaviour has led to several misunderstandings/misinterpretations. To circumvent the problem, a modification is needed in the SCS-CN application procedure, specifically to the S-CN mapping, as follows:

- From given P-Q data, compute S_P from Eq. 4.4 (Chapter 4).
- Derive CN_P for the same P from Eq. 5.3 as follows:

$$CN_P = \frac{100 P}{P + S_P} \quad (5.8a)$$

where subscript 'P' to S or CN refers to their correspondence with P. Similarly, CN corresponding to 254 mm of P can be defined as CN_{10} (or CN) from Eq. 4.4 (Chapter 4). Since CN_{10} is derivable only when S_{10} is available from the runoff generated from 254 mm of rainfall, which is seldom possible to determine in reality, the field application is approximated as follows. Forcing S_{10} to be equal to S_P as per the current practice, it is possible to derive CN_{10} from CN_P (or otherwise) from Eq. 5.8a, as follows:

$$CN_{10} = \frac{100}{1 + \frac{P}{254} \left(\frac{100}{CN_P} - 1 \right)} \quad (5.8b)$$

Thus, for better understanding of the existing SCS-CN method, Eqs. 5.8a and Eq. 5.8b should be used. As seen from Eq. 5.8b, CN_{10} (or CN) represents the runoff potential of a watershed for the fixed 254 mm of rainfall, and thus, is a better indicator to predict the comparative effect of watershed characteristics. This concept is widely used for comparing two watersheds in terms of CN for their runoff-producing (or hydrologic) potential, i.e. whether or not the land use/cover has changed with space/time, using remote sensing (RS) and geographic information system (GIS), ignoring the fact that, as above, CN_P also depends on rainfall.

In this Chapter, as shown above, the use of Eq. 5.8a is proposed instead of Eq. 4.3 (Chapter 4) in computation of Q from P using Eq. 4.2b (Chapter 4). It is recommended for the reason that (a) it holds for boundary conditions: as $S_P \rightarrow 0$, $CN_P \rightarrow 100$ and as $S_P \rightarrow \infty$, $CN_P \rightarrow 0$; and thus, it supports the general notion that CN (or C), as also described above, increases with increasing P, and vice versa. In addition, the available National Engineering Handbook (NEH)-4 table CN (= CN_{10}) values can be directly converted to CN_P using the following relation:

$$CN_P = \frac{1 + S/254}{1 + S/P} CN_{10} \quad (5.9)$$

where $S = S_P = S_{10}$. Here, it worth indicating that any other equation, nearer to Eq. 5.8a, could be recommended for application, as for example:

$$CN_P = \frac{100(P - I_a)}{P - I_a + S_P} = \frac{100}{1 + S_P / (P - I_a)} \quad (5.10)$$

which however is an implicit equation, if I_a is expressed in terms of S (or S_P). This equation also meets both the above boundary conditions. It, however, is valid only for the condition that $P \geq I_a$; it may otherwise lead to impracticable negative CN_P values besides complicating the determination of CN_P .

5.3.1 S-CN mapping based Description of Watershed Behaviour

The description of the watersheds' behaviour based on the existing and the proposed S-CN mapping is discussed in this section using the data of three study watersheds, i.e., West Donaldson Creek, Oregon, Coweeta watershed #2, North Carolina and Berea watershed #6, Kentucky. Notably, the same data set was also used by Hawkins (1993).

(i) Based on the existing S-CN mapping

As discussed above, the watershed behaviour based on the existing S-CN mapping relationship (Eq. 4.3, Chapter 4) as complacent, standard, and violent is shown in Fig. 5.2. As seen, for any fixed C-value, CN decreases with P, as described above. As seen, the complacent behaviour of the watershed closely follows the line $C = 0$. Notably, C can be equal to 0 under three situations: (a) $P \leq 0.2S$, (b) $P = 0$, and (c) $S = \infty$ or infinitely abstracting watershed. Here, the second situation can be easily neglected in runoff estimation (as P has to be non-negative and increasing) whereas the first and last ones are most likely to prevail. In other words, the complacent behaviour is realizable only if it is an absolutely zero runoff potential watershed, an idealized situation. Fig. 2 shows that the CN values can vary in the range 45 to 100. Similarly, the data of the standard watershed exhibits C to vary from 0 to 0.2 (approximate), which is again a low runoff producing watershed whereas CN values are seen to range (45, 100), again a contrasting feature. Lastly, the data of violent watershed shows C to range from 0 to 0.9, which most watersheds do depending on various watershed and AMC features.

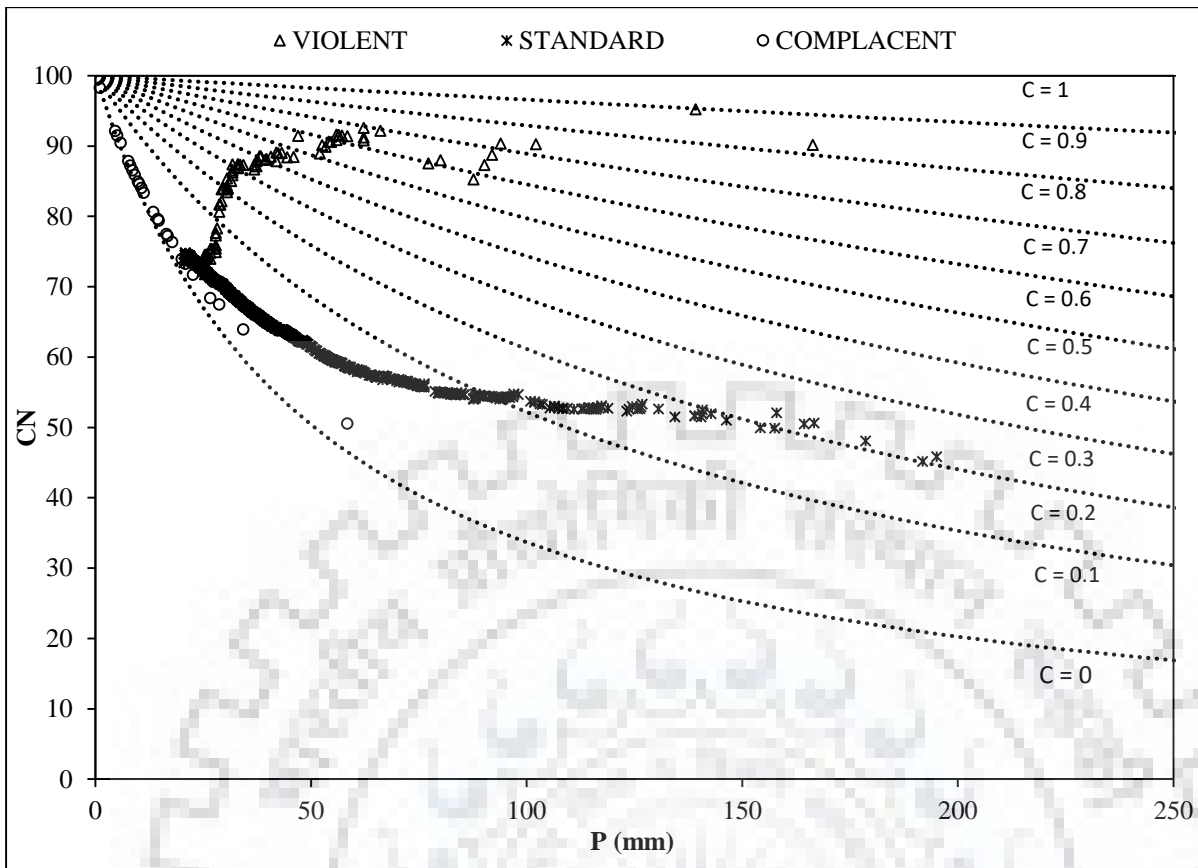


Figure 5.2 Depiction of watershed behaviour in terms of CN-C-P relationship.

Following the present understanding on the existing S-CN relationship (Eq. 4.3, Chapter 4), the behaviour of the above three complacent, standard, and violent watersheds can be described as follows. All the three watersheds closely follow $C = 0$ line until P exceeds I_a , also valid for $S = \infty$. It will continue to exist under all circumstances in nature, and therefore, every watershed has to follow it until runoff starts and, therefore, has to be complacent in nature. When P exceeds I_a , the behaviour of watershed is actually reflected by the increase in both P and P -dependent C , rather than CN (which is for $P = 254$ mm). The gradual and abrupt rate of rise in C (due to several reasons) leads to the description of watersheds as standard and violent, respectively. At what P -magnitude, this rise will be experienced in a watershed will depend on watershed characteristics affecting the runoff generating potential.

The data of standard watershed exhibit C to vary in the range (0, 0.2), which is a reflection of low runoff producing watershed. The watershed which is characterised as violent should be a high runoff producing watershed. As P exceeds I_a , CN (and C as well) increases sharply with little increase in P , and as usual, CN approaches a high (fairly constant) value (as also seen for standard watershed) with increasing P . Such constant values are actually the CN values that are reported in NEH-4 for high storms, and are representative of the watershed runoff potential. For

example, the complacent watershed exhibits lowest runoff potential, violent the highest, and standard the normal.

(ii) Based on the proposed S-CN mapping

Figs. 5.3a&b show CN (or CN₁₀) (Eq. 4.3, Chapter 4) and CN_P (Eq. 5.8) versus P relationships to describe the behaviour of the three watersheds as complacent, standard, and violent. In these figures, solid lines show the variation of CN (= CN₁₀) and CN_P with P for varying C (=Q/P) values derived from Eq. 4.3 (Chapter 4) and Eq. 5.8a, respectively. As seen, CN_P exhibits a more rational behaviour than does CN (or CN₁₀) with increasing P for all three datasets; as P increases, CN_P also increases, and C (not shown) also increases. Thus, it is consistent with the above stated general notion/expectation. Secondly, the low runoff producing watersheds are also seen to exhibit linear P-CN_P relations. CN_P is further seen to exhibit a more consistent (with higher R²) relationship with P; in all three cases, CN_P consistently increases, along with C (not shown), with P. The regression relationships developed between CN- and CN_P-values with P for three types of the watersheds are expressed as:

(a) CN-P relationships

$$CN = 11.506 \ln(P)+41.889 \quad (\text{for Violent watershed}) \quad (5.11a)$$

$$CN = -13.73 \ln(P)+116.04 \quad (\text{for Standard watershed}) \quad (5.11b)$$

$$CN = 95.27e^{-0.012P} \quad (\text{for Complacent watershed}) \quad (5.11c)$$

(b) CN_P-P relationships

$$CN_P = 41.758 \ln(P)-105.95 \quad (\text{for Violent watershed}) \quad (5.12a)$$

$$CN_P = 0.1389P+16.983 \quad (\text{for Standard watershed}) \quad (5.12b)$$

$$CN_P = 0.0289P +17.76 \quad (\text{for Complacent watershed}) \quad (5.12c)$$

In Eqs. 5.11&5.12, $0 \leq CN$ or $CN_P \leq 100$.

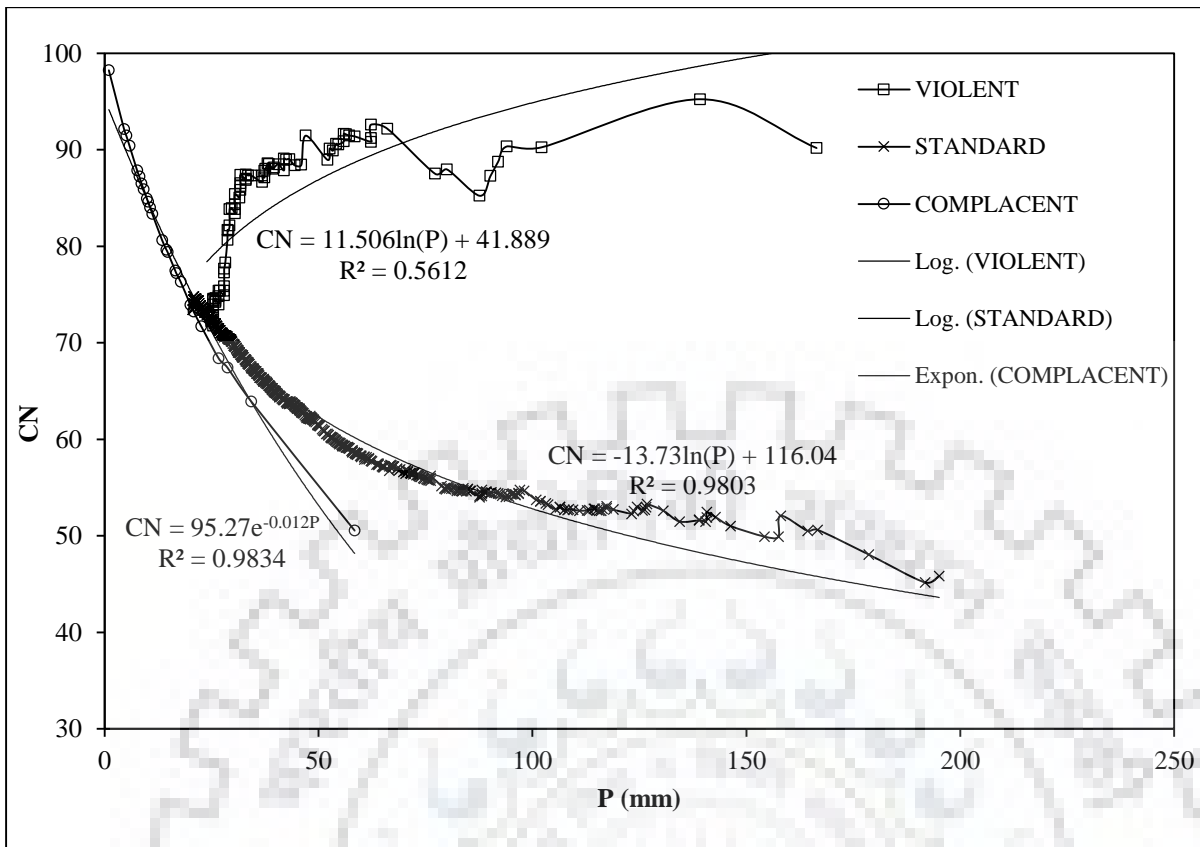


Figure 5.3a CN (or CN₁₀) versus P fitting of the three datasets.

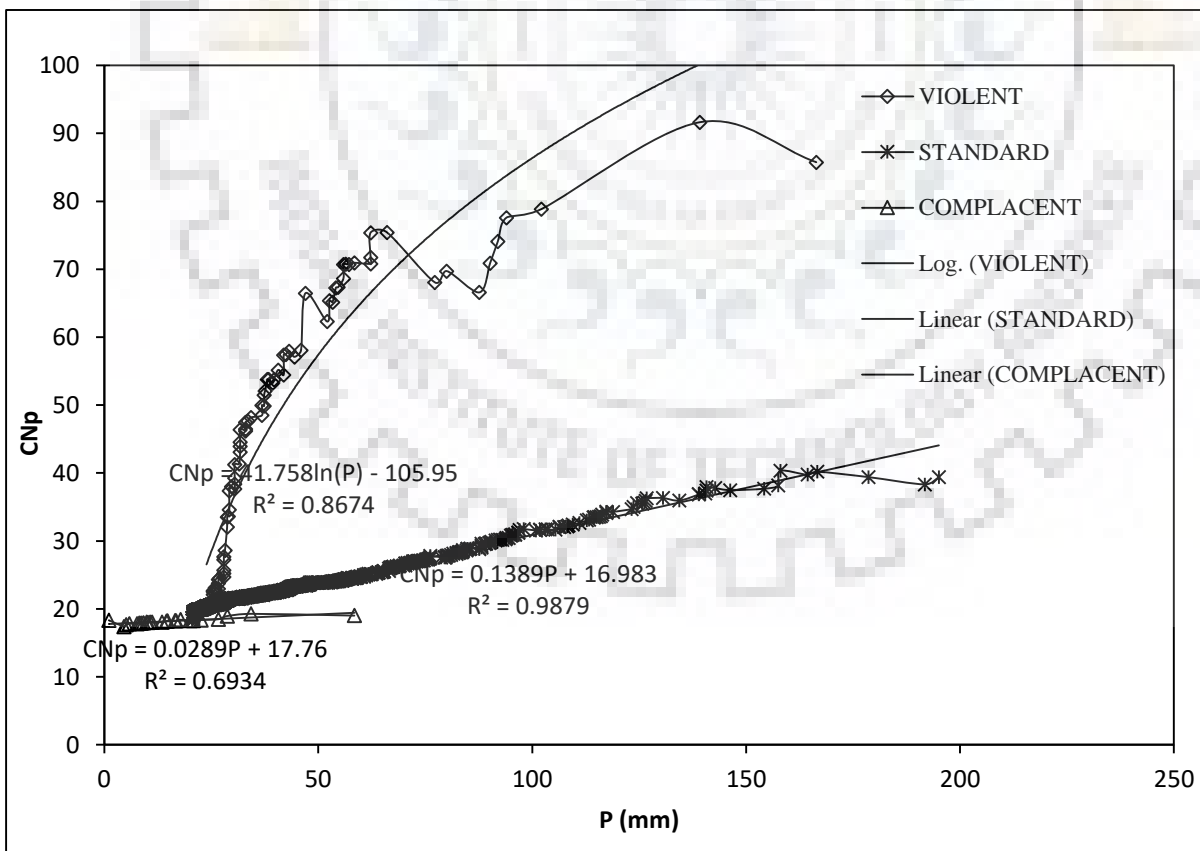


Figure 5.3b CN_p versus P fitting of the three datasets.

5.3.2 Runoff Calculation Approaches Based on Existing and Modified S-CN Mappings

For runoff computations, two approaches can be suggested based the existing and Modified S-CN Mappings and these are named as Model 1 and Model 2.

The application methodology for model 1 can be described as follows:

- a) Determine S from Eq. 4.4 (Chapter 4) using the observed P-Q dataset for a watershed.
- b) Determine CN from Eq. 4.3 (Chapter 4).
- c) Develop a relationship between CN and P for the watershed (Fig. 5.3a and Eq. 4.11) for future applications.

Another method can be proposed by coupling Eq. 4.4 (Chapter 4) with Eq. 5.7, which describes the dependence of CN_p on S/P rather than S alone and the result can be plotted as shown in Fig. 3b. The procedure of Model 2 can be described as follows:

- a) Determine S_p from Eq. 4.4 (Chapter 4) using the observed P-Q dataset for a watershed.
- b) Determine CN_p from Eq. 5.3 or 5.8a.
- c) Develop a relationship between CN_p and P for the watershed (Fig. 5.3b and Eq. 5.12) for future applications.

Notably, Model 2 when depicted graphically describes more elegantly the three types of watersheds based on C or CN; the complacent, the lowest runoff producing (low C and CN), the violent, the highest runoff producing (highest C and CN), and standard, the normal watershed.

5.3.3 Description of Watershed Behaviour based on Strange and Tehri Watershed Data

The description of the watersheds' behaviour based on the existing and the proposed S-CN mapping is discussed in this section using the data of three study watersheds, i.e., good, average and based. The data set are used in this study Strange (1892) and Tehri watershed data. Before describing the watershed behaviour based on proposed S-CN mapping it is important to known the existing relationship of strange table.

5.3.3.1 Existing Relationships based on Strange Data

As above, Strange (1892) described the watersheds as Good, Average, and Bad according to their relative magnitudes of yield or runoff for a given rainfall amount. It is again worth emphasizing here that the Strange monsoon season data (Table 3.1, Chapter 3) was used considering that the SCS-CN concept is applicable to any duration (including seasonal) rainfalls. The correlation equations of best fitting lines relating percentage C are expressed as (Subramanya, 2013):

(i) For Good catchment:

$$\text{For } P < 250 \text{ mm, } C(\%) = 7 \times 10^{-5} P^2 - 0.0003 P, R^2 = 0.9994 \quad (5.13a)$$

$$\text{For } 250 < P < 760 \text{ mm, } C(\%) = 0.0438 P - 7.1671, R^2 = 0.9997 \quad (5.13b)$$

$$\text{For } 760 < P < 1500 \text{ mm, } C(\%) = 0.0443 P - 7.479, R^2 = 1.0 \quad (5.13c)$$

(ii) For Average catchment:

$$\text{For } P < 250 \text{ mm, } C(\%) = 6 \times 10^{-5} P^2 - 0.0022 P + 0.1183, R^2 = 0.9989 \quad (5.14a)$$

$$\text{For } 250 < P < 760 \text{ mm, } C(\%) = 0.0328 P - 5.3933, R^2 = 0.9997 \quad (5.14b)$$

$$\text{For } 760 < P < 1500 \text{ mm, } C(\%) = 0.0333 P - 5.7101, R^2 = 0.9999 \quad (5.14c)$$

(iii) For Bad catchment:

$$\text{For } P < 250 \text{ mm, } C(\%) = 4 \times 10^{-5} P^2 - 0.0011 P + 0.0567, R^2 = 0.9994 \quad (5.15a)$$

$$\text{For } 250 < P < 760 \text{ mm, } C(\%) = 0.0219 P - 3.5918, R^2 = 0.9997 \quad (5.15b)$$

$$\text{For } 760 < P < 1500 \text{ mm, } C(\%) = 0.0221 P - 3.771, R^2 = 1.0 \quad (5.15c)$$

where $C(\%)$ = percentage runoff coefficient = ratio of seasonal runoff to seasonal rainfall in percent (non-dimensional), P = monsoon season rainfall in mm, and R^2 = coefficient of determination. As there is no substantial streamflow from rainfall in dry (non-monsoon) period, the monsoon season runoff volume has been considered as yearly yield of the catchment (Subramanya, 2013). This table can be utilized to determine monthly yields during the monsoon season. However, it must be utilized with the awareness that the table relates cumulative monthly precipitation since the start of the season to the corresponding cumulative runoff.

5.3.3.2 Based on the existing S-CN mapping

Following Hawkins (1993), Strange data (Table 3.1, Chapter 3) is plotted in Fig. 5.4a. In this figure, solid lines show the variation of CN (derived from Eqs. 5.2 and 5.3) with P for varying C ($=Q/P$) values. As seen, for any fixed C -value, CN decreases with P , as described above. The dotted lines correspond to three watersheds described by Strange as Good, Average, and Bad watersheds depending on their runoff generating potential. A Good watershed exhibits a high,

and Bad a low runoff generating potential, and Average falls in between. Thus, consistent with literature, let the Bad watershed be described as Complacent, Average as Standard, and Good as violent watershed. Notably, for a watershed to be violent, CN should increase rapidly with increasing P.

Following the present understanding on the existing S-CN relationship (Eq. 4.3; Chapter 4), the behaviour of the above complacent watersheds can be described as follows. All the three watersheds closely follow $C = 0$ line until P exceeds I_a . It will continue to exist under all circumstances in nature, and therefore, every watershed follows it and, in turn, is complacent in nature. When P exceeds I_a , the behaviour of watershed is reflected by the increase in both P and P-dependent C, rather than CN (which is for $P = 254$ mm). The gradual and abrupt rate of rise in C (due to several reasons) leads to the description of watersheds as standard and violent, respectively. At what P-magnitude, this rise will be experienced in a watershed will depend on watershed characteristics affecting the runoff generating potential.

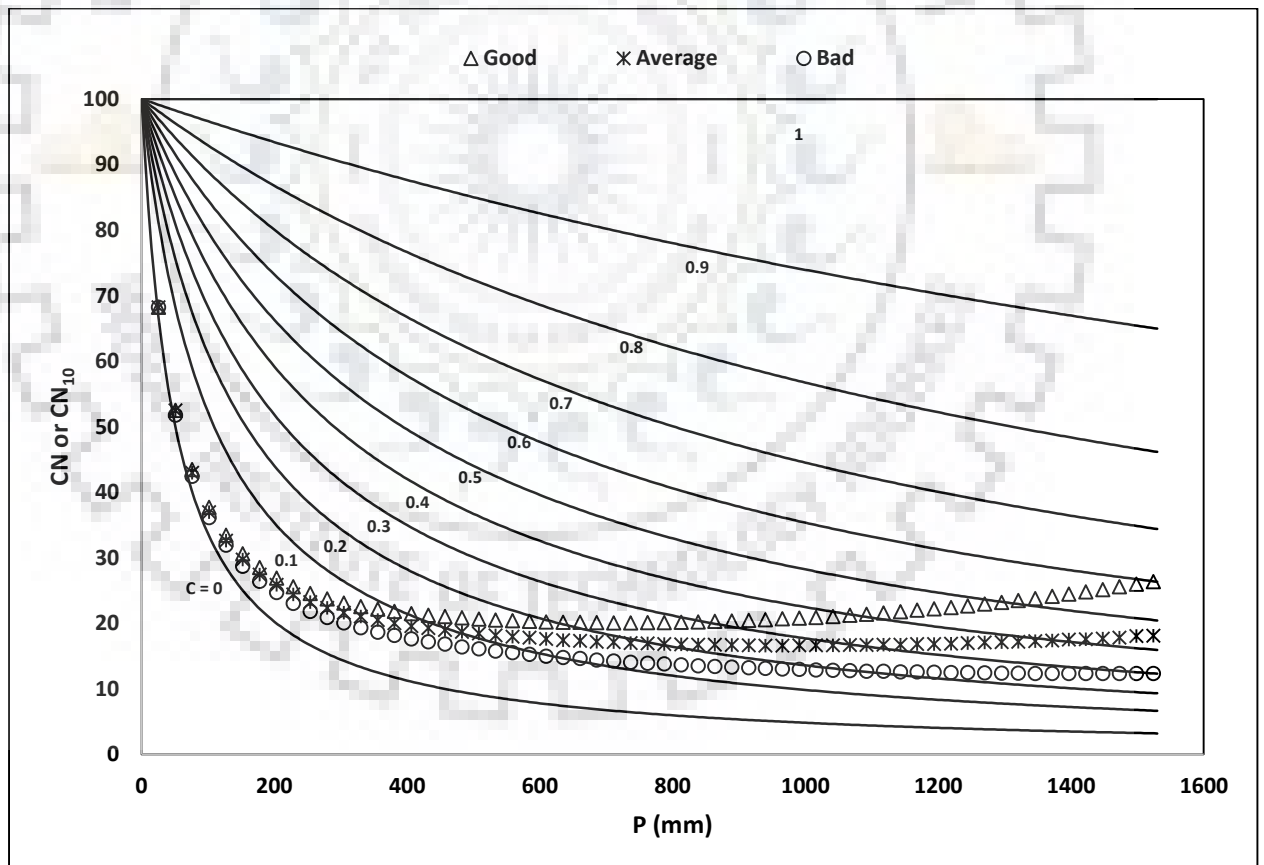


Figure 5.4(a) Plot of Strange data in the existing CN perspective. Third parameter = $C (= Q/P)$.

5.3.3.3 Based on the proposed S-CN mapping

As seen from Fig. 5.4b, the bad (complacent) type behaviour of the watershed closely follows the line $C = 0$. C can however be equal to 0 under three situations: (a) $P \leq 0.2S$, (b) $P = 0$, and (c) $S = \infty$. Here, the second situation is clearly improbable for an event to occur (as $P > 0$) whereas the first and last ones are most likely to prevail. Thus, for $C = 0$, P has always to be less than $0.2S$, and therefore, follow $C = 0$ line. In other words, complacent behaviour is realizable only if it is an absolutely zero runoff potential watershed, an idealized situation. On the other hand, CN values are seen in the same figure to range (12.63, 68.23). Similarly, the data of the average watershed exhibits C to vary from 0.001 to 0.45 and CN values range (16.63, 68.23). The data of Good, Average, and Bad watersheds exhibit C to vary in the range (0.001, 0.6), (0.001, 0.45), and (0.001, 0.3), respectively. Up to the reasonably high rainfall of 254 mm (= 10 inches) (Table 5.3), C -values are seen to range (0.001, 0.043), (0.001, 0.032), and (0.001, 0.021), respectively, indicating all watersheds to be low runoff producing watersheds.

Fig. 5.4b shows CN - P and CN_P - P relations to describe the behaviour of three types of watersheds described by Strange. As seen, CN_P exhibits a more rational behaviour than does CN with increasing P for all three datasets; as P increases, CN_P also increases, and C (not shown) also increases, consistent with the above notion. Considering the above Strange data as observed, the use of both CN and CN_P concepts is shown to describe this data in Fig. 5.6. As seen, CN first decreases with increase in P and then after a certain extent (i.e. $P = 254 \text{ mm} = 10 \text{ inches}$), CN increases with increasing P . Thus, the same CN -concept shows two different types of behaviour with increasing P . It is resolved by plotting CN_P against P (Fig. 5.4b).

Similar to the above, except for cumulative, the Tehri rainfall-runoff data have been categorised so as to represent to good, average, and bad watershed conditions, as described later. These two datasets have been used for performance evaluation of 1 and 2 models described above and summarized in Table 5.2.

The procedure described above was followed to derive CN - P and CN_P - P relations (Table 5.1 and Fig. 5.4b & Fig. 5.5a&b) Strange, and Tehri watershed, as follows:

For Strange (1892) data

For Model 1,

$$CN = 227.29 \times 0.413 \quad (\text{for Good watershed}) \quad (5.16a)$$

$$CN = 134.89P^{0.301} \quad (\text{for Average watershed}) \quad (5.16b)$$

$$CN = 227.29P^{0.413} \quad (\text{for Bad watershed}) \quad (5.16c)$$

These relations can be further improved/simplified significantly by using CN_P in place of CN (for Model 2),

$$CN_p = 0.0343P + 16.435 \quad (\text{for Good watershed}) \quad (5.17a)$$

$$CN_p = 0.0267P + 17.06 \quad (\text{for Average watershed}) \quad (5.17b)$$

$$CN_p = 0.0192P + 17.491 \quad (\text{for Bad watershed}) \quad (5.17c)$$

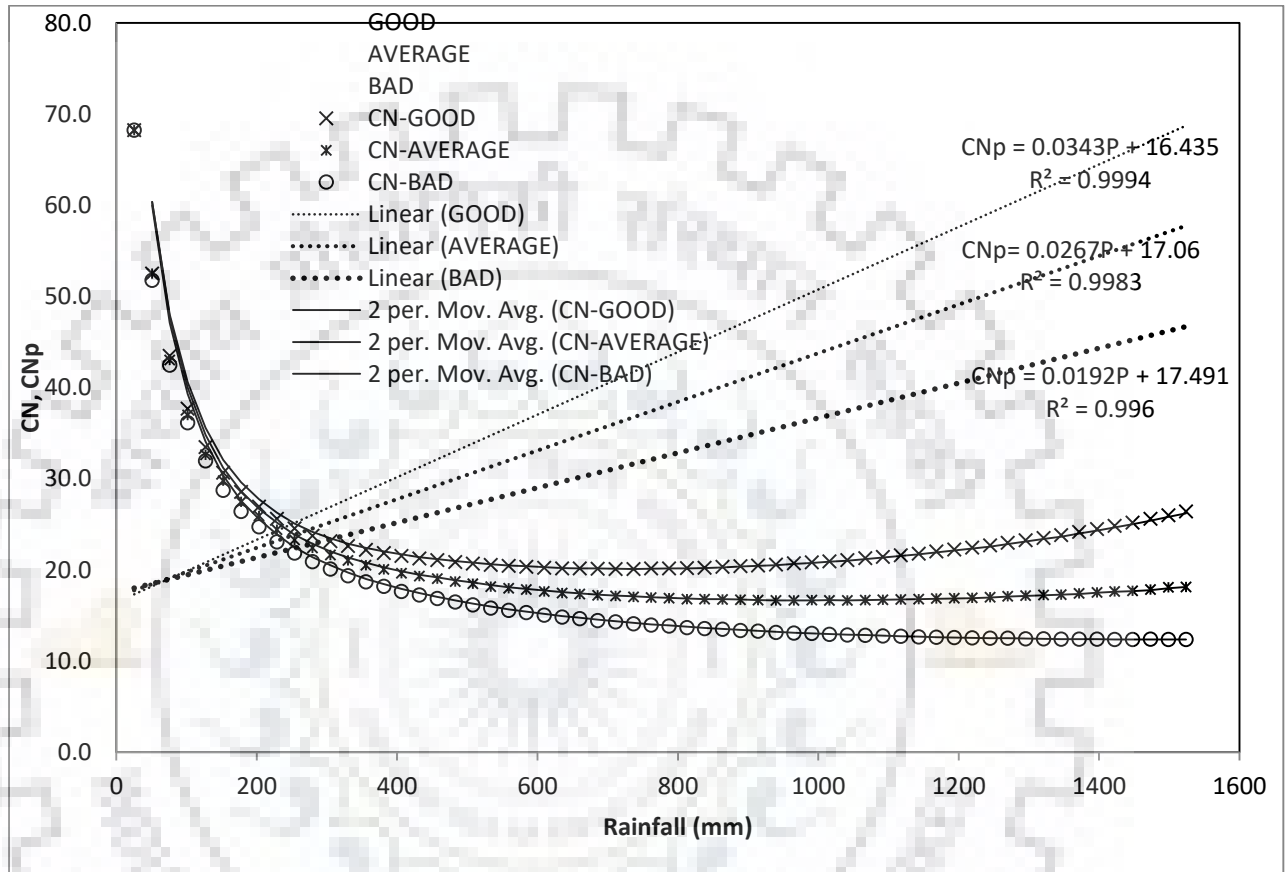


Figure 5.4 (b) CN and CN_P versus P relations for Strange’s datasets. Note: Strange data best fitted with CN using 2 period moving average.

For Tehri Watershed

For Model 1,

$$CN = 0.0007P^2 - 0.3485P + 87.941 \quad (\text{for Good watershed}) \quad (5.18a)$$

$$CN = 0.0013P^2 - 0.3705P + 99.643 \quad (\text{for Average watershed}) \quad (5.18b)$$

$$CN = -2.421 \ln(P) + 104.21 \quad (\text{for Bad watershed}) \quad (5.18c)$$

These relations can be further improved/simplified significantly by using CN_P in place of CN (for Model 2),

$$CN_p = 0.0002P^2 + 0.0023P + 32.61 \quad (\text{for Good watershed}) \quad (5.19a)$$

$$CN_p = 0.0004P^2 + 0.0167P + 48.989 \quad (\text{for Average watershed}) \quad (5.19b)$$

$$CN_p = 1.8527 \ln(P) + 71.899 \quad (\text{for Bad watershed}) \quad (5.19c)$$

In Eqs. 5.16 through 5.19, $0 \leq CN$ or $CN_p \leq 100$, Model 2 is based on Eq. 5.3, and Model 1 on Eq. 4.3 (Chapter 4). The former is the general form of the latter. CN values for both these models are derived from Eq. 4.6 (Chapter 4) to bring all CN-values at one P (=254 mm = 10 inch)-scale.

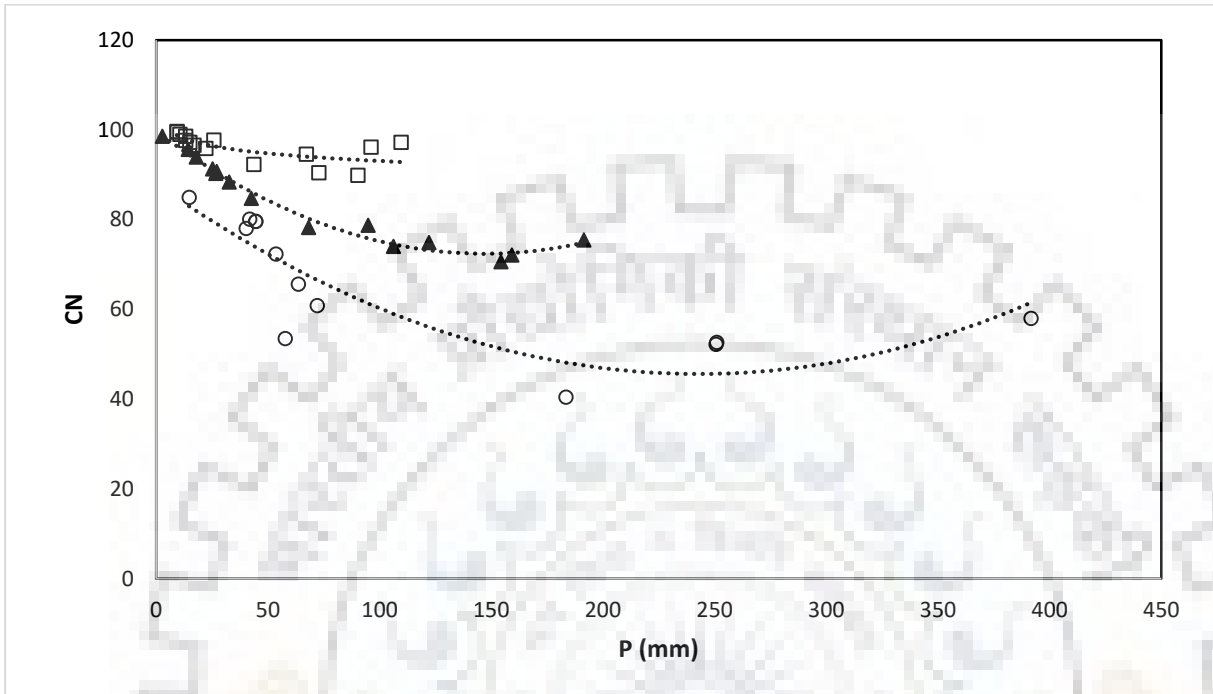


Figure 5.5(a) Plot of Tehri data in the existing CN perspective. Third parameter = $C (= Q/P)$.

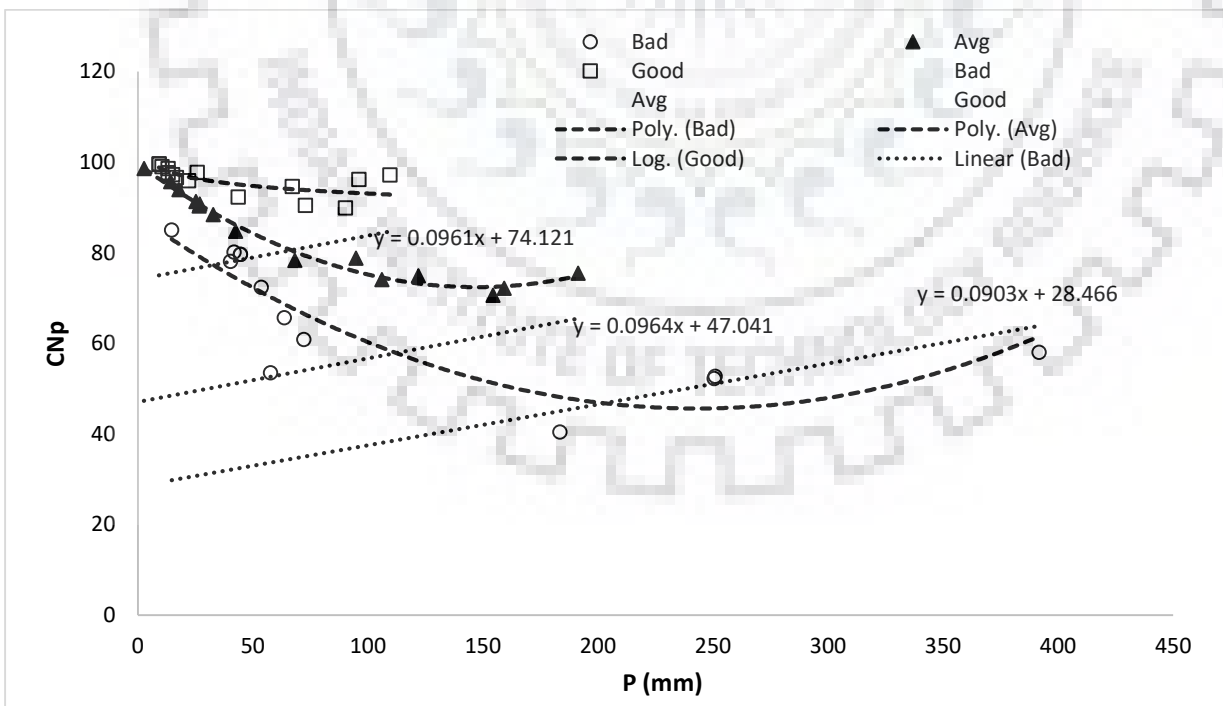


Figure 5.4 (b) CN and CNp versus P relations for Tehri datasets.

5.4 DISCUSSION OF RESULTS

The existing as well as the modified SCS-CN models (Table 5.1) were applied to the data of three study watersheds as discussed above. The performance was evaluated in terms of NSE, RMSE and BIAS, as described in Chapter 4. CN of Models 1 and CN_P of Model 2 were estimated using Eqs. 5.3 & 5.4, respectively. The application results of models are given in Table 5.2 and the results are also graphically shown in Figs. 5.6 to Figs.5.8.

5.4.1 Hawkins Data

As seen from Table 4.2, the violent watershed has the highest ($=0.44$) runoff coefficient (C) (derived from mean values of rainfall and runoff), the complacent the lowest ($=0.003$), and the standard in between these two ($=0.06$). Such order of runoff generating potential is described by CN (or CN_{10}) values derived (for the same $P = 254$ mm) from all model applications except Model 1 (complacent watershed), that is the existing SCS-CN model. This model did not describe the consistent trend because it performed extremely poorly on complacent watershed, perhaps not applicable to such watersheds. Model 2 performed the best of all on complacent, standard and violent watersheds. Bias in Table 2 is presented to indicate whether a model over (positive) - or under (negative)-predicted the runoff.

The application results of Models 1 and 2 indicate that the latter is in general an improvement over the former one, as both performed similarly on violent watershed, and therefore assert that the pre-derived CN_P -P relationship for a watershed can be an improved alternative for runoff predictions using Model 2. In addition, as shown in Fig.5.9, the use of Eq. 5.3 better describes the violent, standard, and complacent watersheds just based on CN_P or C-values.

5.4.2 Strange and Tehri data

Both the models generally performed extremely well on both Strange and Tehri data and their three watershed conditions. For the former, CN ($P=254$ mm) of Model 1 ranges from 30.66 (for Bad watershed) to 23.09 (for Good watershed) for Starnge data. Similarly for Tehri catchment, these values are 90.81 to 44.58.

The application results of Models 1 and 2 indicate that the latter is in general an improvement over the former one and, therefore, assert that the pre-derived CN_P -P relationship for a watershed can be an improved alternative for runoff predictions using Model 2. In addition, as shown in Fig. 6.10, the use of Eq. 5 better describes the Good, Average, and Bad watersheds just based on CN_P or C-values. Thus, in order of preference, all the models are equally well for all watershed

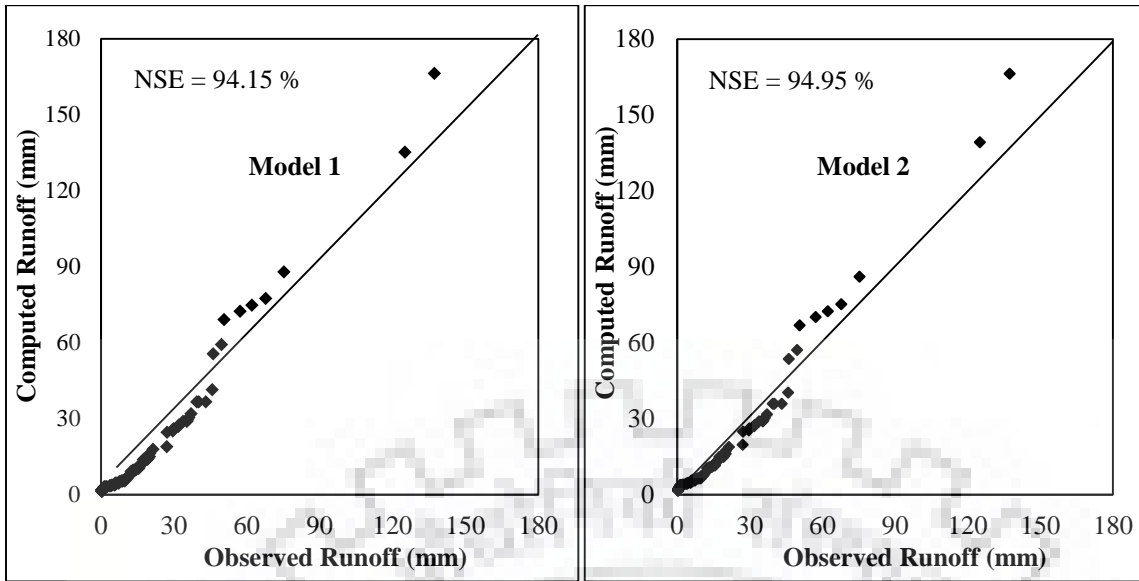
conditions in both cases, indicating their applicability to any duration rainfall values. Between the two, Model 1 is less preferable. For improved applications, mean $C-\lambda$ relationship may be prescribed for a watershed. Model 2 can be preferred if CN_p-P relations are established for watersheds. Notably, Both the models work almost equally well if the data are categorized (using CN_p-P relationship) such that they represent three good, average, and bad watershed conditions.

Table 5.1 Model formulations/procedures.

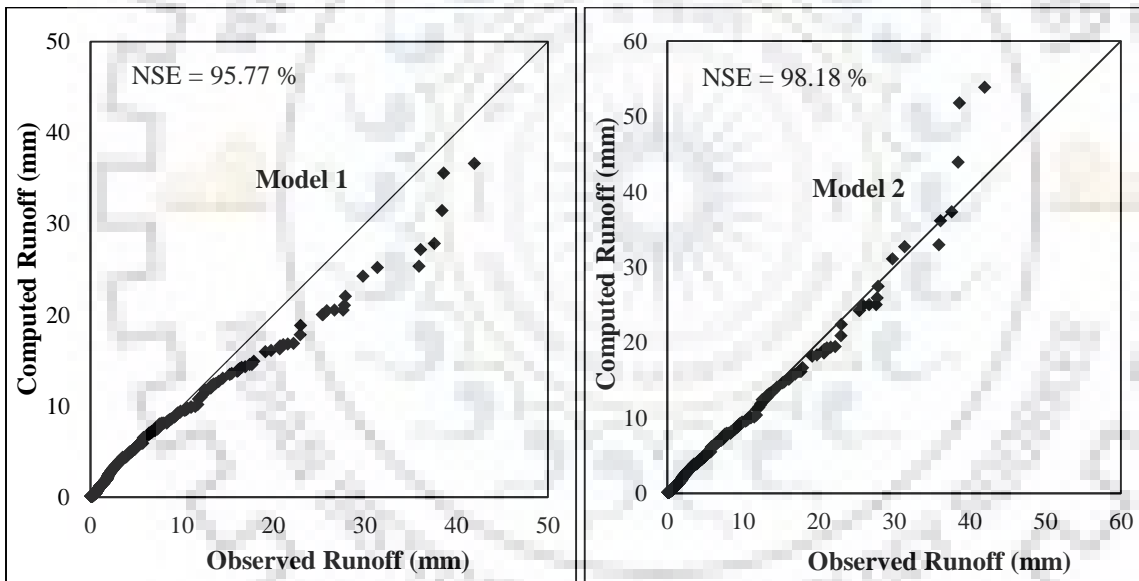
Model No.	Equations	Parameter(s)	Procedure
1	4.2b, 4.3, 4.4 (Chapter 4)	CN (for $P = 254$ mm)	<ul style="list-style-type: none"> a) Determine S from Eq. 4.4 (Chapter 4) for each P-Q dataset for a watershed. b) Determine CN from Eq. 4.3 (Chapter 4). c) Develop a relationship between CN and P for the watershed (Fig. 5.5) for future applications. d) Derive CN from P, then S from Eq. 4.3 (Chapter 4), and then Q from Eq. 4.2b (Chapter 4).
2	4.2b, 4.4 (Chapter 4), 5.3 (or 5.8a)	CN_p (for any value of P)	<ul style="list-style-type: none"> a) Determine S_p from Eq. 4.4 (Chapter 4) for each P-Q dataset for a watershed. b) Determine CN_p from Eq. 5.3 or 5.8a. c) Develop a relationship between CN_p and P for the watershed (Fig. 5.5) for future applications. d) Derive CN_p from P, then S_p from Eq. 5.3 or 5.8a, and then Q from Eq. 4.2b (Chapter 4).

Table 5.2 Performance evaluation of various models. C = Mean runoff/ Mean rainfall.

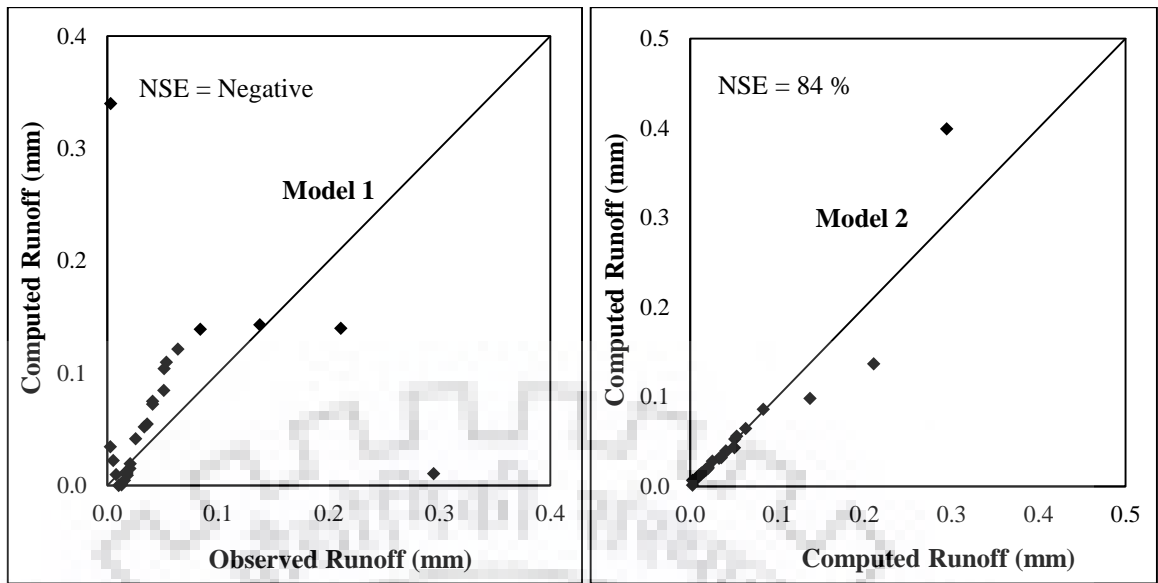
Sl. No.	Watershed Type	C =	Model 1				Model 2			
			CN (for P=254 mm)	NSE	RMSE	BIAS	CNp	NSE	RMSE	BIAS
				(%)	(mm)	(mm)		(%)	(mm)	(mm)
Hawkins (1993)										
1	Violent	0.44	100	94.15	6.00	0.40	100	94.95	5.58	-0.05
2	Standard	0.06	40.01	95.77	1.13	0.12	52.26	98.18	0.74	0.00
3	Complacent	0.003	4.52	Negative	0.09	-0.01	25.10	84.00	0.03	0.00
Strange (1992)										
1	Good	0.38	30.66	94.90		-40.05	25.15	99.98	3.33	-0.27
2	Average	0.28	25.48	96.98		-8.78	23.84	99.95	4.81	0.05
3	Bad	0.19	23.09	99.82		-4.49	22.37	99.82	5.62	0.46
Tehri Watershed										
1	Good	0.76	90.81	96.66	10.97	-0.29	82.16	96.89	10.59	0.49
2	Average	0.47	89.41	99.32	2.68	0.78	79.04	99.27	2.78	-0.62
3	Bad	0.34	44.58	96.97	5.47	-2.57	32.61	96.81	6.78	-3.83



(a)

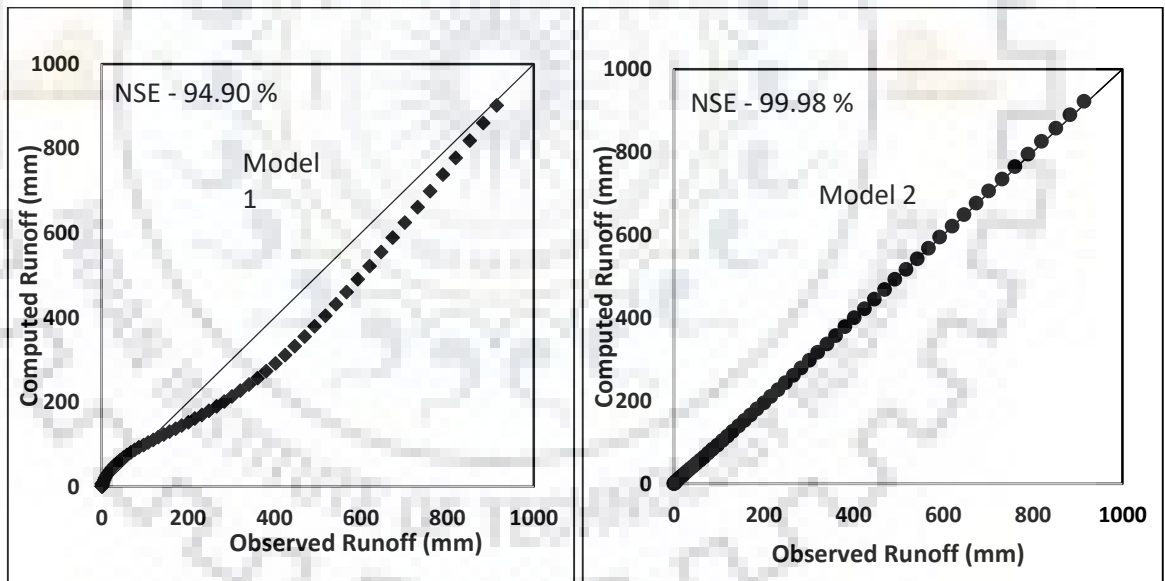


(b)

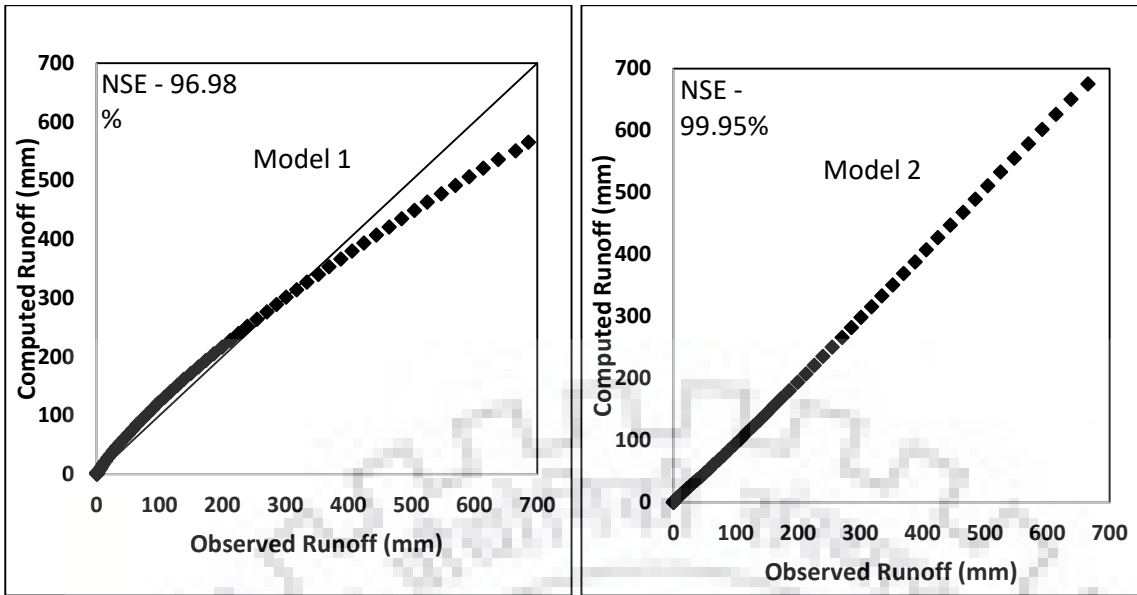


(c)

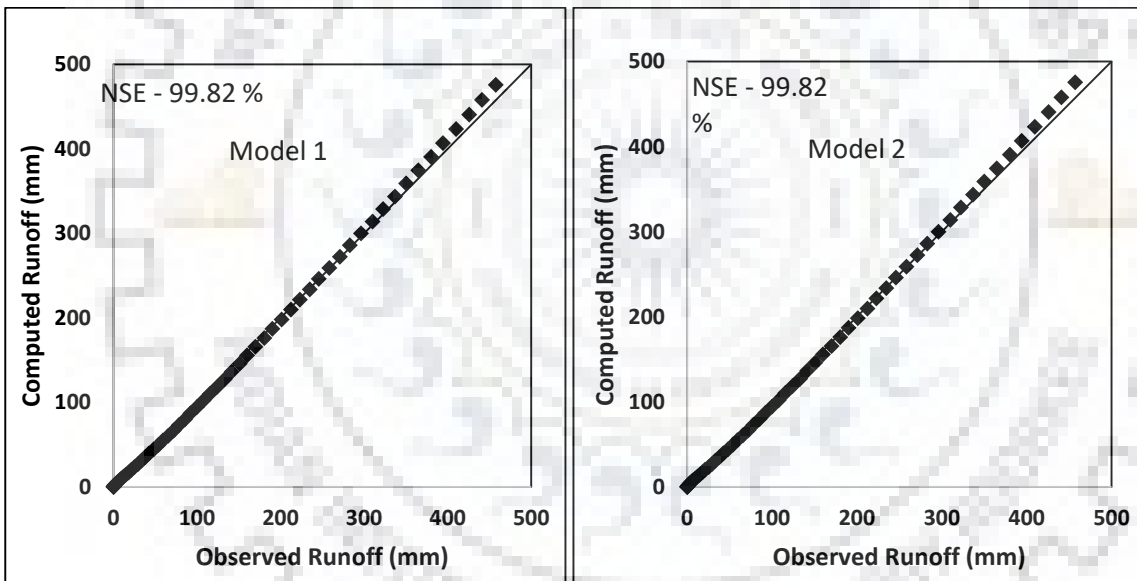
Figure 5.6 Evaluation of Models 1-2 by comparing the computed runoff (mm) with the observed runoff (mm) of (a) Violent, (b) Standard and (c) Complacent watershed (Hawkins, 1993).



(a)

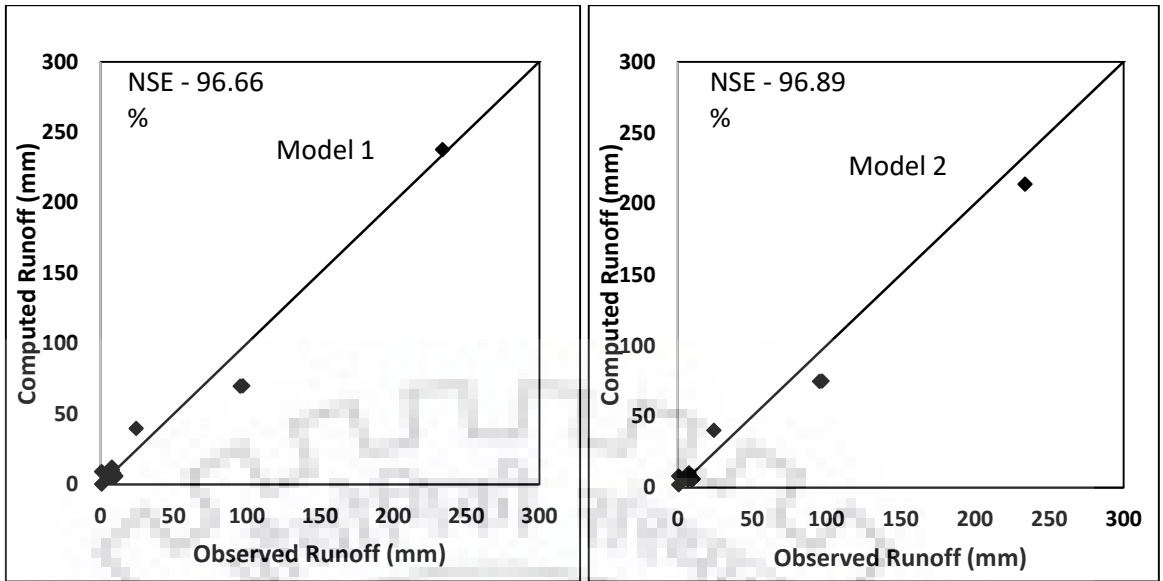


(b)

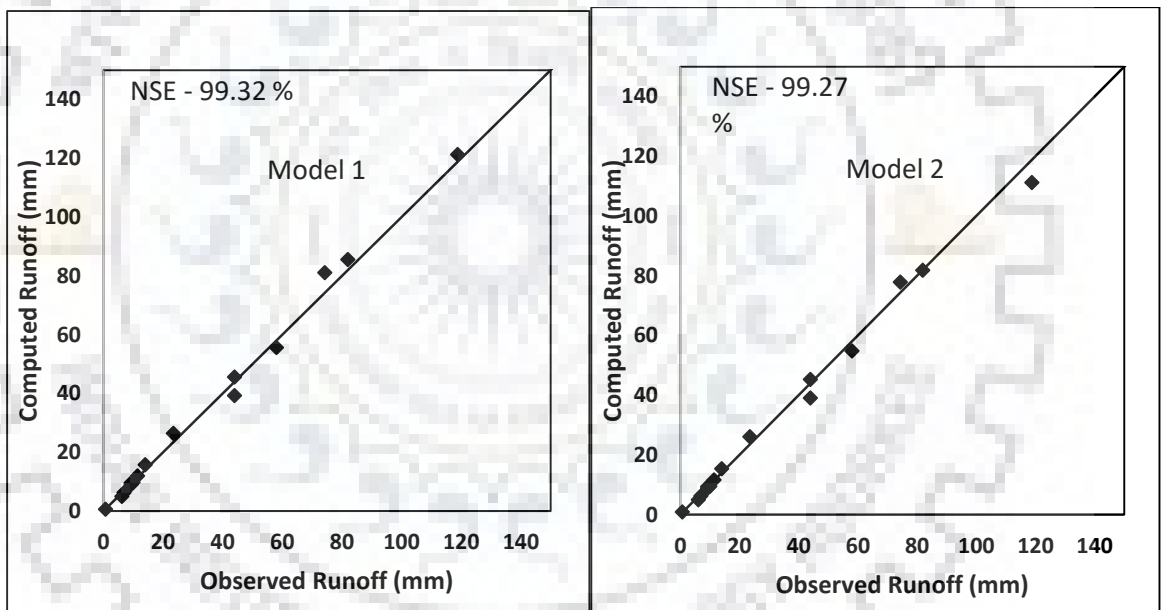


(c)

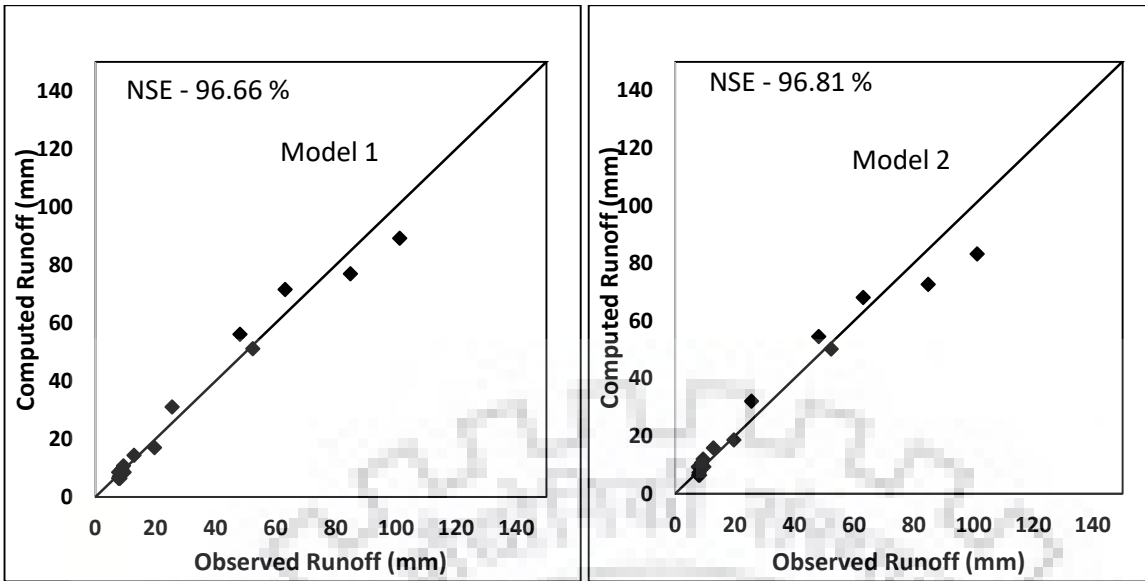
Figure 5.7 Evaluation of Models 1-2 by comparing the computed runoff (mm) with the observed runoff (mm) of (a) Good, (b) Average and (c) Bad watershed (Strange, 1992).



(a)



(b)



(c)

Figure 5.8 Evaluation of Models 1-2 by comparing the computed runoff (mm) with the observed runoff (mm) of (a) Good, (b) Average and (c) Bad watershed (Tehri Watershed).

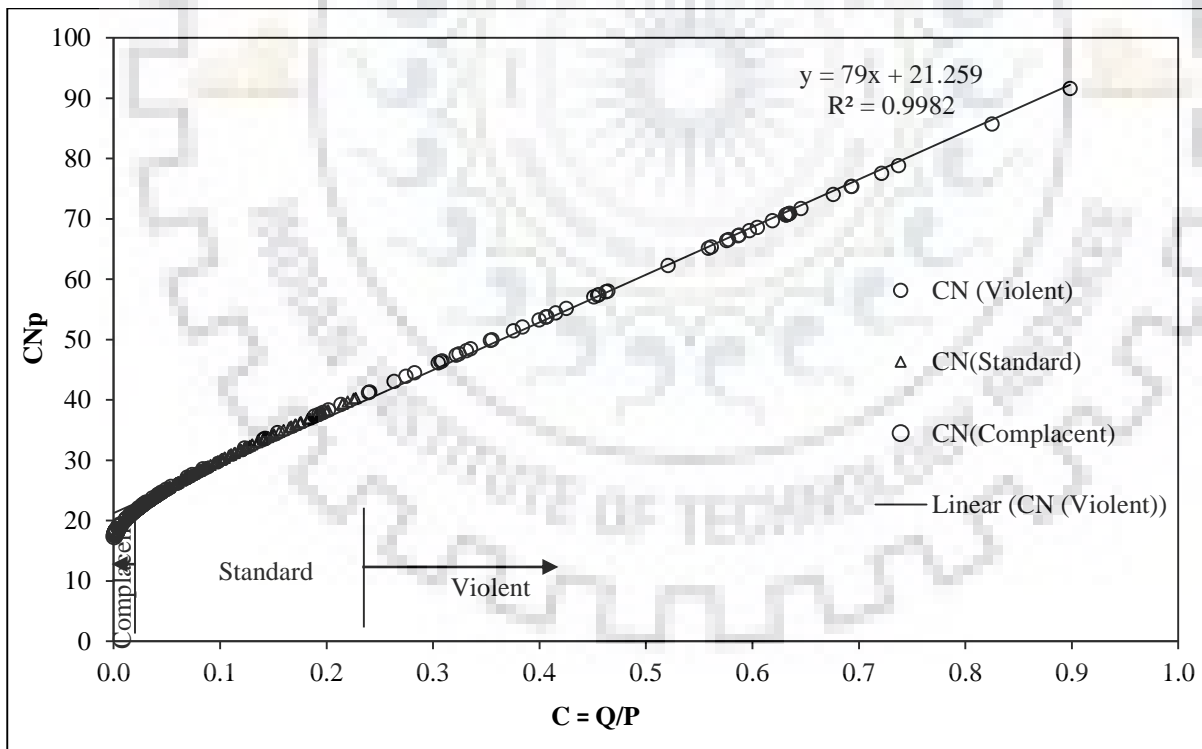
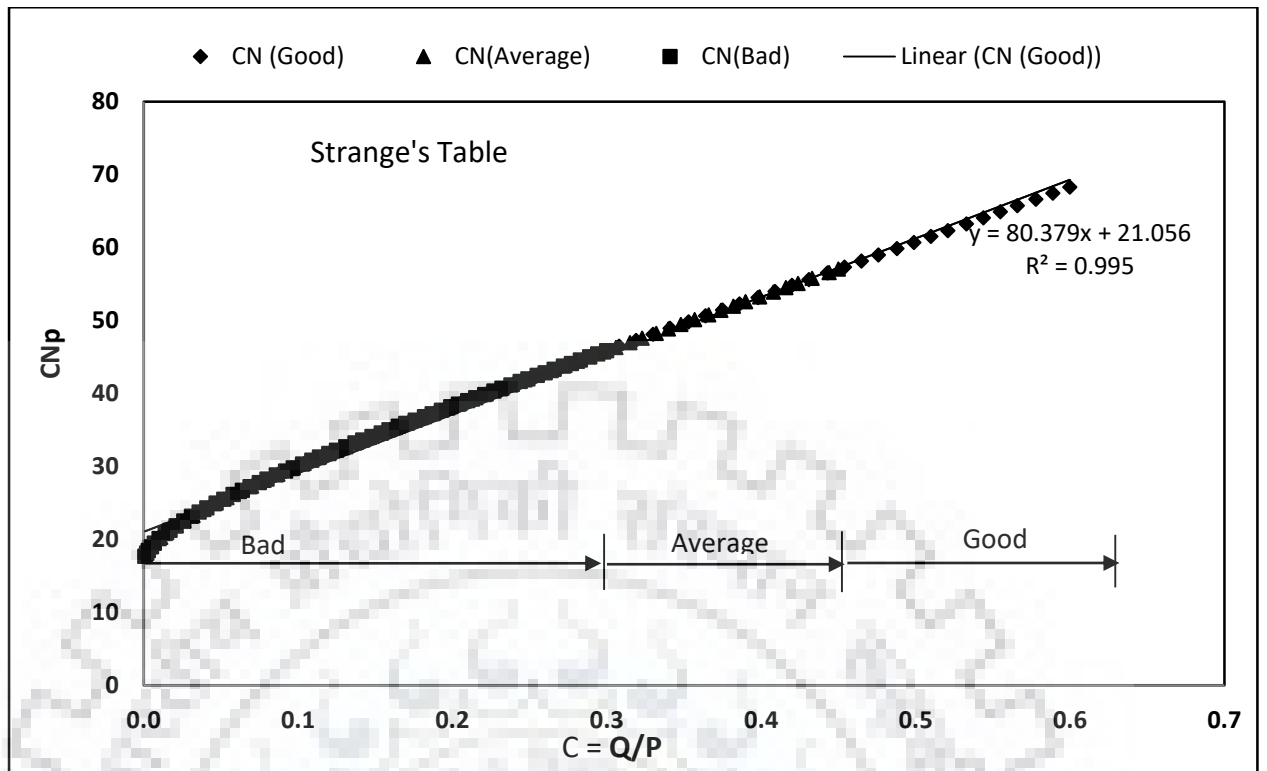
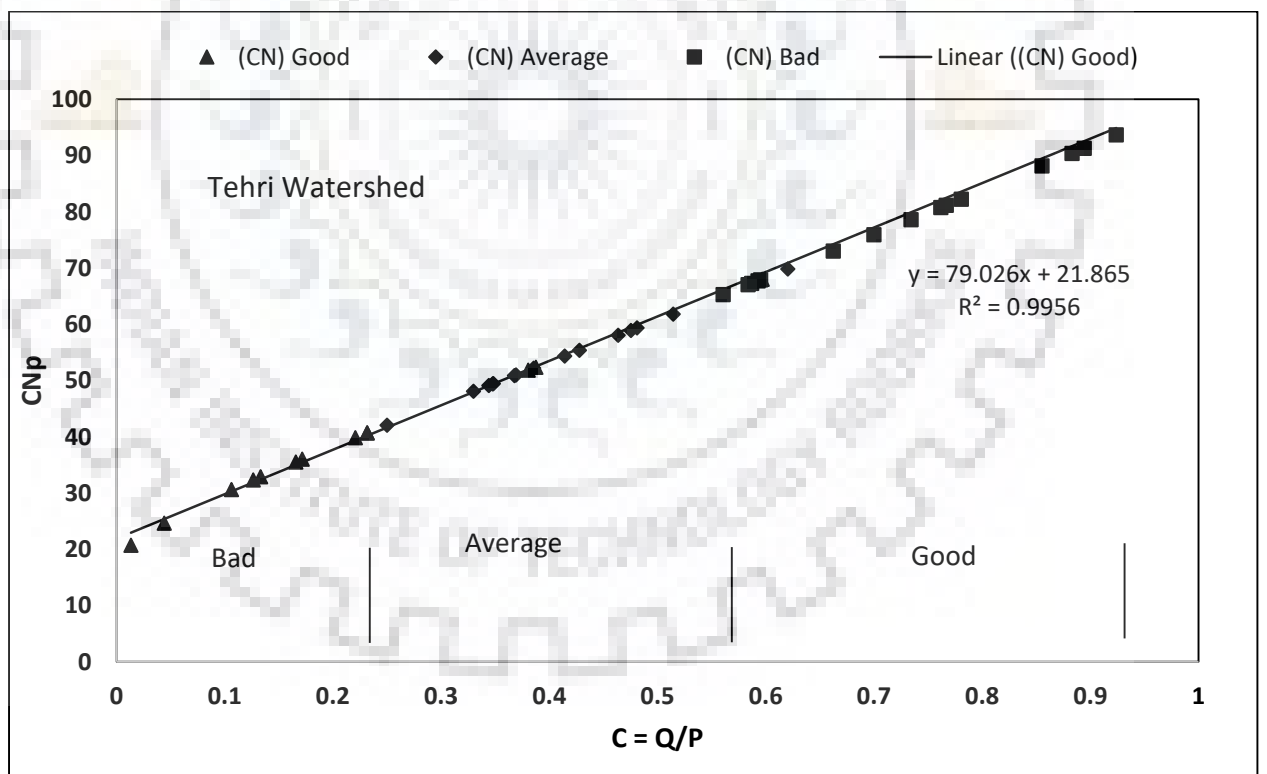


Figure 5.9 C-CNp relationship (Model-2 consisting of Eqs. 4.2b, 4.4 (Chapter 4) and 5.3) description of watershed behaviour (Hawkins, 1993).



(a)



(b)

Figure 5.10 C-CNp relationship (Model-2 consisting of Eqs. 4.2b, 4.4 (Chapter 4) and 5.3) for description of watershed behaviour (Strange data and Tehri watershed).

5.5 SUMMARY AND CONCLUSIONS

In the present chapter, a major modification to the S-CN mapping relationship of the popular SCS-CN methodology was proposed to solve abnormality in watersheds behavior, i.e. complacent, standard, and violent. The proposed modification affectively resolves the abnormalities and supports the general notion that the runoff coefficient (C) (or CN, another form of C) increases with increasing P. This modification also describes the CN_p -P relationship and, in turn, the behavior of three watersheds for growing rainfall. The results show that the pre-derived CN_p -P relationship for a watershed can be an improved alternative for runoff prediction using SCS-CN methodology. These relationships were also derived for Strange and Tehri catchment data and results showed that both the both models performed well on these data sets. The proposed modification also showed an enhanced model performance based on NSE, RMSE and Bias error criteria.

The available description of watersheds behavior as standard, complacent, and violent (Hawkins data) based on the abnormal CN-P behaviour is rectified by proposing an application modification to the existing S-CN mapping, physically justifying the general notion that runoff coefficient (C) (or CN, another form of C) increases with increasing P. For Strange and Tehri data, the description of good, average, and bad watersheds based on decreasing CN trend with increasing P is physically not justifiable as it contrasts the increasing trend of C (or CN) with increasing P. The proposed CN_p -P relation more rationally describes the behaviour of the above three types of watersheds. The prescription of mean $C-\lambda$ (Model 1) and/or CN_p -P (Model 2) relationships for a watershed can improve the application results of the existing SCS-CN methodology significantly.

CN_p values are consistently lower than CN_{10} values for all the three types of watersheds in Starng and Tehri data. However for the Hawkins data, for the complacent and standard watersheds, CN_p values are much lower than CN_{10} values than for the violent watershed. The CN-values based on 254 mm of rainfall (or C values based on mean runoff and mean rainfall values) have the efficacy to distinguish the watersheds for their runoff potentials, a remarkable feature of CN.

Model 2 performed best in all three data sets viz., those of Hawkins, Strange and Tehri. Model 2 performed extremely well in case of complacent watershed, where existing model yields negative efficiency, and the purposed model very high efficiency (84 %).

6.1 INTRODUCTION

Estimates of runoff and sediment yield are necessary for several hydrological issues such as droughts, floods, soil erosion etc. Furthermore, the estimation of reservoir sedimentation has been the subject of several studies since the 1950s. However, this prediction has never been an easy task due to complicated simultaneous processes involved such as sediment transport, erosion and deposition. It is of common knowledge that the sediment yield directly relies upon the direct surface runoff, LULC and soil moisture. In this regard, a silt yield model either estimates the runoff in a lumped manner to calculate total sediment yield from a storm event or, mostly, generates the temporal rainfall-excess rate (or runoff rate) using an appropriate infiltration model to simulate temporally varying sediment rate at the catchment outlet.

For estimating the potential soil erosion and direct surface runoff from small catchments, USLE (Wischmeier and Smith, 1965) and the SCS-CN method (SCS, 1956), respectively, are most popularly and commonly used in the field of hydrology and water resources engineering. A lot of published material and literature is available globally on these methods and their hydrological applications, which has already been discussed earlier (Chapter 2). The works of Singh (1988, 1992), Ponce (1989), and Novotny & Olem (1994) are worth citing. The USLE was developed with an intent to determine yearly soil loss from small plots of an average length of 22 m. Therefore, it may lead to significant errors if applied upon large plots or for a single rainfall event. However, its accuracy is enhanced upon coupling with a rainfall-excess model (Novotny and Olem, 1994). In current practice, USLE collects hydrological information from a rainfall-runoff model and use it to estimate the soil loss potential and the consequent sediment yield (Williams, 1975; Knisel, 1980; Leonard et al., 1987; Young et al., 1987; Rode and Frede, 1997), which is significant in watershed management. The effects of erosion on the environment, especially for water quality was studied by Clark et al. (1985), which is a remarkable contribution.

The USLE and SCS-CN method were first coupled by Mishra et al. (2006) for modeling rain-storm generated sediment yield from a watershed. Both USLE and SCS-CN models share common watershed characteristics like rainfall, soil type, land use and antecedent soil moisture condition etc. to account for direct surface runoff and potential soil erosion. The coupling is based on three hypotheses:

- (a) The runoff coefficient (C) is equal to the degree of saturation (Sr),
- (b) USLE parameters can be expressed in terms of potential maximum retention (S), and
- (c) The sediment delivery ratio (DR) is equal to the runoff coefficient (C).

Some more researchers (Jasrotia et al., 2002; Garen & Moore, 2005; Tyagi et al., 2008; Singh et al., 2008; Bhunya et al., 2010; and Gao et.al., 2012) explore the applicability of SCS-CN method in the field of soil erosion, sedimentation and water quality. Thus, the present chapter aims at to check the applicability USLE-based SCS-CN models for computing total sediment yield from a storm event. The sediment yield models are applied to rainfall-runoff-sediment yield data observed from 09 experimental watersheds (plot size 12×3 m²) of different land uses, soils, and slopes.

6.2 METHODOLOGY

The SCS-CN method is discussed in detail in Chapter 4. This chapter focuses on the explanation of USLE and its coupling with SCS-CN method to formulate a sediment yield model.

6.2.1 Universal Soil Loss Equation

The erosion plot data used by Musgrave (1947) and the US Weather Bureau rainfall data was re-evaluated by Wischmeier and Smith (1958), which finally led to the development of USLE. Based on over 10,000 plot years of natural and simulated runoff data, USLE was developed by Wischmeier and Smith (1965). USLE is expressed as:

$$A=RKLSCP \quad (6.1)$$

Wischmeier and Smith (1965) proposed a method for estimating the value of R in USLE, which can be applied to estimate only the annual erosion, and hence, its application over a single rainfall event would produce erroneous results (Haan et al., 1994). Foster et al. (1977b) proposed a modified equation for computation of R that will be applicable to individual storm events as:

$$R = 0.5Rr + 0.35Qq^{1/3} \quad (6.2)$$

As q (peak runoff rate) has more liability towards the removal of soil particles than the runoff volume (Q), a decline in its peak due to vegetative cover or any other change in physical characteristic may result in reduced sediment yield (Williams and Berndt, 1977). Renard et al. (1991) proposed a Revised USLE (RUSLE) method to compute R-values for distinct storm events. In another approach, Williams (1975) replaced R-factor of USLE by runoff factor to compute sediment yield for distinct runoff events.

6.2.2 Computation of Sediment Yield

In order to determine the sediment yield from the computed potential erosion, sediment delivery ratio (DR) is needed. Erosion and sediment yield are quite different terms, for the erosion can be explained as the potential erosion equivalent to the sum of upland (sheet) erosion whereas sediment yield refers to the quantity (volume) of sediment in the receiving water body for a particular period of time. Vegetation increases porosity by its root system, dissipates rainfall energy, reduces the soil moisture by ET and binds the soil to affect the sediment yield. DR being dimensionless entity can be expressed mathematically as:

$$DR = Y/A \quad (6.3)$$

where Y is the total sediment yield and A is the total potential erosion in the same contributing watershed. The value of DR lies between 0 and 1. Higher values of DR are obtained for smaller watersheds while its value decreases with increase in size of the watershed (Roehl, 1962).

Relationship between non-point pollution and soil loss was developed and calibrated with DR in order to minimize the difference between estimates of sediment yield and computed sheet erosion (through USLE) (Novotny and Olem, 1994). DR is affected by a number of processes that influence deposition of eroded sediments (permanent or ephemeral) in any watershed. These processes are significantly intermittent and variable in nature and can only be described statistically. The correlation between DR and the runoff coefficient implies a substantial effect of infiltration and other losses on the magnitude of DR (Novotny and Olem, 1994). A number of factors influence the magnitude of DR, namely, vegetation, infiltration, depression, overland flow energy, rainfall impact, drainage, change of slope of overland flow and ponding storage (Novotny et al., 1979, 1986; Novotny, 1980; Novotny and Chesters, 1989). As these factors show a temporal variation across the year, the magnitude of DR also varies accordingly.

Both erodibility and permeability of soil determine the soil texture. Soil permeability governs infiltration, which effects soil erosion and generation of runoff. Erosion is basically influenced by surface runoff (Gottschalk, 1964; Langbein and Schumm, 1958; Leopold et al., 1964; Singh, 1985; Walling and Webb, 1983). As per SCS-CN concept, if wind effects are ignored, runoff generation is closely related with infiltration. Hence, runoff generation and soil erosion are highly interrelated. In the practical world, the peak rate of runoff and its volume are estimated using SCS-CN method (Blaszczynski, 2003) or any apt hydrological model. Williams (1975) and Foster et al. (1977b) utilized them for estimation of sediment yield and potential erosion, respectively.

6.3 FORMULATION OF SEDIMENT YIELD MODEL

As stated above, the coupling of SCS-CN method and USLE based on three hypotheses (Mishra et al., 2006): (a) the SCS-CN method can be reformulated using the $C = S_r$ concept; (b) the USLE can be signified using the SCS-CN parameter S ; and (c) the delivery ratio (DR) can be equated to C or S_r . These hypotheses are described below.

6.3.1 Hypothesis: $C = S_r$

The basic SCS-CN proportionality hypothesis (Eq. 4.1b, Chapter 4) can be expressed as runoff factor for $I_a = 0$, i.e. immediate ponding situation,

$$C = Q/P = S_r \quad (6.4)$$

where C = runoff coefficient and S_r = degree of saturation) (Mishra and Singh, 2003), which is defined using the soil-water-air schematic diagram shown in Fig. 6.1 as:

$$\frac{Q}{P} = \frac{F}{S} = C \quad (6.5)$$

$$C = S_r = \frac{F}{S} = \frac{V_w}{V_v} \quad (6.6)$$

where V_v is volume of voids and V_w is volume of water present in form of infiltrated moisture. Eq. 6.6 holds for S of a completely dry AMC, i.e. for $V_v = S_1$, where S_1 = potential maximum retention S of AMC 1. V_a is the volume of air after infiltration and V_s is the volume of the solids as shown in Fig. 6.1. Thus, sum of V_v and V_s is equal to the total volume V . For a unit surface area these quantities can also be expressed in terms of depth.

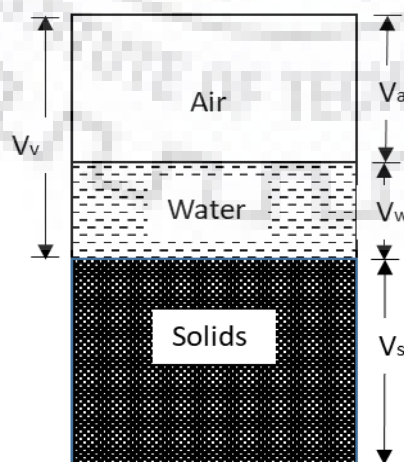


Figure 6.1: Schematic diagram showing soil-water-air

6.3.2 Hypothesis: A - S Relationship

The Universal Soil Loss Equation (Eq. 6.1) calculates the potential soil erosion (A) from a watershed. Since A is the potential mass of soil per unit watershed area, it is equivalent to the product of the volume of solids per unit surface area (V_s) and the density of solids (ρ_s). According to Mishra et al. (2006), USLE parameters can be expressed in terms of potential maximum retention (S) mathematically, which forms the second hypothesis. They gave a relationship between actual potential maximum erosion and actual potential maximum retention as:

$$\frac{A}{S} = \frac{(1-n)}{n} \rho_s \quad (6.7a)$$

or

$$A = \frac{S(1-n)}{n} \rho_s \quad (6.7b)$$

where A is the actual potential maximum erosion, S is the actual potential maximum retention, n is the porosity of soil, and ρ_s is the density of solids. In Eq. 6.7a, left hand side term can be a constant value for a watershed. It further allows Eq. 6.7b to couple with Eq. 6.1, leading to

$$RKLSCP = \frac{S(1-n)\rho_s}{n} \quad (6.8)$$

From Eq. 6.8, it is clear that the actual potential maximum erosion (A) depends on n , ρ_s , and S for a watershed. Since n and ρ_s are constant for a soil, the potential erosion (A) is directly related with potential retention (S) of a watershed. The latter relies on a number factors governing the curve number (CN) (Chapter 4). In the form of the actual potential maximum erodible soil depth (V_{pe}), Eq. 6.8 can be also written as:

$$V_{pe} = (1/\rho_s)RKLSCP + S \quad (6.9)$$

From Eq. 6.9, it is possible to determine V_{pe} of a watershed by using NEH-4 tables and USLE. The description of A based on catchment characteristics in the form of S and the soil particles is presented in Eq. 6.7b. The important factors over which the erodibility of unconsolidated geological materials (sand dunes, river deposits, soil etc.) depends are water content, composition of material, particle size/texture and structure of the material, and the existence or nonexistence of protective surface cover (Novotny and Olem 1994). Moreover, the coarse textured soils are highly erodible due to less chemical and clay content. The interdependence of USLE derived 'A' and SCS-CN parameter 'S' is presented in Eq. 6.8.

6.3.3 Hypothesis: DR = C

Similar to the SCS-CN proportional equality (or $C = S_r$) concept, it is possible to extend it for sediment delivery ratio, DR, as:

$$C = S_r = DR \quad (6.10)$$

in which all variables range from 0 to 1.

6.3.4 Coupling of the SCS-CN Method with USLE

Initial abstraction $I_a = 0$, Eq. 6.10 can be rewritten as:

$$\frac{Q}{P} = \frac{F}{S} = \frac{P}{P+S} = \frac{Y}{A} \quad (6.11)$$

Thus, sediment yield Y can be described by Eq. 6.11 as:

$$Y = CA \quad (6.12)$$

It is clear from Eq. 6.12 that the sediment yield (Y) is directly proportional to the potential maximum erosion (A), while the runoff factor (C) is the constant of proportionality.

Alternatively,

$$Y = \frac{AP}{P+S} \quad (6.13)$$

Above equation designated as model 1 for estimation of sediment yield.

Thus, the actual amount of sediment yield Y increases with the increasing rainfall, for given catchment characteristics, A and S . This concludes that the higher the rainfall, the higher will be the sediment erosion and its transport and hence higher the sediment yield, and vice versa. As $S \rightarrow 0$ (or $CN \rightarrow 100$), $Y \rightarrow A$ since $Q \rightarrow P$. Similarly, as $S \rightarrow \infty$ (or $CN \rightarrow 0$), $Y \rightarrow 0$ since $Q \rightarrow 0$. Here, it is noted that the condition Y approaches 0 does not mean that A approaches 0, rather it is due to the condition that C approaches 0. It also shows that the major factor affecting sediment yield is direct surface runoff.

Furthermore, for a given watershed, the A/S ratio is constant as shown in Eq. 6.7a. Thus, Eq. 6.11 describes the basic theory of the rainfall-sediment yield model as a proportional equality which makes the ratio of actual potential maximum erosion (A) to actual potential maximum retention (S) equal to the ratio of actual erosion (sediment yield) to the actual retention (infiltration). Expressed mathematically,

$$\frac{A}{S} = \frac{Y}{P} = \text{Constant} \quad (6.14)$$

The ratio (= constant) depends on the soil mass of the watershed.

If the initial abstraction (I_a) incorporated in Eq. 6.13, the equation can be re-written as:

$$Y = \frac{(P - I_a)A}{P - I_a + S} \quad (6.15)$$

Taking $I_a = 0.2S$, Eq. 6.15 leads to

$$Y = \frac{(P - 0.2S)A}{P + 0.8S} \quad (6.16)$$

Eq. 6.15 and 6.16 designated as model 2 and model 3.

Eq. 6.15 shows that the sediment yield varies inversely with the initial abstraction. Mishra et al. (2016) proposed 09 rainfall - runoff and rainfall - sediment yield models incorporating initial abstraction, antecedent moisture and initial flush with Eq. 6.13. In the present study, only three rainfall-sediment yield and rainfall-runoff models are considered and these are shown in Table 6.1.

6.4 PROPOSED SEDIMENT YIELD MODEL

The proposed modification in SCS-CN method is discussed in detail in Chapter 4. In this chapter, USLE is coupled with the proposed modification of the SCS-CN method to formulate a new sediment yield model. The proposed model is mathematically expressed (for $I_a = 0$) as:

$$Q = \frac{P^2}{P + S_o e^{-\alpha P}} \quad (6.17)$$

Incorporating potential maximum erosion (A), Eq. 6.17 can be re-written as:

$$Y = \frac{AP}{P + S_o e^{-\alpha P}} \quad (6.18)$$

Eq. 6.17 and Eq. 6.18 are designated as PS1 for estimation of sediment yield, and PR1 for runoff depth. Similarly, two more models for estimation of both sediment yield and runoff have been proposed and shown in Table 6.1. The results due to the existing (Mishra and Singh, 2006) are compared with those due to Proposed models (Table 6.3 to 6.5).

Table 6.1: Formulation of Rainfall-Sediment Yield and Rainfall-Runoff Models.

Model	Rainfall-sediment yield models	Model	Rainfall-runoff models
Existing (Mishra and Singh, 2006)			

S1	$Y = \frac{AP}{P+S}$	R1	$Q = \frac{P^2}{P+S}$
S2	$Y = \frac{A(P-0.2S)}{P+0.8S}$	R2	$Q = \frac{(P-0.2S)^2}{P+0.8S}$
S3	$Y = \frac{A(P-\lambda S)}{P+(1-\lambda)S}$	R3	$Q = \frac{(P-\lambda S)^2}{P+(1-\lambda)S}$
Proposed			
PS1	$Y = \frac{AP}{P+S_0e^{-\alpha P}}$	PR1	$Y = \frac{P^2}{P+S_0e^{-\alpha P}}$
PS2	$Y = \frac{A(P-0.2S_0e^{-\alpha P})}{P+0.8S_0e^{-\alpha P}}$	PR2	$Y = \frac{(P-0.2S_0e^{-\alpha P})^2}{P+0.8S_0e^{-\alpha P}}$
PS3	$Y = \frac{A(P-\lambda S_0e^{-\alpha P})}{P+(1-\lambda)S_0e^{-\alpha P}}$	PR3	$Y = \frac{(P-\lambda S_0e^{-\alpha P})^2}{P+(1-\lambda)S_0e^{-\alpha P}}$

6.5 APPLICATION

6.5.1 Data Used

The data used in the present study were derived from the nine experimental plots, which contain three land slopes (8%, 12% and 16%) and three types of land uses (maize, finger millet and fallow land). The description of study area has been provided in Chapter 3. Rainfall-runoff-sediment yield data collected during monsoon season in years 2016 and 2017. In total, 31 events are observed in 2016, and 40 events in 2017. For this research purpose, the events having rainfall less than 10 mm were eliminated, and thus, 17 events of 2016 and 19 events of 2017 (total events = 40) produced runoff and these have been used in testing of the above discussed S1-S3 & R1-R3 and PS1-PS3 & PR1-PR3 models (Table 6.1).

6.5.2 Model Formulations and Parameter estimation

Table 6.1 shows 12 models including six existing (S1 to S3 sediment and R1 to R3 runoff) models and six proposed (PS1 to PS3 rainfall-sediment and PR1-PR3 rainfall-runoff) models and these are used in this study. From the table, models S1 and R1 considered $I_a = 0$ (by eliminating initial abstraction I_a , antecedent moisture M , and initial flush I_f). Models S2 and R2 considered only initial abstraction $I_a = \lambda S$, where $\lambda = 0.2$ and Model S3 and R3 allowed λ to vary for watersheds between 0 to ∞ . The proposed models (PR1) have two parameters different from the existing models, S_0 is the maximum possible amount of infiltration or the potential maximum space available for moisture retention and α is the decay constant. In the proposed models, parameter S_0 is introduced in place of S of the existing models and it varies from 0 to ∞ . All rainfall-sediment yield models have parameters similar to rainfall-runoff models, except potential maximum erosion (A). Table 6.2 shows the models and their parameters.

Table 6.2 Model procedures of Rainfall-Sediment Yield and rainfall-Runoff models.

Model	Parameters	Model	Parameter(s)
S1	A, S (or CN)	R1	S (or CN)
S2	A, S (or CN)	R2	S (or CN)
S3	A, λ , S (or CN _o)	R3	λ , S (or CN _o)
PS1	A, α , S _o (or CN _o)	PR1	α , S _o (or CN _o)
PS2	A, α , S _o (or CN _o)	PR2	α , S _o (or CN _o)
PS3	A, α , λ , S _o (or CN _o)	PR3	α , λ , S _o (or CN _o)

Model parameters were optimized using the Solver routine of the Microsoft Excel software. Constraining all parameters to be greater than zero in model applications, their initial estimates were set by trial and error such that the resulting model efficiency is maximized. The model performance is evaluated using the Goodness of Fit statistic and Nash and Sutcliffe efficiency.

6.6 RESULTS AND DISCUSSION

6.6.1 Development of Sediment Yield - Runoff Relationship

The relationship between runoff and sediment yield was established using the observed runoff-sediment data. The data were collected for storm events during the monsoon period (2016 and 2017) from the experimental plots of the above three slopes (8%, 12% and 16%) having fallow land, maize and finger millet crops. The sediment rating curves were drawn between the observed sediment and observed runoff for the plots of different slopes as shown in Figs. 6.2 to 6.4. Due to inconsistency reasons, the observed data of 28.06.2017 was excluded from analysis.

It can be seen from Figs. 6.2 to 6.4 that the trend of increase in sediment yield (mass) with runoff and slope is same for all land uses, viz., maize, finger millet, and fallow land. In other words, for a given slope, as the runoff increases, the sediment yield increases, and vice versa. The rate of increase in sediment yield with runoff is sharper for greater slope, and vice versa. It can also be inferred from Figs. 6.2 to 6.4 that higher density and higher canopy crop (Finger millet) exhibit lower runoff and sediment yield. It can be witnessed from these figures that the coefficient of determination (R^2) is higher in the year 2016 than 2017. For 2016, R^2 values of maize for 8%, 12% and 16% slopes are 0.50, 0.45 and 0.77, respectively. Similarly, for 2017, these are 0.56, 0.34 and 0.24 for 8%, 12%

and 16% slopes. In case of Finger millet, R^2 are 0.32, 0.41, 0.77 (for year 2016) and 0.12, 0.12, 15 (for year 2017) respectively for slopes of 8%, 12% and 16%. Similarly, for Fallow land, R^2 values are 0.78, 0.44 and 0.79 for year 2016 and 0.061, 0.33, 0.15 for year 2017.

Similar to the above, sediment rating curves for varied land uses are shown in Figs. 6.5 to 6.7 for years 2016 and 2017. These rating curves can be used for estimation of direct sediment yield for a given runoff depth. From Figs. 6.5 to 6.7, it can be seen that fallow land shows the higher correlation compared to other two crops on all slopes in both years. The maize and fallow land generated approximately similar amount of runoff and sediment in high slopes (12% and 16%). In 2017, the correlation was poorer than that in 2016. The lower slope generated low runoff and sediment, and vice versa. The table 6.3 to 6.4 shows the maximum potential retention (S) and curve number (CN) calculated from the observed rainfall and runoff.

6.6.2 Model Calibration and Verification

The existing as well as the proposed SCS-CN models were tested with observed sediment and runoff data. Model performance was evaluated in terms of Nash-Sutcliffe Efficiency (NSE) and Goodness of fit statistic. The parameters of rainfall-runoff models were optimized using the excel Solver for maximum NSE. In case of rainfall-sediment yield model, the initial optimization results yielded very high values of S (or S_0). Therefore, the value of S (or S_0) was selected by trial and error while the other parameters were optimized for each step until the efficiency is maximized. The final optimized values of model parameters and the resulting efficiencies or NSEs are presented in Tables 6.3 to 6.5 and graphically in Figs. 6.8 to 6.10. It can be seen from these figures that the proposed models (PS1 and PS3) have performed much better than the existing models (S1 and S3), and significantly better than S2 with $\lambda = 0.2$ in both years 2016 and 2017.

Tables 6.3 to 6.5 show the optimized parameters of all rainfall-sediment yield models and rainfall-runoff models. All the models were tested for data sets of both years 2016 and 2017. The parameters of rainfall-sediment yield model and rainfall-runoff model were optimized separately. Models S1, S2, S3 and PS1, PS2, PS3 determine sediment yield using rainfall only, i.e. ignoring the direct involvement of the observed runoff. The optimized maximum potential erosion (A) are also estimated which is impossible to measure in field. It can be observed from these tables that higher slope plots generated higher sediment yield and runoff. From Table 6.5, in case of existing sediment yield models, the value of λ ranged from 0.11 to 0.23 in 2016, and from 0.07 to 0.10 in 2017 in their application to data of all the plots. In case of the proposed models, λ varied from 0.03 to 0.1 in 2016 and from 0 to 0.01 in 2017. The decay coefficient (α) is almost zero for

rainfall-runoff model (PR3) and it however lies between 0.03 and 0.14 in 2016 and 0.02 and 0.05 in 2017 in case of the proposed rainfall-sediment yield model (PS3). It implies that So approaches (or equal to) S in case of rainfall-runoff models whereas it is non-zero in case of rainfall-sediment models, a finding of the study.

The proposed models resulted into highest NSE values in all land uses and slopes and in both years. Figs. 6.11 to 6.13 shows a correlation between the CN-values optimized using rainfall-sediment yield and rainfall-sediment yield models. From Figs. 6.11, the highest R^2 ($=0.84$) was obtained for model S1 in the year 2016. Models S2 and PS2 yield approximately similar correlation of CN derived from rainfall-runoff and rainfall-sediment models (Fig. 6.12). From Fig. 6.13, R^2 for the proposed (PS3 and PR3) model is higher (0.65) than the existing (0.38) S3 and R3 models, which exhibited lowest correlation 0.10 for the year 2016.

Consistent with Mishra and Singh (2003), it is in order to investigate the variation of A/S ratio, as shown in Tables 6.3 to 6.5, which, according to Eq. 6.7a, should be a constant value for a watershed. In these tables, A/S ratio ranged from 0.06-0.68 for 2016 and 0.18-0.28 from 2017 kg/mm for existing model (S1), from 0.10-0.87 for 2016 and from 0.11-0.53 for 2017 for model (S2), from 0.08-0.81 for 2016 and from 0.10-0.38 for 2017 for model (S3). The A/S ratio for the proposed models ranged from 0.0-0.0.1 for 2016 and from 0.00-0.08 for 2017 for model PS1, from 0.0 to 0.32 for 2016 and from 0.05 to 0.34 for 2017 for model PS2, from 2.64 to 83.35 for 2016 and 16.62 to 75.1 for 2017. It can be seen from Table 6.5 that these values vary in a very narrow range for model PS3. The highest A/S ratio (0.87) was found for fallow land for 16% slope in 2016.

Fig. 6.14 and Fig. 6.15 show the goodness-of-fit of the model PS1 and PR1 evaluated using NSE in the year of 2016 and 2017. The results of sediment yield computations using Model PS1 and runoff computations using Model PR1 are shown in Figures 6.8-6.10 for all nine plots of different land use and slopes. The closeness of data points to the line of perfect fit indicates a satisfactory model performance. In these figures, if the model computed results are the same as the observed ones, the data points will lie on the line of perfect fit. From Fig. 6.14 and Fig. 6.15, the model show better goodness-of-fit in computation of runoff depth as compare to computation of sediment yield. Figures also indicates that the higher slopes gave higher correlation and data point were near to the line of perfect fit in both year than the other slope. Fig. 6.14 and Fig. 6.15 shows the land use maize at 16 % slope shows the higher goodness of fit than the other land use in both year and fallow land (2016) and figure millet (2017) at 8 % slope shows the poor goodness of fit. The higher NSE show the higher goodness-of-fit of the models. According to result from Tables 6.4 to 6.5, the sediment yield models can be ranked as PS3>PS1>PS2. The runoff models

PR3 and PR1 performed approximately similar and model PR2 performed poorer than any other proposed models.

It is of common experience that the sediment erosion and sediment yield directly depend on the amount of runoff generated, which is a function of land use/land cover. It is expected that for a given rainfall intensity, soil type, and slope, the Fallow land should exhibit the maximum sediment yield and lesser threshold runoff (R_o), and the Finger millet the minimum and the Maize in between. With the increase in slope, R_o should decrease, and vice versa. The results of the analysis presented in Table 6.6 does however not show the consistency and the expected trends, which might be due to human error in data observations. Such an inference is not beyond reality as the behaviour of sediment is too complex to understand fully.

6.6.3 Data observed from artificial rains

6.6.3.1 Sediment Yield - Runoff Relationship

Similar to the relationship developed between runoff and sediment yield using natural rainfall and sediment yield data, analysis has been carried out using the data observed from artificial rain events. These data were collected during January to April of year 2018 from the above 12 experimental plots of three slopes (8%, 12% and 16%) having wheat, lentil and fallow land crops. Rainfall was measured in fallow land of each slope on the day of experimentation using one non-recording rain gauge and a number of plastic jugs placed at several locations of the plot and assumed that similar rainfall occurred in other two plots of that slope. The sediment rating curves were drawn between the observed runoff and sediment yield, as shown in Figs. 6.16 to 6.17. From these figures, it can be observed that sediment yield (mass) increases with runoff and slope for all land uses. The fallow land generated highest, and maize the lowest runoff and sediment yield. In general, higher canopy crop (such as wheat) generated lower runoff and sediment yield, and vice versa. R^2 values for maize crop on 8%, 12% and 16% slopes are 0.58, 0.67 and 0.75, respectively; for lentil, these are 0.64, 0.66 and 0.59, respectively; and for fallow land, these are 0.88, 0.58 and 0.77, respectively. The generally high R^2 values are indicative of good relationship between runoff and sediment yield. These rating curves can be used for direct estimation of sediment yield for a given runoff depth.

6.6.3.2 Calibration and Verification of SCS-CN Inspired models

All the SCS-CN inspired models were tested with observed sediment and runoff data generated from artificial rains. The parameters of rainfall-runoff models were optimized using the excel Solver for maximum NSE. The optimized value of S from rainfall-runoff models was used in rainfall-sediment yield models to optimize other parameters. The optimized values of model parameters and the resulting NSEs are presented in Tables 6.7 to 6.9 and depicted graphically in Fig. 6.18. It can be

seen from these figures that the proposed model (PS1) performed much better than the existing model (S1), and proposed models (PS2 & PS3) slightly better than the existing models (S2 & S3).

Tables 6.7 to 6.9 show the optimized parameters of all rainfall-sediment yield models and rainfall-runoff models. The table also includes mean rainfall and runoff coefficient (C) of events. It can be seen from the table that the mean rainfall was not similar on all plots, largely because of water pressure in pipeline. However, it is observed that C increases with slope for all land uses, and parameters A & CN increase with slope for all models. The fallow land at 16% slope yielded the highest CN values (93, 96 and 93) in all model applications. From Table 6.7, in case of existing sediment yield models, 'A' ranged from 1.28 to 2.79 kg; and in case of the proposed models, A varied from 0.74 to 2.29 kg. The decay coefficient (α) is seen to decrease with increasing slope for rainfall sediment yield model, and for rainfall-runoff model, it was zero. It can be observed from Tables 6.8 and 6.9, the optimized values of CN from the proposed and existing models were approximately same, largely because α -value being zero or very close to zero. Table 6.8 shows that decay coefficient is zero for model (R2), and 0.1 for model (PS2) for all plots. Λ -values lie between 0.17 and 0.68 for existing model (S3), and these lie between 0.25 and 0.68 and for the proposed rainfall-sediment yield model (PS3), as shown in Table 6.9. It can also be seen that the value of λ increases with slope for rainfall-sediment yield model whereas it is zero for rainfall-runoff model. Similarly, for PS1, (α) is decreased with increasing slope in case of model PS3. Figs. 6.19 show a correlation between the CN-values optimized using existing and proposed rainfall-sediment yield models. It can be seen that $R^2 = 1$ for model S3 and PS3 CNs, 0.97 for CNs from models S1 and PS1, and 0.74 for CNs from models S2 and PS2. Notably, $R^2 = 1$ indicates that $\alpha = 0$ and as α deviates from 0, the value of R^2 decreases.

Consistent with Mishra and Singh (2003), it is in order to investigate the variation of A/S ratio, as shown in Tables 6.7 to 6.9, which, according to Eq. 6.7, should be a constant value for a watershed. In these tables, A/S ratio ranged from 0.03-0.16 for model (S1) and 0.02-0.13 for model (PS1), from 0.04-0.21 for model (S2) and from 0.03-0.19 for model (PS2), from 1.82-5.19 for model (S3) and from 1.09-5.19 for model (PS3). It can be seen from Tables 6.7 to 6.9 that A/S ratio generally increases with increasing slope or decreasing S or increasing A. Models S3 and PS3 yielded higher values of A/S than the other respective models. The A/S ratio values from proposed modes were generally lower than those due to existing models.

Figs. 6.20 shows the goodness-of-fit of the models PS1 and PR1 evaluated using NSE using artificial rainfall-runoff-sediment yield data observed in the year 2018. The results of sediment yield computations using Model PS1 and runoff computations using Model PR1 are shown in

Table 6.7 for all nine plots of different land use and slopes. The general closeness of data points to the line of perfect fit indicates a satisfactory model performance. In these figures, if the model computed results are the same as the observed ones, the data points will lie on the line of perfect fit. From Fig. 6.21, the model shows better goodness-of-fit in computation of runoff depth as compared to computation of sediment yield. Figures also indicate that the slope 12% plots yielded highest correlation for rainfall-sediment yield model and 8% slope for rainfall-runoff model. Fig. 6.21 shows the wheat crop at 12% slope yields higher goodness of fit than the other land uses, and lentil at 16 % slope shows the poorest goodness of fit. From Tables 6.7 to 6.9, the sediment yield models can be ranked as PS3>PS2>PS1 in order of their performance. The runoff models PR3 and PR1 performed approximately similar and model PR2 performed poorer than any other proposed models. Table 6.10 shows the Linear [$y = m (x - c/m)$] fitting of sediment yield (kg) and runoff (mm) plots. Here, m is the slope and c is the constant and $R_o (mm) = c/m$ represents the threshold runoff generating sediment yield. The results however do not exhibit consistency with the trends expected and it might be due to small size of plots, uniform rainfall, high slopes and resulting very less time of concentration providing no opportunity for eroded particles to settle within the watershed. Therefore, sediment yield will occur due to runoff only when it occurs after condition of initial abstraction is satisfied.

Table 6.3 Observed Runoff, Potential maximum retention (S) and Curve Number (CN) data for experimental plot (2016).

Event No.	Date	Rainfall (mm)	Runoff(Q) mm			Potential maximum retention (S) (mm)			Curve Number (CN)		
			Slope (16%)	Slope (12%)	Slope (8%)	Slope (16%)	Slope (12%)	Slope (8%)	Slope (16%)	Slope (12%)	Slope (8%)
Maize											
1	15-Jun-16	17	10.66	4.86	1.28	7.17	20.95	44.05	97.26	92.38	85.22
2	16-Jun-16	46.5	35.50	27.10	22.24	10.98	22.92	32.14	95.85	91.72	88.77
3	22-Jun-16	39.2	27.23	21.53	14.31	12.70	21.61	38.10	95.24	92.16	86.96
4	7-Feb-16	35	26.75	18.41	17.72	8.24	20.81	22.16	96.86	92.43	91.98
5	3-Jul-16	22.8	11.20	9.81	7.04	15.13	18.23	26.23	94.38	93.30	90.64
6	6-Jul-16	13	8.27	8.41	4.28	5.29	5.09	14.06	97.96	98.04	94.75
7	16-Jul-16	19.1	8.97	6.88	3.41	13.56	18.83	33.13	94.93	93.10	88.46
8	22-Jul-16	65	49.43	45.82	40.61	15.59	20.15	27.62	94.22	92.65	90.19
9	23-Jul-16	36	30.07	25.90	16.18	5.58	10.47	27.17	97.85	96.04	90.34
10	25-Jul-16	23.8	18.28	15.50	11.06	5.49	9.16	17.16	97.88	96.52	93.67
11	6-Aug-16	24	5.47	4.08	0.75	35.40	42.87	79.50	87.77	85.56	76.16
12	8-Aug-16	20.8	11.64	6.36	3.16	11.09	24.15	39.58	95.82	91.32	86.52
13	11-Aug-16	12.4	0.89	1.59	0.20	32.69	25.81	46.28	88.60	90.78	84.59
14	14-Aug-16	22	15.49	14.10	9.93	6.85	8.81	16.50	97.37	96.65	93.90
15	14-Aug-16	12	5.81	4.42	0.95	8.15	11.56	30.62	96.89	95.65	89.24
16	29-Aug-16	46.5	31.27	25.02	16.13	16.49	26.61	47.73	93.90	90.52	84.18
17	22-Sep-16	20	9.11	7.45	4.81	14.81	19.02	28.36	94.49	93.03	89.95
Finger Millet											
1	15-Jun-16	17	9.86	9.27	5.35	8.46	9.50	19.22	96.78	96.40	92.97
2	16-Jun-16	46.5	32.65	21.82	24.49	14.59	33.04	27.59	94.57	88.49	90.20
3	22-Jun-16	39.2	24.03	19.87	15.70	17.38	24.78	34.29	93.60	91.11	88.11
4	7-Feb-16	35	21.89	19.80	19.11	14.85	18.27	19.51	94.48	93.29	92.87

5	3-Jul-16	22.8	12.59	9.81	5.65	12.45	18.23	31.60	95.33	93.30	88.93
6	6-Jul-16	13	7.23	8.62	7.06	7.00	4.78	7.32	97.32	98.15	97.20
7	16-Jul-16	19.1	7.30	7.58	6.88	17.64	16.89	18.83	93.51	93.76	93.10
8	22-Jul-16	65	51.62	47.66	40.61	13.02	17.77	27.62	95.12	93.46	90.19
9	23-Jul-16	36	25.21	25.21	21.74	11.39	11.39	16.49	95.71	95.71	93.90
10	25-Jul-16	23.8	20.78	13.83	12.45	2.76	11.79	14.30	98.92	95.56	94.67
11	6-Aug-16	24	4.08	6.86	2.00	42.87	29.58	60.01	85.56	89.57	80.89
12	8-Aug-16	20.8	12.19	5.66	2.19	10.13	26.72	47.32	96.16	90.48	84.30
13	11-Aug-16	12.4	1.59	0.89	0.20	25.81	32.69	46.28	90.78	88.60	84.59
14	14-Aug-16	22	10.63	11.32	9.93	14.98	13.57	16.50	94.43	94.93	93.90
15	14-Aug-16	12	7.20	3.03	3.03	5.58	16.39	16.39	97.85	93.94	93.94
16	29-Aug-16	46.5	28.77	28.49	27.79	20.21	20.65	21.77	92.63	92.48	92.11
17	22-Sep-16	20	8.84	5.78	5.36	15.45	24.42	26.02	94.27	91.23	90.71
Fellow Land											
1	15-Jun-16	17	11.77	7.88	2.68	5.56	12.29	31.73	97.86	95.38	88.90
2	16-Jun-16	46.5	36.82	30.92	18.17	9.44	16.99	41.86	96.42	93.73	85.85
3	22-Jun-16	39.2	31.67	20.98	16.26	7.25	22.64	32.86	97.23	91.82	88.54
4	7-Feb-16	35	18.41	12.16	16.33	20.81	35.84	25.07	92.43	87.63	91.02
5	3-Jul-16	22.8	9.81	11.20	5.65	18.23	15.13	31.60	93.30	94.38	88.93
6	6-Jul-16	13	9.32	6.71	8.45	3.83	7.98	5.03	98.51	96.96	98.06
7	16-Jul-16	19.1	4.80	6.88	6.61	26.18	18.83	19.66	90.66	93.10	92.82
8	22-Jul-16	65	53.11	49.99	45.89	11.36	14.92	20.06	95.72	94.45	92.68
9	23-Jul-16	36	27.29	17.57	24.51	8.74	24.13	12.34	96.68	91.32	95.37
10	25-Jul-16	23.8	16.61	16.61	9.67	7.60	7.60	20.47	97.09	97.09	92.54
11	6-Aug-16	24	5.47	2.69	1.30	35.40	53.10	69.14	87.77	82.71	78.60
12	8-Aug-16	20.8	10.94	5.39	9.97	12.37	27.84	14.33	95.36	90.12	94.66
13	11-Aug-16	12.4	2.97	0.89	0.89	17.62	32.69	32.69	93.51	88.60	88.60
14	14-Aug-16	22	15.49	11.32	11.32	6.85	13.57	13.57	97.37	94.93	94.93
15	14-Aug-16	12	5.81	3.03	1.64	8.15	16.39	24.16	96.89	93.94	91.32
16	29-Aug-16	46.5	29.88	29.18	24.32	18.51	19.56	27.92	93.21	92.85	90.10

17	22-Sep-16	20	7.45	3.28	4.95	19.02	36.49	27.75	93.03	87.44	90.15
----	-----------	----	------	------	------	-------	-------	-------	-------	-------	-------

Table 6.4 Observed Runoff, Potential maximum retention (S) and Curve Number (CN) data for experimental plot (2017).

Event No.	Date	Rainfall (mm)	Runoff(Q) mm			Potential maximum retention (S) (mm)			Curve Number (CN)		
			Slope (16%)	Slope (12%)	Slope (8%)	Slope (16%)	Slope (12%)	Slope (8%)	Slope (16%)	Slope (12%)	Slope (8%)
Maize											
1	19-Jun-17	44	34.29	27.12	14.21	9.57	19.28	48.50	96.37	92.95	83.97
2	26-Jun-17	34.2	26.63	26.45	13.4	7.46	7.68	30.70	97.15	97.07	89.22
3	29-Jun-17	17.7	10.99	10.56	6.39	7.63	8.32	17.41	97.08	96.83	93.58
4	30-Jun-17	15	13.39	9.83	7.06	1.45	5.69	10.61	99.43	97.81	95.99
5	6-Jul-17	36.4	29.01	28.68	19.12	7.18	7.55	21.70	97.25	97.11	92.13
6	24-Jul-17	14	7.41	4.14	0.67	8.24	16.75	41.81	96.86	93.81	85.87
7	2-Aug-17	79.5	51.73	42.51	33.2	30.68	45.97	66.06	89.22	84.67	79.36
8	3-Aug-17	9.6	5.66	3.35	1.96	4.62	9.79	15.29	98.21	96.29	94.32
9	7-Aug-17	27.4	25.51	20.94	18.86	1.65	6.45	9.11	99.35	97.52	96.54
10	10-Aug-17	43.4	37.29	26.87	19.93	5.65	18.83	31.80	97.83	93.10	88.87
11	19-Aug-17	22.3	12.61	9.19	2.94	11.65	18.84	45.72	95.61	93.10	84.75
12	22-Aug-17	58.1	46.25	30.9	28.95	11.52	33.91	37.73	95.66	88.22	87.07
13	23-Aug-17	15.5	8.64	2.54	2.32	8.32	28.29	29.75	96.83	89.98	89.51
14	25-Aug-17	61.8	52.04	36.59	32.28	9.14	29.50	37.19	96.53	89.59	87.23
15	1-Sep-17	44	36.24	20.53	14.98	7.37	31.52	46.03	97.18	88.96	84.66
16	1-Sep-17	23	21.27	18.81	14.65	1.52	4.00	9.35	99.40	98.45	96.45
17	2-Sep-17	61.1	32.9	33.22	26.27	34.90	34.31	48.92	87.92	88.10	83.85
18	3-Sep-17	26	19.34	13.51	9.06	6.76	15.78	26.56	97.41	94.15	90.53

Finger Millet											
1	19-Jun-17	44	27.2	17.75	13.03	19.15	38.15	52.57	92.99	86.94	82.85
2	26-Jun-17	34.2	26.17	15.06	11.59	8.01	26.54	35.94	96.94	90.54	87.60
3	29-Jun-17	17.7	13.34	7.78	10.56	4.39	13.77	8.32	98.30	94.86	96.83
4	30-Jun-17	15	12.33	9.14	6.78	2.54	6.74	11.24	99.01	97.42	95.76
5	6-Jul-17	36.4	30.01	24.29	13.34	6.07	13.17	35.23	97.67	95.07	87.82
6	24-Jul-17	14	2.75	2.75	2.75	22.88	22.88	22.88	91.74	91.74	91.74
7	2-Aug-17	79.5	41.53	34.87	24.17	47.83	62.01	92.75	84.15	80.38	73.25
8	3-Aug-17	9.6	6.13	4.74	0.57	3.88	6.32	26.93	98.50	97.57	90.41
9	7-Aug-17	27.4	25.8	20.25	17.47	1.39	7.29	11.11	99.46	97.21	95.81
10	10-Aug-17	43.4	33.12	26.18	22.01	10.27	19.93	27.41	96.11	92.73	90.26
11	19-Aug-17	22.3	10.44	5.72	1.55	15.90	30.08	59.47	94.11	89.41	81.03
12	22-Aug-17	58.1	35.06	25.34	16.31	26.65	45.66	72.74	90.50	84.76	77.74
13	23-Aug-17	15.5	3.93	3.15	2.54	21.10	24.77	28.29	92.33	91.12	89.98
14	25-Aug-17	61.8	50.47	38.67	28.42	10.83	26.18	45.19	95.91	90.66	84.90
15	1-Sep-17	44	17.75	18.98	10.81	38.15	35.08	61.38	86.94	87.86	80.54
16	1-Sep-17	23	16.73	16.04	12.56	6.46	7.36	12.82	97.52	97.18	95.20
17	2-Sep-17	61.1	42.94	24.05	29.05	19.12	54.55	42.59	93.00	82.32	85.64
18	3-Sep-17	26	20.45	9.34	6.56	5.44	25.72	35.53	97.90	90.81	87.73
Fellow land											
1	19-Jun-17	44	29.56	20.39	12.31	15.64	31.83	55.25	94.20	88.86	82.13
2	26-Jun-17	34.2	20.62	18.12	8.12	15.72	20.09	48.96	94.17	92.67	83.84
3	29-Jun-17	17.7	14.72	13.34	5	2.81	4.39	22.04	98.90	98.30	92.02
4	30-Jun-17	15	10.94	10.17	5.39	4.18	5.20	14.83	98.38	97.99	94.48
5	6-Jul-17	36.4	32.29	26.07	17.79	3.72	10.75	24.35	98.56	95.94	91.25
6	24-Jul-17	14	4.14	2.75	1.36	16.75	22.88	32.95	93.81	91.74	88.52

7	2-Aug-17	79.5	40.14	38.2	22.09	50.56	54.56	100.41	83.40	82.32	71.67
8	3-Aug-17	9.6	5.71	3.35	0.57	4.54	9.79	26.93	98.24	96.29	90.41
9	7-Aug-17	27.4	20.25	13.3	16	7.29	18.52	13.45	97.21	93.20	94.97
10	10-Aug-17	43.4	34.65	19.93	20.07	8.49	31.80	31.49	96.77	88.87	88.97
11	19-Aug-17	22.3	14.94	6.42	4.61	7.99	27.32	35.23	96.95	90.29	87.82
12	22-Aug-17	58.1	35.9	33.67	23.26	25.32	28.96	50.84	90.94	89.77	83.32
13	23-Aug-17	15.5	4.54	5.32	2.54	18.70	16.08	28.29	93.14	94.05	89.98
14	25-Aug-17	61.8	45.61	31.45	38.67	16.53	38.81	26.18	93.89	86.75	90.66
15	1-Sep-17	44	30.7	17.75	12.2	14.07	38.15	55.67	94.75	86.94	82.02
16	1-Sep-17	23	20.9	13.81	14.65	1.87	10.66	9.35	99.27	95.97	96.45
17	2-Sep-17	61.1	48.5	25.72	33.22	12.27	50.27	34.31	95.39	83.48	88.10
18	3-Sep-17	26	19.06	10.68	13.51	7.11	22.05	15.78	97.28	92.01	94.15



Table 6.5 Results of existing (S1 & R1) and proposed (PS1 & PR1) models.

Data observed in 2016																				
Plot no.	Land use	Slope (%)	S1					R1			PS1					PR1				
			A (Kg)	CN	S (mm)	NSE	A/S (kg/mm)	CN	S (mm)	NSE	A (kg)	α	CN	S (mm)	NSE	A/S (kg)	α	CN	S (mm)	NSE
1	Maize	8	4.63	81	61	38	0.08	87	39	91	3.14	0.12	19	1100	71	0	0	85	45	91
2	Finger Millet		3.68	80	62	34	0.06	86	40	87	2.61	0.12	17	1200	64	0	0.01	82	57	88
3	Fallow land		5.36	75	84	40	0.06	83	52	90	12.29	0.04	19	1100	72	0.01	0.01	76	79	91
4	Maize	12	10.14	79	66	29	0.15	90	29	92	8.67	0.09	19	1100	57	0.01	0	90	29	92
5	Finger Millet		6.72	85	44	30	0.15	90	30	92	7.25	0.08	27	700	62	0.01	0	89	32	92
6	Fallow land		7.44	85	45	21	0.17	89	30	91	8.61	0.09	20	1000	49	0.01	0.01	82	56	92
7	Maize	16	13.93	92	23	24	0.61	94	17	93	44.55	0.04	30	600	79	0.07	0	94	17	93
8	Finger Millet		17.08	90	29	25	0.59	93	20	92	50.69	0.04	34	500	74	0.1	0	92	22	92
9	Fallow land		16.8	91	25	21	0.68	93	18	92	70.61	0.04	22	900	82	0.08	0.01	91	24	92
Data observed in 2017																				
1	Maize	8	25.42	45	310	22	0.08	80	62	83	22.86	0.05	5.97	4000	43	0.01	0	80	62	83
2	Finger Millet		17.26	46	300	18	0.06	76	80	69	15.54	0.05	5.34	4500	38	0	0	76	80	69
3	Fallow land		24.14	42	350	22	0.07	78	71	70	19.77	0.05	4.06	6000	40	0	0	78	70	70
4	Maize	12	56.15	39	390	29	0.14	88	36	80	43.26	0.03	14.48	1500	41	0.03	0	87	36	80
5	Finger Millet		44.29	50	250	24	0.18	84	50	76	39.81	0.02	24.1	800	31	0.05	0	83	50	76
6	Fallow land		47.82	47	290	28	0.16	84	48	81	48.56	0.03	11.79	1900	43	0.03	0	84	48	81
7	Maize	16	96.58	41	360	35	0.27	94	14	86	73.23	0.02	19.48	1050	47	0.07	0	94	15	86
8	Finger Millet		94.34	41	370	32	0.25	92	22	79	70.03	0.02	22.01	900	41	0.08	0	92	22	79
9	Fallow land		96.39	42	350	33	0.28	93	20	80	67.87	0.02	24.1	800	42	0.08	0	93	20	80

Table 6.6 Results of existing (S2 & R2) and proposed (PS2 & PR2) models.

Data observed in 2016																				
Plot no.	Land use	Slope (%)	S2					R2			PS2					PR2				
			A (kg)	CN	S (mm)	NSE	A/S (kg)	CN	S (mm)	NSE	A (kg)	α	CN	S _o (mm)	NSE	A/S (kg/mm)	α	CN	S _o (mm)	NSE
1	Maize	8	21.51	76	82	51	0.26	93	19	91	2.98	0.14	19	1069	55	0	0	91	25	91
2	Finger Millet		17.37	76	78	57	0.22	93	20	87	2.49	0.12	26	739	60	0	0	91	25	87
3	Fallow land		21.33	75	83	43	0.26	93	20	90	5.86	0.02	68	121	47	0.05	0	89	31	90
4	Maize	12	8.49	78	72	60	0.12	91	25	91	8.42	0.07	45	306	69	0.03	0	93	19	91
5	Finger Millet		7.09	77	74	56	0.1	91	25	92	7.22	0.06	54	216	63	0.03	0	93	20	92
6	Fallow land		9.68	75	83	66	0.12	89	31	91	8.22	0.07	41	365	69	0.02	0.01	91	24	92
7	Maize	16	61.66	75	85	70	0.72	96	12	93	36.28	0.02	65	137	75	0.27	0	96	12	93
8	Finger Millet		65.18	75	84	63	0.77	95	14	92	41.01	0.02	66	129	67	0.32	0	95	14	92
9	Fallow land		76.52	74	88	63	0.87	95	13	92	46.54	0.02	62	153	69	0.3	0	95	14	92
Data observed in 2017																				
1	Maize	8	16.83	71	103	31	0.16	87	38	71	10.66	0.02	53	230	32	0.05	0	87	38	78
2	Finger Millet		11.76	71	103	26	0.11	85	46	70	7.39	0.03	49	263	27	0.03	0	85	46	70
3	Fallow land		13.32	72	97	31	0.14	86	42	76	8.88	0.02	60	171	32	0.05	0	86	42	76
4	Maize	12	24.02	75	84	26	0.29	90	29	78	17.61	0.01	70	110	30	0.16	0	91	24	74
5	Finger Millet		27.21	76	82	21	0.33	89	32	62	20.32	0.01	72	100	24	0.2	0	89	32	70
6	Fallow land		27.85	74	88	25	0.32	89	30	63	19.83	0.01	67	123	27	0.16	0	89	30	76
7	Maize	16	42.25	76	81	36	0.52	96	11	85	31.64	0.01	72	100	38	0.32	0	94	15	83
8	Finger Millet		38.54	77	77	33	0.5	94	15	77	29.53	0.01	74	91	34	0.32	0	94	15	77
9	Fallow land		40.42	77	76	33	0.53	95	14	79	30.83	0.01	74	91	34	0.34	0	95	14	79

Table 6.7 Results of existing (S3 & R3) and proposed (PS3 & PR3) models.

Data observed in 2016																								
Plot no.	Land use	Slope (%)	S3						R3				PS3						PR3					
			A (kg)	λ	CN	S (mm)	NSE	A/S (mm)	λ	CN	S (mm)	NSE	A (kg)	λ	α	CN	S _o (mm)	NSE	A/S (kg/mm)	λ	α	CN	S _o (mm)	NSE
1	Maize	8	7.79	0.23	73	95	60	0.08	0	90	29	91	3.12	0.07	0.14	14	1500	73	0	0.07	0	89	32	91
2	Finger Millet		7.74	0.17	74	90	56	0.09	0	90	30	87	2.64	0.1	0.11	24	800	65	0	0	0.01	82	57	88
3	Fallow land		11.1	0.16	72	100	67	0.11	0.23	93	19	91	11.63	0.06	0.02	42	350	73	0.03	0	0.01	76	79	91
4	Maize	12	23.95	0.17	80	63	51	0.38	0.07	89	32	92	8.74	0.07	0.09	22	900	58	0.01	0	0	90	29	92
5	Finger Millet		19.13	0.17	75	85	57	0.23	0.07	89	33	92	7.2	0.06	0.08	27	700	63	0.01	0	0	89	32	92
6	Fallow land		24.36	0.16	72	100	43	0.24	0.12	87	37	91	8.76	0.08	0.08	24	800	50	0.01	0	0.01	82	56	92
7	Maize	16	96.27	0.11	63	150	73	0.64	0.01	94	17	93	70.71	0.05	0.03	34	500	82	0.14	0	0	94	17	93
8	Finger Millet		79.21	0.15	70	110	65	0.72	0	93	20	92	83.35	0.04	0.03	30	600	79	0.14	0	0	92	22	92
9	Fallow land		96.93	0.14	68	120	65	0.81	0.16	95	13	92	98.7	0.03	0.03	24	800	85	0.12	0	0.01	91	24	92
Data observed in 2017																								
1	Maize	8	38.75	0.07	48	280	30	0.14	0	80	62	80	24.89	0.01	0.05	6	4000	44	0.01	0	0	80	62	80
2	Finger Millet		27.96	0.07	47	290	24	0.1	0	76	80	76	16.62	0.01	0.05	5	4500	38	0	0	0	76	80	76
3	Fallow land		28.54	0.07	50	250	28	0.11	0	78	70	81	19.77	0	0.05	4	6000	40	0	0	0	78	70	81
4	Maize	12	43.69	0.08	57	190	33	0.23	0	87	36	83	43.26	0	0.03	14	1500	41	0.03	0	0	87	36	83
5	Finger Millet		41.51	0.1	63	150	28	0.28	0	83	50	69	46.62	0.01	0.02	24	800	31	0.06	0	0	83	50	69
6	Fallow land		55.99	0.08	54	220	34	0.25	0	84	48	70	48.93	0	0.03	12	1900	43	0.03	0	0	84	48	70
7	Maize	16	88.66	0.07	54	220	40	0.4	0	94	15	86	75.1	0	0.02	19	1050	47	0.07	0	0	94	15	86
8	Finger Millet		79.41	0.07	55	210	36	0.38	0	92	22	79	70.03	0	0.02	22	900	41	0.08	0	0	92	22	79
9	Fallow land		70.95	0.08	60	170	36	0.42	0	93	20	80	67.87	0	0.02	24	800	42	0.08	0	0	93	20	80

Table 6.8 Linear [$y = m(x - c/m)$] fitting of sediment yield (kg) and runoff (mm) plots. Here, m is the slope and c is the constant and R_o (mm) = c/m represents the threshold runoff generating sediment yield.

Slope (%)	Land use	2016			2017		
		m (kg/mm)	c (kg)	$R_o = c/m$ (mm)	m (kg/mm)	c (kg)	$\gamma = c/m$ (mm)
8	Maize	0.09	0.05	0.56	0.06	0.07	1.17
	Finger millet	0.06	0.18	3.00	0.03	0.22	7.33
	Fallow land	0.12	0.24	2.00	0.03	0.49	16.33
12	Maize	0.22	0.82	3.73	0.18	0.95	5.28
	Finger millet	0.16	0.23	1.44	0.16	0.55	3.44
	Fallow land	0.21	0.69	3.29	0.21	0.78	3.71
16	Maize	0.59	4.63	7.85	0.26	1.06	4.08
	Finger millet	0.68	4.81	7.07	0.22	0.62	2.82
	Fallow land	0.74	5.9	7.97	0.2	1.13	5.65

Table 6.9 Results of existing (S1 & R1) and proposed (PS1 & PR1) models.

Plot no.	Land use	Slope (%)	Mean rainfall (mm)	C	Existing models						Proposed models							
					A (kg)	S (mm)	CN	A/S (kg/mm)	NSE ^{S1}	NSE ^{R1}	A (kg)	α^{PS1}	α^{PR1}	S (mm)	CN	A/S (kg/m ²)	NSE ^{PS1}	NSE ^{PR1}
1	Wheat	8	21.12	0.30	1.69	59	81	0.03	37	65	0.91	0.05	0	59	81	0.02	45	65
2	Lentil		21.12	0.33	1.28	48	84	0.03	34	83	0.74	0.04	0	48	84	0.02	40	83
3	Fallow land		21.12	0.39	1.79	37	87	0.05	40	86	1.22	0.03	0	37	87	0.03	46	86
4	Wheat	12	22.08	0.36	2.09	44	83	0.05	39	65	1.33	0.04	0	44	85	0.03	46	65
5	Lentil		22.08	0.36	2.05	45	85	0.05	36	62	1.30	0.04	0	45	85	0.03	43	62
6	Fallow land		22.08	0.40	1.76	35	88	0.05	27	81	1.21	0.03	0	35	88	0.03	31	81
7	Wheat	16	19.69	0.47	1.94	24	92	0.08	21	67	1.52	0.03	0	24	92	0.06	24	67
8	Lentil		19.69	0.50	1.86	21	92	0.09	17	71	1.47	0.03	0	21	92	0.07	18	71
9	Fallow land		19.69	0.54	2.79	18	93	0.16	19	73	2.29	0.02	0	18	93	0.13	21	73

Table 6.10 Results of existing (S2 & R2) and proposed (PS2 & PR2) models.

Plot no.	Land use	Slope (%)	Existing models						Proposed models							
			A (kg)	S (mm)	CN	A/S (kg/mm)	NSE ^{S1}	NSE ^{R1}	A	α^{PS2}	α^{PR2}	S _o (mm)	CN	A/S _o (kg/mm)	NSE ^{PS1}	NSE ^{PR1}
1	Wheat	8	1.33	29	90	0.05	42	39	1.11	0.01	0	29	90	0.04	43	39
2	Lentil		1.04	26	91	0.04	38	73	0.87	0.01	0	26	91	0.03	38	73
3	Fallow land		1.50	21	92	0.07	43	82	1.30	0.01	0	21	92	0.06	43	82
4	Wheat	12	1.70	24	87	0.07	43	54	1.46	0.01	0	24	91	0.06	43	54
5	Lentil		1.67	24	91	0.07	40	44	1.43	0.01	0	24	91	0.06	41	44
6	Fallow land		1.48	21	93	0.07	29	77	1.29	0.01	0	21	93	0.06	29	77
7	Wheat	16	1.68	15	95	0.11	21	64	1.52	0.01	0	15	95	0.10	21	64
8	Lentil		1.62	13	95	0.12	17	68	1.47	0.01	0	13	95	0.11	17	68
9	Fallow land		2.47	12	96	0.21	19	70	2.27	0.01	0	12	96	0.19	19	70

Table 6.11 Results of existing (S3 & R3) and proposed (PS3 & PR3) models.

Plot no.	Land use	Slope (%)	Existing models								proposed models									
			A (kg)	λ^{S3}	λ^{R3}	S (mm)	CN	A/S (kg/mm)	NSE ^{S1}	NSE ^{R1}	A (kg)	α^{PS3}	α^{PR3}	λ^{PS3}	λ^{PR3}	S _o (mm)	CN	A/S _o (kg/mm)	NSE ^{PS1}	NSE ^{PR1}
1	Wheat	8	2.70	0.17	0.00	59	81	0.05	51	65	1.09	0.05	0	0.26	0	59	81	0.02	52	65
2	Lentil		1.82	0.17	0.00	48	84	0.04	44	83	0.83	0.04	0	0.25	0	48	84	0.02	45	83
3	Fallow land		2.93	0.29	0.00	37	87	0.08	63	86	2.26	0.01	0	0.32	0	37	87	0.06	63	86
4	Wheat	12	3.63	0.27	0.00	44	85	0.08	64	65	2.86	0.01	0	0.29	0	44	85	0.07	64	65
5	Lentil		3.62	0.27	0.00	45	85	0.08	60	62	2.77	0.01	0	0.30	0	45	85	0.06	61	62
6	Fallow land		2.96	0.33	0.00	35	88	0.08	45	81	2.34	0.01	0	0.37	0	35	88	0.07	45	81
7	Wheat	16	3.75	0.52	0.00	24	92	0.16	47	67	3.75	0.00	0	0.52	0	24	92	0.16	47	67
8	Lentil		3.27	0.55	0.00	21	92	0.16	34	71	3.27	0.00	0	0.55	0	21	92	0.16	34	71
9	Fallow land		5.19	0.68	0.00	18	93	0.29	46	73	5.19	0.00	0	0.68	0	18	93	0.29	46	73

Table 6.12 Linear [$y = m (x - c/m)$] fitting of sediment yield (kg) and runoff (mm) plots. Here, m is the slope and c is the constant and R_o (mm) = c/m represents the threshold runoff generating sediment yield.

Slope (%)	Land use	m (kg/mm)	c (kg)	$R_o = c/m$ (mm)
8	Wheat	0.08	0.11	1.38
	Lentil	0.05	0.01	0.20
	Fallow land	0.09	0.13	1.44
12	Wheat	0.1	0.14	1.40
	Lentil	0.12	0.29	2.42
	Fallow land	0.09	0.14	1.56
16	Wheat	0.14	0.52	3.71
	Lentil	0.14	0.54	3.86
	Fallow land	0.24	1.16	4.83

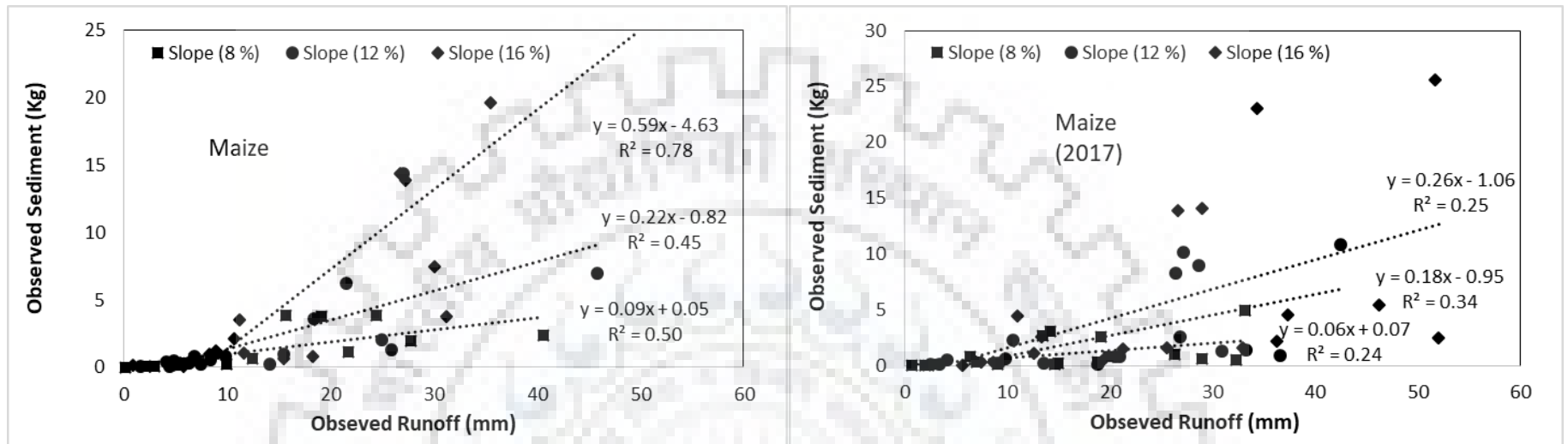


Figure 6.2. Sediment rating curve of different slope of maize.

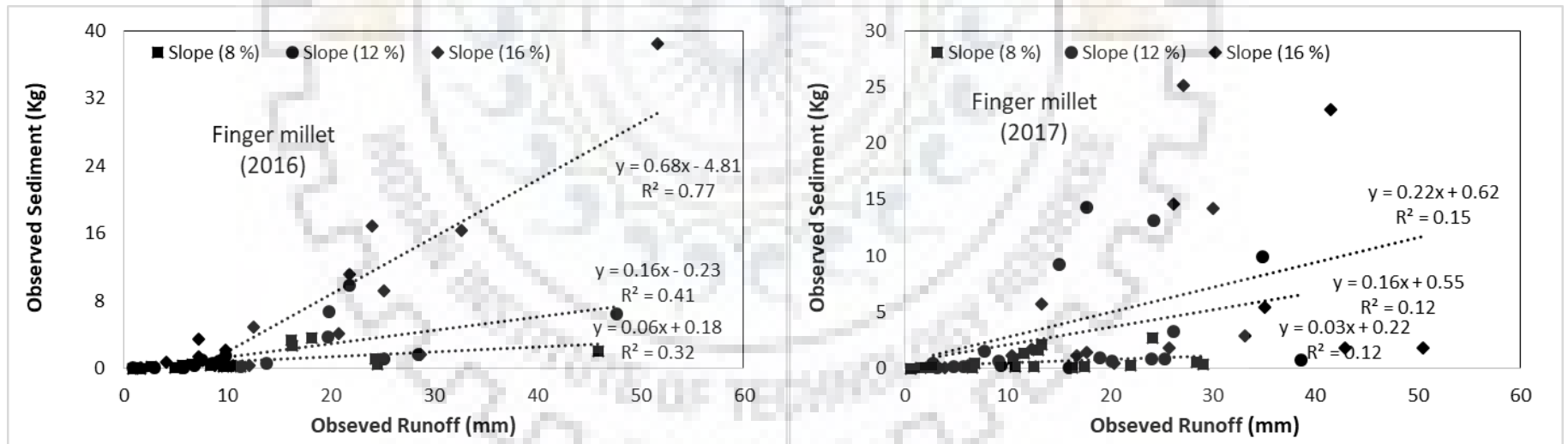


Figure 6.3. Sediment rating curve of different slope of finger millet.

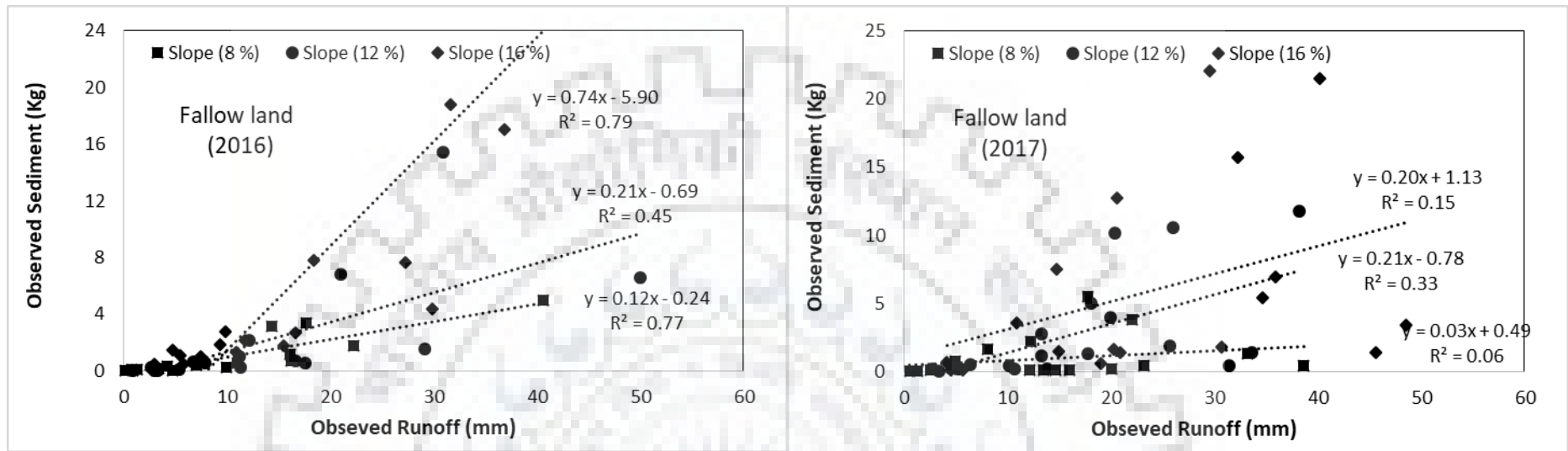


Figure 6.4. Sediment rating curve of different slope of fallow land.

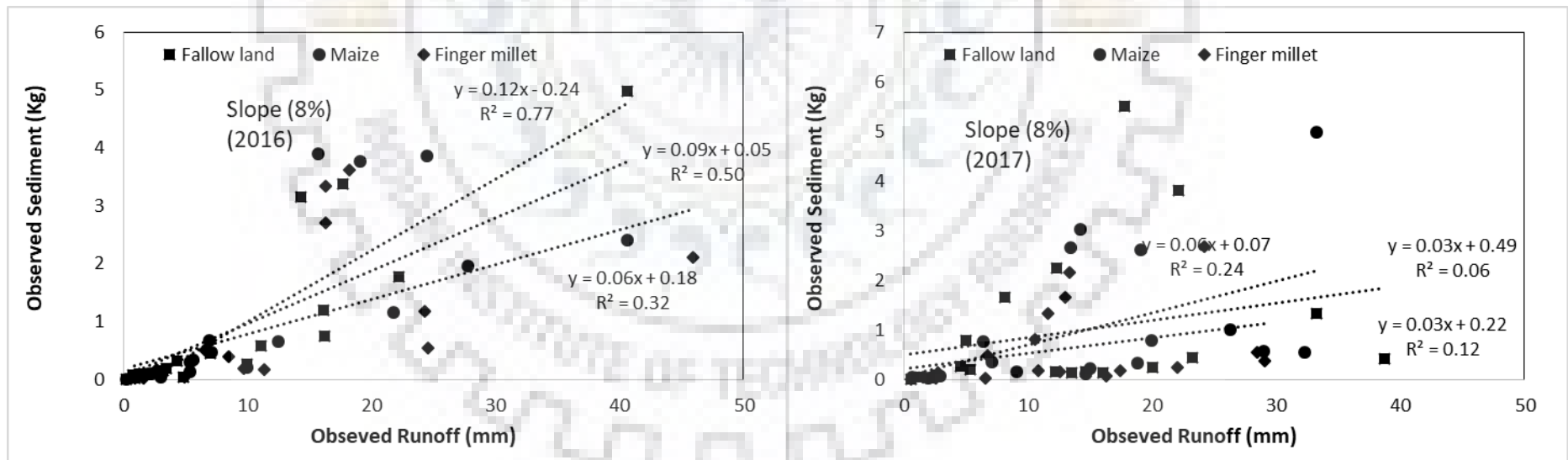


Figure 6.5. Sediment rating curve of different land use on 8% slope.

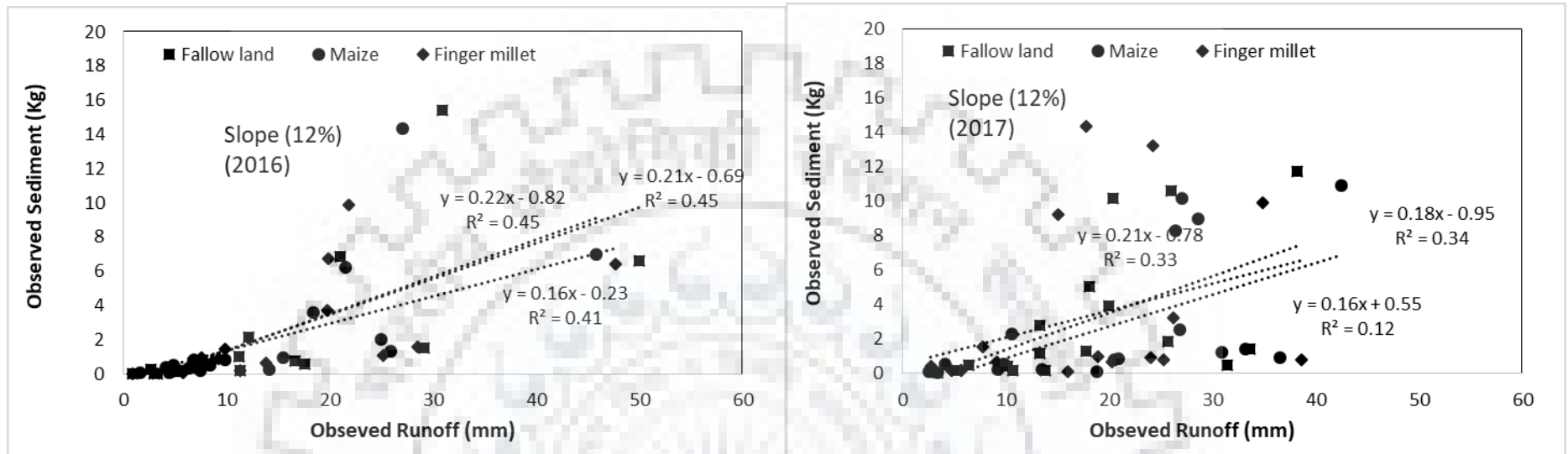


Figure 6.6. Sediment rating curve of different land use on 12% slope.

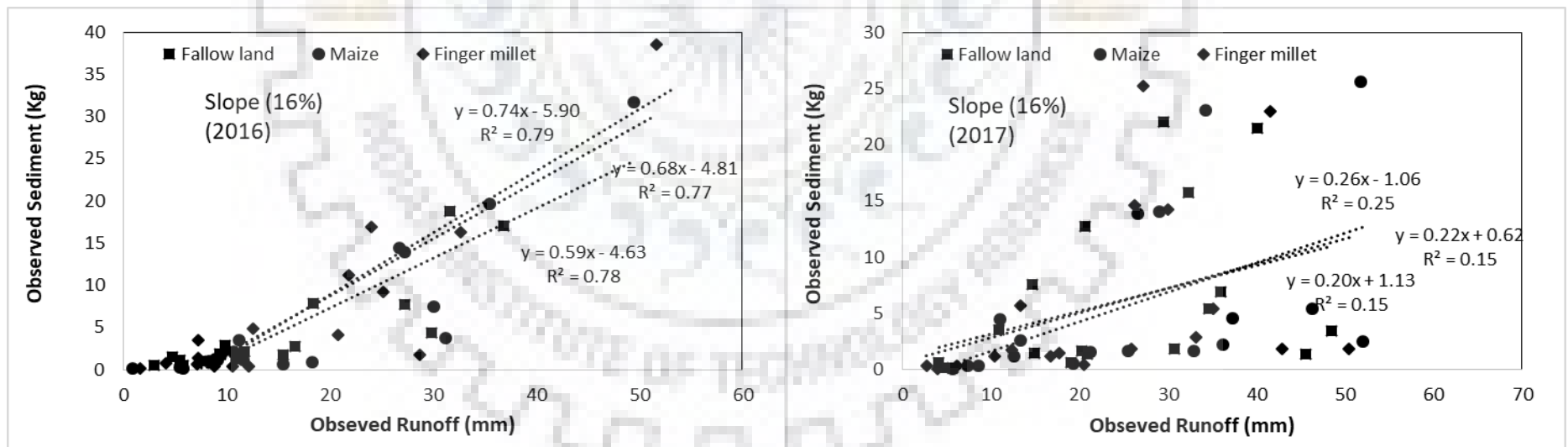


Figure 6.7. Sediment rating curve of different land use on 16% slope.

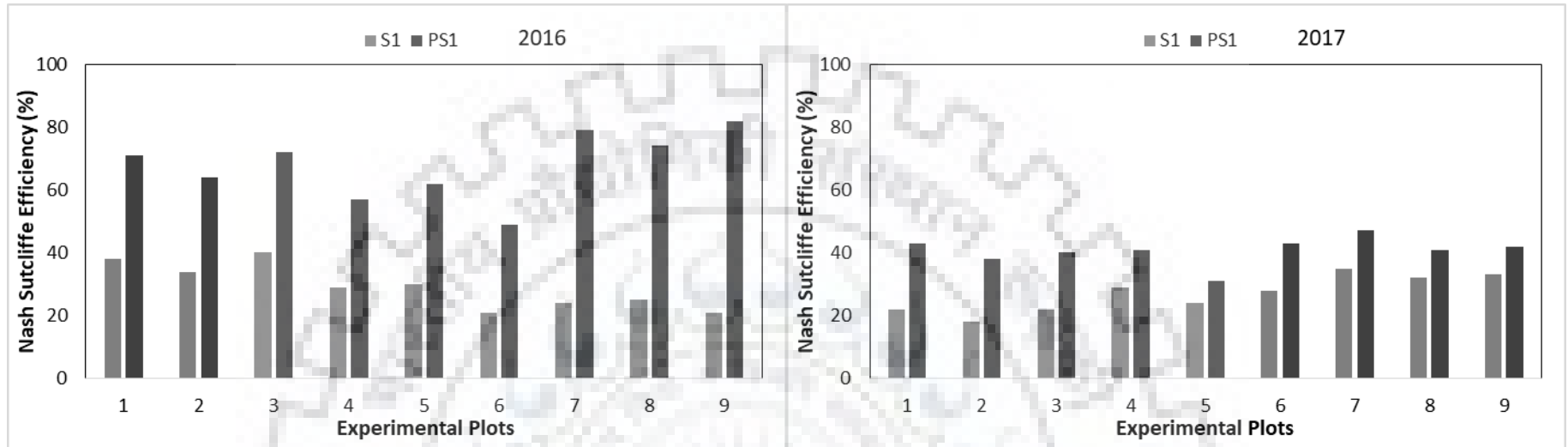


Figure 6.8 Nash Sutcliffe Efficiency of existing and proposed Rainfall-Sediment Yield models (S1 and PS1).

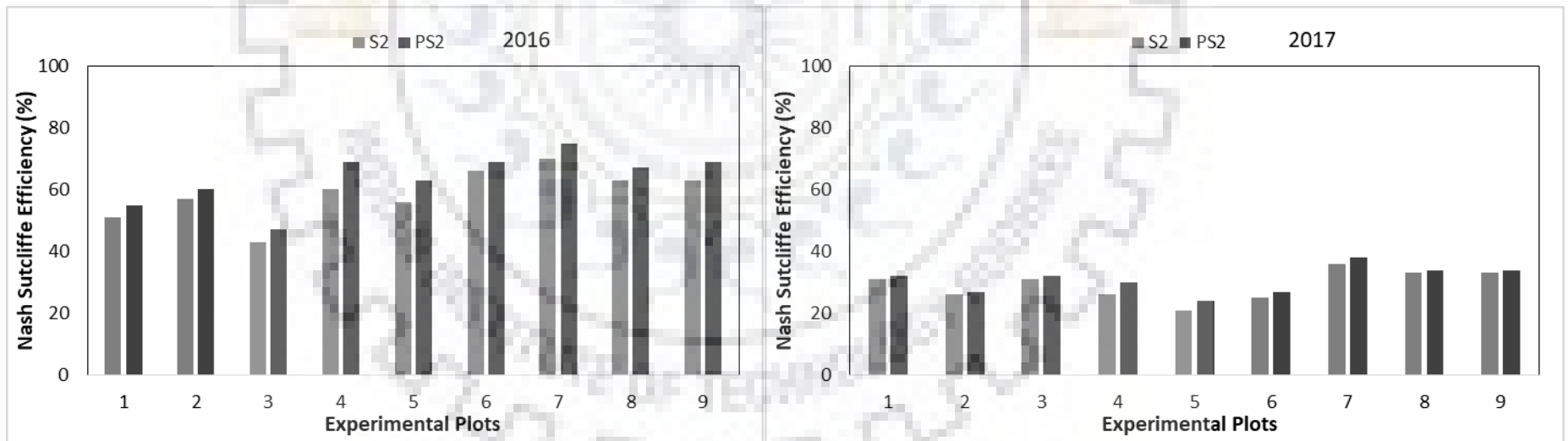


Figure 6.9 Nash Sutcliffe Efficiency of existing and proposed Rainfall-Sediment Yield models (S2 and PS2).

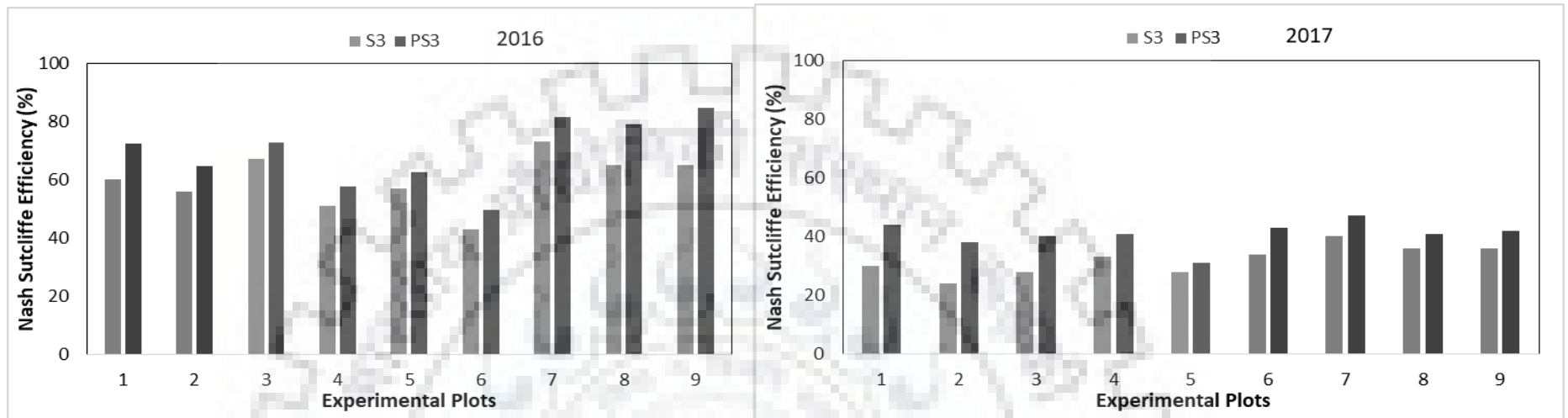


Figure 6.10 Nash Sutcliffe Efficiency of existing and proposed Rainfall-Sediment Yield models (S3 and PS3).

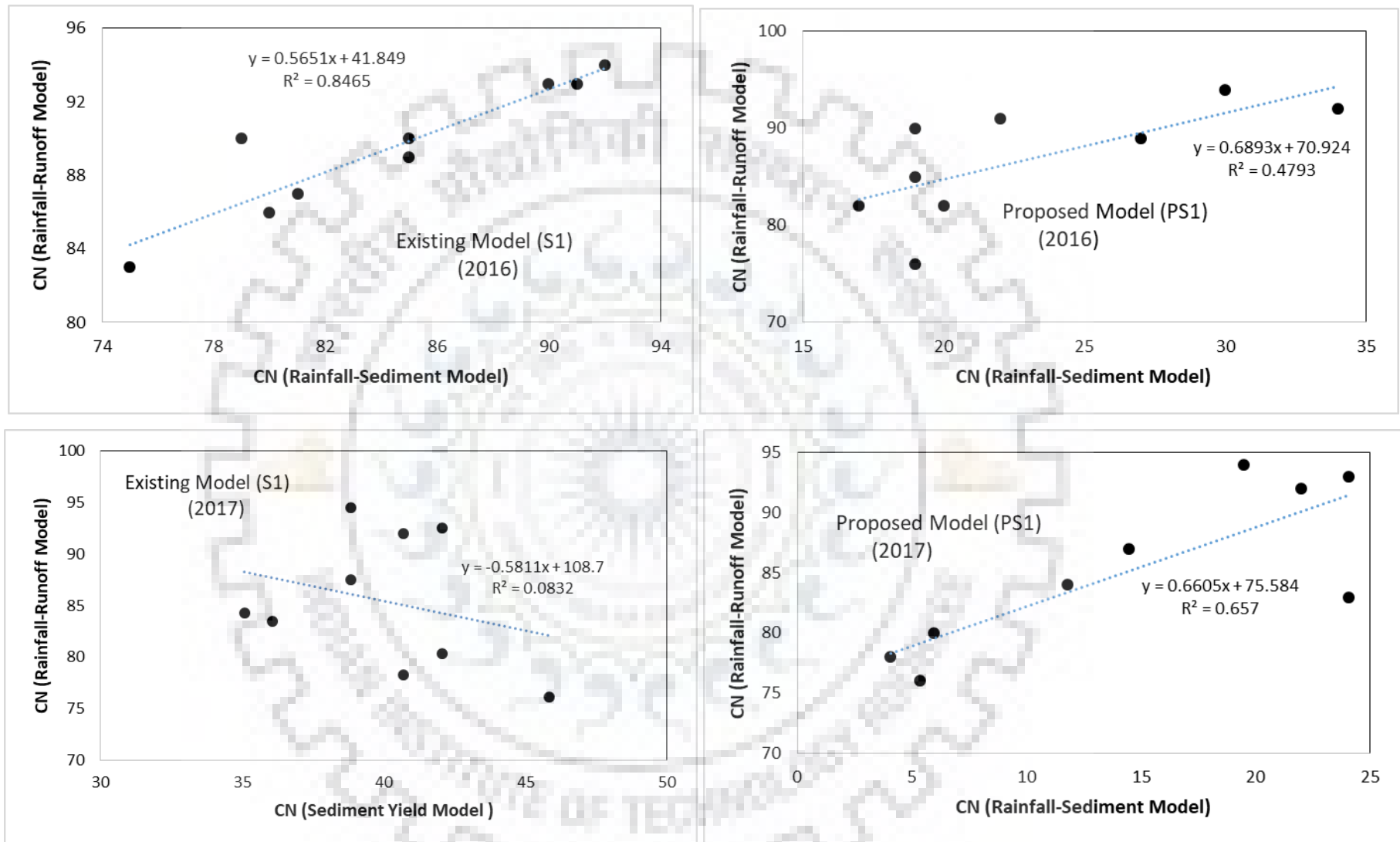


Figure 6.11 Relationship between CN values derived from rainfall-sediment yield and rainfall-runoff models (Model 1).

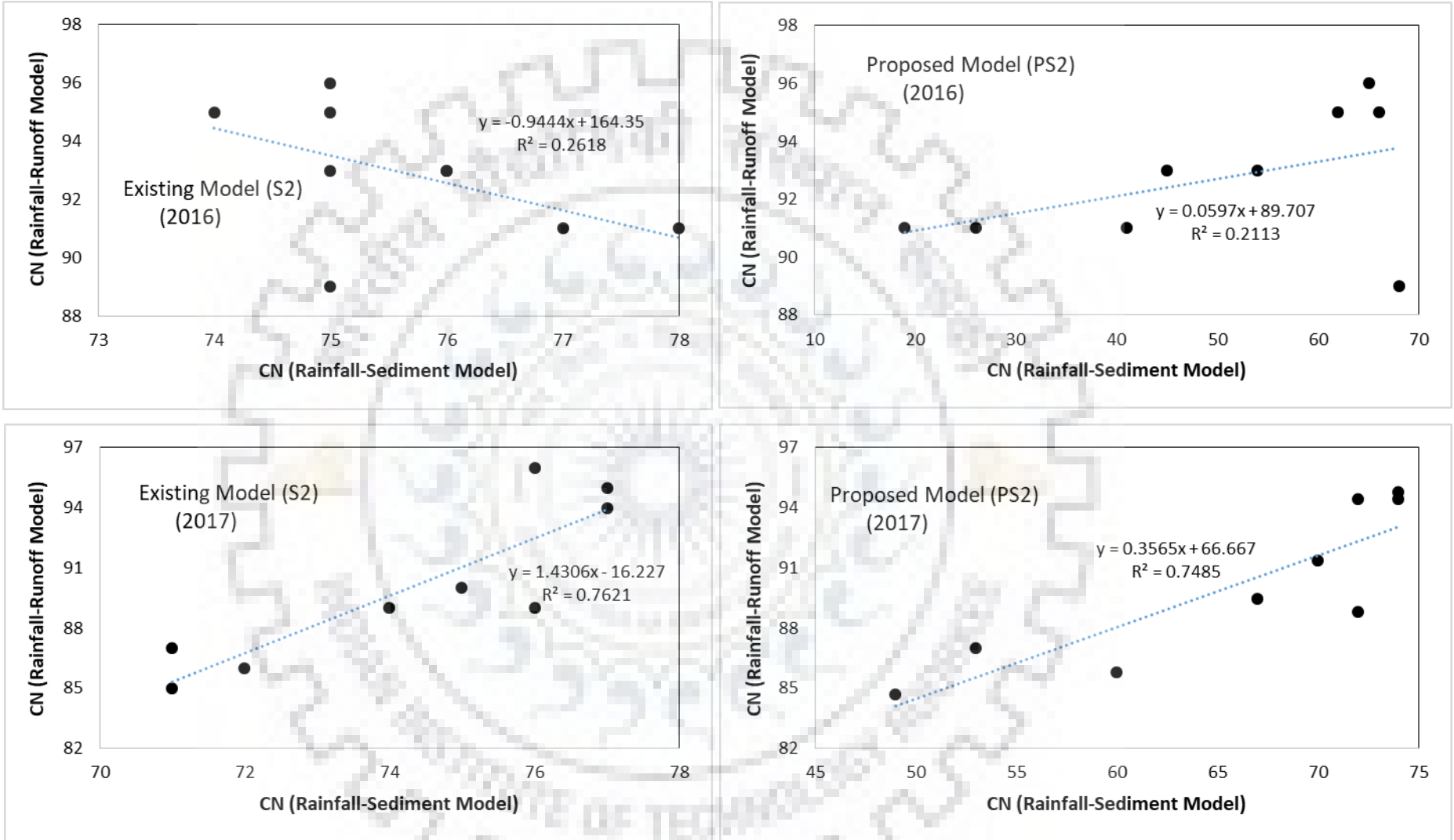


Figure 6.12 Relationship between CN values derived from rainfall-sediment yield and rainfall-runoff models (Model 2).

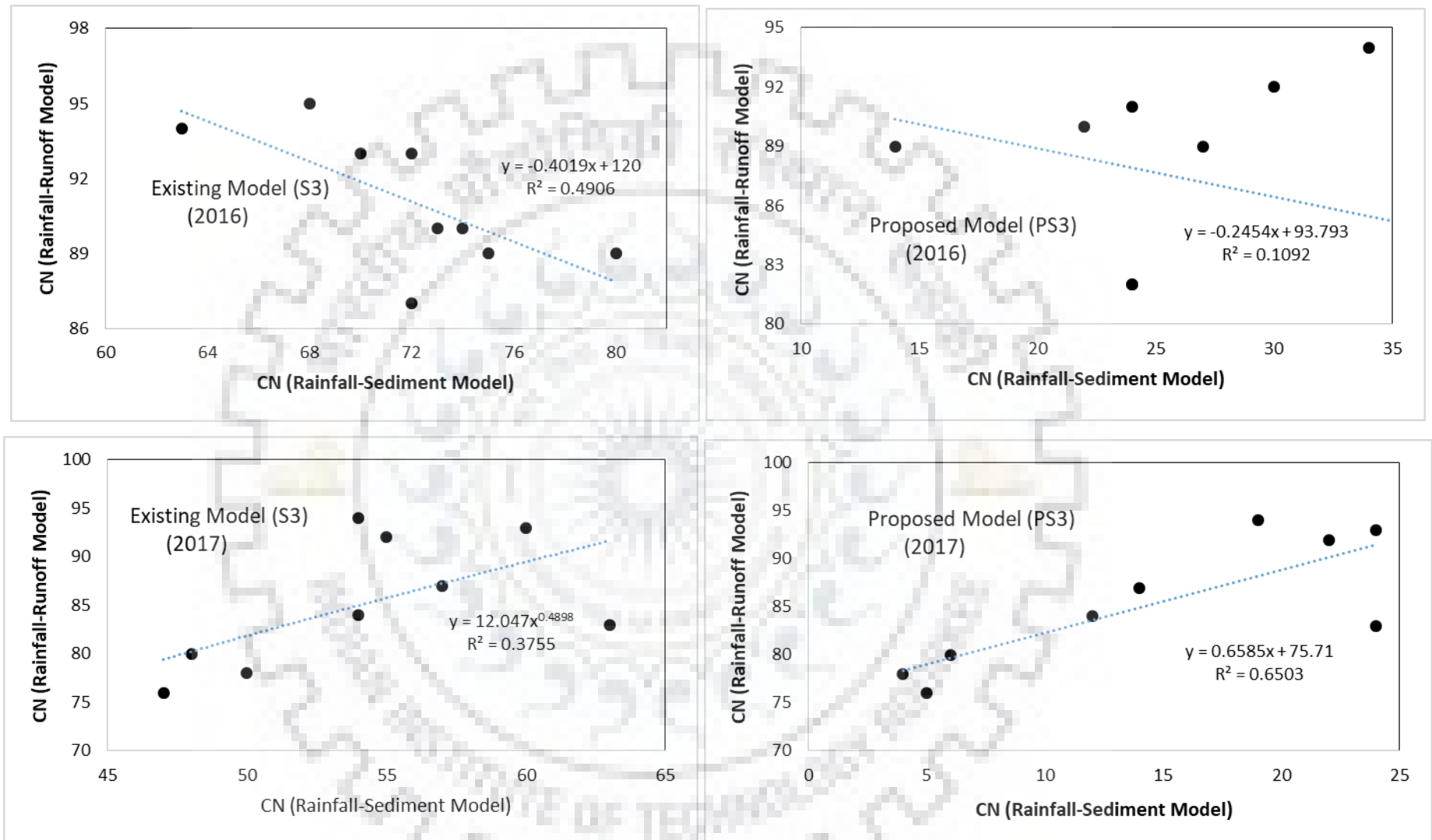
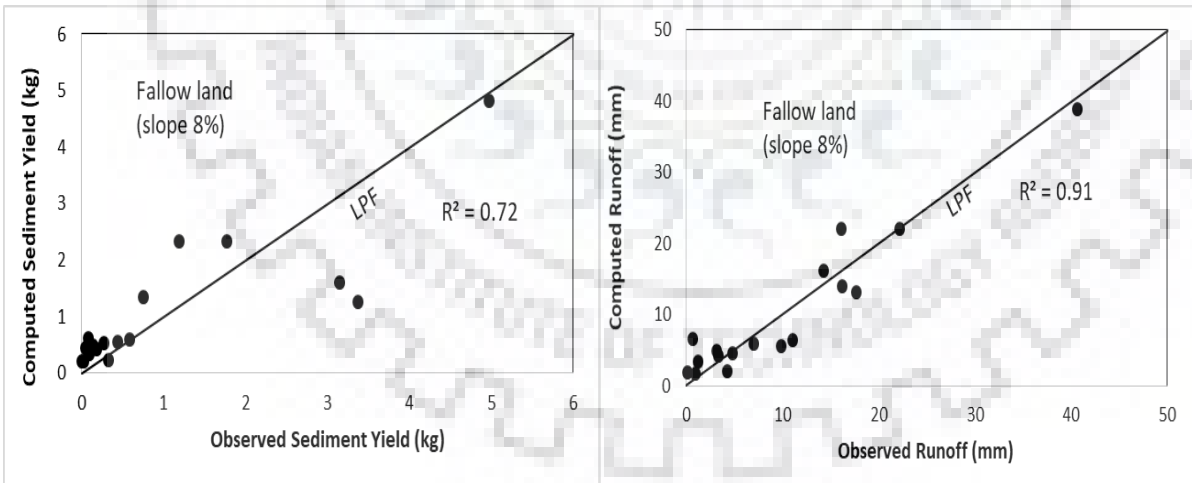
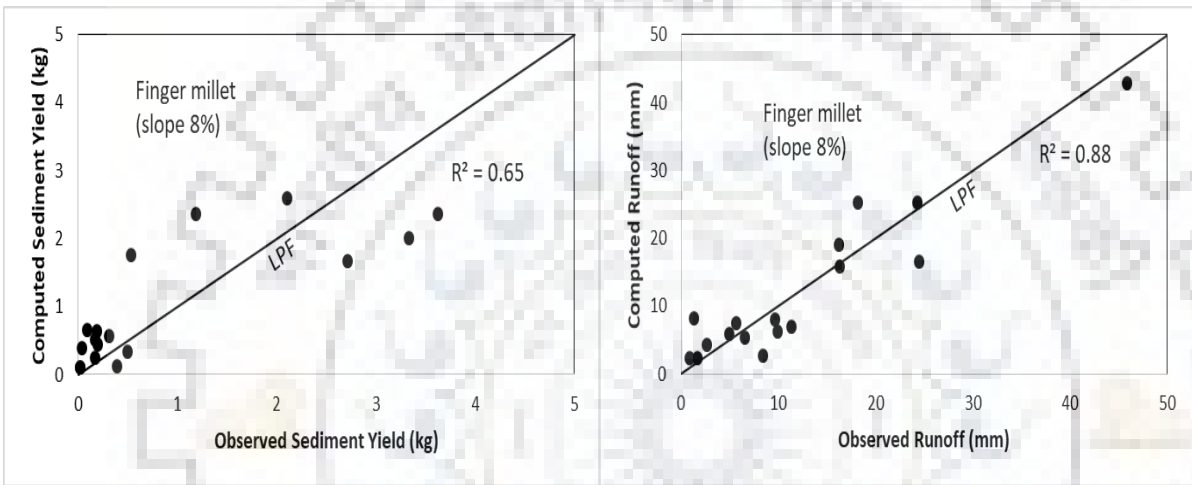
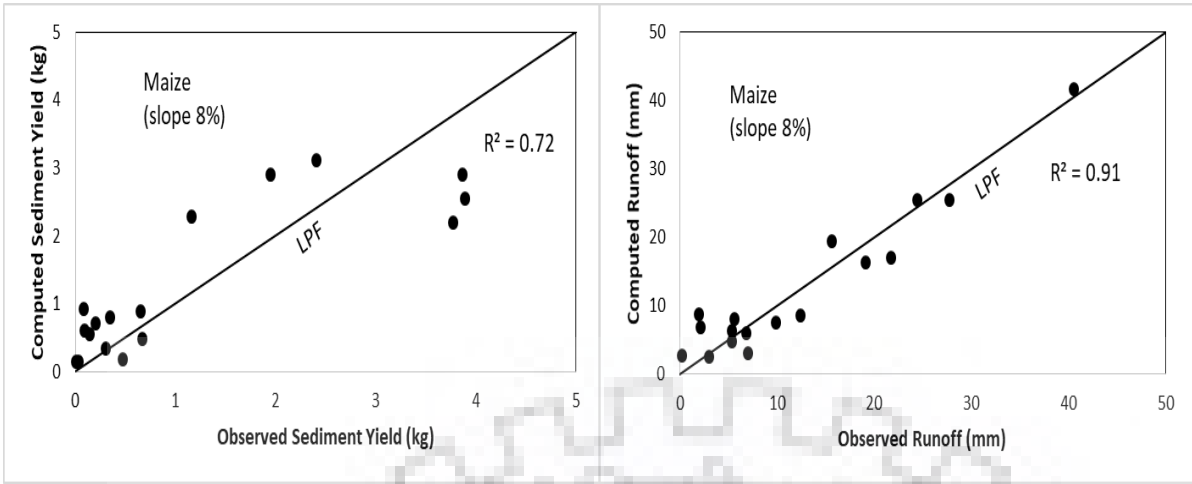
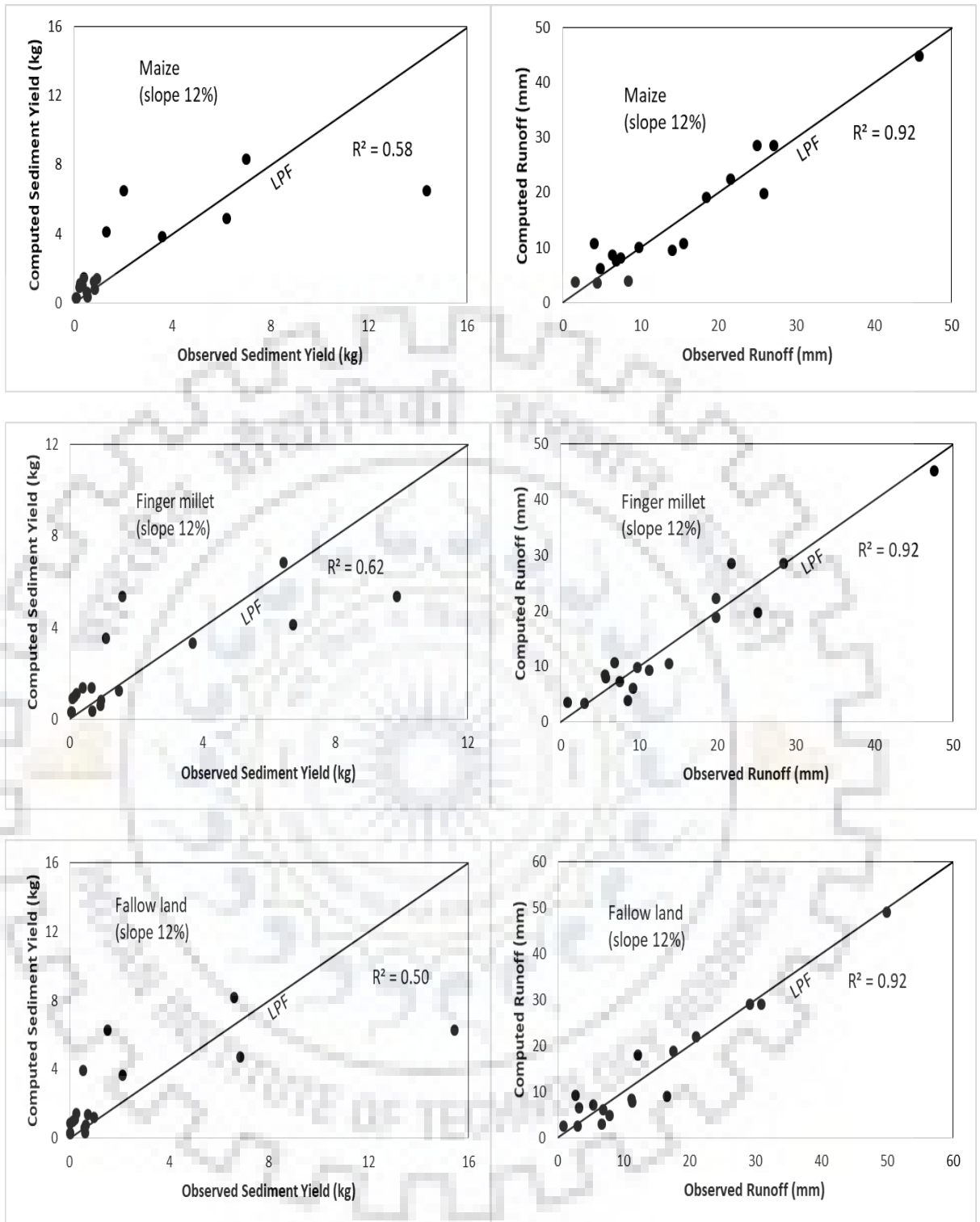


Figure 6.13 Relationship between CN values derived from rainfall-sediment yield and rainfall-runoff models (Model 3).





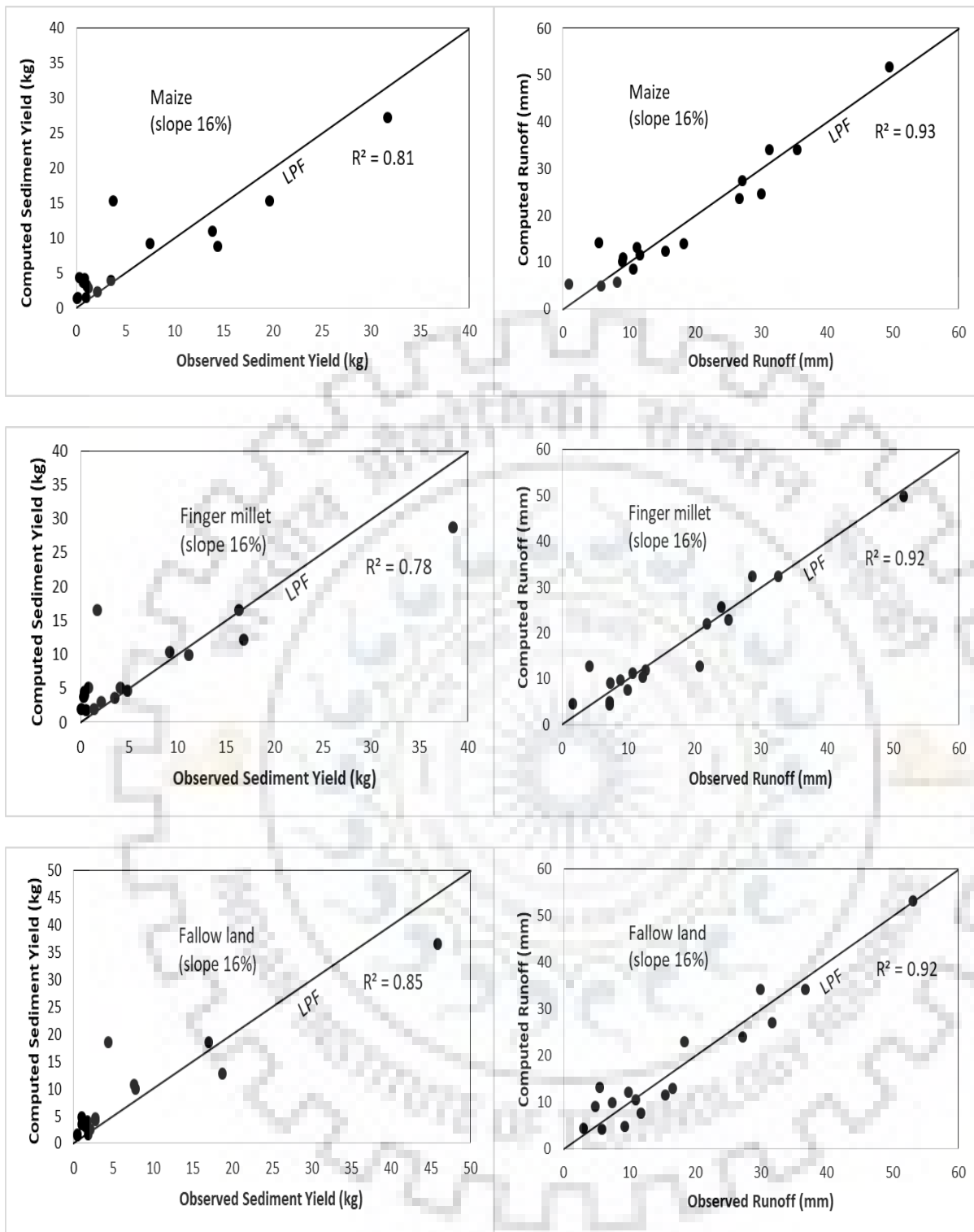
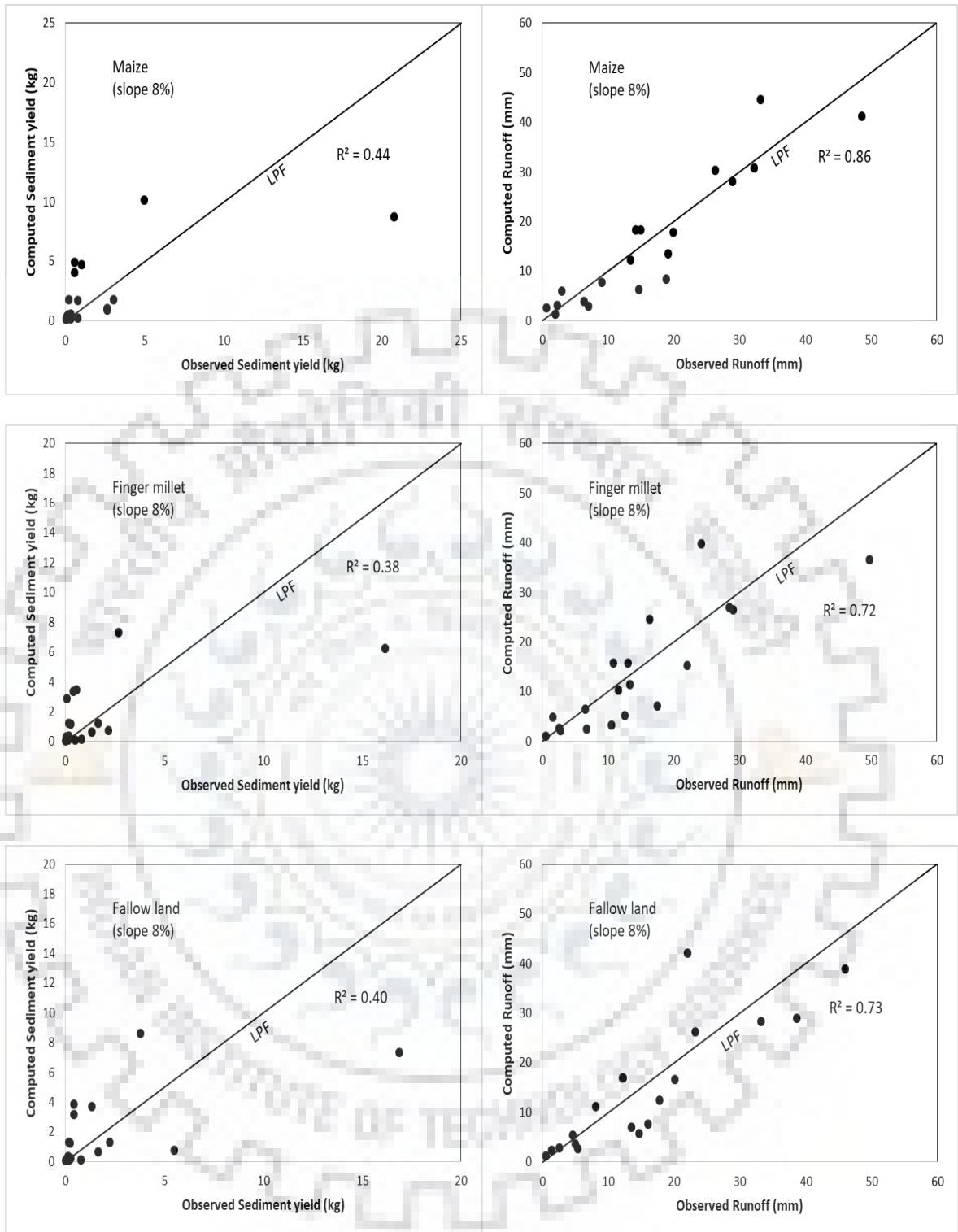
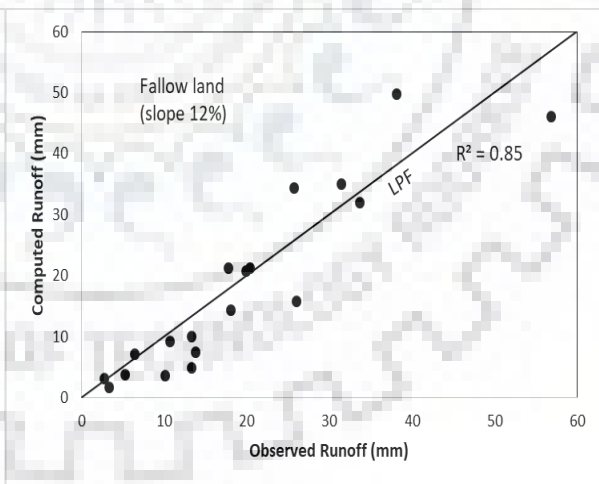
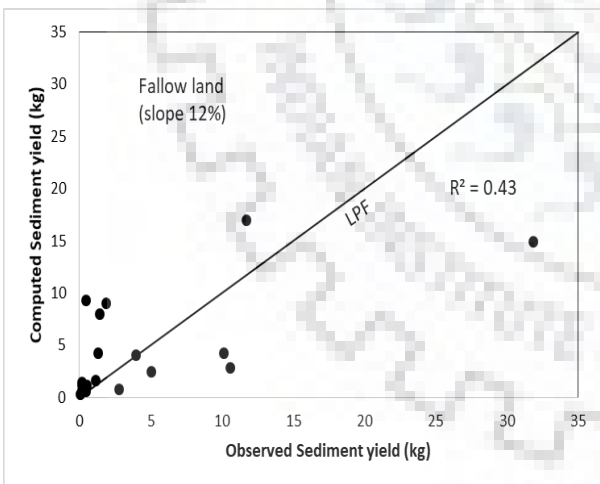
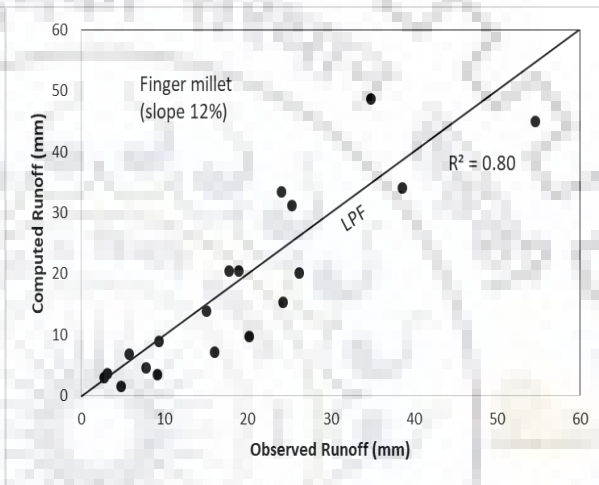
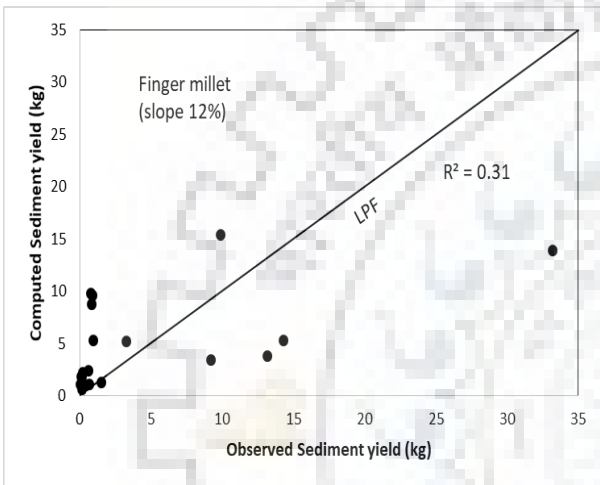
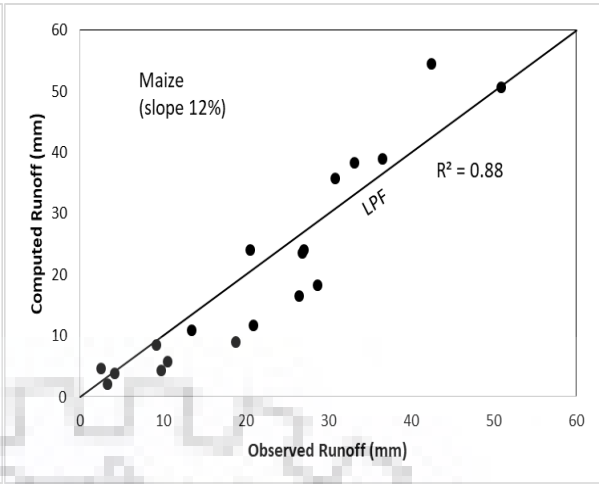
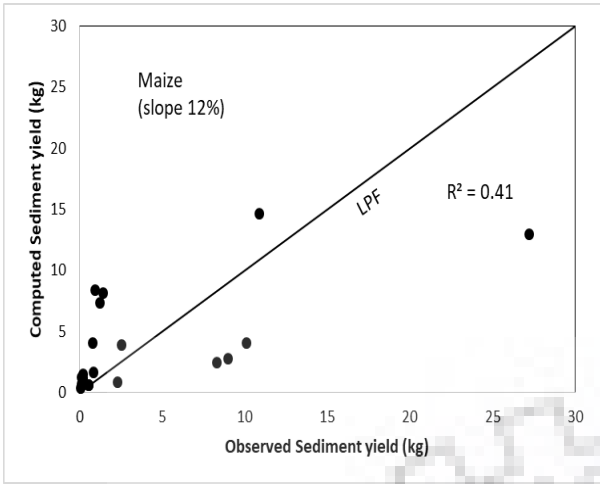


Figure 6.14 Performance of PS1 and PR1 models in application to 2016 data of different land uses/slopes. Sediment yield in kg and runoff in mm. (LPF = Line of perfect fit)





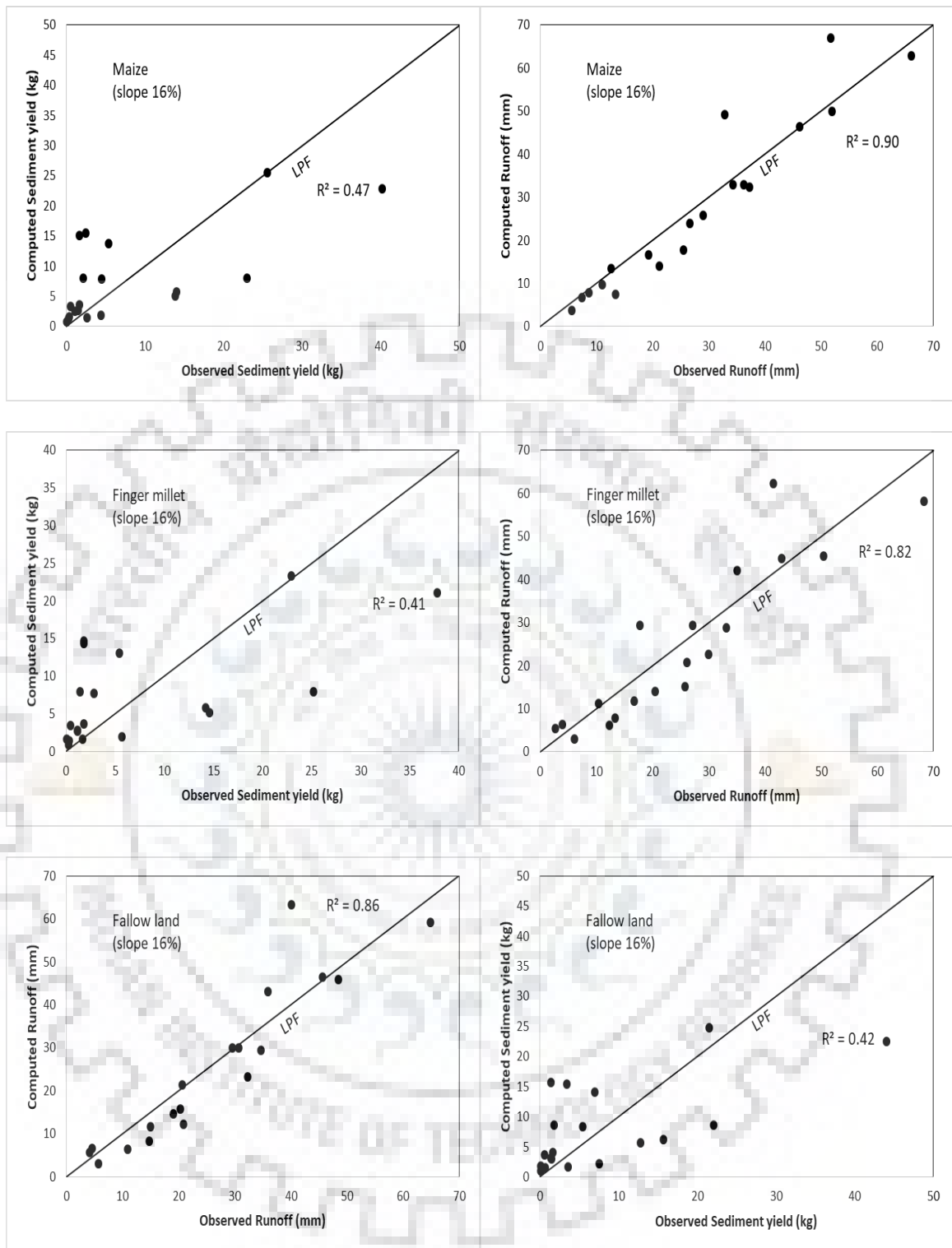


Figure 6.15 Performance of PS1 and PR1 models in application to 2017 data of different land uses/slopes. Sediment yield in kg and runoff in mm. (LPF = Line of perfect fit)

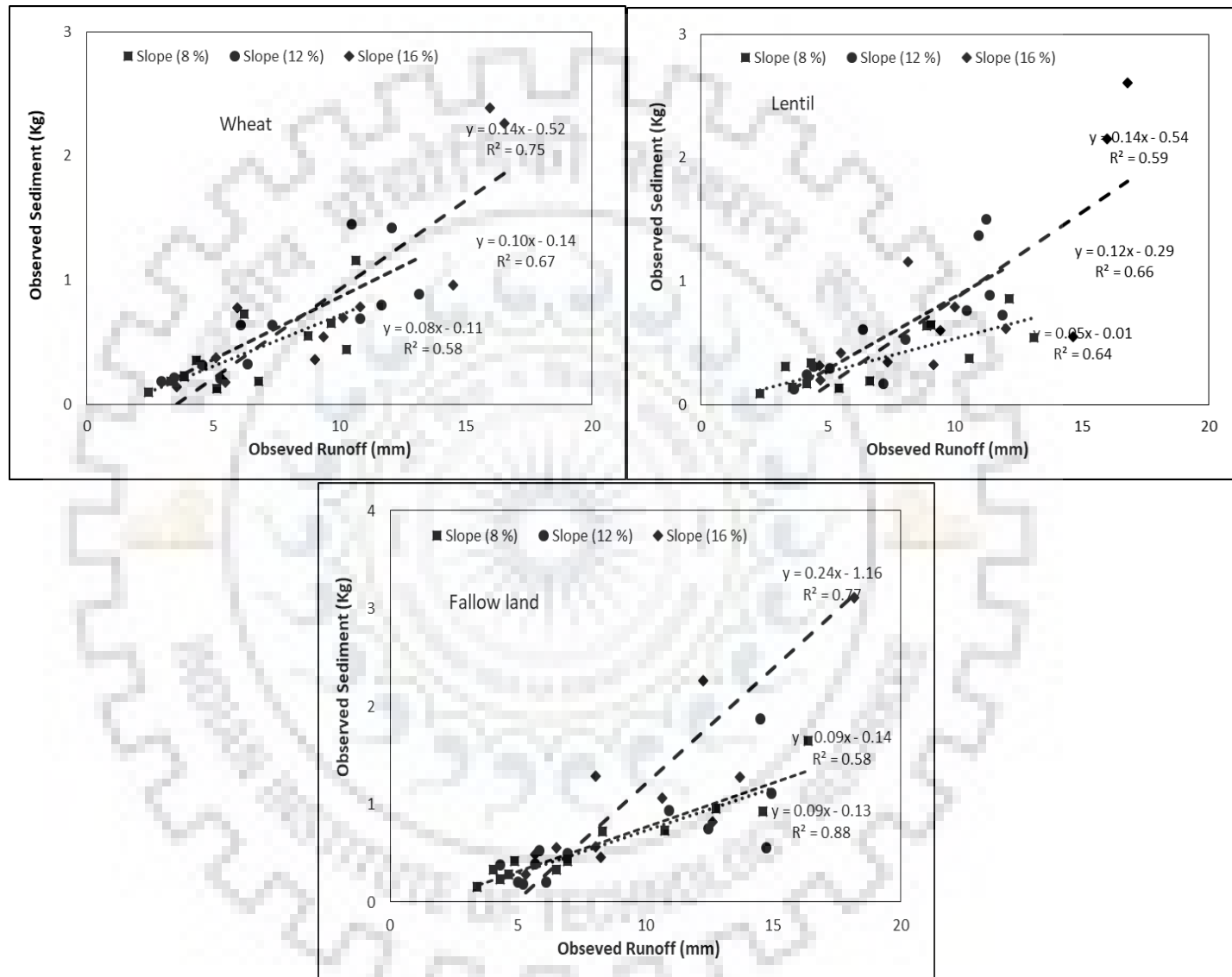


Figure 6.16. Sediment rating curve for different land uses on different slopes.

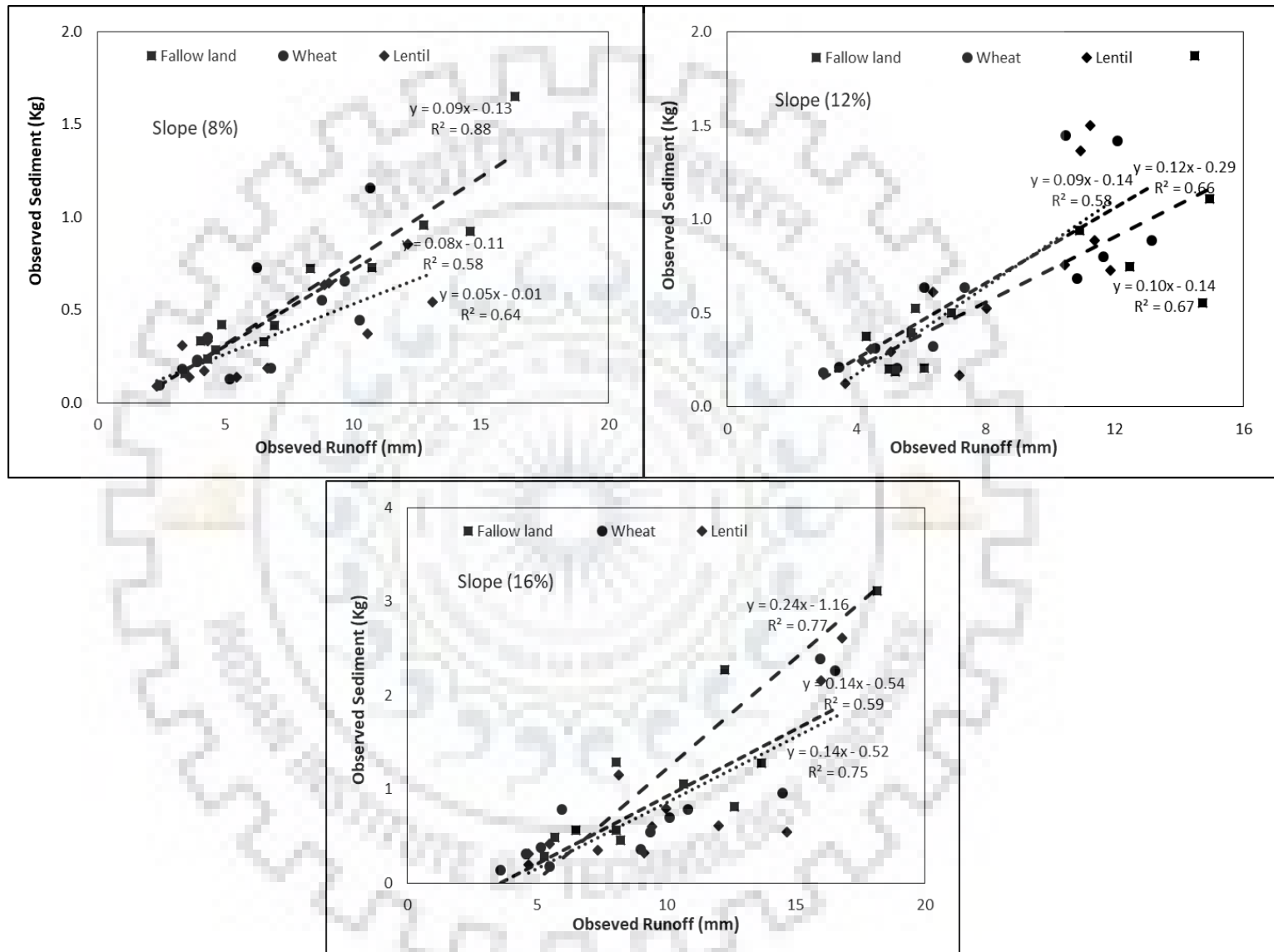
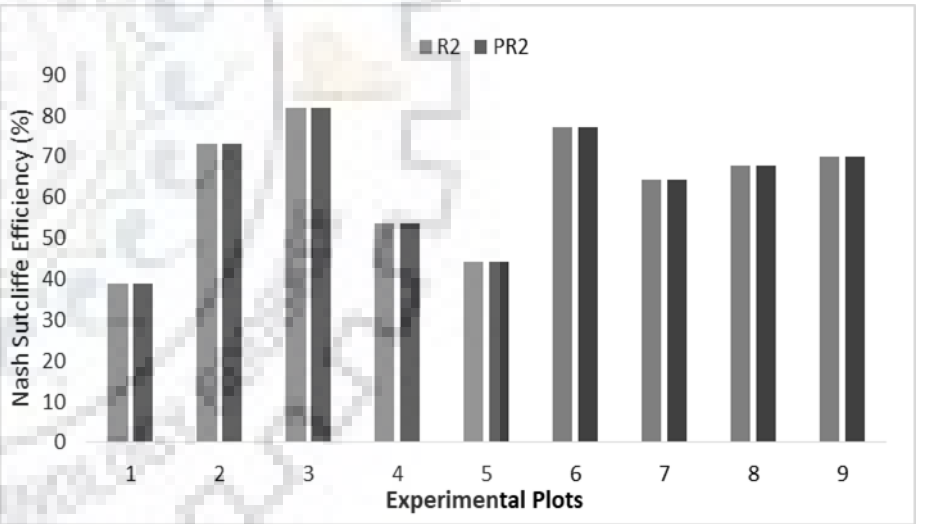
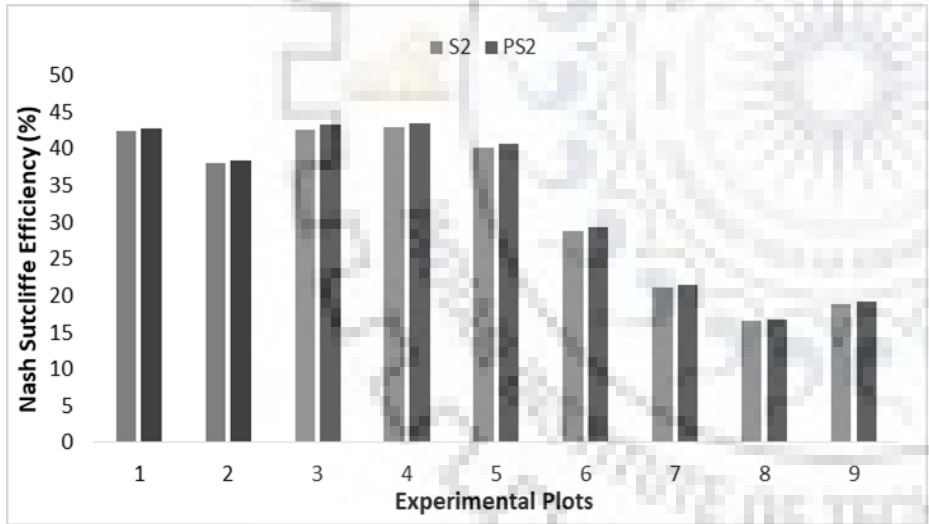
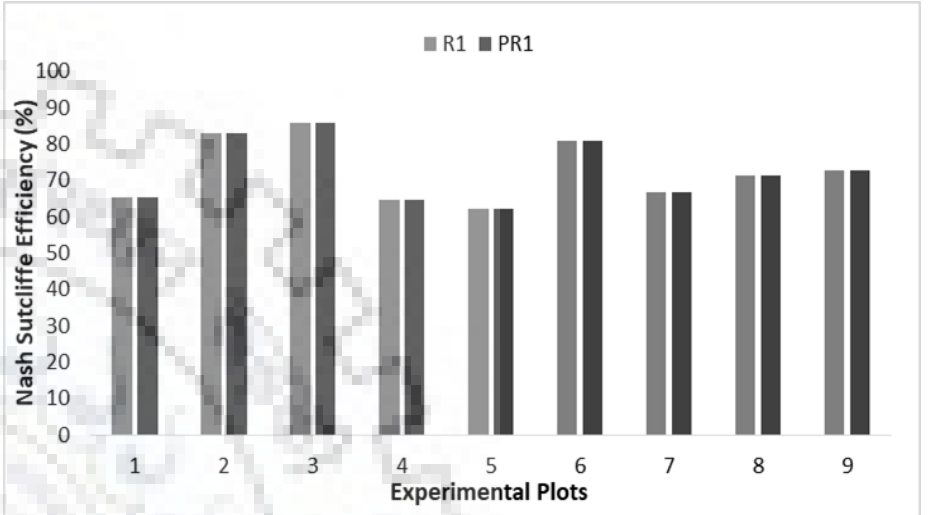
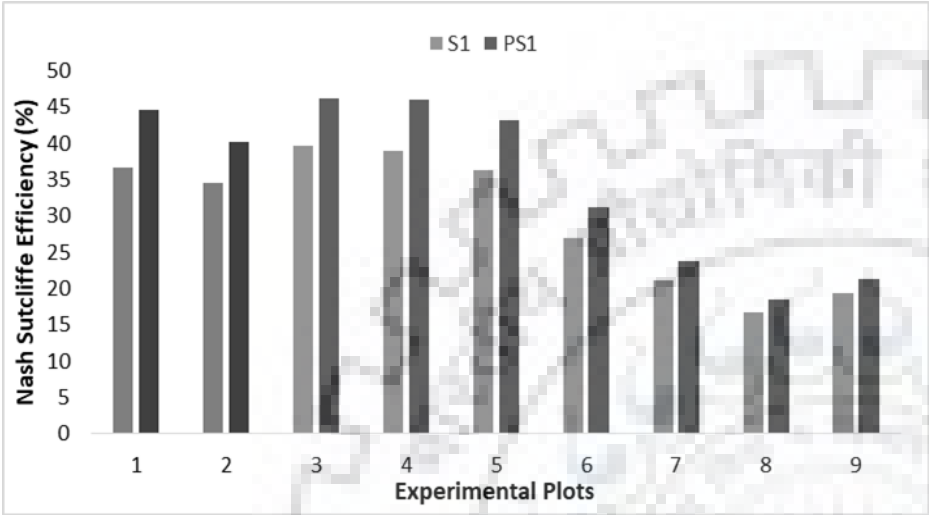


Figure 6.17. Sediment rating curve for different land uses on different slopes.



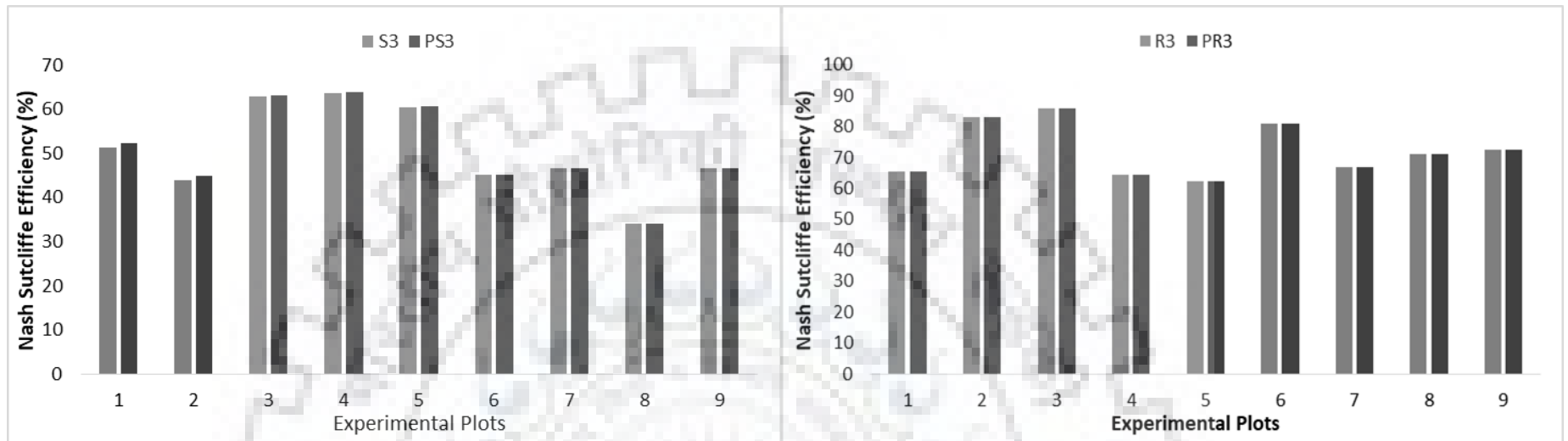


Figure 6.18 Nash Sutcliffe Efficiency of existing and proposed Rainfall-Sediment Yield models.

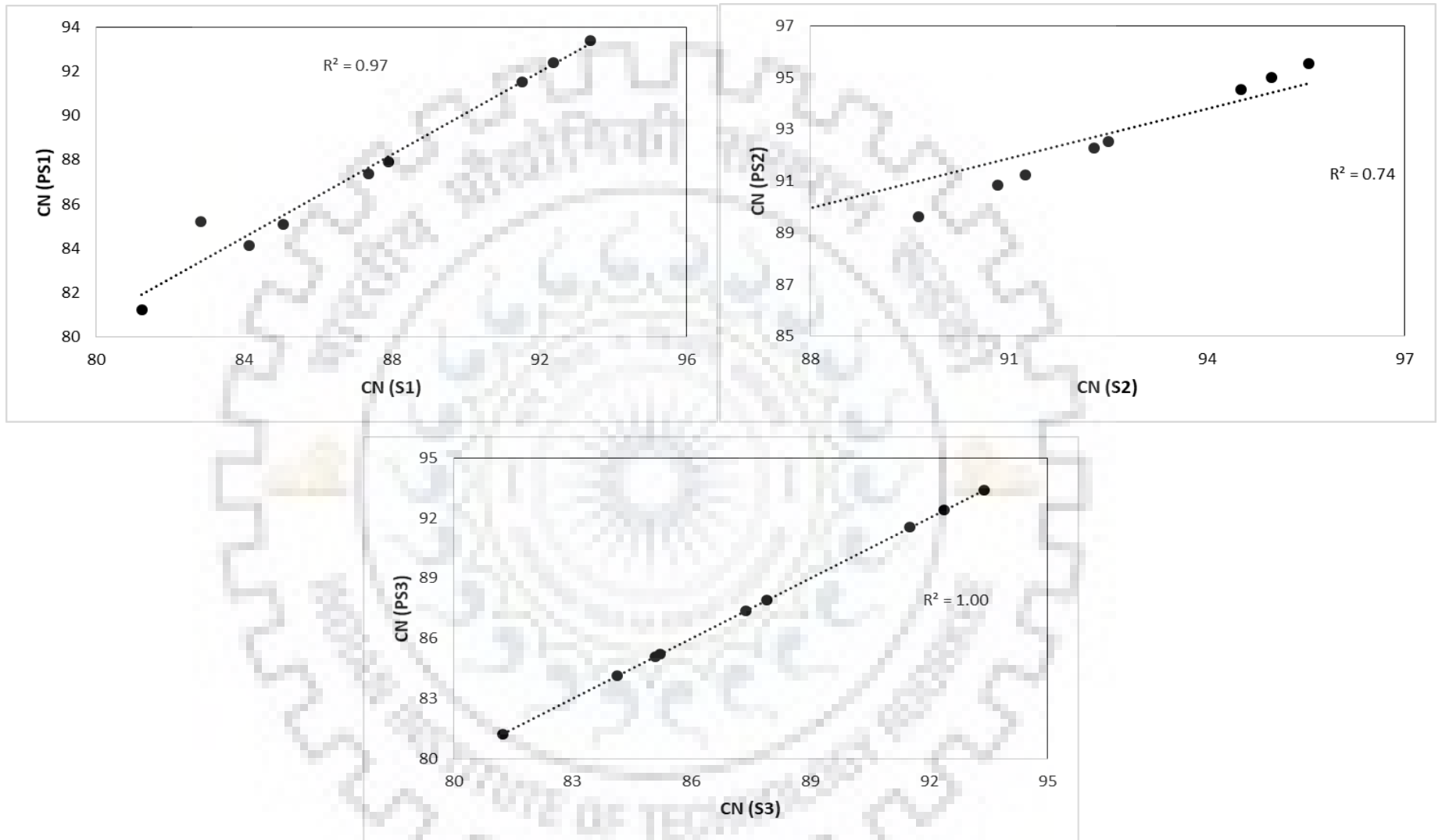
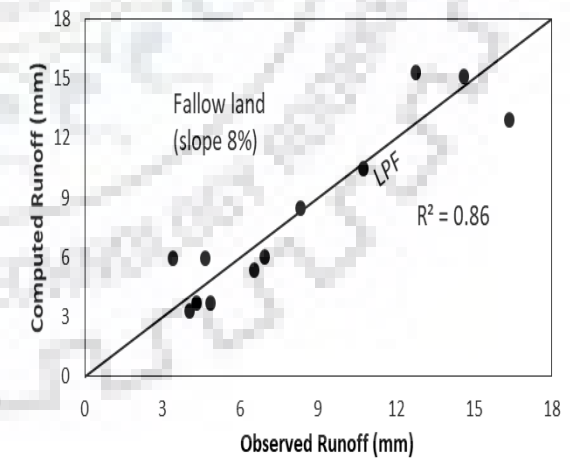
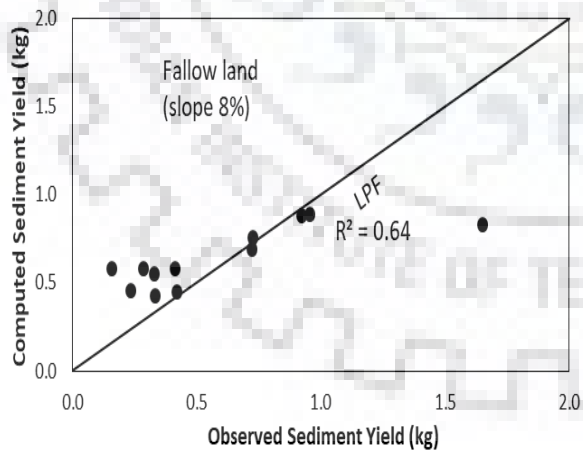
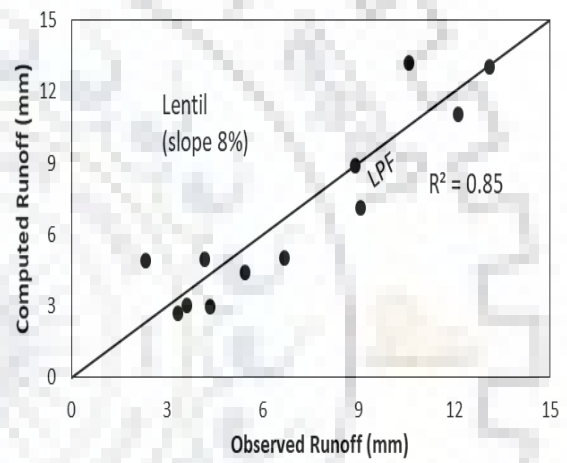
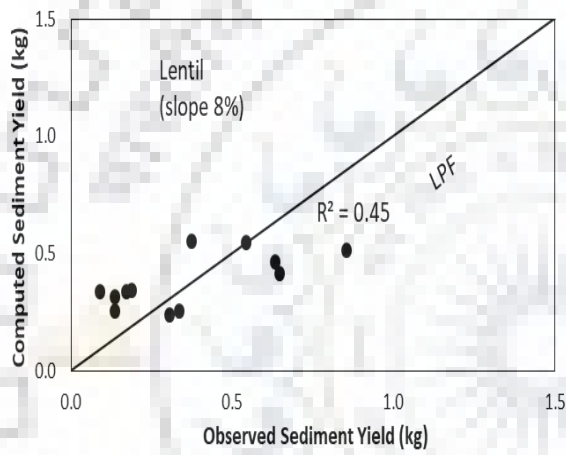
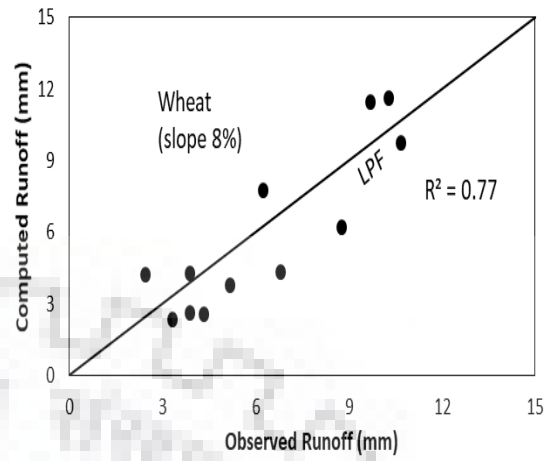
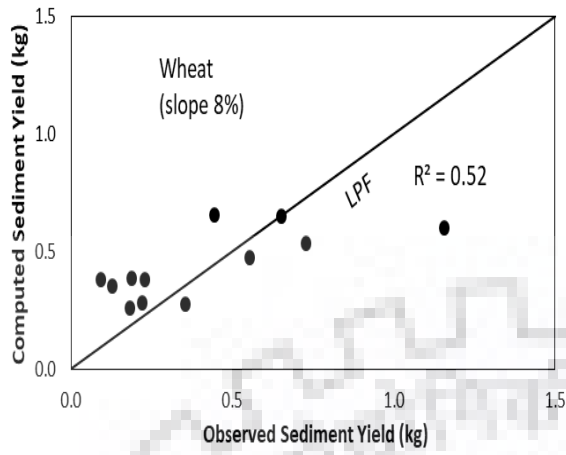
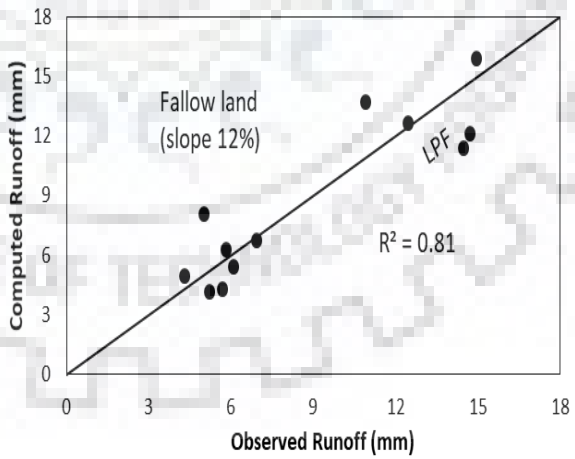
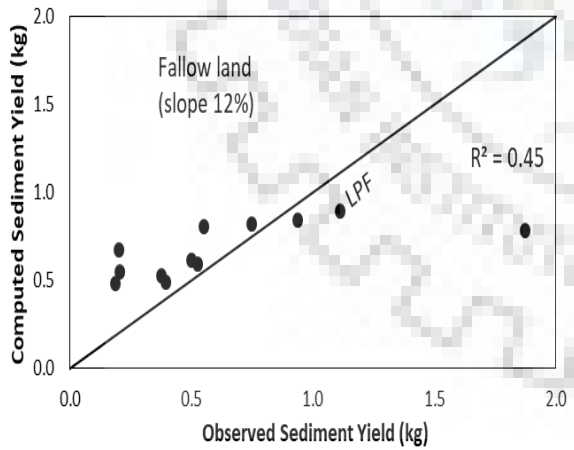
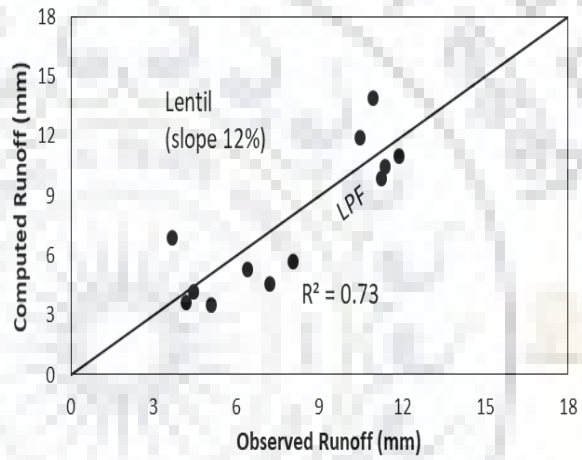
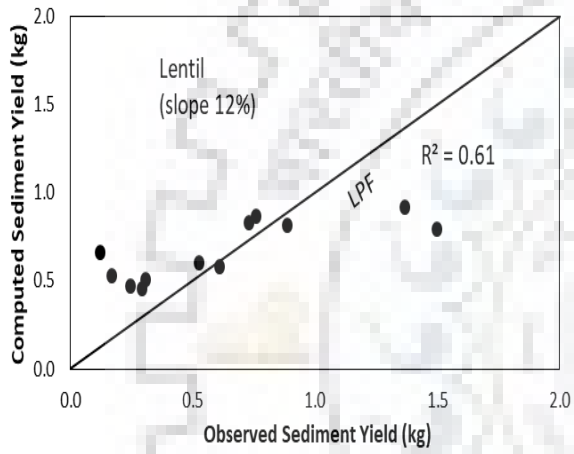
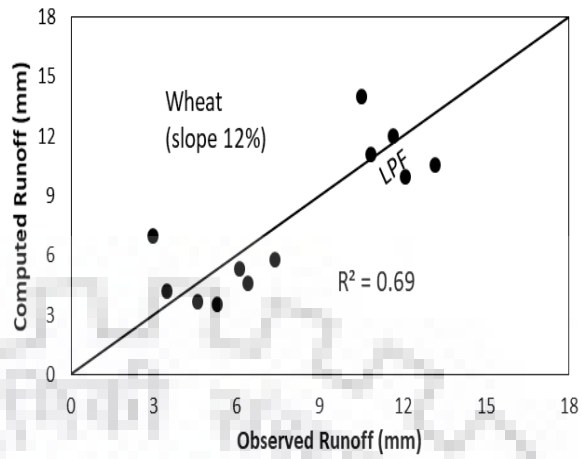
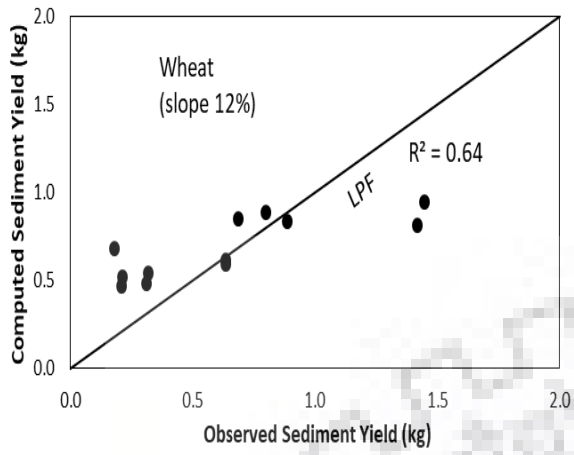


Figure 6.19 Relationship between CN values derived from existing and proposed rainfall-runoff models.





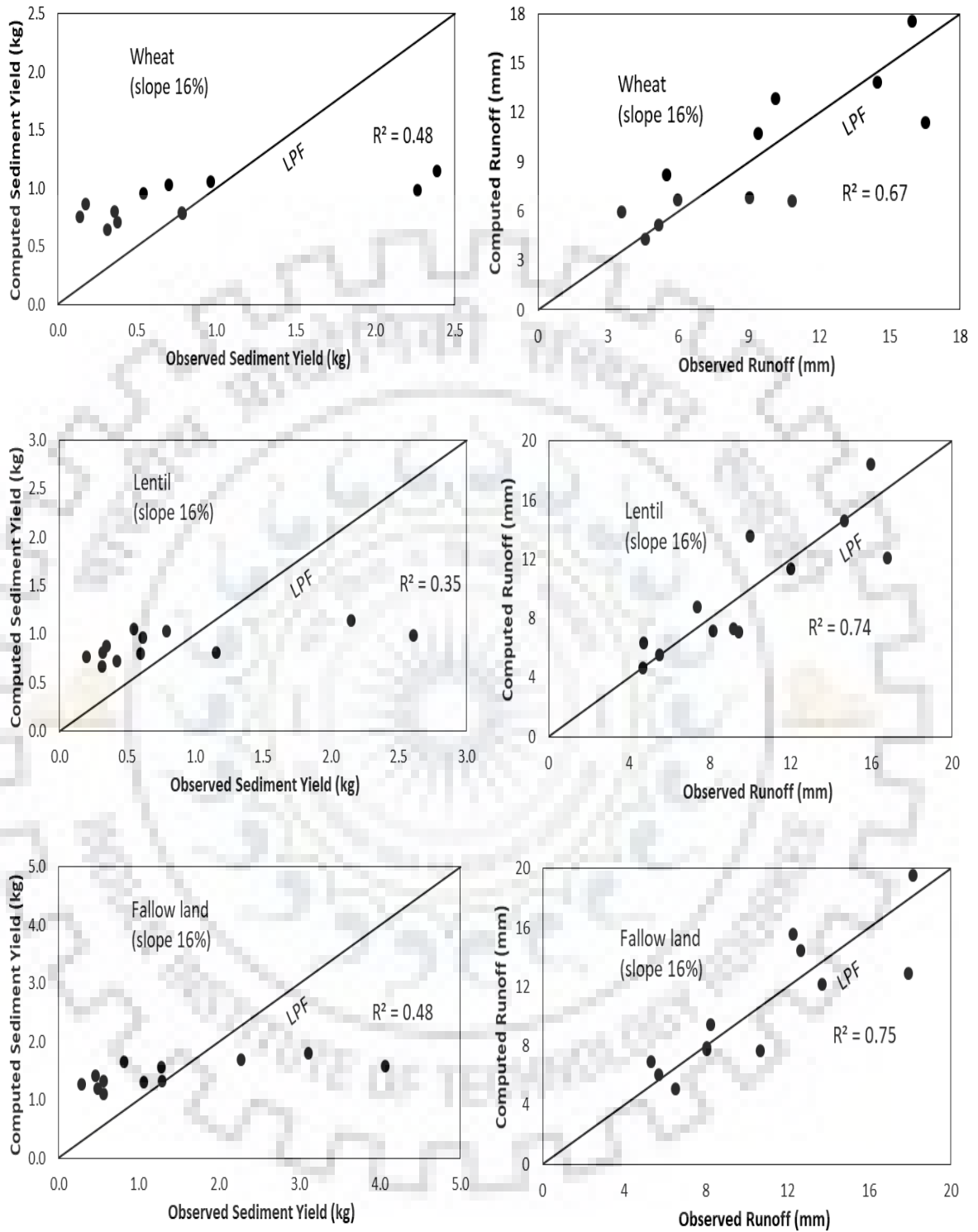


Figure 6.20 Performance of PS1 and PR1 models in application to 2017 data observed using artificial rainfall of different land uses/slopes. Sediment yield in kg and runoff in mm. (LPF = Line of perfect fit)

6.7 SUMMARY AND CONCLUSIONS

The present chapter investigated the applicability of USLE-based SCS-CN models for computing total sediment yield from a storm event using the rainfall-runoff-sediment yield data observed from 09 experimental watersheds (plot size 12×3 m²) of different land uses, soils, and slopes. The sediment rating curves were drawn between the observed sediment and observed runoff for the plots of different slopes. The trend of increase in sediment yield (mass) with runoff and slope is same for all land uses, viz., maize, finger millet, and fallow land. The rate of increase in sediment yield with runoff is sharper for greater slope, and vice versa.

In this chapter, the modified SCS-CN based models (considering $S = S_0 e^{-\alpha P}$), which removes the structural inconsistencies of the SCS-CN method, are examined with respect to the existing models for sediment yield estimation. Three models viz., PS1, PS2 and PS3 are proposed for different initial abstractions ($I_a = 0$, $I_a = 0.2S$, $I_a = \lambda S$) and compared with the corresponding existing models i.e. S1, S2 and S3. All these models were tested with observed sediment data. Similarly, three proposed models (PR1, PR2 and PR3) and existing models (R1, R2 and R3) are tested against the observed runoff.

For naturally occurring rainfall events, the coefficient of determination (R^2) is higher in the year 2016 than 2017. For 2016, R^2 values of maize for 8%, 12% and 16% slopes are 0.50, 0.45 and 0.77, respectively. Similarly, for 2017, these are 0.56, 0.34 and 0.24 for 8%, 12% and 16% slopes. In case of Finger millet, R^2 are 0.32, 0.41, 0.77 (for year 2016) and 0.12, 0.12, 0.15 (for year 2017) respectively for slopes of 8%, 12% and 16%. Similarly, for Fallow land, R^2 values are 0.78, 0.44 and 0.79 for year 2016 and 0.061, 0.33, 0.15 for year 2017.

From the artificial rainfall experiments, higher canopy crop (such as wheat) generated lower runoff and sediment yield, and vice versa. R^2 values for maize crop on 8%, 12% and 16% slopes are 0.58, 0.67 and 0.75, respectively; for lentil, these are 0.64, 0.66 and 0.59, respectively; and for fallow land, these are 0.88, 0.58 and 0.77, respectively.

The proposed models performed much better than the existing models for sediment yield estimation in both 2016 and 2017 data. In performance the sediment yield models are ranked as: PS3>PS1>PS2. Among the proposed runoff models, PR3 and PR1 performed approximately similar, whereas PR2 performed poorly.

7.1 INTRODUCTION

Human interventions such as dam construction, channelization and gravel extraction affects the physical and ecological processes in rivers from many years across the world (Gore, 1985; Gregory, 2006). Today in the world of increasing water demand, the restoration of rivers has drawn the attention of researchers around the globe (Bates et al., 2008; Vörösmarty et al., 2010). Meier (1998) defines *river restoration* as, “an attempt to bring the river back to as high a level of ecological integrity as possible, taking into account the prevailing socio-economic, political, and technological constraints. In highly managed rivers, the objective should be to maintain a healthy ecosystem that is able to meet the societal needs in a sustainable manner.” Despite of lot of efforts and funds devoted for the river recovery, the rate of success for river restoration is not up to the mark (Bernhardt et al., 2005; Roni et al., 2008).

The dynamics of runoff are regulated by different mechanisms, which act on a range of spatial and temporal scale (Sivakumar et al., 2001). The health of river ecosystem can be determined by many factors such as flow, channel structure and riparian zone, quality of water, exploitation level and macrophyte cutting and dredging (Norris and Thoms, 1999). Initially, it was believed that all the problems related to health of the river are associated with low flows and that the river ecosystem will be conserved till a minimum flow is maintained in the river, but as time lapses people become more aware about importance of all the other elements of flow regimes such as floods, medium and low flows (Poff et al., 1997; Hill et al., 1991).

The increasing demand of water around the globe draws the attention of researchers to ponder about the estimation of environmental flow requirement. A number of studies have been done in different parts of the world for the formulation, implementation and adaptation of various approaches for environmental flow assessment (EFA). The various methods of EFA have been often reviewed critically in several studies (Stalnaker and Arnette 1976; Jowett 1997; Arthington 2012; Linnansaari et al. 2012; Hatfield et al. 2013). The methods for environmental flow assessment were developed initially for the estimation of in-stream flow needs of fish residing below the irrigation and

hydroelectric dams over large rivers (Dunbar et al. 1998; Tharme and Smakhtin 2003; Kumar et al., 2007; Amrit et al., 2019) with the objective of setting the flow requirement during low flow periods (Leathe and Nelson, 1986). There are large number of methods/approaches presently being used for the estimation of environmental flow requirement to sustain the river in good condition during different flow (low and high) periods (Tharme, 2003; Amrit et al., 2019). The methods for estimation of environmental flow requirement are grouped as (a) hydrological, (b) hydraulic rating, (c) habitat simulation, and (d) holistic methods.

The simplest hydrological methods for EF estimation require flow data of rivers. These methods assume a relationship between stream flow and certain biological parameters. Many hydrological methods are available for estimation of EF, however Tennant method is quite popular worldwide. Smakhtin and Masse (2000) proposed a method for the generation of time series of daily flow data using the observed daily precipitation in a catchment. The application of the suggested approach was demonstrated on the various catchments located in South Africa, and was very useful for the ungauged or poorly gauged sites. Gupta (2008) studied about the implication of environmental flow (EF) in management of river basin. The approaches for the assessment of environmental flow are evaluated in perspective of flow characteristics of river. The study revealed that EF can be integrated in the mainstream of operation of infrastructure (such as dams and pumps) to modulate the flow of water for the aquatic and other environment in the basins having regulated flows. Vaughan et al., (2009) integrated the ecology and hydromorphology for river management. The study indicated that the assessment of relations between ecology and physical habitat are serious problem in river research and management.

Haghighi and Klove (2017) suggested release of EF in areas where irrigation demand is high. Mishra et al. (2019) correlated %AAF and SPI for the prediction of environmental flow condition during low flow season (October-June), using rainfall-runoff data of five catchments of Godavari basin. The analysis revealed that the EF condition of the studied catchments during low flow season could be ascertained through rainfall-based SPI (9-month scale).

The Curve Number (CN) parameter of the SCS-CN methodology (SCS, 1956) describes the runoff potential of the watershed (Mishra and Singh, 2003), for it is based on the major runoff producing watershed characteristics, such as soil type, land use/ treatment, surface condition, and antecedent moisture conditions (AMCs).

EF assessment using Tennant method (hydrological method), assumes the existence of relationship between flow alteration and specific environmental responses. Generally, Tennant method is used to recommend instream flows and Curve Number (CN) is used to describe the runoff potential of catchment. In spite of the fact that both the ideas infer levels of water supply for natural ecosystems or anthropogenic activities, they manage the issue at various spatiotemporal scales in hydrology.

As above, CN is used to describe the runoff potential of catchment from low to high based on catchment characteristics (i.e. soil type, land use/treatment, surface condition, and antecedent moisture conditions) whereas, Tennant method is utilized to represent the EF state of a stream from flushing flow to serious degradation depending on if the river has maximum flow or runs dry, based on percentage of AAF (%AAF) computed using the flow data. As the flow through the catchment depends on its characteristics and Tennant method is used to describe the EF condition based on flow data, so there might be a possibility of relationship between CN and Tennant method.

The CN is directly related to precipitation and %AAF is related to flow, since both are equally dynamic parameter but the %AAF can only be used in gauged catchments for the prediction of environmental flow condition, while the relationship between CN and %AAF enables us to predict the environmental flow condition of the ungauged (where flow data is not available) catchments too which forms the primary objective of this chapter.

The application of this study has been demonstrated on 17 catchments, a summary of their characteristics is given in Table 7.1. Some of the study catchments and data used in the analysis have been taken from the study entitled “Study of regional drought characteristics and environment” by Kumar Amrit (2018)

Table 7.1 Summary characteristics of study catchments

S. No.	Catchment	River	Major River Basin	Area (Km ²)	Data Length	Latitude (N)	Longitude (E)	Elevation Range (m)	Climatic region
1	Ghatora	Arpa	Mahanadi	3035	1991-2010	22 ⁰ 02'31"	82 ⁰ 13'22"	246	Sub-humid
2	Rampur	Jonk	Mahanadi	2920	1991-2010	21 ⁰ 39'19"	82 ⁰ 31'17"	231.88	Sub-humid
3	Baronda	Pairi	Mahanadi	3225	1990-2010	20 ⁰ 54'40"	81 ⁰ 53'05"	289.37	Sub-humid
4	Basantpur	Mahanadi	Mahanadi	57780	1990-2010	21 ⁰ 43'19"	82 ⁰ 47'22"	206	Sub-humid
5	Chakaliya	Anas	Mahi	3121	1991-2010	23 ⁰ 03'16"	74 ⁰ 91'10"	215	Semi-arid
6	Hivra	Wardha	Godavari	10240	1991-2010	20 ⁰ 32'52"	78 ⁰ 31'25"	230	Semi-arid
7	Nandgaon	Wunna	Godavari	4580	1990-2010	20 ⁰ 30'59"	78 ⁰ 48'12"	198	Semi-arid
8	Dhariawad	Jakham	Mahi	1510	1990-2010	24 ⁰ 05'12"	74 ⁰ 47'10"	203	arid
9	Ashti	Wainganga	Godavari	50990	1990-2010	19 ⁰ 41'04"	79 ⁰ 22'52"	141.42	Semi-arid
10	Bamini	wardha	Godavari	46020	1990-2010	19 ⁰ 48'47"	79 ⁰ 22'52"	157.97	Semi-arid
11	Bhatpalli	Peddavagu	Godavari	3100	1990-2009	19 ⁰ 18'57"	79 ⁰ 28'16"	156	Sub-humid
12	Satrapur	Kanhan	Godavari	11100	1990-2010	21 ⁰ 13'24"	79 ⁰ 13'48"	263.30	Dry sub-humid

13	Jagdapur	Indravathi	Godavari	7380	1990-2010	19 ⁰ 06'27"	82 ⁰ 01'23"	543	Semi-arid
14	Ramakona	Kanhan	Godavari	2500	1990-2010	21 ⁰ 43'05"	78 ⁰ 49'08"	336.38	Dry sub-humid
15	P.G. penganga	Penganga	Godavari	18441	1990-2008	19 ⁰ 48'57"	78 ⁰ 34'29"	198	Semi-arid
16	Jenepur	Brahmni	Brahmni-Baitarni	33955	1990-2010	20 ⁰ 53'05"	86 ⁰ 34'29"	13	Sub-humid
17	Kogaon	Kundi	Narmada	3919	1990-2010	22 ⁰ 06'10"	75 ⁰ 41'53"	151	Semi-arid

7.2 METHODOLOGY

7.2.1 Tennant method

In this method, the various streamflow conditions are classified using Average Annual Flow (AAF). This method uses percentages for classification of conditions (Table 7.2). This method is a globally accepted for the assessment of environmental flow. Tennant Method relates AAF percentage on a seasonal basis to flows that uphold geomorphic function (flushing flows) and flows that preserve instream habitat condition. This approach also called as Montana method and was developed in USA considering the data from eleven streams comprising 38 different flows and 58 cross section (Mann, 2006). The data related to different aspects over which both (warm and cold water) fish habitats depends, were collected for the study. The Some fraction of average flow is essential to maintain a good stream environment, is the basic assumption of this method. For temporary survival, the average velocity and depth of flow should not be less than 0.3m and 0.25m/s, respectively. The flow depth of 0.45 to 0.6m and flow velocity of 0.45 to 0.6m/s were found optimum for the survival of fish. These situations corresponded to 10% and 30% of average annual flow (AAF), respectively, in various streams that were analysed. Different flow conditions described based on percentage of AAF for low (October-March) flow periods (Tennant, 1975) are given in Table 7.2.

Table 7.2 Flow conditions based on percentage of AAF for low flow season (October-March) (Tennant, 1975)

Flow Condition	% of AAF
Flushing flow	200
Optimum range of flow	60-100
Outstanding	40
Excellent	30
Good	20
Fair or Degrading	10
Poor or Minimum	10
Severe Degradation	Less than 10

7.2.2 SCS-CN method

The detailed description of SCS-CN method has been provided in Section 4.2. (Chapter 4).

7.3 ANALYSIS AND DISCUSSION OF RESULTS

The analysis has been carried out using the data of different catchments for exploration of the existence of a relationship between %AAF, which describes EF condition in Tennant (1976) approach, and CN, which describes the runoff potential of the watershed for the non-monsoon season from October-June. The following two cases are considered:

Case 1: Relationship derived between CN and %AAF is calibrated and validated for each of the seventeen catchments using split datasets.

Case 2: A general relationship between CN and %AAF is derived using the calibration dataset of all the watersheds, and tested on the combined validation dataset of all watersheds.

Case 1

Relationship derived between CN and %AAF is calibrated and validated for each of the eleven catchments using split datasets, as follows.

Ghatora catchment: The data for rainfall-runoff pertaining to 1991-2008 were utilized. The mean flow of nine months i.e. from October to June for each year was calculated to determine AAF. Based on the %AAF, the various flow conditions of the catchment are described. Similarly, from the rainfall-runoff data, CN was also estimated for the same duration for each year. CN was optimized, considering λ to be zero, for each year. The rainfall-runoff data of non-monsoon season (October to June) were used for the optimization of CN. A plot between %AAF and CN for the split data is shown in Fig. 7.1(a) for the period of 1991-2000. It is seen that, as CN increases, %AAF also increases, and vice versa. The value of R^2 is 0.574, which shows a very good fit. Further, the remaining data of the same period (2001-2008) were used for validation of the derived relationship. The observed and computed %AAF of the corresponding CN values when plotted in Fig. 7.1(b) show the observed and computed %AAF values are generally close to the line of perfect fit (LPF), indicating a satisfactory fit.

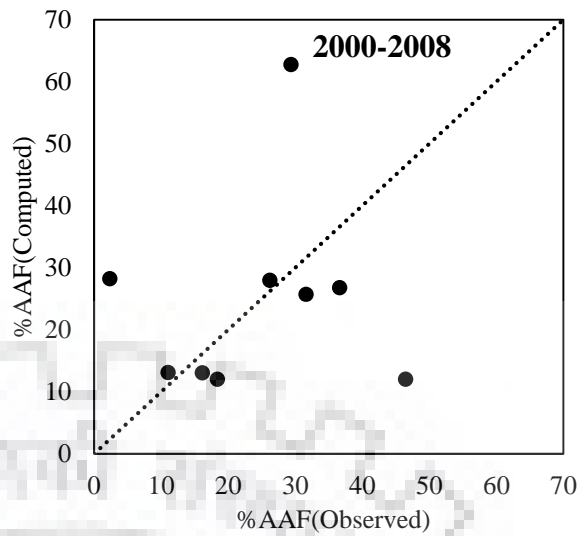
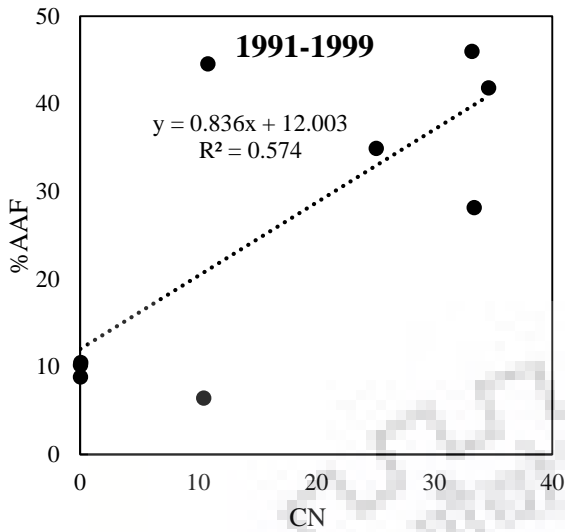


Figure 7.1(a) %AAF versus CN values for Ghatora catchment

Figure 7.1(b) Observed and computed %AAF for Ghatora catchment.

Jagadapur catchment: The data for rainfall-runoff pertaining to 1991-2009 were utilized. Following the similar procedure as above, the derived %AAF is plotted against the corresponding CN for Kurubhata catchment in Fig. 7.2 (a) with $R^2 = 0.607$, showing a good agreement between %AAF and the corresponding CN. Thus, CN can be used to ascertain the EF condition over this catchment. Further, %AAF has been computed for the period 2001-2009 and plot of observed and computed %AAF is shown in Fig. 7.2(b), leading to similar inference as above.

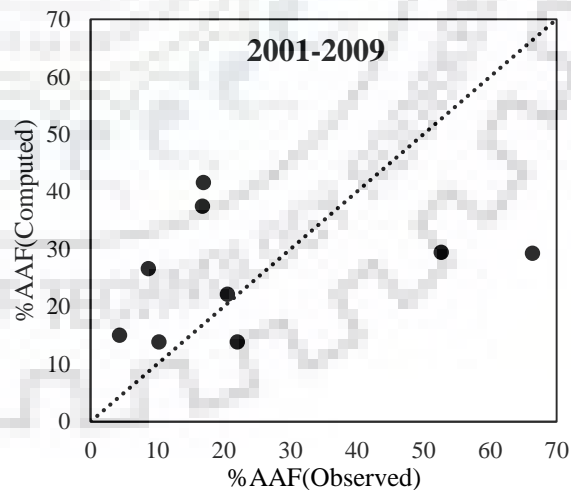
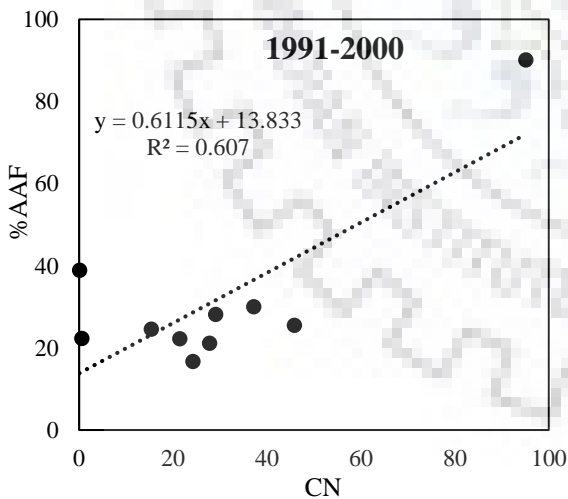


Figure 7.2(a) %AAF versus CN values for Jagadapur catchment

Figure 7.2(b) Observed and computed %AAF for Jagadapur catchment

P. G. Penganga Catchment: The data of 17 years (1991-2007) were used, and the requisite plot using the data of 10 years (1990-2000) is shown in Fig.7.3(a), again indicating a very good fit

($R^2 = 0.596$). The observed and computed values of %AAF for the period 2001-2007 are seen to be in good agreement (Fig. 7.3b).

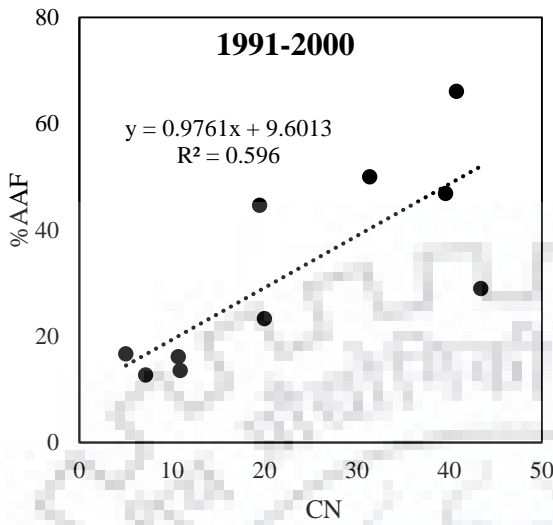


Figure 7.3(a) %AAF versus CN values for P. G. Penganga catchment

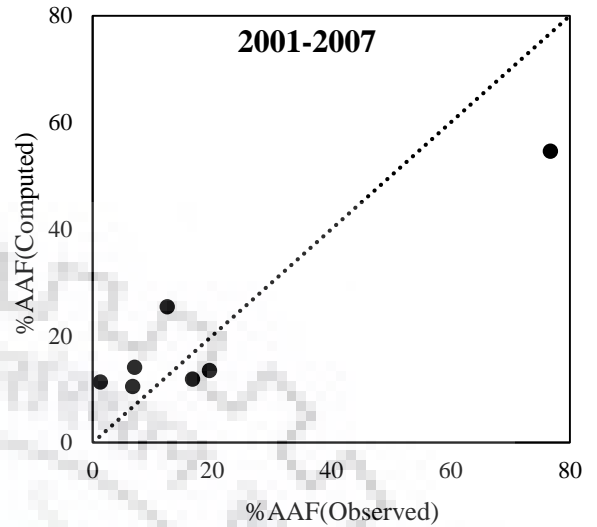


Figure 7.3(b) Observed and computed %AAF for P. G. Penganga catchment

Ramakona Catchment: The data for rainfall-runoff pertaining to 1990-2009 were utilized. The %AAF derived for 1990-2000 is plotted against the corresponding CN for Ramakona catchment in Fig. 7.4(a) with $R^2 = 0.547$, exhibiting a very good %AAF - CN relationship. Thus, EF condition for this catchment can be ascertained using CN. The observed and computed %AAF (for the period 2001-2006) of the corresponding CN values were plotted in Fig. 7.4(b), which shows the observed and computed %AAF values are generally close to LPF.

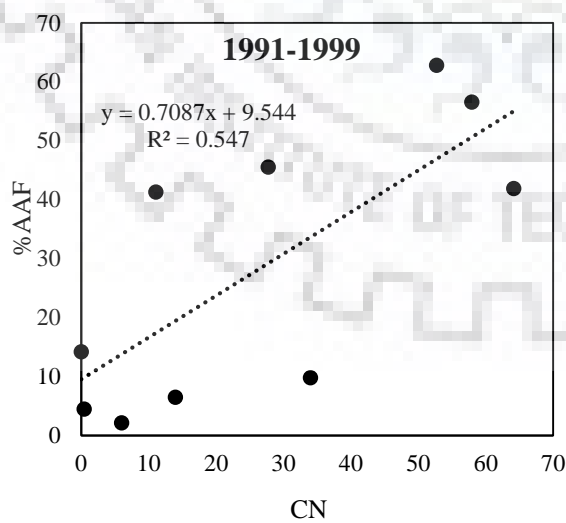


Figure 7.4(a) %AAF versus CN values for Ramakona catchment

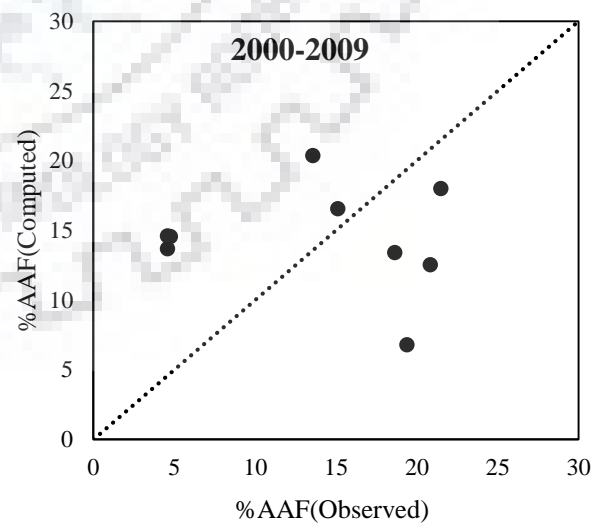


Figure 7.4(b) Observed and computed %AAF for Ramakona catchment

Rampur Catchment: The data of 19 years (1991-2008) were used, and the requisite plot using the data of 10 years (1991-2000) is shown in Fig. 7.5(a), again indicating a very good fit ($R^2 = 0.511$). Further, %AAF has been computed for the period 2001-2009 and plot between observed and computed %AAF is presented in Fig. 7.5(b), leading to similar inference as above.

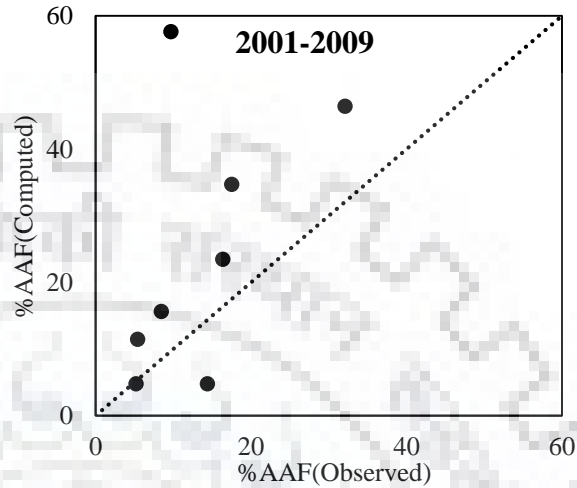
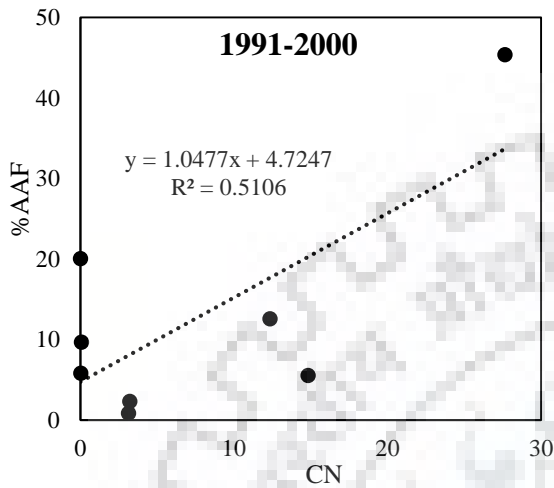


Figure 7.5(a) %AAF versus CN values for Rampur catchment

Figure 7.5(b) Observed and computed %AAF for Rampur catchment.

Hivra Catchment: The data for rainfall-runoff pertaining to 1991-2008 were utilized. The %AAF derived for 1991-2000 is plotted against the corresponding CN for Hivra catchment in Fig. 7.6(a) with $R^2 = 0.556$, exhibiting a very good relationship. Thus, EF condition for this catchment can be ascertained using CN. The observed and computed %AAF (for the period 2001-2008) of the corresponding CN values were plotted in Fig. 7.6(b), which shows the observed and computed %AAF values are generally close to LPF.

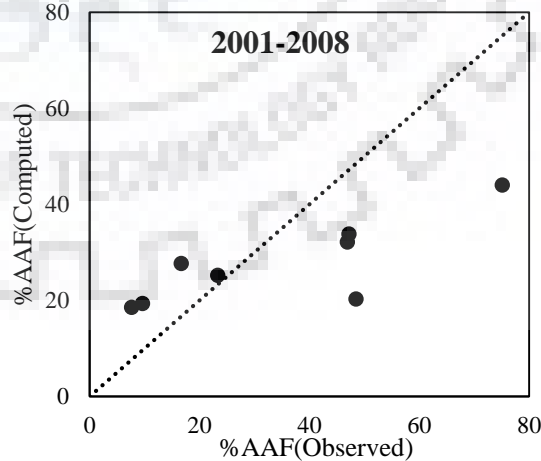
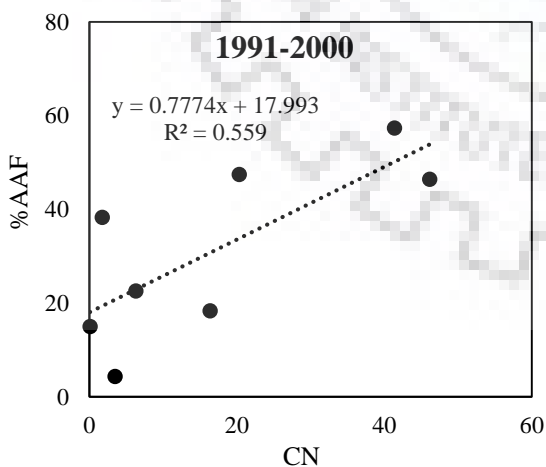


Figure 7.6(a) %AAF versus CN values for Hivra catchment

Figure 7.6(b) Observed and computed %AAF for Hivra catchment

Nandgaon Catchment: The data of 17 years (1991-2008) were used, and the requisite plot using the data of 9 years (1991-2000) is shown in Fig. 7.7(a) ($R^2 = 0.428$). Further, %AAF has been computed for the period 2001-2009 and plot between observed and computed %AAF is presented in Fig. 7.7(b) leading to similar inference as above.

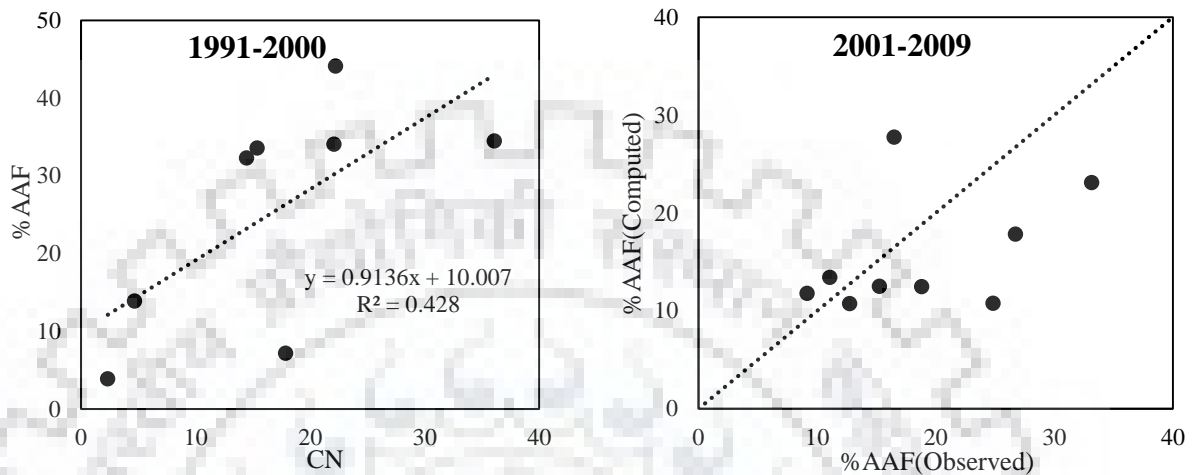


Figure 7.7(a) %AAF versus CN values for Nandgaon catchment

Figure 7.7(b) Observed and computed %AAF for Nandgaon catchment

Chakaliya catchment: The data for rainfall-runoff pertaining to 1991-2009 were utilized. The mean flow of nine months i.e. from October to June for each year was calculated to determine AAF. Based on the %AAF, the various flow conditions of the catchment are described. Similarly, from the rainfall-runoff data, CN was also estimated for the same duration for each year. A plot between %AAF and CN for the calibration data (1991-2000) is shown in Fig. 7.8(a). The value of R^2 is 0.507 shows a very good fit. Further, the remaining data (2001-2009) were used for validation of the relationship. The observed and computed %AAF of the corresponding CN values when plotted in Fig. 7.8(b) show the observed and computed %AAF values to be generally close to LPF, indicating a satisfactory fit.

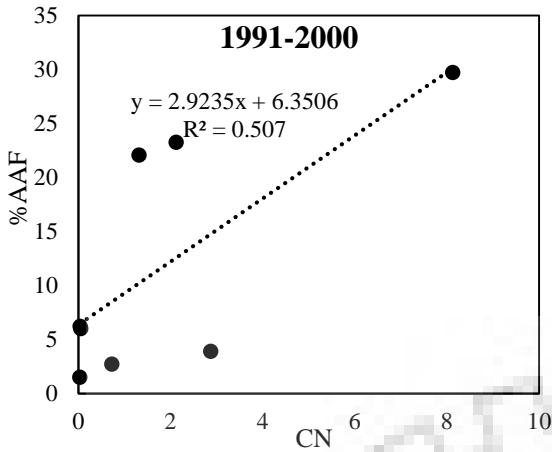


Figure 7.8(a) %AAF versus CN values for Chakaliya catchment

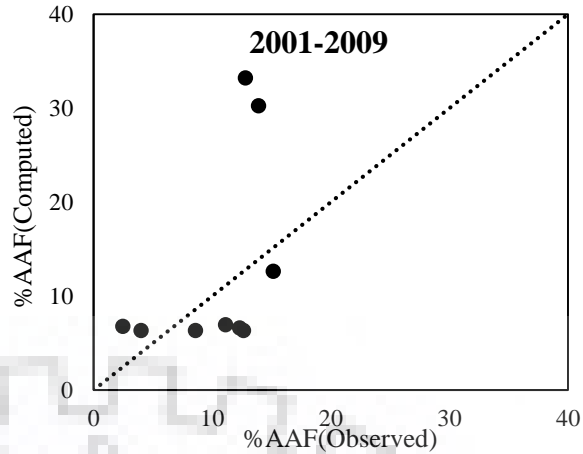


Figure 7.8(b) Observed and computed %AAF for Chakaliya catchment

Dhariawad catchment: The data for rainfall-runoff pertaining to 20 years i.e. 1990-2009 were utilized. A plot between the %AAF and CN for this catchment is shown in Fig. 7.9(a) for the period of 1990-1999 with $R^2 = 0.899$, exhibiting a good relationship between %AAF and CN. The observed and computed %AAF for 2000-2009 data plotted in Fig. 7.9(b) are generally close to LPF.

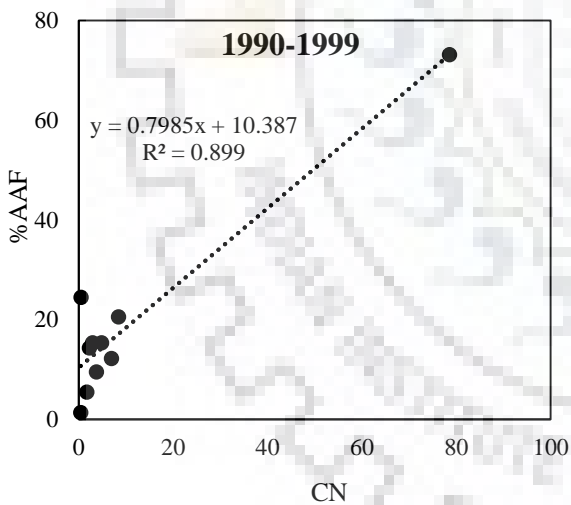


Figure 7.9(a) %AAF versus CN values for Dhariawad catchment

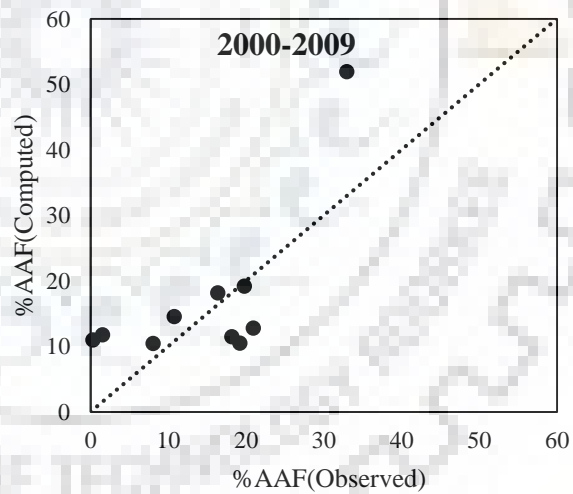


Figure 7.9(b) Observed and computed %AAF for Dhariawad catchment

Koegon Catchment: The data of 20 years (1991 – 2010) were used, and the requisite calibration plot for the period of 1991-1999 is shown in Fig. 7.10(a), fitting with $R^2 = 0.624$. The validation plot (Fig. 7.10b) from 2000-2009 imply similar inferences as above.

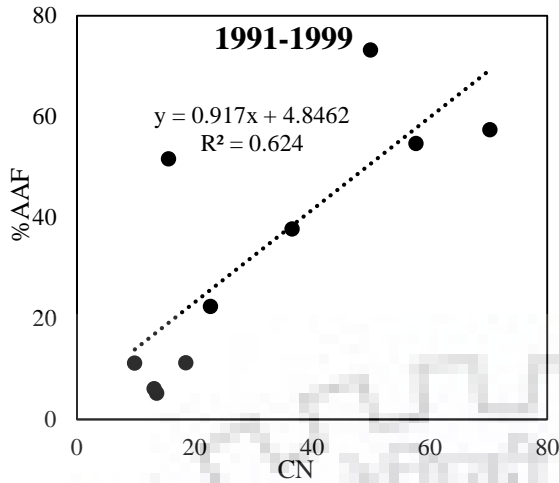


Figure 7.10(a) %AAF versus CN values for Koegeon catchment

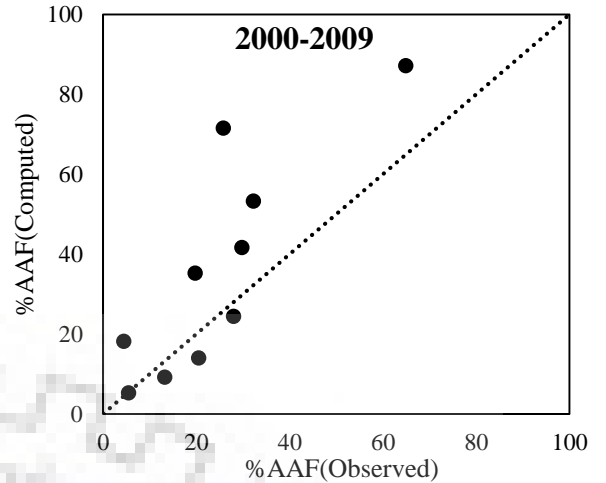


Figure 7.10(b) Observed and computed %AAF for Koegeon catchment

Jenepur Catchment: Fig. 7.11(a) shows good ($R^2=0.554$) %AAF-CN relation from 1990-2009 data. The observed and computed %AAF for 2000-2009 data points are close to LPF, as shown in Fig. 7.11 (b).

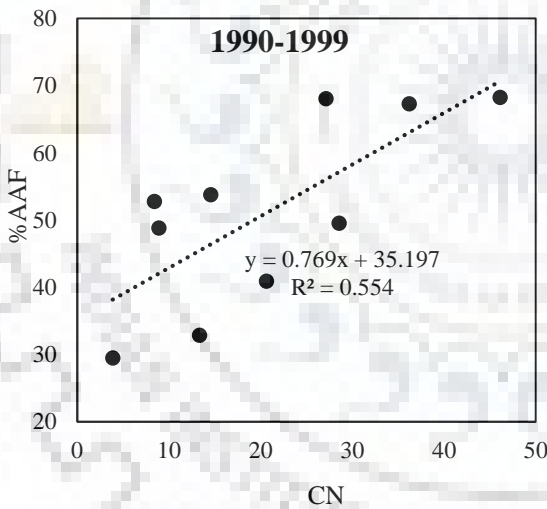


Figure 7.11(a) %AAF versus CN values for Jenepur catchment

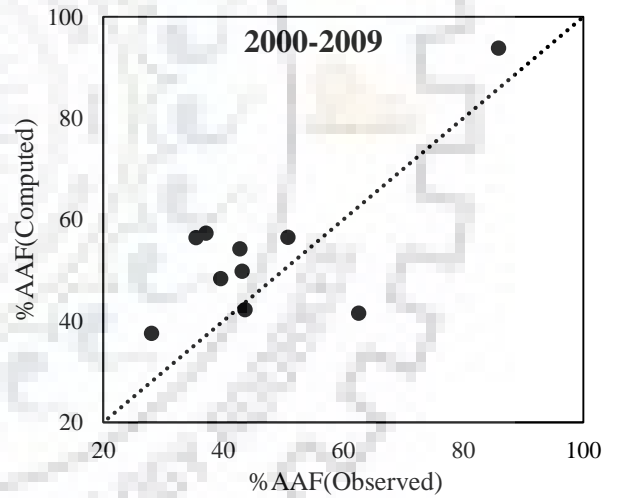


Figure 7.11(b) Observed and computed %AAF for Jenepur catchment

Ashti Catchment: The data of 21 years (1990-2010) were used, and the derived %AAF for the period of 1990-1999 is plotted against the corresponding CN in Fig 7.12(a) with $R^2=0.516$, which shows a good relationship between %AAF and CN. Further, the observed and computed %AAF for the period 2000-2009 data plotted in Fig. 7.12 (b) are close to line of perfect fit.

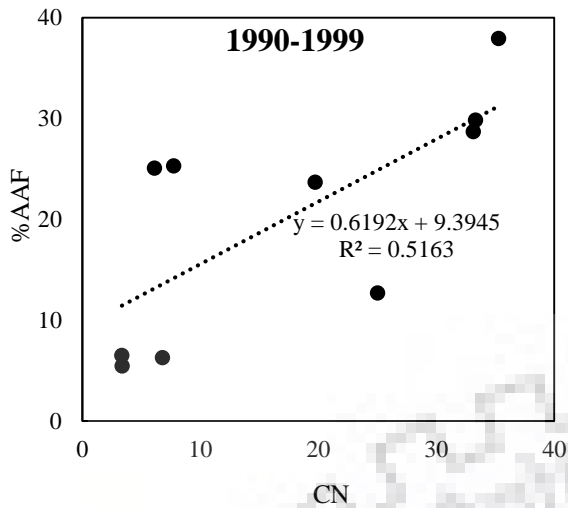


Figure 7.12(a) %AAF versus CN values for Ashti catchment

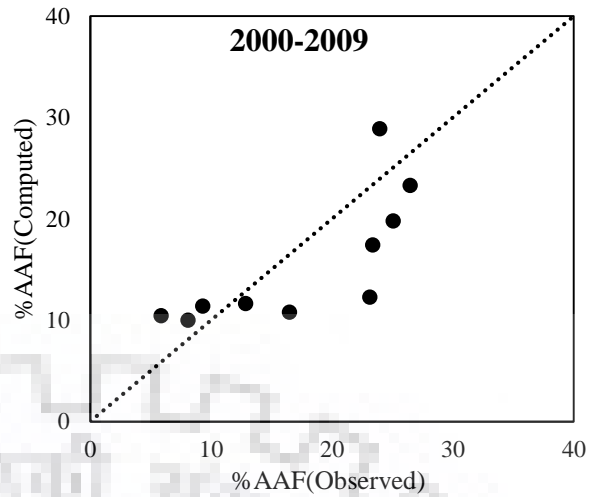


Figure 7.12(b) Observed and computed %AAF for Ashti catchment

Bamini Catchment: Fig. 7.13 (a) shows good ($R^2= 0.646$) %AAF-CN relation for the period 1990-1999. The observed and computed %AAF plotted (7.13 (b)) and found close to LPF.

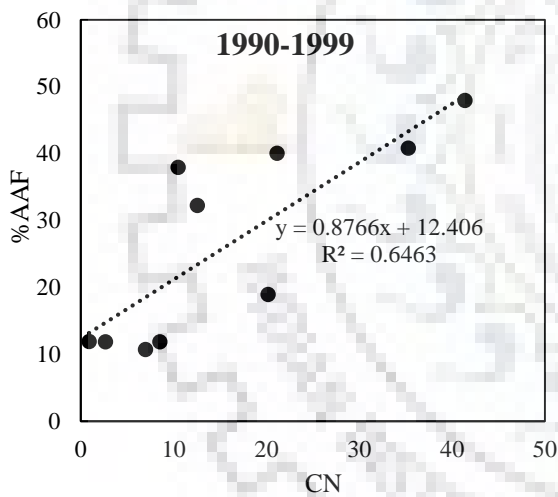


Figure 7.13(a) %AAF versus CN values for Bamini catchment

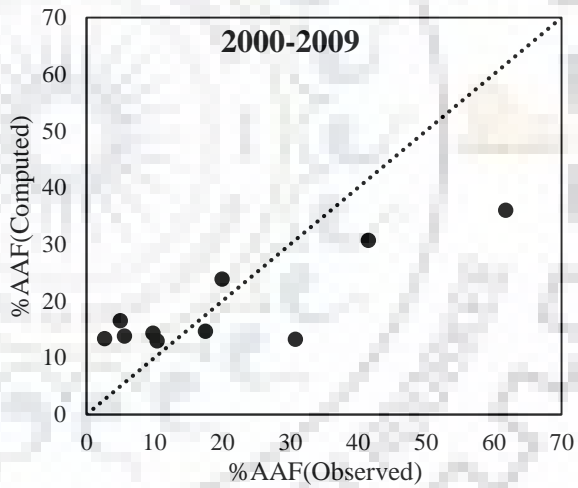


Figure 7.13(b) Observed and computed %AAF for Bamini catchment

Baronda Catchment: Following the similar procedure as above, the requisite %AAF-CN ($R^2= 0.813$) plot using the data of 10 years (1990-1999) is shown in Fig. 7.14 showing excellent relation. The validation plot shows the similar inference as above.

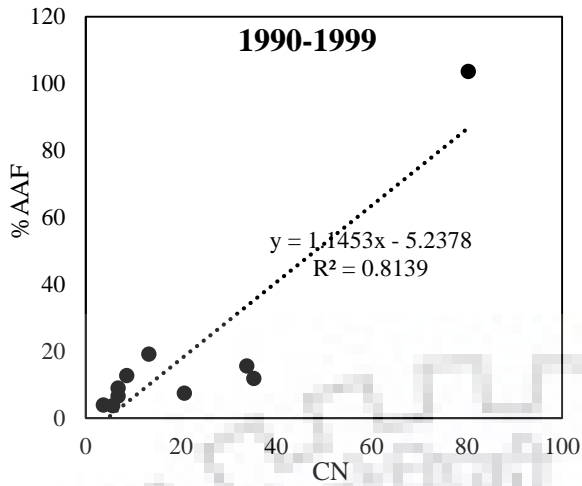


Figure 7.14(a) % AAF versus CN values for Baronda catchment

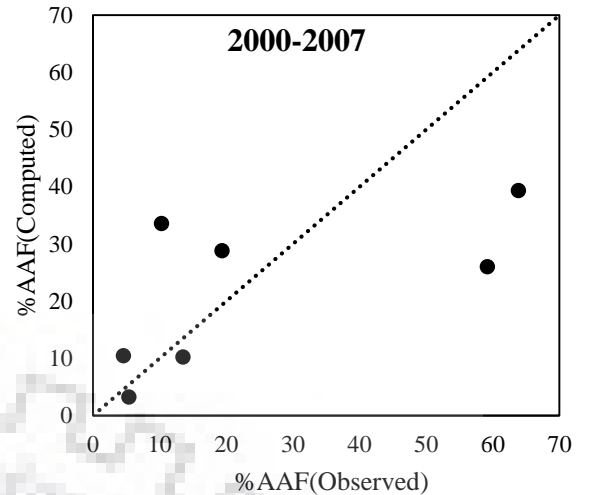


Figure 7.14(b) Observed and computed % AAF for Baronda catchment

Basantpur Catchment: Following the similar procedure as above, the requisite plot (7.15 (a)) with $R^2 = 0.573$ (1990-1999) shows good % AAF-CN relation. The observed and computed % AAF (7.15 (a)) for 2000-2009 are found to be close to line of perfect fit.

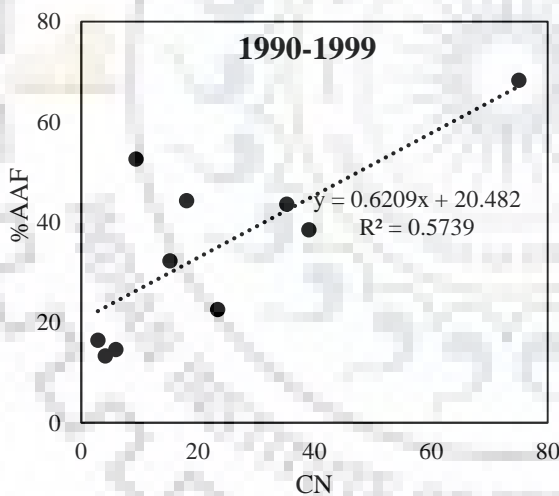


Figure 7.15 (a) % AAF versus CN values for Basantpur catchment

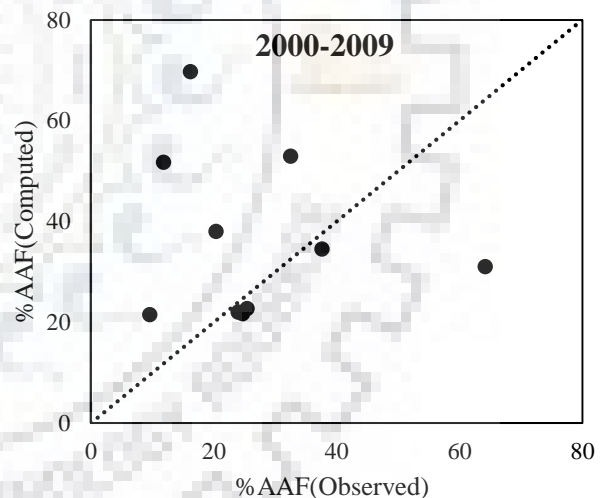


Figure 7.15 (b) Observed and computed % AAF for Basantpur catchment

Bhatpalli Catchment: The data of 21 years (1990-2009) were used, the requisite calibration ($R^2 = 0.657$) and validation plot shown in Fig 7.16 (a) and Fig. 7.16 (b) respectively, showing the similar inference as above.

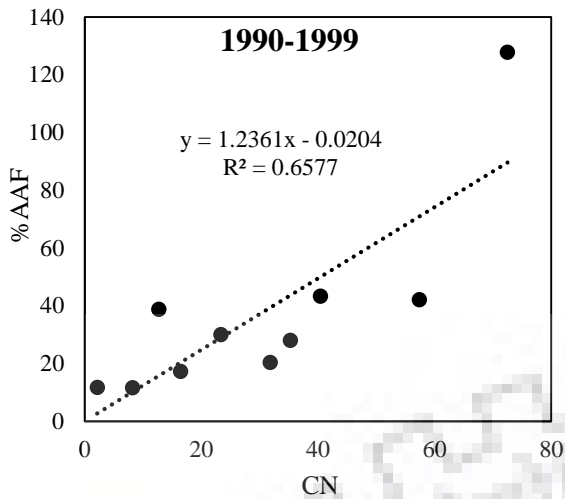


Figure 7.16 (a) %AAF versus CN values for Bhatpalli catchment

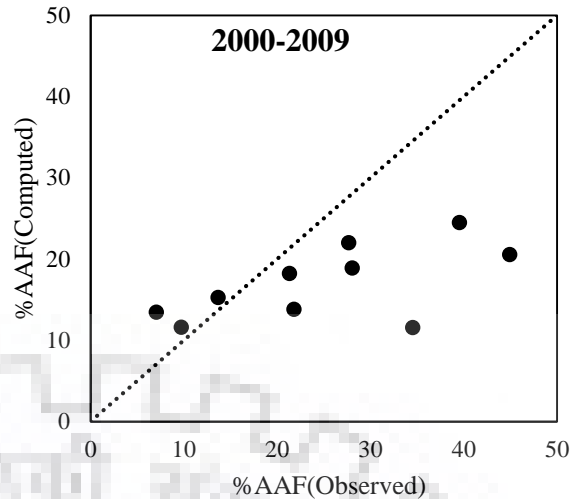


Figure 7.16 (b) Observed and computed %AAF for Bhatpalli catchment

Satrapur Catchment: The requisite calibration plot (Fig. 7.17 (a)) for 1990-1999 shows good %AAF-CN relation. The observed and computed %AAF plotted in Fig. 7.17 (b) shows the similar inference as above.

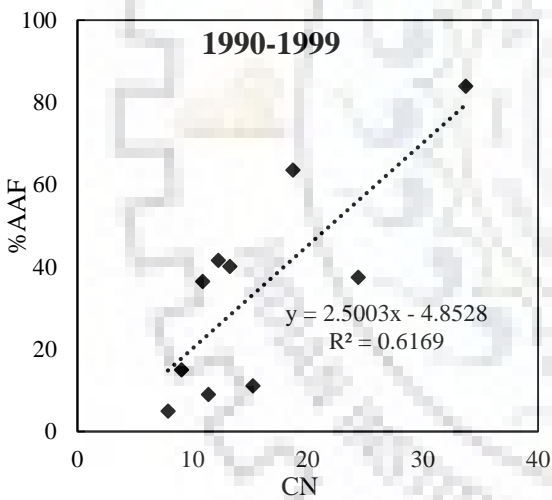


Figure 7.17(a) %AAF versus CN values for Satrapur catchment

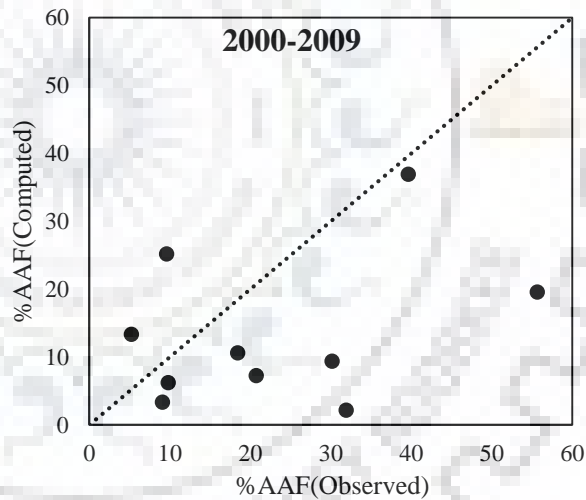


Figure 7.17(b) Observed and computed %AAF for Satrapur catchment

It can be seen from the above that %AAF of the non-monsoon season (from October-June) is significantly related with CN computed from the corresponding rainfall and runoff data for all the catchments.

Case 2

The calibration datasets of each of eleven watersheds were taken together for deriving a general relationship between CN and %AAF, as shown in Fig. 7.18 ($R^2 = 0.6104$), and then tested on the combined validation data of these watersheds. As shown in Fig. 7.19, the observed and computed %AAF values are generally close to LPF, implying that there exists a relationship between CN and %AAF, and CN can be used for derivation of %AAF for describing the EF condition of a watershed during low flow season (October-June) based on CN values, as shown in Table 6.6 derived from the results of Fig. 7.18. Here, it is worth emphasizing that the approach presented in this study includes all the shortcomings of the Tennant method.

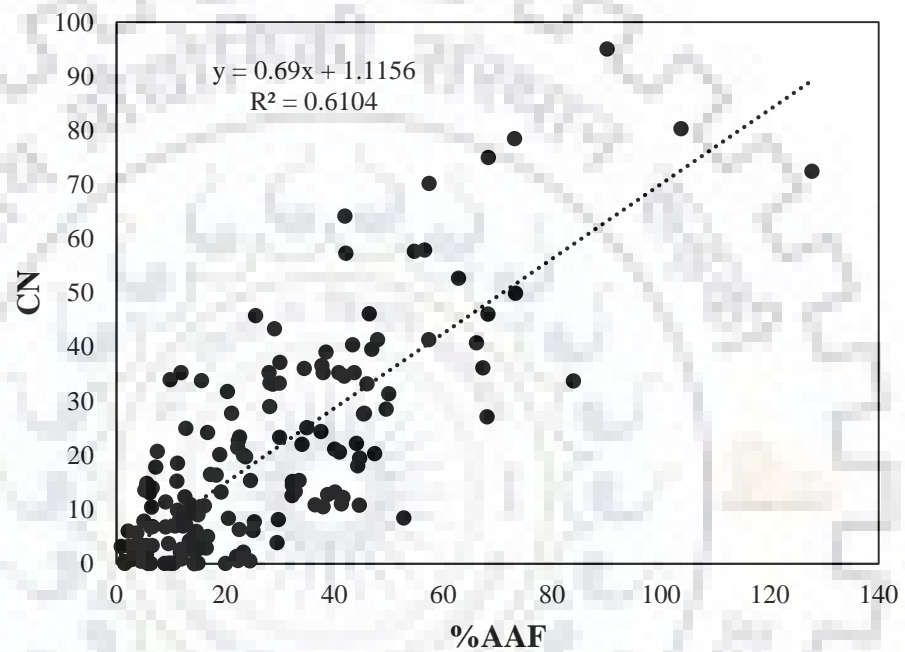


Figure 7.18 %AAF versus CN values for all the catchments used in the study

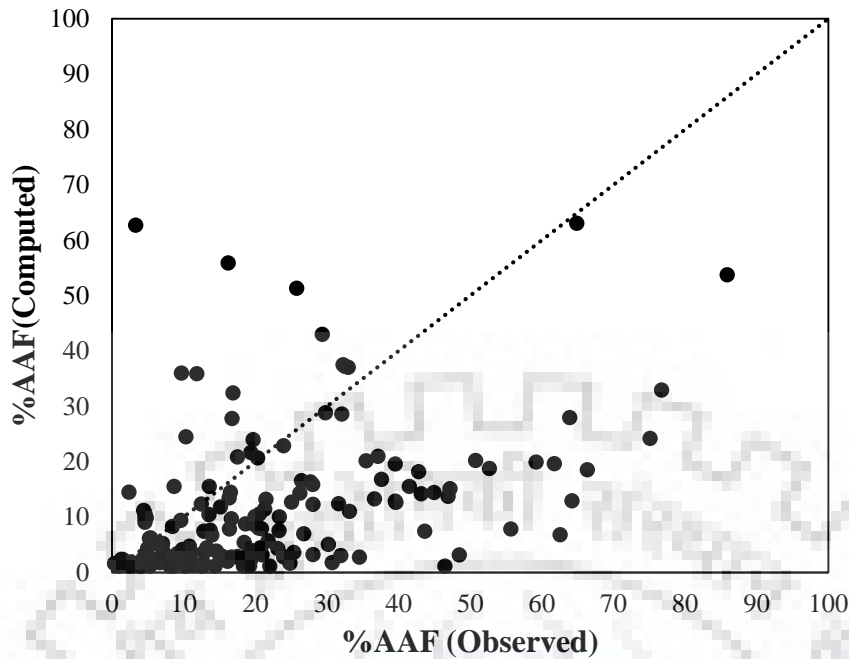


Figure 7.19 Observed and computed %AAF for all catchments used in the analysis.

Table 7.3 Description of flow condition based on %AAF or CN during low flow season

Flow Condition	%AAF	CN
Optimum range of flow	$\geq 60\%$	≥ 85
Outstanding	40%	56 to 84
Excellent	30%	42 to 55
Good	20%	27 to 41
Fair or Degrading	10%	13 to 26
Poor or Minimum	10% or less	< 13

7.5 SUMMARY AND CONCLUSIONS

The assessment of Environmental flow is very important for the survival of the healthy ecosystem. However, it is quite difficult to estimate the environmental flow condition in ungauged catchments. Therefore, it is essential to develop a robust measure which can be used for the assessment of EF condition of a catchment. Though a very few recent studies have been carried out recently to link the EF condition with the standardized precipitation index. However, the EF (characterized by average flow conditions) is significantly affected by the processes of the hydrological cycle. These processes are significantly dependent on the surface characteristics of the catchment. Therefore, it is crucial to develop a method to establish a relationship between

EF and the catchment surface characteristics, which can be instrumental for the ungauged catchments.

The investigation was executed using the rainfall-runoff data of seventeen catchments, viz., Ghatora, Rampur, Baronda, Basantpur of Mahanadi basin; Chakaliya, Hivra, Nandgaon, Dhariawad, Asthi, Bamini, Bhatapalli, Satrapur, Jagdalpur, Ramakona, P.G. Penganga of Godavari basin; Jenapur in Brahmani-Baitaini basin; and Kogaon of Narmada basin. For each of the catchments, the percentage of average annual flow (%AAF) and Curve Number were computed for low flow season. The conclusions of the study are as follows:

1. The %AAF is observed to increase linearly with increasing CN and vice versa, for all the catchments. R^2 greater than 0.55 for 13 (out of 17) catchments was found. The correlation between %AAF and CN is maximum for Dhariawad ($R^2 = 0.899$) and Baronda ($R^2 = 0.814$) catchments. This reveals an excellent correlation between %AAF and CN.
2. The excellent %AAF-CN relationship over all the catchments signifies that the EF conditions of the catchments may be estimated using CN (derivable from catchment characteristics) during low flow season. Moreover, this will also play a key role in monitoring the EF conditions over the ungauged catchments using the catchment characteristics only.
3. Since the proposed approach inheres all limitations of the Tennant method, it is not applicable to catchments severely disturbed by anthropogenic activities.



CHAPTER 8

SUMMARY AND CONCLUSIONS

Water is regarded as a necessity for survival and existence of life on the planet the Earth. Furthermore, it is vital for growth and sustainability of the ecosystem. Amongst the climate changes, global population growth is perhaps the most compelling reason for concern, leading to the problems of water management that can be well addressed with the aid of watershed models. Attempts are being continuously made for improving the existing models and to develop new models to address these issues more effectively. These models are used to analyze the quantity and quality of streamflow, erosion and sediment yield, irrigation water use, water distribution systems, conjunctive use of surface water and groundwater, groundwater development, reservoir system operations, and a range of such water management activities.

The rainfall passes through a number processes of hydrologic cycle in a watershed, such as interception, infiltration, percolation, interflow, overland flow, evaporation and evapotranspiration, base flow etc., and it finally emerges as runoff at the outlet of watershed. These processes largely depend on climatic (rainfall intensity, frequency, amount and duration) and catchment (geology, drainage density, drainage pattern, land use/ vegetation cover, topography) characteristics which vary both spatially and temporally. Therefore, reliable predictions of runoff and sediment yield from land mass into streams and rivers are difficult, expensive and time consuming. The hydrological models used for the purpose should therefore be parametrically efficient and identifiable from the available data.

There are a number of rainfall-runoff models to estimate the runoff from ungauged catchments from a given amount of rainfall. However, the Soil Conservation Service Curve Number (SCS-CN) method is one of the simplest and most widely used methods for accomplishing the aforementioned assignments. This technique is the consequence of comprehensive field examinations performed amid the late 1930s and 1940s and the modifications made by various researchers. The estimation of direct runoff for ungauged watersheds depends on soils, landuse, antecedent rainfall, duration of storm and rainfall amount associated, and average annual temperature and date of storm.

The SCS-CN method has been used by a number of researchers for runoff estimation world over and, in turn, has attracted investigations into its formation, physical significance, applicability, extendibility, and rationality, etc. The SCS-CN method still inherits major

structural inconsistency associated with the potential maximum retention (S)- curve number (CN mapping) resulting into erroneous description of watershed behavior as complacent, standard, and violent and, in turn, the estimation of runoff from the existing SCS-CN method. It invoked the need for development of a revised S-CN mapping relationship employing sounder hydrological perception. The existing SCS-CN method is modified using the proposed S-CN mapping and improved SCS-CN methodology based on the revised proportional equality for variation of S with rainfall (P) as per first order linear hypothesis.

Sediment yield represents the total sediment outflow reaching the outlet of a drainage basin in a specified period of time. Accurate estimation of soil erosion and sediment yield are essential for design of erosion control structures, reservoir sedimentation, water quality management, and design of future water resources management policies. Sediment yield depends on a number of complex factors such as flow, precipitation, topography and soil characteristics of the watershed.

The popular approach for the assessment of soil erosion and sediment yield is the Universal Soil Loss Equation (USLE) or its extensions. Since sediment yield is a surface runoff-dependent process, the erosion models are often coupled with the models capable of simulating the rainfall-runoff response of watershed. In this study, USLE coupled with SCS-CN method has been further improved and modified for sediment yield estimation.

The demand for water is rising due to rapid population growth as well as industrialization. For the protection of the natural ecosystem, water must be preserved in the streams/rivers. More importantly, it should be clean so as to maintain healthy environmental conditions. The minimum threshold quantity of water needed for the survival of streams/rivers is called Environmental flow (EF), which is a key factor for a healthy ecosystem. There are more than 240 methods available to describe the environmental flow condition based on flow data only. Tennant method is widely used hydrological method to describe the EF condition of river from severe degradation to flushing flow based on percentage of AAF (%AAF) using the flow data, whereas Curve number (CN) is used to describe the runoff potential of catchment from low to high based on catchment characteristics (i.e. soil type, land use/treatment, surface condition, and antecedent moisture conditions). As the flow through the catchment depends on its characteristics and Tennant method is used to describe the EF condition based on flow data. Since both the concepts imply levels of water supply for human activities or natural ecosystems so, an effort has been made to establish a relationship between these two which helps to describe the EF condition using Curve Number (based on catchment characteristics) during low flow season.

8.1 CONCLUSIONS

The following conclusions can be derived from the study:

1. The modified proportional equality of SCS-CN methodology describes the watershed behavior more rationally and realistically. It describes the increasing trend of runoff coefficient C with rainfall, consistent with reality. Furthermore, it has the efficacy to resolve the issue of CN decaying with increasing rainfall (P).
2. CN represents the runoff potential for a watershed given amount of rainfall, which at present is considered as 10 inch (= 254 mm). Therefore, it should be modified as CN_P for the actual amount of rainfall P in real-world applications. Such a modification also solves problematic description of watershed behavior, i.e. complacent, standard, and violent. It also supports the general notion that the runoff coefficient (C) (or CN) increases with increasing P and improves runoff prediction.
3. The models based on CN_P relationships performed well on all Strange and Tehri data. The proposed modification also showed an enhanced model performance based on NSE, RMSE and Bias error criteria.
4. The proposed sediment yield models (PS1 and PS3) performed much better than the models based on existing SCS-CN concept (S1 and S3), and significantly better than S2 with $\lambda = 0.2$ in both years 2016 and 2017 data.
5. The higher slope plots generated higher sediment yield and runoff, and vice versa. In performance the sediment yield models are ranked as: PS3>PS1>PS2.
6. The runoff models PR3 and PR1 performed approximately similar and model PR2 performed poorer than any other proposed models.
7. The existence of remarkable %AAF-CN relationship with R^2 greater than 0.55 for 13 (out of 17) catchments underlines the significance of the study, the EF condition of the studied catchments can be ascertained using Curve Number (i.e. catchment characteristics) during low flow season.

8.2 MAJOR RESEARCH CONTRIBUTIONS

The major contributions of the study are as follows:

1. The modification proposed to the proportional equality of SCS-CN methodology describes the realistic increasing trend of runoff coefficient C with rainfall and resolves the issue of CN decaying unrealistically with increasing rainfall (P).
2. CN is presented as an index of describing runoff potential of a watershed for given amount of rainfall (it is 10 inch = 254 mm at present).
3. The proposed variation of CN-with P in real world applications has the efficacy to describe watershed behaviour. It supports the fact that runoff coefficient (C) (or CN) increases with increasing P and improves runoff prediction.
4. Proposed a modified USLE-based modified SCS-CN model for improved prediction of sediment yield.
5. A CN based method for the prediction of environmental flow condition using the data of 17 catchments located in different river basins, has been proposed for low flow season.

8.3 LIMITATION OF THE STUDY

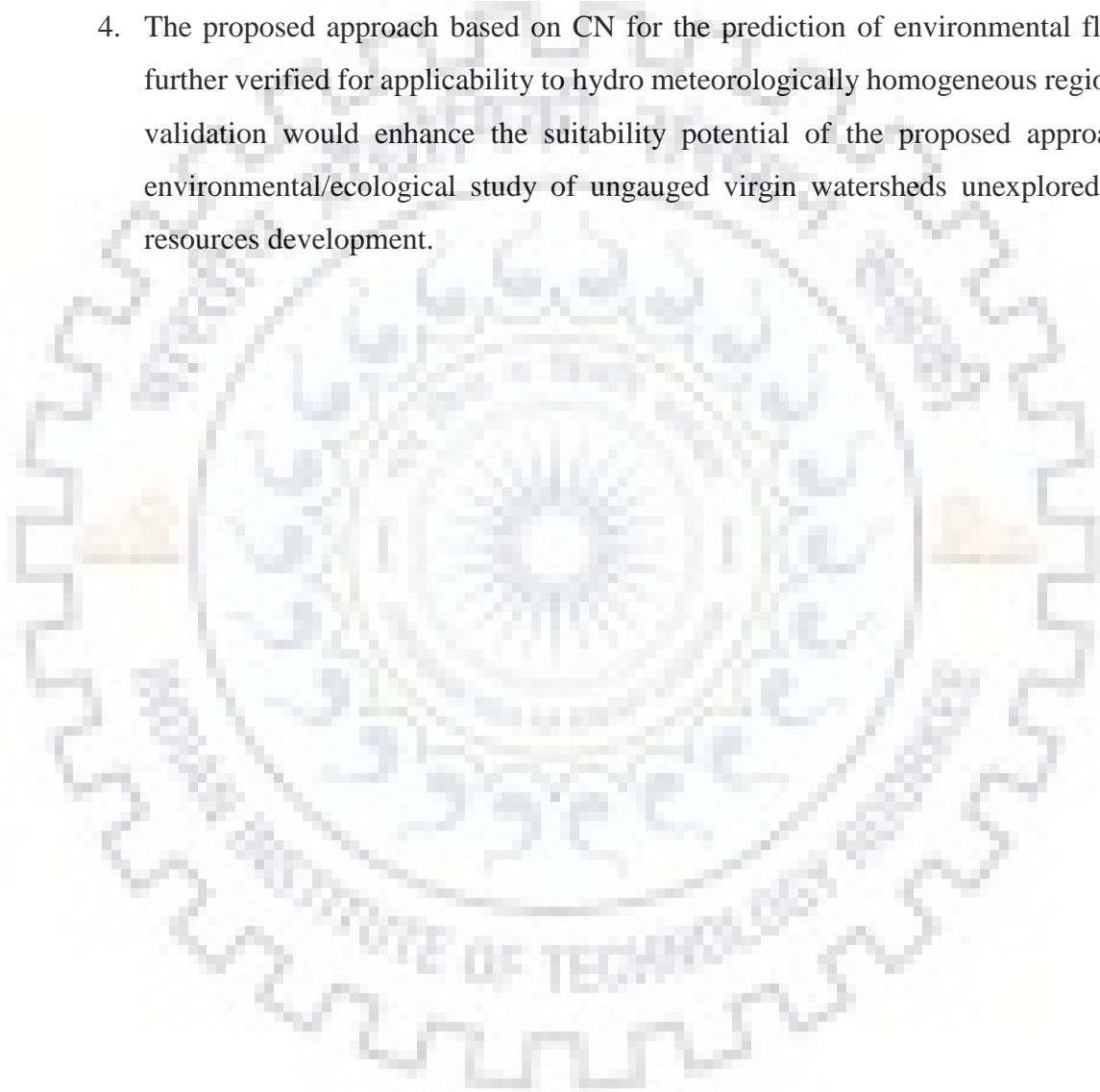
1. The derivation involving S-CN mapping is based on the assumption that $I_a = 0$, which is possible only when the soil is initially moist and it contrasts the assumption of the initially dry soil. It needs to be explored further.
2. The proposed model needs to be tested on a much wider data base.
3. The approach suggested for the estimation of environmental flow based on catchment characteristics (i.e. CN) inheres all the limitations of the Tennant's method. The proposed method holds good for the watersheds having little or no human interventions. It might not be possible in the present modern world where human interventions are increasing rapidly.

8.4 FUTURE SCOPE OF WORK

1. This study makes use of the same dataset as used by Hawkins (1993) having one watershed of each kind. The relationships and models proposed in this study may be further explored for their versatility using a large set of rainfall-runoff data from the watersheds having different soil-vegetation-land use (SVL) complex.
2. The models developed in this study may be further improved through their coupling with SMA procedure to address the issues of initial abstraction (in terms of threshold soil moisture) and

quantum jump in runoff estimation corresponding to change in antecedent moisture conditions; the continuous function for antecedent soil moisture obviates the sudden jumps in runoff estimations.

3. Being simple in model formulation and its structure and attempting to describe an extremely complex process of rainfall-runoff modelling, the SCS-CN methodology has several myths, limitations, and structural inconsistencies yet to be resolved in future using a large data base.
4. The proposed approach based on CN for the prediction of environmental flow can be further verified for applicability to hydro meteorologically homogeneous regions. Such a validation would enhance the suitability potential of the proposed approach to the environmental/ecological study of ungauged virgin watersheds unexplored for water resources development.





REFERENCES

- Aggarwal, S.P., Garg, V., Gupta, P.K., Nikam, B.R., Thakur, P.K., & Roy P.S. (2013). Runoff potential assessment over Indian landmass: A macro-scale hydrological modeling approach. *Current Science*, 104(7), 950-959. (IF 2014: 0.833)
- Ajmal, M., & Kim, T. W. (2014). Quantifying excess storm water using SCS-CN-based rainfall runoff models and different curve number determination methods. *Journal of Irrigation and Drainage Engineering*, 141(3), 04014058.
- Ajmal, M., Moon, G. W., Ahn, J. H., & Kim, T. W. (2015). Investigation of SCS-CN and its inspired modified models for runoff estimation in South Korean watersheds. *Journal of Hydro-environment Research*, 9(4), 592-603.
- Ajmal, M., Waseem, M., Ahn, J. H., & Kim, T. W. (2016). Runoff estimation using the NRCS slope-adjusted curve number in mountainous watersheds. *Journal of Irrigation and Drainage Engineering*, 142(4), 04016002.
- Aksoy, H., & Kavvas, M. L. (2005). A review of hillslope and watershed scale erosion and sediment transport models. *Catena*, 64(2-3), 247-271.
- Alberts, E. E., Moldenhauer, W. C., & Foster, G. R. (1980). Soil Aggregates and Primary Particles Transported in Rill and Inter rill Flow 1. *Soil Science Society of America Journal*, 44(3), 590-595.
- Amrit, K., Mishra, S. K., & Pandey, R. P. (2017). Tennant Concept Coupled with Standardized Precipitation Index for Environmental Flow Prediction from Rainfall. *Journal of Hydrologic Engineering*, (ASCE), 23(2), 05017031.
- Amrit, K., Mishra, S. K., & Pandey, R. P. (2018). Coupling of Tennant Concept with Standardized Precipitation Index (SPI) for the Prediction of Environmental Flow Condition from Rainfall in Upper Narmada Basin. In *Climate Change Impacts* (pp. 265-272). Springer, Singapore.
- Amrit, K., Mishra, S. K., Pandey, R. P., Himanshu, S. K., & Singh, S. STANDARDIZED PRECIPITATION INDEX BASED APPROACH TO PREDICT ENVIRONMENTAL FLOW CONDITION. *Ecohydrology*, e2127.

- Andrews, R. G. (1954). The use of relative infiltration indices in computing runoff. (unpublished) Soil Conservation Service, Forth Worth Texas.
- Arnold, J. G., Williams, J. R., Nicks, A. D., & Sammons, N. B. (1990). SWRRB; a basin scale simulation model for soil and water resources management. SWRRB; a basin scale simulation model for soil and water resources management.
- Arnold, J.G., Williams, J.R., Srinivasan, R., & King, K.W. (1996). SWAT: Soil and Water Assessment Tool. USDA-ARS, Grassland, Soil and Water Research Laboratory. Temple, TX. 1990.
- Aron, G., Miller, A. C., & Lakatos, D. F. (1977). Infiltration formula based on SCS curve number. *Journal of Irrigation and Drainage Engineering*, 103(ASCE 13427 Proceeding).
- Arthington, A.H. 2012. *Environmental Flows: Saving Rivers in the Third Millennium*. University of California Press, Berkeley. 424 pages.
- Arthington, A. H., King, J. M., O'keeffe, J. H., Bunn, S. E., Day, J. A., Pusey, B. J., & Tharme, R. (1992). Development of an holistic approach for assessing environmental flow requirements of riverine ecosystems. In *Proceedings of an international seminar and workshop on water allocation for the environment* (Vol. 69, p. 76). The Centre for Water Policy Research, University of New England: Armidale, Australia.
- Arthington, A. H., Bunn, S. E., Poff, N. L. & Naiman, R. J. The challenge of providing environmental flow rules to sustain river ecosystems. *Ecol. Appl.* 16, 1311–1318 (2006).
- ASCE Task Committee on Definition of Criteria for Evaluation of Watershed Models of the Watershed Management Committee, Irrigation and Drainage Division. (1993). Criteria for evaluation of watershed models. *Journal of Irrigation and Drainage Engineering*, 119(3), 429-442.
- Banks, S. A., & Docker, B. B. (2013). Delivering environmental flows in the Murray-Darling Basin (Australia)—legal and governance aspects. *Hydrological Sciences Journal*, 59(3-4), 688-699.
- Bates, B., Kundzewicz, Z., & Wu, S. (2008). *Climate change and water*. Intergovernmental Panel on Climate Change Secretariat.

- Belmar, O., Velasco, J., Gutiérrez-Cánovas, C., Mellado-Díaz, A., Millán, A., & Wood, P. J. (2013). The influence of natural flow regimes on macroinvertebrate assemblages in a semiarid Mediterranean basin. *Ecohydrology*, 6(3), 363-379.
- Bernhardt, E. S., Palmer, M. A., Allan, J. D., Alexander, G., Barnas, K., Brooks, S., & Galat, D. (2005). Synthesizing US river restoration efforts.
- Bhunya, P. K., Jain, S. K., Singh, P. K., & Mishra, S. K. (2010). A simple conceptual model of sediment yield. *Water Resources Management*, 24(8), 1697-1716.
- Blaszczynski, J. (2003). Estimating watershed runoff and sediment yield using a GIS interface to curve number and MUSLE models. *Bureau of Land Management Resource Notes*, 66.
- Bonta, J. V. (1997) Determination of watershed curve number using derived distributions. *Journal of Irrigation and Drainage Engineering*, 123 (1), 28-36.
- Bosznay, M. (1989). Generalization of SCS curve number method. *Journal of Irrigation and Drainage Engineering*, 115(1), 139-144.
- Brisbane Declaration. (2007). “The Brisbane Declaration: Environmental Flows are Essential for Freshwater Ecosystem Health and Human Well-Being.” September 3–6, Brisbane, Australia.
- Brown, L. C., & Foster, G. R. (1987). Storm erosivity using idealized intensity distributions. *Transactions of the ASAE*, 30(2), 379-0386.
- Bunn, S. E., & Arthington, A. H. (2002). Basic principles and ecological consequences of altered flow regimes for aquatic biodiversity. *Environmental management*, 30(4), 492-507.
- Bunn, S. E., Bond, N. R., Davis, J. A., Gawne, B., Kennard, M. J., King, A. J., & Peterson, E. E. (2014). Ecological responses to altered flow regimes: synthesis report.
- Cazier, D. J., & Hawkins, R. H. (1984). Regional application of the curve number method. In *Water Today and Tomorrow* (pp. 710-710). ASCE.
- Chakraborty, S., Pandey, R. P., Mishra, S. K., & Chaube, U. C. (2015). Relation between Runoff Curve Number and Irrigation Water Requirement. *Agricultural research*, 4(4), 378-387.

- Changyeol P., Hayoung K., Chulsang Y., Sang Y. S., (2016). Evaluating Estimation Method of Sediment Yield Coupling with SCS-CN. *Journal of the Korean Society of Hazard Mitigation*, 16(2), 455-462.
- Chen, C. L. (1982). An evaluation of the mathematics and physical significance of the soil conservation service curve number procedure for estimating runoff volume. In *Proc., Int. Symp. on Rainfall-Runoff Modeling*, Water Resources Publ., Littleton, Colo (pp. 387-418).
- Chen, H., & Zhao, Y. W. (2011). Evaluating the environmental flows of China's Wolonghu wetland and land use changes using a hydrological model, a water balance model, and remote sensing. *Ecological Modelling*, 222(2), 253-260.
- Cheng, X., Chen, L., Sun, R., & Kong, P. (2018). Land use changes and socio-economic development strongly deteriorate river ecosystem health in one of the largest basins in China. *Science of the Total Environment*, 616, 376-385.
- Chessman, B. C., Fryirs, K. A., & Brierley, G. J. (2006). Linking geomorphic character, behaviour and condition to fluvial biodiversity: implications for river management. *Aquatic Conservation: Marine and Freshwater Ecosystems*, 16(3), 267-288.
- Choi, J. Y., Engel, B. A., & Chung, H. W. (2002). Daily streamflow modelling and assessment based on the curve-number technique. *Hydrological Processes*, 16(16), 3131-3150.
- Chow, V. T. (1959). *Open channel hydraulics*. McGraw-Hill Book Company, Inc; New York.
- Chow, V. T., Maidment, D. R., & Mays, L. W. (1988). *Applied hydrology*, 572 pp. Editions McGraw-Hill, New York.
- Clark, E. H. (1985). The off-site costs of soil erosion. *Journal of soil and water conservation*, 40(1), 19-22.
- Coffey, M. E., Workman, S. R., Taraba, J. L., & Fogle, A. W. (2004). Statistical procedures for evaluating daily and monthly hydrologic model predictions. *Transactions of the ASAE*, 47(1), 59.
- Cogo, N. P., Moldenhauer, W. C., & Foster, G. R. (1984). Soil Loss Reductions from Conservation Tillage Practices 1. *Soil Science Society of America Journal*, 48(2), 368-373.

- Coustau, M., Ricci, S., Borrell-Estupina, V., Bouvier, C., & Thual, O. (2013). Benefits and limitations of data assimilation for discharge forecasting using an event-based rainfall-runoff model. *Natural Hazards and Earth System Science*, 13, pp-583.
- David, W. P., & Beer, C. E. (1975a). Simulation of soil erosion—Part I. Development of a mathematical erosion model. *Transactions of the ASAE*, 18(1), 126-0129.
- David, W. P., & Beer, C. E. (1975b). Simulation of soil erosion—Part II. Streamflow and suspended sediment simulation results. *Transactions of the ASAE*, 18(1), 130-0133.
- Dickey, E. C., Shelton, D. P., Jasa, P. J., & Peterson, T. R. (1985). Soil erosion from tillage systems used in soybean and corn residues. *Transactions of the ASAE*, 28(4), 1124-1130.
- Dunbar, M.J.; Gustard, A.; Acreman, M.C., & Elliot, C.R.N. (1998). Review of Overseas Approaches to Setting River Flow Objectives, Environment Agency R and D Technical Report W6B 96 (4). Institute of Hydrology, Wallingford, U.K. 61 pages
- Durbude, D. G., Jain, M. K., & Mishra, S. K. (2011). Long-term hydrologic simulation using SCS-CN-based improved soil moisture accounting procedure. *Hydrological processes*, 25(4), 561-579.
- Dyson M., Bergkamp M., & Scanlon J. (2003). *Flow: The Essentials of Environmental Flows*. IUCN, Gland, Switzerland and Cambridge, U.K.
- EEA, 1999. *Environment in the European Union at the Turn of the Century – Environmental Assessment Report No. 2*, European Environment Agency, Copenhagen.
- Eldho, T. I., Singh, A. K., Jha, A., & Jana, R. (2007). A GIS and SCS-CN based integrated model for rainfall-runoff simulation of ungauged watershed. *Water and Energy International*, 64(4), 30-38.
- Epps, T. H., Hitchcock, D. R., Jayakaran, A. D., Loflin, D. R., Williams, T. M., & Amatya, D. M. (2013). Curve Number derivation for watersheds draining two headwater streams in lower coastal plain South Carolina, USA. *JAWRA Journal of the American Water Resources Association*, 49(6), 1284-1295.
- Evans, E. A. (1980). Analysis of adhesion of large vesicles to surfaces. *Biophysical journal*, 31(3), 425-431.

- Fentie, B., Yu, B., Silburn, M. D., & Ciesiolka, C. A. A. (2002). Evaluation of eight different methods to predict hillslope runoff rates for a grazing catchment in Australia. *Journal of Hydrology*, 261(1-4), 102-114.
- Fischer, G., & Heilig, G. K. (1997). Population momentum and the demand on land and water resources. *Philosophical Transactions of the Royal Society of London B: Biological Sciences*, 352(1356), 869-889.
- Flaxman, E. M. (1972). Predicting sediment yield in western USA. *Journal of the Hydraulics Division*, 98 (Hy 12).
- Foster, G. R. (1982). Modeling the erosion process. *Hydrologic modeling of small watersheds*.
- Foster, G. R., & Meyer, L. D. (1972a). Closed-form soil erosion equation for upland areas. In *Sedimentation Symposium To Honor Professor HA Einstein, Berkeley, 1971.(Papers)*.
- Foster, G. R., & Meyer, L. D. (1972b). Transport of soil particles by shallow flow. *Transactions of the ASAE*, 15(1), 99-0102.
- Foster, G. R., Meyer, L. D., & Onstad, C. A. (1977). An erosion equation derived from basic erosion principles. *Transactions of the ASAE*, 20(4), 678-0682.
- Franti, T. G., Foster, G. R., & Monke, E. J. (1996). Modeling the Effects of Incorporated Residue on Rill Erosion Part I: Model Development and Sensitivity Analysis. *Transactions of the ASAE*, 39(2), 535-542.
- Fryirs, K., Chessman, B., & Rutherford, I. (2013). Progress, problems and prospects in Australian river repair. *Marine and Freshwater Research*, 64(7), 642-654.
- Galay, V. J. (1983). Causes of river bed degradation. *Water resources research*, 19(5), 1057-1090.
- Gao, G. Y., Fu, B. J., Lü, Y. H., Liu, Y., Wang, S., & Zhou, J. (2012). Coupling the modified SCS-CN and RUSLE models to simulate hydrological effects of restoring vegetation in the Loess Plateau of China. *Hydrology and Earth System Sciences*, 16(7), 2347-2364.
- Garde, R. J., & Kothiyari, U. C. (1987). Estimation of sediment yield. *J. Central Board of Irrigation and Power (CBIP)*, 44(3), 7.

- Garen, D., & Moore, D. S. (2005). Curve number hydrology in water quality modeling: use, abuse, and future directions. *J. Am. Water Resource. Assoc.*, 41 (2), 377–388.
- Garg, V., Nikam, B.R., Thakur, P.K. and Aggarwal, S.P. (2013). Assessment of the effect of slope on runoff potential of a watershed using NRCS-CN Method. *International Journal of Hydrology Science and Technology*, 3(2), 141–159.
- Geetha, K., Mishra, S. K., Eldho, T. I., Rastogi, A. K., & Pandey, R. P. (2008). SCS-CN-based continuous simulation model for hydrologic forecasting. *Water Resources Management*, 22(2), 165-190.
- Gilley, J. E., Finkner, S. C., Spomer, R. G., & Mielke, L. N. (1986). Runoff and erosion as affected by corn residue: Part I. Total losses. *Transactions of the ASAE*, 29(1), 157-0160.
- Gippel, C. J., Marsh, N., & Grice, T. (2012). Flow Health: Software to Assess Deviation of River Flows from Reference and to Design a Monthly Environmental Flow Regime. Technical Manual and User Guide Version, 2.
- Gleick, P. H. (1993). *Water in crisis: a guide to the worlds fresh water resources*.
- Glenn, E. P., Nagler, P. L., Shafroth, P. B., & Jarchow, C. J. (2017). Effectiveness of environmental flows for riparian restoration in arid regions: A tale of four rivers. *Ecological engineering*, 106, 695-703.
- Golding, B. L. (1979). Discussion of runoff curve numbers with varying soil moisture. *Journal of the Irrigation and Drainage Division, ASCE* 105 (IR4), 441–442.
- Golubev, G. N., & Biswas, A. K. (1984). Large-scale water transfers: emerging environmental and social issues. *International Journal of Water Resources Development*, 2(2-3), 1-5.
- González-Villela, R., Martínez, M. J. M., & Sepúlveda, J. S. S. (2018). Effects of climate change on the environmental flows in the Conchos River (Chihuahua, Mexico). *Ecohydrology & Hydrobiology*, 18(4), 431-440.
- Gore, J. A. (1978). A technique for predicting in-stream flow requirements of benthic macroinvertebrates. *Freshwater Biology*, 8(2), 141-151.
- Gore, J. A. (1985). *Restoration of rivers and streams*.

- Gottschalk, L.C. (1964), 'Sedimentation, Part 1: Reservoir sedimentation,' In: Handbook of Applied Hydrology, V.T. Cow (ed), McGraw Hill, New York.
- Govindaraju, R. S., & Kavvas, M. L. (1991). Modeling the erosion process over steep slopes: approximate analytical solutions. *Journal of Hydrology*, 127(1-4), 279-305.
- Grayson, R.B., Moore, I.D., McMahon, T.A. (1992). Physically based hydrologic modelling 2. Is the concept realistic? *Water Resource Research* 28, 2659–2666.
- Gregory, K. J. (2006). The human role in changing river channels. *Geomorphology*, 79(3-4), 172-191.
- Grimaldi, S., Petroselli, A., & Romano, N. (2013a). Green-Ampt Curve-Number mixed procedure as an empirical tool for rainfall–runoff modelling in small and ungauged basins. *Hydrological processes*, 27(8), 1253-1264.
- Grimaldi, S., Petroselli, A., & Romano, N. (2013b). Curve-Number/Green–Ampt mixed procedure for streamflow predictions in ungauged basins: Parameter sensitivity analysis. *Hydrological Processes*, 27(8), 1265-1275.
- Gupta, A. D. (2008). Implication of environmental flows in river basin management. *Physics and Chemistry of the Earth, Parts A/B/C*, 33(5), 298-303.
- Haan, C. T., Barfield, B. J., & Hayes, J. C. (1994). *Design hydrology and sedimentology for small catchments*. Elsevier.
- Haghighi Ali Torabi and Bjørn. (2017). Design of environmental flow regimes to maintain lakes and wetlands in regions with high seasonal irrigation demand. *Ecological Engineering*, 100:120-129.
- Haith, D. A., & Shoenaker, L. L. (1987). Generalized watershed loading functions for stream flow nutrients. *JAWRA Journal of the American Water Resources Association*, 23(3), 471-478.
- Hatfield, T.; Wright, N.; Buchanan, S. and Faulkner, S. 2013. A Review of Environmental Flow Assessment Methods for Application to Northeastern British Columbia. Consultant's report prepared for the Canadian Association of Petroleum Producers by Solander Ecological Research Ltd. (Victoria, B.C.) and Ecofish Research Ltd (Courtenay, B.C.), August 2012. 96 pages.

- Hawkins, R. H. (1975). The importance of accurate curve numbers in the estimation of storm runoff. *JAWRA Journal of the American Water Resources Association*, 11(5), 887-890.
- Hawkins, R. H. (1978). Runoff curve numbers with varying site moisture. *Journal of the irrigation and drainage division*, 104(4), 389-398.
- Hawkins, R. H. (1993). Asymptotic determination of runoff curve numbers from data. *Journal of Irrigation and Drainage Engineering*, 119(2), 334-345.
- Hawkins, R. H., Hjelmfelt Jr, A. T., & Zevenbergen, A. W. (1985). Runoff probability, storm depth, and curve numbers. *Journal of Irrigation and Drainage Engineering*, 111(4), 330-340.
- Hawkins, R. H., Steenhuis, T. S., Frankenberger, J. R., Winchell, M., Zollweg, J. A., & Walter, M. F. (1996). Discussion and Closure: SCS Runoff Equation Revisited for Variable-Source Runoff Areas. *Journal of Irrigation and Drainage Engineering*, 122(5), 319-320.
- Hawkins, R. H., Woodward, D. E. & Jiang, R. (2001). Investigation of the runoff curve number abstraction ratio. Pap. Presented at USDA-NRCS Hydraulic Engineering Workshop, Tucson, Arizona.
- Himanshu, S. K., Pandey, A., & Patil, A. (2018). Hydrologic Evaluation of the TMPA-3B42V7 Precipitation Data Set over an Agricultural Watershed Using the SWAT Model. *Journal of Hydrologic Engineering*, 23(4), 05018003.
- Himanshu, S. K., Pandey, A., Yadav, B., & Gupta, A. (2019). Evaluation of best management practices for sediment and nutrient loss control using SWAT model. *Soil and Tillage Research*, 192, 42-58.
- Hirji, R., & Davis, R. (2009). Environmental flows in water resources policies, plans, and projects: findings and recommendations. The World Bank.
- Hjelmfelt, A. T. (1980). Empirical investigation of curve number technique. *Journal of the Hydraulics Division*, 106(9), 1471-1476.
- Horton, R. E. (1932). Drainage-basin characteristics. *Eos, Transactions American Geophysical Union*, 13(1), 350-361.

- Horton, R. E. (1938). The interpretation and application of runoff plot experiments with reference to soil erosion problems. In *Soil Science Society of America Proceedings* (Vol. 3, pp. 340-349).
- Huang, M., Gallichand, J., Wang, Z., & Goulet, M. (2006). A modification to the Soil Conservation Service curve number method for steep slopes in the Loess Plateau of China. *Hydrological processes*, 20(3), 579-589.
- Hussein, M. H., & Laflen, J. M. (1982). Effects of crop canopy and residue on rill and interrill soil erosion. *Transactions of the ASAE*, 25(5), 1310-1315.
- Iyer, R. R. (2005). The notion of environmental flows: a caution NIE. In *IWMI Workshop on Environmental Flows*, New Delhi (pp. 23-24).
- Jacobsen, D., Milner, A. M., Brown, L. E., & Dangles, O. (2012). Biodiversity under threat in glacier-fed river systems. *Nature Climate Change*, 2(5), 361-364.
- Jain, M. K., Kothiyari, U. C., & Raju, K. G. (2005). GIS based distributed model for soil erosion and rate of sediment outflow from catchments. *Journal of hydraulic engineering*, 131(9), 755-769.
- Jain, M. K., Mishra, S. K., Babu, S. & Venugopal, K. (2006a). On the Ia–S relation of the SCS-CN method. *Nord. Hydrol.* 37 (3), 261–275.
- Jain, M. K., Mishra, S. K., Babu, S. & Singh, V. P. (2006b). Enhanced runoff curve number model incorporating storm duration and a nonlinear Ia–S relation. *Journal Hydrologic Engineering*. 11 (6), 631–635.
- Jain, M. K., Durbude, D. G., & Mishra, S. K. (2012). Improved CN-based long-term hydrologic simulation model. *Journal of Hydrologic Engineering*, 17(11), 1204-1220.
- Jansen, I. M. L., & Painter, R. B. (1974). Predicting sediment yield from climate and topography. *Journal of Hydrology*, 21(4), 371-380.
- Jasrotia, A. S., Dhiman, S. D., & Aggarwal, S. P. (2002). Rainfall-runoff and soil erosion modeling using remote sensing and GIS technique—a case study of tons watershed. *Journal of the Indian Society of Remote Sensing*, 30(3), 167-180.
- Johnson, J. W. (1943). Distribution graphs of suspended-matter concentration. *Transactions of the American Society of Civil Engineers*, 108(1), 941-956.

- Johnson, M. S., Coon, W. F., Mehta, V. K., Steenhuis, T. S., Brooks, E. S., & Boll, J. (2003). Application of two hydrologic models with different runoff mechanisms to a hillslope dominated watershed in the northeastern US: a comparison of HSPF and SMR. *Journal of Hydrology*, 284(1-4), 57-76.
- Jowett, I.G. 1997. Instream flow methods: a comparison of approaches. *Regulated Rivers Research and Management* 13: 115-127..
- Kannan, N., Santhi, C., Williams, J. R., & Arnold, J. G. (2008). Development of a continuous soil moisture accounting procedure for curve number methodology and its behaviour with different evapotranspiration methods. *Hydrological Processes*, 22(13), 2114-2121.
- King, A. J., Tonkin, Z., & Mahoney, J. (2009). Environmental flow enhances native fish spawning and recruitment in the Murray River, Australia. *River Research and Applications*, 25(10), 1205-1218.
- King, J., Brown, C., & Sabet, H. (2003). A scenario-based holistic approach to environmental flow assessments for rivers. *River research and applications*, 19(5-6), 619-639.
- Kisi, O., Haktanir, T., Ardiclioglu, M., Ozturk, O., Yalcin, E., & Uludag, S. (2009). Adaptive neuro-fuzzy computing technique for suspended sediment estimation. *Advances in Engineering Software*, 40(6), 438-444.
- Kiwango, H., Njau, K. N., & Wolanski, E. (2015). The need to enforce minimum environmental flow requirements in Tanzania to preserve estuaries: case study of mangrove-fringed Wami River estuary. *Ecohydrology & Hydrobiology*, 15(4), 171-181.
- Knisel, W. G. (1980) CREAMS: a field-scale model for chemical, runoff and erosion from agricultural management systems. Conservation Research Report No. 26, South East Area, US Dept. of Ag., Washington, DC.
- Kostrzewa, H. (1977). Validation of criteria and magnitude of instream flow for Polish rivers. *Mat. Bad., Ser. Gospodarka Wodna i Ochrona Wód*. IMGW Warsaw, Poland.
- Kothyari, U. C., & Jain, S. K. (1997). Sediment yield estimation using GIS. *Hydrological sciences journal*, 42(6), 833-843.
- Koutsoyiannis, D., Makropoulos, C., Langousis, A., Baki, S., Efstratiadis, A., Christofides, A. & Mamassis, N. (2009). HESS Opinions:" Climate, hydrology, energy, water: recognizing

- uncertainty and seeking sustainability". *Hydrology and Earth System Sciences*, 13(2), 247-257.
- Kumar, P., Chaube, U. C., & Mishra, S. K. (2007, October). Environmental flows for hydropower projects—a case study. In *International conference on small hydropower-hydro Sri Lanka* (Vol. 22, p. 24).
- Lafren, J. M., & Colvin, T. S. (1981). Effect of crop residue on soil loss from continuous row cropping. *Transactions of the ASAE*, 24(3), 605-0609.
- Lal, R. (1976). Soil erosion problems on an Alfisol in Western Nigeria and their control.
- Langbein, W.B. and S.A. Schumm (1958), 'Yield of sediment in relation to mean annual precipitation,' *Trans. Am. Geophys. Union* 39, pp. 1076-84.
- Langhans, S. D., Lienert, J., Schuwirth, N., & Reichert, P. (2013). How to make river assessments comparable: A demonstration for hydromorphology. *Ecological indicators*, 32, 264-275.
- Leathe, S.A. and Nelson, F.A., (1986). A Literature Evaluation of Montana's Wetted Perimeter Inflection Point Method for Deriving Instream Flow Recommendations: Department of Fish, and Wildlife, and Parks, Helena, MT. 70 pages.
- Leonard, R. A., Knisel, W. G., & Still, D. A. (1987). GLEAMS: Groundwater loading effects of agricultural management systems. *Transactions of the ASAE*, 30(5), 1403-1418.
- Leopold, L.B., M.G. Wolman, and J.P. Miller (1964), 'Fluvial Processes in Geomorphology,' W.H. Freeman, San Francisco.
- Linnansaari, T.; Monk, W.A.; Baird, D.J. and Curry, R.A (2012). Review of Approaches and Methods to Assess Environmental Flows across Canada and internationally. Dept Fisheries and Oceans, Can. Sci. Advis. Sec. Res. Doc. 2012/039.
- Liu, B. Y., Nearing, M. A., & Risse, L. M. (1994). Slope gradient effects on soil loss for steep slopes. *Transactions of the ASAE*, 37(6), 1835-1840.
- Mackay, S. J., Arthington, A. H., & James, C. S. (2014). Classification and comparison of natural and altered flow regimes to support an Australian trial of the Ecological Limits of Hydrologic Alteration framework. *Ecohydrology*, 7(6), 1485-1507.

- Malone, R. W., Yagow, G., Baffaut, C., Gitau, M. W., Qi, Z., Amatya, D. M., & Green, T. R. (2015). Parameterization guidelines and considerations for hydrologic models. *Transactions of the ASABE*, 58(6), 1681-1703.
- Mann, J.L. (2006). "Instream Flow Methodologies: An Evaluation of the Tennant Method for Higher Gradients Streams in National Forest System Land in Western U.S. M.Tech. Thesis Colorado State University, 158.
- Mao, L., Carrillo, R., Escauriaza, C., & Iroume, A. (2016). Flume and field-based calibration of surrogate sensors for monitoring bedload transport. *Geomorphology*, 253, 10-21.
- Martin L., & Morgan, R.P.C. 1979: The impact of drought and post drought on soil erosion in mid-Bedfordshire. In *Atlas of drought in Britain, 1975-76*, London: Institute of British Geographers.
- Mathews R., & Richter BD (2007). Application of the indicators of hydrologic alteration software in environmental flow setting. *American Water Resources Association*, 43: 1400–1413.
- McCuen, R. H., & Bondelid, T. R. (1981). Relation between curve number and runoff coefficient. In *Journal of the Irrigation and Drainage Division, Proceedings of the American Society of Civil Engineers* (Vol. 107).
- McCuen, R. H. (1982). *A guide to hydrologic analysis using SCS methods*. Prentice-Hall, Inc..
- McCuen, R. H. (1983). Closure to "Relation Between Curve Number and Runoff Coefficient" by Richard H. McCuen and Timothy R. Bondelid (December, 1981). *Journal of Irrigation and Drainage Engineering*, 109(1), 195-198.
- McCuen, R. H. (1989). *Hydrologic analysis and design*. Prentice-Hall, Inc., Englewood Cliffs, N.J., 143-147.
- McCuen, R. H. (2003). *Modeling hydrologic change: Statistical methods*, Lewis, Boca Raton, Fla.
- McCuen, R. H., Knight, Z., & Cutter, A. G. (2006). Evaluation of the Nash–Sutcliffe efficiency index. *Journal of Hydrologic Engineering*, 11(6), 597-602.
- Meador, M. R., Brown, L. R., & Short, T. (2003). Relations between introduced fish and environmental conditions at large geographic scales. *Ecological Indicators*, 3(2), 81-92.

- Meier, C. I. (1998). The ecological basis of river restoration: 2. Defining restoration from an ecological perspective. In *Engineering Approaches to Ecosystem Restoration* (pp. 392-397).
- Meng, W., Zhang, N., Zhang, Y., & Zheng, B. (2009). Integrated assessment of river health based on water quality, aquatic life and physical habitat. *Journal of Environmental Sciences*, 21(8), 1017-1027.
- Merritt, W. S., Letcher, R. A., & Jakeman, A. J. (2003). A review of erosion and sediment transport models. *Environmental Modelling & Software*, 18(8-9), 761-799.
- Metcalf and Eddy Inc., University of Florida, and Water Resources Engineers Inc. (1971). "Storm Water Management Model, volume 1: final report." EPA Rep. 11024 DOC 07-71, (NTIS PB-203289), Environmental Protection Agency, Washington, D.C
- Meyer, L. D. (1981). How rain intensity affects inter rill erosion. *Transactions of the ASAE*, 24(6), 1472-1475.
- Meyer, L. D., Foster, G. R., & Nikolov, S. (1975). Effect of flow rate and canopy on rill erosion. *Transactions of the ASAE*, 18(5), 905-911.
- Michel, C., Andréassian, V., & Perrin, C. (2005). Soil conservation service curve number method: How to mend a wrong soil moisture accounting procedure?. *Water Resources Research*, 41(2).
- Millennium Ecosystem Assessment (2005). *Millennium Ecosystem Assessment Synthesis Report*. Island Press, Washington DC.
- Mishra, S. K., & Singh, V. P. (1999). Another look at SCS-CN method. *Journal of Hydrologic Engineering*, 4(3), 257-264.
- Mishra, S. K., & Singh, V. P. (2002a). SCS-CN-based hydrologic simulation package (pp. 391-464). *Water Resources Publications*: Littleton, CO.
- Mishra, S. K., & Singh, V. P. (2002b). SCS-CN method. Part I: derivation of SCS-CN-based models.
- Mishra, S. K. and Singh, V. P. (2003a). *Soil conservation service curve number (SCS-CN) methodology*. Kluwer, Dordrecht, The Netherlands. ISBN: 1-4020-1132-6.

- Mishra, S. K. and Singh, V. P. (2003b). SCS-CN method: Part-II: Analytical treatment. *Acta Geophysica Polonica*, 51(1), 107–123.
- Mishra, S. K. and Singh, V. P. (2004a). Long-term hydrological simulation based on soil conservation service curve number. *Hydrological processes*, 18(7), 1291–1313.
- Mishra, S. K. & Singh, V. P. (2004b). Validity and extension of the SCS-CN method for computing infiltration and rainfall-excess rates. *Hydrological processes*, 18, 3323–3345.
- Mishra, S. K. & Singh, V. P. (2006b). A re-look at NEH-4 curve number data and antecedent moisture condition criteria. *Hydrologic Process*. 20, 2755–2768.
- Mishra, S. K., & Singh, V. P. (2013). Soil conservation service curve number (SCS-CN) methodology (Vol. 42). Springer Science & Business Media.
- Mishra, S. K., Singh, V. P., Sansalone, J. J., & Aravamuthan, V. (2003a). A modified SCS-CN method: characterization and testing. *Water Resources Management*, 17(1), 37-68.
- Mishra, S. K., Sansalone, J. J., & Singh, V. P. (2003b). Hysteresis-based analysis of overland metal transport. *Hydrological processes*, 17(8), 1579-1606.
- Mishra, S. K., Tyagi, J. V., & Singh, V. P. (2003c). Comparison of infiltration models. *Hydrological processes*, 17(13), 2629-2652.
- Mishra, S. K., Jain, M. K., & Singh, V. P. (2004a). Evaluation of the SCS-CN-based model incorporating antecedent moisture. *Water resources management*, 18(6), 567-589.
- Mishra, S. K., Sansalone, J. J. & Singh, V. P. (2004b). Partitioning analog for metal elements in urban rainfall-runoff overland flow using the soil conservation service curve number concept. *Journal of Environmental Engineering*, 130 (2), 145–154.
- Mishra, S. K., Sansalone, J. J., Glenn, D. W., III & Singh, V. P. (2004c). PCN based metal partitioning in urban snow melt, rainfall/runoff, and river flow systems. *J. Am. Water Resource. Association*, 40 (5), 1315–1337.
- Mishra, S. K., Geetha, K., Rastogi, A. K., & Pandey, R. P. (2005). Long-term hydrologic simulation using storage and source area concepts. *Hydrological Processes: An International Journal*, 19(14), 2845-2861.

- Mishra, S. K., Sahu, R. K., Eldho, T. I. & Jain, M. K. (2006a). An improved Ia–S relation incorporating antecedent moisture in SCS-CN methodology. *Water Resource. Manage.* 20, 643–660.
- Mishra, S. K., Sahu, R. K., Eldho, T. I., & Jain, M. K. (2006b). A generalized relation between initial abstraction and potential maximum retention in SCS-CN-based model. *International Journal of River Basin Management*, 4(4), 245-253.
- Mishra, S. K., Tyagi, J. V., Singh, V. P., and Singh, R. (2006). SCS-CN based modeling of sediment yield. *Journal of Hydrology*, 324, 301-322.
- Mishra, S. K., Pandey, R. P., Jain, M. K., & Singh, V. P. (2008). A rain duration and modified AMC-dependent SCS-CN procedure for long duration rainfall-runoff events. *Water resources management*, 22(7), 861-876.
- Mishra, S. K., Rawat, S. S., Chakraborty, S., Pandey, R. P., & Jain, M. K. (2013). Relation between runoff curve number and PET. *J Hydrologic Engineering*, Manuscript No. HEENG-1496.
- Mishra, S. K., Chaudhary, A., Shrestha, R. K., Pandey, A., & Lal, M. (2014). Experimental verification of the effect of slope and land use on SCS runoff curve number. *Water resources management*, 28(11), 3407-3416.
- Mishra, S. K., Amrit, K., & Pandey, R. P. (2019). Correlation between Tennant method and Standardized Precipitation Index for predicting environmental flow condition using rainfall in Godavari Basin. *Paddy and Water Environment*, 1-7.
- Mockus, V. (1949). Estimation of total (and peak rates of) surface runoff for individual storms. Exhibit A in Appendix B, Interim Survey Report, Grand (Neosho) River Watershed, USDA, Washington DC.
- Mockus, V., Woodward, D., Neilsen, R. D., Kluth, R., Plummer, A., Van Mullem, J. A., & Hawkins, R. H. (2002). Land use and treatment classes. US NRCS, National Engineering Handbook. Washington DC.
- Moldenhauer, W. C., & Long, D. C. (1964). Influence of Rainfall Energy on Soil Loss and Infiltration Rates: I. Effect over a Range of Texture 1. *Soil Science Society of America Journal*, 28(6), 813-817.

- Morgan, R. P. C. (1995). Soil erosion and conservation. John Wiley & Sons.
- Musgrave, G. W. (1947). The quantitative evaluation of factors in water erosion-a first approximation. *Journal of Soil and Water conservation*, 2, 133-138.
- Naiman RJ, Bunn SE, Nilsson C, Petts GE, Thompson LC (2002). Legitimizing fluvial ecosystems as users of water. *Environmental Management*, 30:455-467.
- Nash, J. E. (1957). The form of the instantaneous unit hydrograph. *International Association of Scientific Hydrology, Publication*, 3, 114-121.
- Natural Resources Conservation Service (NRCS), 2004. Estimation of direct runoff from storm rainfall. In NRCS. *National Engineering Handbook: Part 630 Hydrology*. USDA, Washington DC.
- Nearing, M. A., Foster, G. R., Lane, L. J., & Finkner, S. C. (1989). A process-based soil erosion model for USDA-Water Erosion Prediction Project technology. *Transactions of the ASAE*, 32(5), 1587-1593.
- Neitsch, S. L., Arnold, J. G., Kiniry, J. E. A., Srinivasan, R., & Williams, J. R. (2002). Soil and water assessment tool user's manual version 2000. GSWRL report, 202(02-06).
- Nia, E. S., Asadollahfardi, G., & Heidarzadeh, N. (2016). Study of the environmental flow of rivers, a case study, Kashkan River, Iran. *Journal of Water Supply: Research and Technology-Aqua*, 65(2), 181-194.
- Nilsson, C., & Berggren, K. (2000). Alterations of riparian ecosystems caused by river regulation: Dam operations have caused global-scale ecological changes in riparian ecosystems. How to protect river environments and human needs of rivers remains one of the most important questions of our time. *BioScience*, 50(9), 783-792.
- Novotny, V. (1979). Simulation of pollutant loadings and runoff quality. US Environmental Protection Agency.
- Novotny, V. (1980). Delivery of Suspended Sediment and Pollutants from Nonpoint Sources during Overland Flow. *JAWRA Journal of the American Water Resources Association*, 16(6), 1057-1065.
- Norton, L. D. (1985). Erosion-sedimentation in a Closed Drainage Basin in Northwest Indiana 1. *Soil Science Society of America Journal*, 50(1), 209-213.

- Novotny, V. (1986). A review of hydrologic and water quality models used for simulation of agricultural pollution. In *Developments in environmental modelling* (Vol. 10, pp. 9-35). Elsevier.
- Novotny V., & Chesters G., (1989). *Handbook of Nonpoint Pollution: Sources and Management* Van Nostrand Reinhold, New York (1989).
- Novotny, V. and H. Olem (1994), 'Water Quality: Prevention, Identification, and Management of Diffuse Pollution,' John Wiley & Sons, New York, N.Y.
- Ogrosky, H. O. (1956). *Several Objectives in the field of hydrology*. USDA, SCS (unpublished), 5.
- Ojha, C. S. P. (2011). Simulating turbidity removal at a river bank filtration site in India using SCS-CN approach. *Journal of Hydrologic Engineering*, 17(11), 1240-1244.
- O'Keefe, J. (2009). Sustaining river ecosystems: Balancing use and protection. *Progress in Physical Geography*, 33(3), 339-357.
- Oki, T., & Kanae, S. (2006). Global hydrological cycles and world water resources. *Science*, 313(5790), 1068-1072.
- Operacz, A., Wałęga, A., Cupak, A., & Tomaszewska, B. (2018). The comparison of environmental flow assessment-The barrier for investment in Poland or river protection?. *Journal of cleaner production*, 193, 575-592.
- Overton, I. C., Smith, D. M., Dalton, J., Barchiesi, S., Acreman, M. C., Stromberg, J. C., & Kirby, J. M. (2014). Implementing environmental flows in integrated water resources management and the ecosystem approach. *Hydrological Sciences Journal*, 59(3-4), 860-877.
- Padikkal, S., Sumam, K. S., & Sajikumar, N. (2019). Environmental flow modelling of the Chalakkudi Sub-basin using 'Flow Health'. *Ecohydrology & Hydrobiology*, 19(1), 119-130.
- Paillex, A., Schuwirth, N., Lorenz, A. W., Januschke, K., Peter, A., & Reichert, P. (2017). Integrating and extending ecological river assessment: Concept and test with two restoration projects. *Ecological indicators*, 72, 131-141.

- Palmer, M. A., Reidy Liermann, C. A., Nilsson, C., Flörke, M., Alcamo, J., Lake, P. S., & Bond, N. (2008). Climate change and the world's river basins: anticipating management options. *Frontiers in Ecology and the Environment*, 6(2), 81-89.
- Pan, B., Yuan, J., Zhang, X., Wang, Z., Chen, J., Lu, J., & Xu, M. (2016). A review of ecological restoration techniques in fluvial rivers. *International Journal of Sediment Research*, 31(2), 110-119.
- Pandey, A., Himanshu, S. K., Mishra, S. K., & Singh, V. P. (2016). Physically based soil erosion and sediment yield models revisited. *Catena*, 147, 595-620.
- Pandit, A., & Gopalakrishnan, G. (1996). Estimation of annual storm runoff coefficients by continuous simulation. *Journal of irrigation and drainage engineering*, 122(4), 211-220.
- Paukert, C. P., Pitts, K. L., Whittier, J. B., & Olden, J. D. (2011). Development and assessment of a landscape-scale ecological threat index for the Lower Colorado River Basin. *Ecological Indicators*, 11(2), 304-310.
- Pearce F (2007). *When the Rivers Run Dry: What Happens When our Water Runs Out?* Transworld Publishers, London.
- Pearce, F. (2012). *The land grabbers: The new fight over who owns the earth.* Beacon Press.
- Perlman, H. (2016, December 2). Runoff (surface water runoff). Retrieved May 01, 2017, from <https://water.usgs.gov/edu/runoff.html>
- Petroselli, A., Grimaldi, S., & Romano, N. (2013). Curve-Number/Green-Ampt mixed procedure for net rainfall estimation: a case study of the Mignone watershed, IT. *Procedia Environmental Sciences*, 19, 113-121.
- Philip, J. R. (1974). Recent progress in the solution of nonlinear diffusion equations. *Soil Science*, 117(5), 257-264.
- Plummer, A. & Woodward, D. E. (2002). The origin and derivation of Ia/S in the runoff curve number system. Available at the NRCS website: <http://www.wcc.nrcs.usda.gov/water/quality/common/techpaper/don1.pdf>
- Poff N. L., Allan J.D., Bain M. B., Karr J. R., Prestegard K. L., Richter B. D., Sparks R. E., Stromberg J. E., (1997). The natural flow regime: a paradigm for river conservation and restoration. *BioScience*, 47:769-784

- Poff, N. L., & Matthews, J. H. (2013). Environmental flows in the Anthropocene: past progress and future prospects. *Current Opinion in Environmental Sustainability*, 5(6), 667-675.
- Poff, N. L., Richter, B. D., Arthington, A. H., Bunn, S. E., Naiman, R. J., Kendy, E., & Henriksen, J. (2009). The ecological limits of hydrologic alteration (ELOHA): a new framework for developing regional environmental flow standards. *Freshwater Biology*, 55(1), 147-170.
- Poff, N.L. (2009). "Managing for Variability to sustain Freshwater Ecosystems." *Journal of Water Resources Planning and Management*, (21), 435-456.
- Ponce, V. M. (1989). *Engineering hydrology: Principles and practices* (Vol. 640). Englewood Cliffs, NJ: Prentice Hall.
- Ponce, V. M., & Hawkins, R. H. (1996). Runoff curve number: Has it reached maturity?. *Journal of hydrologic engineering*, 1(1), 11-19.
- Postel, S. (1992). *Last oasis*. World watch Institute, Washington, DC.
- Postel, S., & Carpenter, S. (1997). Freshwater ecosystem services. *Nature's services: Societal dependence on natural ecosystems*, 195.
- Postel S, and Richter B. (2003). *Rivers for Life: Managing Water for People and Nature*. Island Press, Washington, DC.
- Rallison, R. E., & Miller, N. (1982). Past, present, and future SCS runoff procedure. In *Rainfall-runoff relationship/proceedings, International Symposium on Rainfall-Runoff Modeling held May 18-21, 1981 at Mississippi State University, Mississippi State, Mississippi, USA*/edited by VP Singh. Littleton, Colo.: Water Resources Publications, c1982.
- Ramasastri, K. S., & Seth, S. M. (1985). *Rainfall-runoff relationships*, Rep. RN-20, National Institute of Hydrology, Roorkee-247667, Uttar Pradesh, India.
- Renard, K. G., Simanton, J. R., & Osborn, H. B. (1974). Applicability of the Universal Soil Loss Equation to semiarid rangeland conditions in the Southwest. In *Hydrology and Water Resources in Arizona and the Southwest*. Arizona-Nevada Academy of Science.
- Renard, K. G., Foster, G. R., Weesies, G. A., & Porter, J. P. (1991). RUSLE: Revised universal soil loss equation. *Journal of soil and Water Conservation*, 46(1), 30-33.

- Rode, M., & Frede, H. G. (1997). Modification of AGNPS for agricultural land and climate conditions in central Germany. *Journal of environmental quality*, 26(1), 165-172.
- Roehl, J. W. (1962). Sediment source areas, delivery ratios and influencing morphological factors. *International Association of Scientific Hydrology*, 59, 202-213.
- Roni, P., Hanson, K., & Beechie, T. (2008). Global review of the physical and biological effectiveness of stream habitat rehabilitation techniques. *North American Journal of Fisheries Management*, 28(3), 856-890.
- Sahu, R. K., Mishra, S. K., Eldho, T. I., & Jain, M. K. (2007). An advanced soil moisture accounting procedure for SCS curve number method. *Hydrological processes*, 21(21), 2872-2881.
- Sahu, R. K., Mishra, S. K., & Eldho, T. I. (2010). An improved AMC-coupled runoff curve number model. *Hydrological processes*, 24(20), 2834-2839.
- Sahu, R. K., Mishra, S. K., & Eldho, T. I. (2012). Improved storm duration and antecedent moisture condition coupled SCS-CN concept-based model. *Journal of Hydrologic Engineering*, 17(11), 1173-1179.
- Saintilan, N., & Overton, I. (2010). *Ecosystem response modelling in the Murray-Darling Basin*. Csiro Publishing.
- Sandoval-Solis, S., & McKinney, D. C. (2014). Integrated water management for environmental flows in the Rio Grande. *Journal of Water Resources Planning and Management*, 140(3), 355-364.
- Schumm, S. A. (1954). The relation of drainage basin relief to sediment loss. *International Association of Scientific Hydrology*, 36(1), 216-219.
- SCS (1956, 1964, 1969, 1971, 1972, 1985, 1993), 'Hydrology,' *National Engineering Handbook, Supplement A, Section 4, Chapter 10*, Soil Conservation Service, USDA, Washington, D.C.
- Senbeta, D. A., Shamseldin, A. Y., & O'Connor, K. M. (1999). Modification of the probability-distributed interacting storage capacity model. *Journal of Hydrology*, 224(3-4), 149-168.

- Sharpley, A. N. & Williams, J. R. (1990). EPIC—Erosion/Productivity Impact Calculator: 1. Model Documentation. US Department of Agriculture Technical Bulletin No. 1768. US Government Printing Office, Washington, DC.
- Shi, W., Huang, M., Gongadze, K., & Wu, L. (2017). A modified SCS-CN method incorporating storm duration and antecedent soil moisture estimation for runoff prediction. *Water resources management*, 31(5), 1713-1727.
- Shi, Zhi-Hua, Chen, Li-Ding, Fang, Nu-Fang, Qin, De-Fu, and Cai, Chong-Fa (2009). Research on the SCS-CN initial abstraction ratio using rainfall-runoff event analysis in the Three Gorges Area, China. *Catena*, pp. 1-7.
- Singh, P. K., Bhunya, P. K., Mishra, S. K., & Chaube, U. C. (2008). A sediment graph model based on SCS-CN method. *Journal of Hydrology*, 349(1-2), 244-255.
- Singh, P. K., Gaur, M. L., Mishra, S. K., & Rawat, S. S. (2010). An updated hydrological review on recent advancements in soil conservation service-curve number technique. *Journal of Water and Climate Change*, 1(2), 118-134.
- Singh, P. K., Maehiwal, D., & Roy, M. K. (2011). Modeling daily runoff and probabilistic estimation of design maximum daily runoff from selected watersheds of Udaipur, Rajasthan. *Indian Journal of Soil Conservation*, 39(3), 176-182.
- Singh, P. K., Yaduvanshi, B. K., Patel, S., & Ray, S. (2013). SCS-CN based quantification of potential of rooftop catchments and computation of ASRC for rainwater harvesting. *Water resources management*, 27(7), 2001-2012.
- Singh, P. K., Mishra, S. K., Berndtsson, R., Jain, M. K., & Pandey, R. P. (2015). Development of a modified SMA based MSCS-CN model for runoff estimation. *Water resources management*, 29(11), 4111-4127.
- Singh, V.P. (1985), 'A mathematical study of erosion from upland areas,' Water resources Report, Dept. of Civil and Env. Engrg., Louisiana State University, Baton Rouge, LA 70803-6405.
- Singh, V. P., & Singh, V. P. (1992). *Elementary hydrology* (pp. 179-182). Englewood Cliffs: Prentice Hall.

- Singh, V. P. (Ed.). (1995). *Computer models of watershed hydrology* (Vol. 1130). Highlands Ranch, CO: Water Resources Publications.
- Singh, V. P. (1997). The use of entropy in hydrology and water resources. *Hydrological processes*, 11(6), 587-626.
- Singh, V. P. (2015). *Entropy theory in hydrologic science and engineering* (p. 848). New York: McGraw-Hill Education.
- Singh, V. P., Baniukiwicz, A., & Chen, V. J. (1982). An instantaneous unit sediment graph study for small upland watersheds. *Applied modeling in catchment hydrology*.
- Singh, V. P., & Frevert, D. K. (Eds.). (2002). *Mathematical models of small watershed hydrology and applications*. Water Resources Publication.
- Singh, V. P., & Woolhiser, D. A. (2002). Mathematical modeling of watershed hydrology. *Journal of hydrologic engineering*, 7(4), 270-292.
- Sivakumar, B., Berndtsson, R., & Persson, M. (2001). Monthly runoff prediction using phase space reconstruction. *Hydrological sciences journal*, 46(3), 377-387.
- Sivapalan, M., Savenije, H. H., & Blöschl, G. (2012). Socio-hydrology: A new science of people and water. *Hydrological Processes*, 26(8), 1270-1276.
- Skaugen, T., Peerebom, I. O., & Nilsson, A. (2015). Use of a parsimonious rainfall-run-off model for predicting hydrological response in ungauged basins. *Hydrological processes*, 29(8), 1999-2013.
- Skoulikidis N. T., Vardakas L., Karaouzas I., Economou A. N., Dimitriou E., & Zogaris S. (2011) Assessing water stress in Mediterranean lotic systems: insights from an artificially intermittent river in Greece. *Aqua Sci*. doi: 10.1007/s00027-011-0228-1.
- Smakhtin, V. U., & Masse, B. (2000). "Continuous Daily Hydrograph Simulation Using Duration Curves of a Precipitation Index". *Hydrological Processes* 14: 1083-1100.
- Sobhani, G. (1975). A review of selected small watershed design methods for possible adoption to Iranian conditions. source pollution model: A large water analysis model,' U.S. Dept. of Agri., Cons. Res. Report No. 35,

- Soulis, K. X., & Valiantzas, J. D. (2013). Identification of the SCS-CN parameter spatial distribution using rainfall-runoff data in heterogeneous watersheds. *Water resources management*, 27(6), 1737-1749.
- Springer, E.P., B.J. McGurk, R.H Hawkins, & G.B. Goltharp (1980), 'Curve numbers from watershed data,' Proc., A.S.C.E. Irrigation and Drainage Symp. on Watershed Management, A.S.C.E., New York, N.Y., Vol. D, 938-950.
- Srinivasan, V., Lambin, E. F., Gorelick, S. M., Thompson, B. H., & Rozelle, S. (2012). The nature and causes of the global water crisis: Syndromes from a meta-analysis of coupled human-water studies. *Water Resources Research*, 48(10).
- Srivastava, R. K., & Imtiyaz, M. (2016). Testing of coupled SCS curve number model for estimating runoff and sediment yield for eleven watersheds. *Journal of the Geological Society of India*, 88(5), 627-636.
- Stalnaker, C. B. (1990). Minimum flow is a myth. In *Ecology and assessment of warmwater streams: workshop synopsis*. Washington (DC): US Fish & Wildlife Service. Biological Report (No. 90, p. 5).
- Stalnaker, C.B. and Arnette, J.L. (Editors). (1976). *Methodologies for the Determination of Stream Resource Flow Requirements: An Assessment*. U.S. Fish and Wildlife Service, Office of Biological Services. 199 pages.
- Stamou, A., Polydera, A., Papadonikolaki, G., Martinez-Capel, F., Muñoz-Mas, R., Papadaki, C., & Dimitriou, E. (2018). Determination of environmental flows in rivers using an integrated hydrological-hydrodynamic-habitat modelling approach. *Journal of environmental management*, 209, 273-285.
- Statzner, B. (1981). The relation between "hydraulic stress" and microdistribution of benthic macroinvertebrates in a lowland running water system, the Schierenseebrooks (North Germany). *Archiv fur Hydrobiologie*, 91, 192-218.
- Statzner, B., & Higler, B. (1986). Stream hydraulics as a major determinant of benthic invertebrate zonation patterns. *Freshwater biology*, 16(1), 127-139.
- Su, Y. Z., Zhao, H. L., Zhao, W. Z., & Zhang, T. H. (2004). Fractal features of soil particle size distribution and the implication for indicating desertification. *Geoderma*, 122(1), 43-49.

- Subramanya, K. (2013), 'Engineering Hydrology,' Fourth Ed., McGraw Hill Edu. (India) Pvt. Ltd., New Delhi, p. 534.
- Tayfur, G. (2001). Modeling two-dimensional erosion process over infiltrating surfaces. *Journal of Hydrologic Engineering*, 6(3), 259-262.
- Tayfur, G. (2002). Applicability of sediment transport capacity models for nonsteady state erosion from steep slopes. *Journal of Hydrologic Engineering*, 7(3), 252-259.
- Tayfur, G., & Kavvas, M. L. (1994). Spatially averaged conservation equations for interacting rill-interrill area overland flows. *Journal of Hydraulic Engineering*, 120(12), 1426-1448.
- Taylor, B. D. (1983). Sediment yields in coastal southern California. *Journal of Hydraulic Engineering*, 109(1), 71-85.
- Tennant, D.L. (1975). "Instream Flow Regimens for Fish, Wildlife, Recreation and Related Environmental Resources." U.S. Fish and Wildlife Service, Federal Building, Billings, MT. 30 pages.
- Tharme, R. E. (2003). A global perspective on environmental flow assessment: emerging trends in the development and application of environmental flow methodologies for rivers. *River research and applications*, 19(5-6), 397-441.
- Tharme, R. E., Webb, S. C., & Brown, A. C. (1996). Organisms associated with the sandy-beach bivalve *Donax serra* Röding, with a description of *Cercaria serra* sp. nov. (Trematoda). *South African Journal of Zoology*, 31(2), 86-90.
- Tharme, R.E. and Smakhtin, V. (2003). Environmental Flow Assessment in Asia: Capitalizing on existing momentum. *Proceedings of the First Southeast Asia Water Forum*, 17-21 November 2003, Chiang Mai, Thailand. Volume 2: p 301-313. Thailand Water Resources Association, Bangkok, Thailand.
- Trihey, E.W. and Stalnaker, C.B. (1985). Evolution and application of instream flow methodologies to small hydropower development: an overview of the issues. Pages 176-183, In: Olson, G.W.; White, R.G. and Hamre, R.H. (Editors) *Proceedings of the Symposium on Small Hydropower and Fisheries*. American Fisheries Society, Bethesda, MD, USA. 497 pages.

- Turnbull, L., Wilcox, B. P., Belnap, J., Ravi, S., D'odorico, P., Childers, D., & Sankey, T. (2012). Understanding the role of ecohydrological feedbacks in ecosystem state change in drylands. *Ecohydrology*, 5(2), 174-183.
- Tyagi, J. V., Mishra, S. K., Singh, R., & Singh, V. P. (2008). SCS-CN based time-distributed sediment yield model. *Journal of hydrology*, 352(3-4), 388-403.
- Van Vliet, M.T.H., Franssen, W.H.P., Yearsley, J.R., Ludwig, F., Haddeland, I., Lettenmaier, D.P., Kabat, P.(2013). "Global river discharge and water temperature under climate change." *Glob. Environ. Change*, 23, 450–464.
- Van-Mullem, J. A. (1989). Runoff and peak discharges using Green-Ampt model. *Journal of Hydrologic Engineering*, ASCE 117 (3), 354–370.
- Váňová, V., & Langhammer, J. (2011). Modelling the impact of land cover changes on flood mitigation in the upper Lužnice basin. *Journal of Hydrology and Hydromechanics*, 59(4), 262-274.
- Verma, S., Singh, P. K., Mishra, S. K., Jain, S. K., Berndtsson, R., Singh, A., & Verma, R. K. (2018). Simplified SMA-inspired 1-parameter SCS-CN model for runoff estimation. *Arabian Journal of Geosciences*, 11(15), 420.
- Vogel, E. F. (2011). *Deng Xiaoping and the transformation of China (Vol. 10)*. Cambridge, MA: Belknap Press of Harvard University Press.
- Volchek, A., Kirvel, I., & Sheshko, N. (2019). Environmental flow assessment for the Yaselda River in its Selets reservoir section. *Ecohydrology & Hydrobiology*, 19(1), 109-118.
- Vorosmarty, C. J. (1997). The storage and aging of continental runoff in large reservoir systems of the world. *Ambio*, 26, 210-219.
- Vörösmarty, C. J., McIntyre, P. B., Gessner, M. O., Dudgeon, D., Prusevich, A., Green, P., & Davies, P. M. (2010). Global threats to human water security and river biodiversity. *Nature*, 467(7315), 555.
- Walega, A., & Salata, T. (2019). Influence of land cover data sources on estimation of direct runoff according to SCS-CN and modified SME methods. *Catena*, 172, 232-242.

- Wałęga, A., Michalec, B., Cupak, A., & Grzebinoga, M. (2015). Comparison of SCS-CN determination methodologies in a heterogeneous catchment. *Journal of Mountain Science*, 12(5), 1084-1094.
- Wałęga, A., Młyński, D., & Wachulec, K. (2017). The use of asymptotic functions for determining empirical values of CN parameter in selected catchments of variable land cover. *Studia Geotechnica et Mechanica*, 39(4), 111-120.
- Walling, D.E. and B.W. Webb (1983), 'Patterns of sediment yield,' In: *Background to Paleohydrology*, K.J. Gregory (ed.), Wiley, New York.
- Walter, M. T., & Shaw, S. B. (2005). DISCUSSION 1: "Curve Number Hydrology in Water Quality Modeling: Uses, Abuses, and Future Directions," by David C. Garen and Daniel S. Moore. 2. *JAWRA Journal of the American Water Resources Association*, 41(6), 1491-1492.
- Wang and Lu, (2009). "Quantitative Estimation Models and their Application of Ecological Water Use at a Basin Scale." *Procedia Environmental Science*, 13, 1559-1568.
- Warner, A. T., Bach, L. B., & Hickey, J. T. (2014). Restoring environmental flows through adaptive reservoir management: planning, science, and implementation through the Sustainable Rivers Project. *Hydrological Sciences Journal*, 59(3-4), 770-785.
- Webb, J. A., Nichols, S. J., Norris, R. H., Stewardson, M. J., Wealands, S. R., & Lea, P. (2012). Ecological responses to flow alteration: assessing causal relationships with Eco Evidence. *Wetlands*, 32(2), 203-213.
- Williams, J. R. (1975). Sediment-yield prediction with universal equation using runoff energy factor.
- Williams, J. R. (1978). A sediment graph model based on an instantaneous unit sediment graph. *Water Resources Research*, 14(4), 659-664.
- Williams, J. R., & LaSeur, W. V. (1976). Water yield model using SCS curve numbers. *Journal of the hydraulics division*, 102(ASCE# 12379).
- Williams, J. R., & Berndt, H. D. (1977). Sediment yield prediction based on watershed hydrology. *Transactions of the ASAE*, 20(6), 1100-1104.

- Williams, J. R., Kannan, N., Wang, X., Santhi, C., & Arnold, J. G. (2011). Evolution of the SCS runoff curve number method and its application to continuous runoff simulation. *Journal of Hydrologic Engineering*, 17(11), 1221-1229.
- Wilson, L. (1973). Variations in mean annual sediment yield as a function of mean annual precipitation. *American Journal of Science*, 273(4), 335-349.
- Wischmeier, W. H. (1975). Estimating the soil loss equation's cover and management factor for undisturbed areas. Present and prospective technology for predicting sediment yields and sources, 118-124.
- Wischmeier, W. H., & Mannering, J. V. (1969). Relation of Soil Properties to its Erodibility 1. *Soil Science Society of America Journal*, 33(1), 131-137.
- Wischmeier, W. H., & Smith, D. D. (1958). Rainfall energy and its relationship to soil loss. *Eos, Transactions American Geophysical Union*, 39(2), 285-291.
- Wischmeier, W. H., & Smith, D. D. (1965). Rainfall-erosion losses from cropland east of the Rocky Mountains, guide for selection of practices for soil and water conservation. *Agriculture Handbook*, 282.
- Wischmeier, W. H., & Smith, D. D. (1978). Predicting rainfall erosion losses-a guide to conservation planning. *Predicting rainfall erosion losses-a guide to conservation planning*.
- Wischmeier, W. H., Johnson, C. B., & Cross, B. V. (1971). Soil erodibility nomograph for farmland and construction sites. *Journal of soil and water conservation*.
- Wohl, E., Palmer, M., Kondolf, G. M., Brierley, G. J., & Fryirs, K. A. (2012). River management in the United States. *River futures: an integrative scientific approach to river repair*. Island Press, Washington, DC, 174-200.
- Woodward, D. E. and Gbuerek, W. J. (1992). Progress report ARS/SCS curve number work group. *Proceedings of ASCE Water Forum*. ASCE, New York, 378-382.
- Woolhiser, D. A., Smith, R. E., & Goodrich, D. C. (1990). KINEROS: A kinematic runoff and erosion model: documentation and user manual, USDA Agricultural Research Service ARS-77.

- Wu, T. H., Hall, J. A., & Bonta, J. V. (1993). Evaluation of runoff and erosion models. *Journal of irrigation and drainage engineering*, 119(2), 364-382.
- Wurbs, R. A. (1998). Dissemination of generalized water resources models in the United States. *Water International*, 23(3), 190-198.
- Xu, C. Y. (2002). *Hydrologic models*. Textbooks of Uppsala University. Department of Earth Sciences Hydrology.
- Yang, C. T., Marsooli, R., & Aalami, M. T. (2009). Evaluation of total load sediment transport formulas using ANN. *International Journal of Sediment Research*, 24(3), 274-286.
- Yang, W. Y., Li, D., Sun, T., & Ni, G. H. (2015). Saturation-excess and infiltration-excess runoff on green roofs. *Ecological Engineering*, 74, 327-336.
- Yang, Z. F., Sun, T., Cui, B. S., Chen, B., & Chen, G. Q. (2009). Environmental flow requirements for integrated water resources allocation in the Yellow River Basin, China. *Communications in Nonlinear Science and Numerical Simulation*, 14(5), 2469-2481.
- Yao, Y., Zheng, C., Tian, Y., Li, X., & Liu, J. (2018). Eco-hydrological effects associated with environmental flow management: A case study from the arid desert region of China. *Ecohydrology*, 11(1), e1914.
- Yin, X. A., & Yang, Z. F. (2011). Development of a coupled reservoir operation and water diversion model: Balancing human and environmental flow requirements. *Ecological Modelling*, 222(2), 224-231.
- Yin, X. A., & Yang, Z. F. (2012). Morphology and associated environmental flow prescriptions for rivers for water supply. *Procedia Environmental Sciences*, 13, 2414-2426.
- Young, R. A. (1987). *AGNPS, Agricultural Non-Point-Source Pollution Model: a watershed analysis tool*. Conservation research report (USA). no. 35. Yu, B. (1998). Theoretical justification of SCS method for runoff estimation. *Journal of irrigation and drainage engineering*, 124(6), 306-310.
- Young, R. A., Onstad, C. A., Bosch, D. D. & Anderson, W. P. (1989). AGNPS: a nonpoint-source pollution model for evaluating agricultural watersheds. *J. Soil & Water Conservation*, 44 (2), 168–173.

Yuan, Y., Mitchell, J. K., Hirschi, M. C. and Cooke, R. A. C. (2001). Modified SCS Curve Number Method for predicting sub surface drainage flow. *Trans. ASAE*. 44(6): 1673-1682.

Zingg, A. W. (1940). Degree and length of land slope as it affects soil loss in run-off. *Agric. Engng.*, 21, 59-64.

Zoch, R. T. (1934). On the relation between rainfall and streamflow-1. *Monthly Weather Review*, 62(9), 315-322.

Zoch, R. T. (1936). On the relation between rainfall and stream flow—II. *Monthly Weather Review*, 64(4), 105-121.



Soil addition



Addition of sandy soil by manual power.

Grain size analysis of soil



Soil sampling for grain size analysis of soil



View of Sieve Analysis of Soil using Sieve Shaker



Double ring infiltration test



Table A1: Computed values of Bulk Density, Particle Density and Porosity. (2016 to 2017)

Plot No.	Land use	Slope	Bulk Density (gm/cc)	Particle Density (gm./cc)	Porosity (%)
2016					
1	Maize	12%	1.46	2.54	42.33
2	Mandua	12%	1.35	2.55	46.89
3	Fallow	12%	1.36	2.68	49.06
4	Maize	8%	1.33	2.53	47.31
5	Mandua	8%	1.48	2.59	43.03
6	Fallow	8%	1.42	2.58	45.00
7	Mandua	16%	1.40	2.61	46.38
8	Maize	16%	1.44	2.59	44.40
9	Fallow	16%	1.40	2.67	47.50
2017					
1	Maize	12%	1.46	2.54	42.34
2	Mandua	12%	1.35	2.55	46.90
3	Fallow	12%	1.36	2.68	49.06
4	Maize	8%	1.33	2.53	47.32
5	Mandua	8%	1.48	2.59	43.03
6	Fallow	8%	1.42	2.58	45.00
7	Mandua	16%	1.40	2.61	46.39
8	Maize	16%	1.44	2.59	44.41
9	Fallow	16%	1.40	2.67	47.51

Table A2: Results of Sieve Analysis of Soil Samples from the different Plots (2017).

S . N	Sieve (mm)	1st Plot(wt. retained) (Grams)	2nd Plot(wt. retained)(Grams)	3rd Plot (Weight retained) (Grams)	4th Plot(wt. retained) (Grams)	5th Plot(wt. retained) (Grams)	6th Plot(wt. retained) (Grams)	7th Plot(wt. retained) (Grams)	8th Plot(wt. retained) (Grams)	9th Plot(wt. retained) (Grams)
2016										
1	0.6	20.12	12.21	11.95	19.42	13.21	14.24	18.46	7.6	13.03
2	0.4	40.21	22.21	36.74	38.93	18.61	34.34	43.42	23.74	33.58
3	0.3	19.82	55.12	34.51	22.32	53.32	30.02	17.84	49.18	33.51
4	0.225	146.73	166.42	151.648	150.23	163.14	146.13	143.585	163.71	153.648
5	0.15	351.21	276.31	322.025	348.94	280.34	300.45	351.02	289.03	320.025
6	0.09	136.32	178.31	160.675	135.67	180.21	188.94	143.71	179.64	161.675
7	0.075	7.68	8.36	5.55	8.92	8.31	6.55	5.72	4.98	5.35
8	0.063	4.97	2.19	3.12	5.21	4.1	5.71	3.21	3.26	3.235
9	pan	68.29	78.71	73.5	68.29	78.71	73.5	68.29	78.71	73.5
2017										
1	0.6	2.5	27		3.2	5	3.5	3.42	2.7	4.7
2	0.4	20.40	29.00		16.20	30.30	31.00	12.20	15.00	26.00
3	0.3	4.50	32.20		13.93	34.40	53.40	0.00	12.20	1.00
4	0.225	78.80	98.80		59.30	74.60	98.00	87.60	90.80	122.80
5	0.15	216.19	122.00		239.00	117.00	138.20	164.63	143.30	130.80
6	0.09	124.21	125.70		106.47	141.30	106.50	162.26	182.50	147.60
7	0.075	3.43	6.60		1.96	7.60	3.00	4.61	2.50	5.10
8	Pan	41.82	50.25		36.61	84.10	65.60	59.12	48.17	60.15

Table A3: Double ring infiltrometer test.

Plot 2 (Date of test: 15/11/2016)				Plot 5 (Date of test: 15/11/2016)				Plot 8 (Date of test: 16/11/2016)			
Time interval(min)	Cumulative time(min)	Infiltration depth(m)	Infiltration Capacity(mm/hr)	Time interval(min)	Cumulative time(min)	Infiltration depth(m)	Infiltration Capacity(mm/hr)	Time interval(min)	Cumulative time(min)	Infiltration depth(m)	Infiltration Capacity(mm/hr)
start	0	0	0	start	0	0.0	0	start	0	0	0
1	1	3	180	1	1	2	120	1	1	5	300
1	2	2	120	1	2	2	120	1	2	3	180
1	3	3	180	1	3	1	60	1	3	3	180
1	4	2	120	1	4	1	60	1	4	2	120
1	5	1	60	1	5	1	60	1	5	2	120
1	6	1	60	1	6	1	60	1	6	2	120
1	7	2	120	1	7	1	60	1	7	2	120
1	8	1	30	1	8	1	60	1	8	1	60
1	9	1	30	1	9	1	60	1	9	1	60
1	10	1	60	1	10	1	60	1	10	1	60
10	20	8	48	10	20	8	48	10	20	13	78
10	30	6	36	10	30	6	36	10	30	9	54
10	40	3	18	10	40	5	30	10	40	8	48
30	70	10	20	30	70	16	32	30	70	25	50
30	100	9	18	30	100	12	24	30	100	23	46
30	130	8	16	30	130	11	22	30	130	21	42
60	190	14	14	60	190	22	22	60	190	40	40
60	250	15	15	60	250	24	24	60	250	39	39
60	310	15	15	60	310	20	20	60	310	35	35
60	370	15	15	60	370	20	20	60	370	34	34
60	430	15	15	60	430	10	10				

Plot 3 (Date of test: 15/11/2016)				Plot 6 (Date of test: 16/11/2016)				Plot 9 (Date of test: 16/11/2016)			
Time interval(min)	Cumulative time(min)	Infiltration depth(mm)	Infiltration Capacity(mm/hr)	Time interval(min)	Cumulative time(min)	Infiltration depth(mm)	Infiltration Capacity(mm/hr)	Time interval(min)	Cumulative time(min)	Infiltration depth(mm)	Infiltration Capacity(mm/hr)
start	0	0	0	start	0	0	0	start	0	0	0
2	2	10	300	1	1	3	180	2	2	8	240
2	4	4	120	1	2	3	180	2	4	5	150
2	6	4	120	1	3	2	120	2	6	3	90
2	8	3	90	1	4	2	120	2	8	3	90
2	10	4	120	1	5	1	60	2	10	2	60
10	20	16	96	1	6	1	60	10	20	6	36
10	30	14	84	1	7	1	60	10	30	5	30
10	40	13	78	1	8	1	60	10	40	4	24
30	70	35	70	1	9	1	60	30	70	13	26
30	100	35	70	1	10	1	90	30	100	6	12
30	130	33	66	10	20	11	63	30	130	5	10
60	190	62	62	10	30	6	36	60	190	10	10
60	250	58	58	10	40	6	36	60	250	7	7
60	310	57	57	30	70	11	22	60	310	7	7
60	370	51	51	30	100	10	20	60	370	7	7
				30	130	9	18				
				60	190	15	15				
				60	250	15	15				

				60	310	14	14				
				60	370	14	14				

Plot 1 (Date of test: 17/11/2016)				Plot 4 (Date of test: 17/11/2016)				Plot 7 (Date of test: 07/07/2016)			
Time interval(min)	Cumulative time(min)	Infiltration depth(mm)	Infiltration Capacity(mm/hr)	Time interval(min)	Cumulative time(min)	Infiltration depth(mm)	Infiltration Capacity(mm/hr)	Time interval(min)	Cumulative time(min)	Infiltration depth(mm)	Infiltration Capacity(m m/hr)
start	0	0.0	0	start	0	0	0	start	0	0.0	0
1	1	1.2	72	2	2	15	450	1	1	5.0	300
1	2	0.4	24	2	4	5	150	1	2	6.0	360
1	3	0.4	24	2	6	4	120	1	3	2.0	120
1	4	0.3	18	2	8	4	120	1	4	5.0	300
1	5	0.3	18	2	10	3	90	1	5	4.0	240
1	6	0.3	18	10	20	13	78	1	6	4.0	240
1	7	0.3	18	10	30	11	66	1	7	2.0	120
1	8	0.3	18	10	40	11	66	1	8	3.0	180
1	9	0.2	12	30	70	27	54	1	9	2.0	120
1	10	0.2	12	30	100	25	50	1	10	2.0	120
10	20	2.2	13	30	130	21	42	10	20	24.0	144
10	30	1.8	11	60	190	39	39	10	30	20.0	120
10	40	1.8	11	60	250	35	35	10	40	19.0	114
10	50	1.8	11	60	310	35	35	30	70	49.0	98
20	70	3.2	10	60	370	33	33	30	100	40.0	80
30	100	4.5	9					30	130	37.0	74
30	130	4.1	8					60	190	67.0	67
30	160	3.8	8					60	250	64.0	64
30	190	3.7	7					60	310	64.0	64
30	220	3.6	7					60	370	62.0	62

30	250	3.4	7							
30	280	3.2	6							
30	310	3.1	6							
30	340	3.1	6							
30	370	3.0	6							

Plot 1 (Date of test: 19/09/2017)				Plot 2 (Date of test: 18/09/2017)				Plot 3 (Date of test: 14/09/2017)			
Time interval(min)	Cumulative time(min)	Infiltration depth(mm)	Infiltration Capacity(mm/hr)	Time interval(min)	Cumulative time(min)	Infiltration depth(mm)	Infiltration Capacity(mm/hr)	Time interval(min)	Cumulative time(min)	Infiltration depth(mm)	Infiltration Capacity(mm/hr)
start	0	0	0	start	0	0	0	start	0	0	0
1	1	10	600	1	1	5	300	1	1	5.0	300.0
1	2	5	300	1	2	9	510	1	2	9.0	540.0
1	3	5	300	1	3	3	210	1	3	3.0	180.0
1	4	5	300	1	4	4	240	1	4	4.0	240.0
1	5	5	300	1	5	3	180	1	5	3.0	180.0
1	6	5	300	1	6	3	180	1	6	4.0	240.0
1	7	2	120	1	7	2	120	1	7	1.0	60.0
1	8	3	180	1	8	2	120	1	8	2.0	120.0
1	9	5	300	1	9	3	180	1	9	3.0	180.0
1	10	3	180	1	10	2	120	1	10	2.0	120.0
2	12	2	60	2	12	2	60	2	12	2.0	60.0
2	14	4	120	2	14	3	90	2	14	3.0	90.0
2	16	9	270	2	16	5	150	2	16	5.0	150.0
2	18	3	90	2	18	2	60	2	18	2.0	60.0
2	20	7	210	2	20	5	150	2	20	5.0	150.0
10	30	17	102	10	30	10	60	10	30	10.0	60.0
10	40	22	132	10	40	8	48	10	40	8.0	48.0
10	50	18	108	10	50	4	24	10	50	4.0	24.0
10	60	20	120	10	60	5	30	10	60	5.0	30.0
30	90	45	90	30	90	5	10	30	90	5.0	10.0
30	120	45	90	30	120	15	30	30	120	15.0	30.0
30	150	40	80	30	150	13	26	30	150	25.0	50.0

30	180	40	80	30	180	11	22	30	180	10.0	20.0
30	210	40	80	30	210	11	22	30	210	10.0	20.0
30	240	40	80	30	240	11	22	30	240	10.0	20.0
30	270	11	22	30	270	11	22	30	270	10.0	20.0
30	300	11	22								
30	330	11	22								

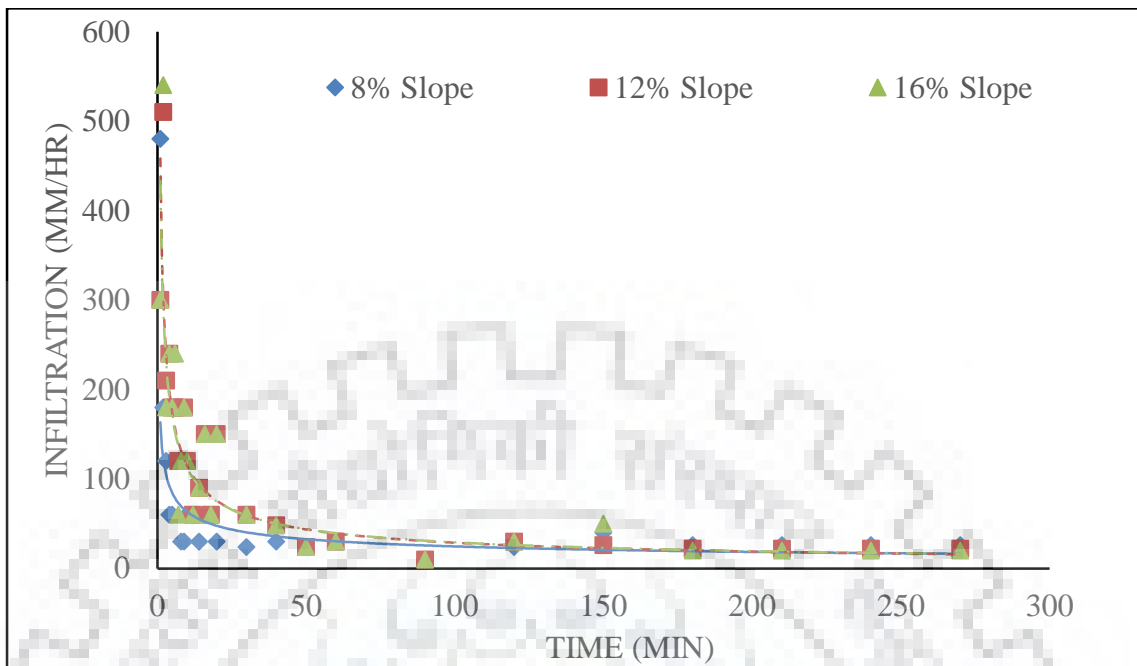
Plot 4 (Date of test: 02/11/2017)				Plot 5 (Date of test: 10/09/2017)				Plot 6 (Date of test: 16/07/2017)			
Time interval(min)	Cumulative time(min)	Infiltration depth(mm)	Infiltration Capacity(mm/hr)	Time interval(min)	Cumulative time(min)	Infiltration depth(mm)	Infiltration Capacity(mm/hr)	Time interval(min)	Cumulative time(min)	Infiltration depth(mm)	Infiltration Capacity(mm/hr)
start	0	0.0	0	start	0	0.0	0	start	0	0.0	0
1	1	6.0	360	1	1	8.0	480	1	1	4.0	240
1	2	3.0	180	1	2	3.0	180	1	2	3.0	180
1	3	2.0	120	1	3	2.0	120	1	3	2.5	150
1	4	1.0	60	1	4	1.0	60	1	4	2.0	120
1	5	1.0	60	1	5	1.0	60	1	5	1.5	90
1	6	2.0	120	1	6	2.0	120	1	6	1.0	60
1	7	3.0	180	1	7	3.0	180	1	7	1.5	90
1	8	2.0	120	1	8	0.5	30	1	8	1.1	66
1	9	1.0	60	1	9	0.5	30	1	9	1.4	84
1	10	1.0	60	1	10	1.0	60	1	10	1.0	60
2	12	1.0	30	2	12	2.0	60	2	12	1.9	57
2	14	1.0	30	2	14	1.0	30	2	14	0.9	27
2	16	1.0	30	2	16	2.0	60	2	16	2.2	66
2	18	2.0	60	2	18	2.0	60	2	18	1.5	45
2	20	1.0	30	2	20	1.0	30	2	20	1.0	30
10	30	9.0	54	10	30	4.0	24	10	30	4.5	27
10	40	9.0	54	10	40	5.0	30	10	40	4.5	27
10	50	10.0	60	10	50	4.0	24	10	50	4.5	27
10	60	10.0	60	10	60	5.0	30	10	60	5.0	30

30	90	10.0	20	30	90	5.0	10	30	90	5.0	10
30	120	27.0	54	30	120	12.0	24	30	120	22.0	44
30	150	20.0	40	30	150	20.0	40	30	150	20.0	40
30	180	30.0	60	30	180	13.0	26	30	180	20.0	40
30	210	30.0	60	30	210	13.0	26	30	210	20.0	40
30	240	30.0	60	30	240	13.0	26	30	240	20.0	40
30	270	30.0	60	30	270	13.0	26	30	270	20.0	40

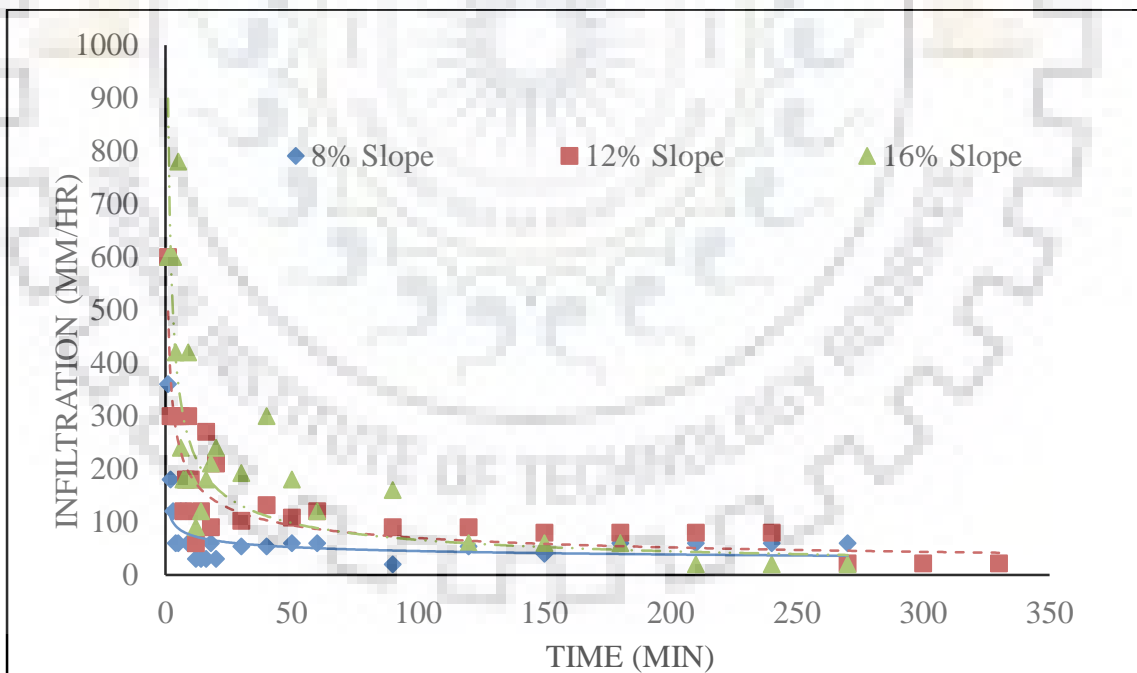
Plot 7 (Date of test: 05/11/2017)				Plot 8 (Date of test: 12/09/2017)				Plot 9 (Date of test: 13/09/2017)			
Time interval(min)	Cumulative time(min)	Infiltration depth(mm)	Infiltration Capacity(mm/hr)	Time interval(min)	Cumulative time(min)	Infiltration depth(mm)	Infiltration Capacity(mm/hr)	Time interval(min)	Cumulative time(min)	Infiltration depth(mm)	Infiltration Capacity(mm/hr)
start	0	0	0	start	0	0.0	0	start	0	0	0
1	1	10	600	1	1	5.0	300	1	1	10	600
1	2	10	600	1	2	9.0	540	1	2	5	300
1	3	10	600	1	3	3.0	180	1	3	5	300
1	4	7	420	1	4	4.0	240	1	4	5	300
1	5	13	780	1	5	3.0	180	1	5	5	300
1	6	4	240	1	6	4.0	240	1	6	5	300
1	7	3	180	1	7	1.0	60	1	7	2	120
1	8	3	180	1	8	2.0	120	1	8	3	180
1	9	7	420	1	9	3.0	180	1	9	2	120
1	10	3	180	1	10	2.0	120	1	10	6	360
2	12	3	90	2	12	2.0	60	2	12	2	60
2	14	4	120	2	14	3.0	90	2	14	4	120
2	16	6	180	2	16	5.0	150	2	16	9	270
2	18	7	210	2	18	2.0	60	2	18	3	90
2	20	8	240	2	20	5.0	150	2	20	4	120
10	30	32	192	10	30	10.0	60	10	30	10	60
10	40	50	300	10	40	8.0	48	10	40	10	60
10	50	30	180	10	50	4.0	24	10	50	10	60
10	60	20	120	10	60	5.0	30	10	60	10	60

30	90	80	160	30	90	5.0	10	30	90	10	20
30	120	30	60	30	120	15.0	30	30	120	10	20
30	150	30	60	30	150	25.0	50	30	150	20	40
30	180	30	60	30	180	10.0	20	30	180	10	20
30	210	10	20	30	210	10.0	20	30	210	14	28
30	240	10	20	30	240	10.0	20	30	240	14	28
30	270	10	20	30	270	10.0	20	30	270	14	28
								30	300	14	28
								30	330	14	28

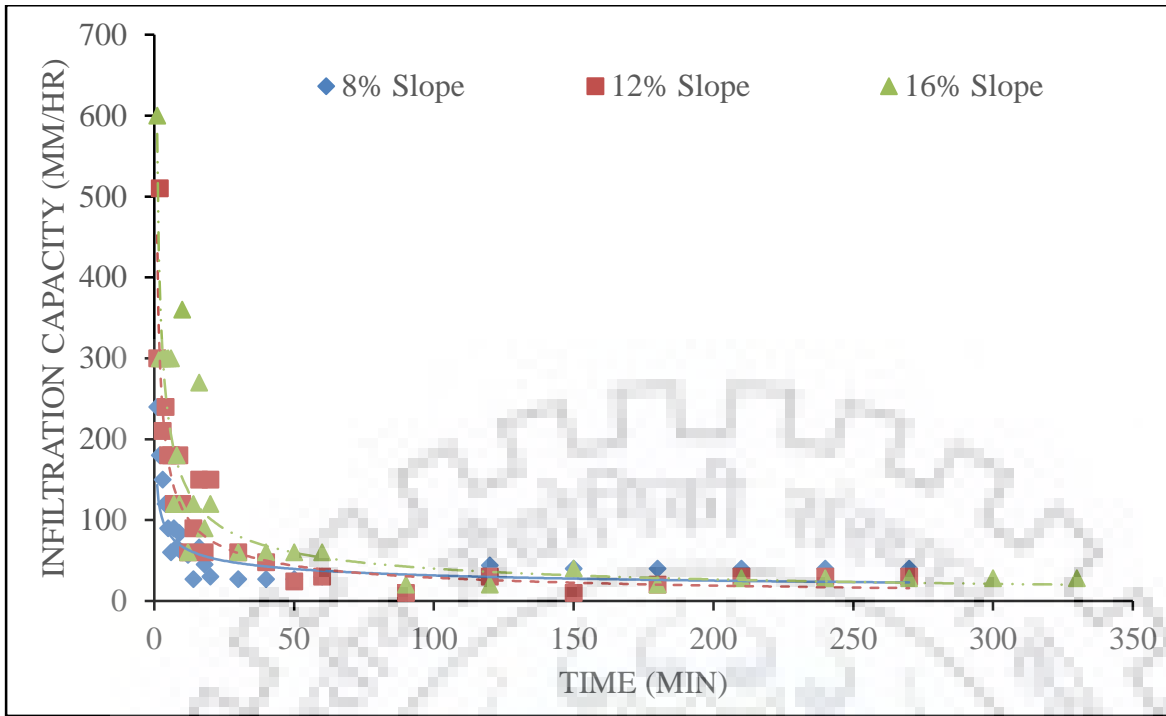




Infiltration capacity curve of maize crops at different slope (Test was carried out in year of 2017)



Infiltration capacity curve of finger millet crops at different slope (Test was carried out in year of 2017)



Infiltration capacity curve of Fellow land at different slope (Test was carried out in year of 2017)

Table A4: Observed rainfall and runoff data for experimental plots (2016).

Event No.	Date	Rainfall (mm)	Runoff (mm)								
			plot 1	plot 2	plot 3	plot 4	plot 5	plot 6	plot 7	plot 8	plot 9
1	15-Jun-16	17	10.66	4.86	1.28	9.86	9.27	5.35	11.77	7.88	2.68
2	16-Jun-16	46.5	35.50	27.10	22.24	32.65	21.82	24.49	36.82	30.92	18.17
3	22-Jun-16	39.2	27.23	21.53	14.31	24.03	19.87	15.70	31.67	20.98	16.26
4	7-Feb-16	35	26.75	18.41	17.72	21.89	19.80	19.11	18.41	12.16	16.33
5	3-Jul-16	22.8	11.20	9.81	7.04	12.59	9.81	5.65	9.81	11.20	5.65
6	6-Jul-16	13	8.27	8.41	4.28	7.23	8.62	7.06	9.32	6.71	8.45
7	16-Jul-16	19.1	8.97	6.88	3.41	7.30	7.58	6.88	4.80	6.88	6.61
8	22-Jul-16	65	49.43	45.82	40.61	51.62	47.66	40.61	53.11	49.99	45.89
9	23-Jul-16	36	30.07	25.90	16.18	25.21	25.21	21.74	27.29	17.57	24.51
10	25-Jul-16	23.8	18.28	15.50	11.06	20.78	13.83	12.45	16.61	16.61	9.67
11	6-Aug-16	24	5.47	4.08	0.75	4.08	6.86	2.00	5.47	2.69	1.30
12	8-Aug-16	20.8	11.64	6.36	3.16	12.19	5.66	2.19	10.94	5.39	9.97
13	11-Aug-16	12.4	0.89	1.59	0.20	1.59	0.89	0.20	2.97	0.89	0.89
14	14-Aug-16	22	15.49	14.10	9.93	10.63	11.32	9.93	15.49	11.32	11.32
15	14-Aug-16	12	5.81	4.42	0.95	7.20	3.03	3.03	5.81	3.03	1.64
16	29-Aug-16	46.5	31.27	25.02	16.13	28.77	28.49	27.79	29.88	29.18	24.32
17	22-Sep-16	20	9.11	7.45	4.81	8.84	5.78	5.36	7.45	3.28	4.95

Table A5: Observed rainfall, runoff and previous day soil moisture data for experimental plots (2017).

Event No.	Date	Rainfall (mm)	Runoff(Q) mm			Previous day soil moisture (%)		
			Plot 1	Plot 2	Plot 3	Plot 1	Plot 2	Plot 3
1	19-Jun-17	44.0	34.29	27.12	14.21	12.30	10.50	13.80
2	26-Jun-17	34.2	26.63	26.45	13.40	25.47	25.87	28.50
3	28-Jun-17	75.2	66.07	50.94	48.66	29.10	27.60	30.40
4	29-Jun-17	17.7	10.99	10.56	6.39	29.80	29.50	30.40
5	30-Jun-17	15.0	13.39	9.83	7.06	29.45	28.55	30.40
6	6-Jul-17	36.4	29.01	28.68	19.12	23.00	18.00	20.00
7	24-Jul-17	14.0	7.41	4.14	0.67	18.00	23.40	20.90
8	2-Aug-17	79.5	51.73	42.51	33.20	17.80	24.00	15.90
9	3-Aug-17	9.6	5.66	3.35	1.96	31.65	30.57	34.30
10	7-Aug-17	27.4	25.51	20.94	18.86	25.70	23.40	31.80
11	10-Aug-17	43.4	37.29	26.87	19.93	26.70	24.10	29.10
12	19-Aug-17	22.3	12.61	9.19	2.94	NA	NA	NA
13	22-Aug-17	58.1	46.25	30.90	28.95	24.00	24.00	25.70
14	23-Aug-17	15.5	8.64	2.54	2.32	33.40	33.30	37.80
15	25-Aug-17	61.8	52.04	36.59	32.28	27.70	26.40	31.00
16	1-Sep-17	44.0	36.24	20.53	14.98	25.85	25.20	28.35
17	1-Sep-17	23.0	21.27	18.81	14.65	32.60	32.87	33.85
18	2-Sep-17	61.1	32.90	33.22	26.27	25.67	26.53	29.47
19	3-Sep-17	26.0	19.34	13.51	9.06	30.25	28.45	32.60

Event No.	Date	Rainfall (mm)	Runoff(Q) mm			Previous day soil moisture (%)		
			Plot 4	Plot 5	Plot 6	Plot 4	Plot 5	Plot 6
1	19-Jun-17	44.0	27.20	17.75	13.03	14.20	12.00	11.30
2	26-Jun-17	34.2	26.17	15.06	11.59	26.87	25.53	30.53
3	28-Jun-17	75.2	68.35	54.61	49.82	31.50	30.60	32.10
4	29-Jun-17	17.7	13.34	7.78	10.56	34.30	35.10	37.60
5	30-Jun-17	15.0	12.33	9.14	6.78	32.90	32.85	34.85
6	6-Jul-17	36.4	30.01	24.29	13.34	21.00	21.00	20.20
7	24-Jul-17	14.0	2.75	2.75	2.75	24.50	25.40	19.80
8	2-Aug-17	79.5	41.53	34.87	24.17	23.70	21.50	22.00
9	3-Aug-17	9.6	6.13	4.74	0.57	32.30	32.23	35.25
10	7-Aug-17	27.4	25.80	20.25	17.47	26.20	25.90	24.50
11	10-Aug-17	43.4	33.12	26.18	22.01	26.03	28.83	32.30
12	19-Aug-17	22.3	10.44	5.72	1.55	NA	NA	NA
13	22-Aug-17	58.1	35.06	25.34	16.31	23.00	26.20	29.00
14	23-Aug-17	15.5	3.93	3.15	2.54	30.30	25.60	35.30
15	25-Aug-17	61.8	50.47	38.67	28.42	25.60	28.90	28.00
16	1-Sep-17	44.0	17.75	18.98	10.81	24.30	27.55	28.50
17	1-Sep-17	23.0	16.73	16.04	12.56	35.05	33.07	33.55
18	2-Sep-17	61.1	42.94	24.05	29.05	25.10	26.77	26.80
19	3-Sep-17	26.0	20.45	9.34	6.56	32.05	31.60	29.33

Event No.	Date	Rainfall (mm)	Runoff(Q) mm			Previous day soil moisture (%)		
			Plot 7	Plot 8	Plot 9	Plot 7	Plot 8	Plot 9
1	19-Jun-17	44.0	29.56	20.39	12.31	10.10	7.30	10.50
2	26-Jun-17	34.2	20.62	18.12	8.12	26.13	23.90	30.87
3	28-Jun-17	75.2	64.92	56.87	45.98	24.00	24.90	28.70
4	29-Jun-17	17.7	14.72	13.34	5.00	39.00	30.70	37.00
5	30-Jun-17	15.0	10.94	10.17	5.39	31.50	27.80	32.85
6	6-Jul-17	36.4	32.29	26.07	17.79	16.00	19.00	22.00
7	24-Jul-17	14.0	4.14	2.75	1.36	18.30	18.40	19.00
8	2-Aug-17	79.5	40.14	38.20	22.09	17.00	24.50	20.50
9	3-Aug-17	9.6	5.71	3.35	0.57	33.00	30.87	35.67
10	7-Aug-17	27.4	20.25	13.30	16.00	25.40	29.00	30.20
11	10-Aug-17	43.4	34.65	19.93	20.07	28.00	30.83	32.20
12	19-Aug-17	22.3	14.94	6.42	4.61	NA	NA	NA
13	22-Aug-17	58.1	35.90	33.67	23.26	22.50	29.20	31.20
14	23-Aug-17	15.5	4.54	5.32	2.54	32.80	32.80	35.60
15	25-Aug-17	61.8	45.61	31.45	38.67	24.40	28.10	26.20
16	1-Sep-17	44.0	30.70	17.75	12.20	23.45	28.65	28.70
17	1-Sep-17	23.0	20.90	13.81	14.65	31.90	34.63	34.83
18	2-Sep-17	61.1	48.50	25.72	33.22	24.10	27.10	26.30
19	3-Sep-17	26.0	19.06	10.68	13.51	27.40	32.10	31.23

Table A6: Strange data of total monsoon rainfall and estimated percent runoff coefficients.

Total monsoon rainfall (in)	Total monsoon rainfall (mm)	Percent runoff coefficient			Total monsoon rainfall (in)	Total monsoon rainfall (mm)	Percent runoff coefficient		
		Good catchment	Average catchment	Bad catchment			Good catchment	Average catchment	Bad catchment
1.0	25.4	0.1	0.1	0.1	31.0	787.4	27.4	20.5	13.7
2.0	50.8	0.2	0.2	0.1	32.0	812.8	28.5	21.3	14.2
3.0	76.2	0.4	0.3	0.2	33.0	838.2	29.6	22.2	14.8
4.0	101.6	0.7	0.5	0.3	34.0	863.6	30.8	23.1	15.4
5.0	127.0	1.0	0.7	0.5	35.0	889.0	31.9	23.9	15.9
6.0	152.4	1.5	1.1	0.7	36.0	914.4	33.0	24.7	16.5
7.0	177.8	2.1	1.5	1.0	37.0	939.8	34.1	25.5	17.0
8.0	203.2	2.8	2.1	1.4	38.0	965.2	35.3	26.4	17.6
9.0	228.6	3.5	2.6	1.7	39.0	990.6	36.4	27.3	18.2
10.0	254.0	4.3	3.2	2.1	40.0	1016.0	37.5	28.1	18.7
11.0	279.4	5.2	3.9	2.6	41.0	1041.4	38.6	28.9	19.3
12.0	304.8	6.2	4.6	3.1	42.0	1066.8	39.8	29.8	19.9
13.0	330.2	7.2	5.4	3.6	43.0	1092.2	40.9	30.6	20.4
14.0	355.6	8.3	6.2	4.1	44.0	1117.6	42.0	31.5	21.0
15.0	381.0	9.4	7.0	4.7	45.0	1143.0	43.1	32.3	21.5
16.0	406.4	10.5	7.8	5.2	46.0	1168.4	44.3	33.2	22.1
17.0	431.8	11.6	8.7	5.8	47.0	1193.8	45.4	34.0	22.7
18.0	457.2	12.8	9.6	6.4	48.0	1219.2	46.5	34.8	23.2

19.0	482.6	13.9	10.4	6.9	49.0	1244.6	47.6	35.7	23.8
20.0	508.0	15.0	11.3	7.5	50.0	1270.0	48.8	36.6	24.4
21.0	533.4	16.1	12.0	8.0	51.0	1295.4	49.9	37.4	24.9
22.0	558.8	17.3	12.9	8.6	52.0	1320.8	51.0	38.2	25.5
23.0	584.2	18.4	13.8	9.2	53.0	1346.2	52.1	39.0	26.0
24.0	609.6	19.5	14.6	9.7	54.0	1371.6	53.3	39.9	26.6
25.0	635.0	20.6	15.4	10.3	55.0	1397.0	54.4	40.8	27.2
26.0	660.4	21.8	16.3	10.9	56.0	1422.4	55.5	41.6	27.7
27.0	685.8	22.9	17.1	11.4	57.0	1447.8	56.6	42.4	28.3
28.0	711.2	24.0	18.0	12.0	58.0	1473.2	57.8	43.3	28.9
29.0	736.6	25.1	18.8	12.5	59.0	1498.6	58.9	44.4	29.4
30.0	762.0	26.3	19.7	13.1	60.0	1524.0	60.0	45.0	30.0



Name : **Shailendra Kumar Kumre**
Address : Room No. F-64, Azad Bhawan
IIT Roorkee, Roorkee
Dist. Haridwar, Uttarakhand – 247667
India
Email ID : skumre@wr.iitr.ac.in; skumre159@gmail.com
Educational Qualifications : B.Tech. (Agricultural Engineering), June-2011
J. N. K. V. V., India
M.Tech. (Hydrology), June-2013
IIT Roorkee, Uttarakhand, India

Publications from the Ph.D. research work

1. **Kumre S. K.**, Mishra S. K., Pandey A., (2019). “Application of SCS-CN based sediment yield models on small scale experimental plots using artificial rainfall”. In International Conference EGU general assembly, 2019, Vienna, Austria.
 2. **Kumre S. K.**, Mishra S. K., Pandey A., (2018). "SCS-CN method revisited in perspective of strange data". In International Conference on Sustainable Technologies for Intelligent Water Management, 2018, IIT Roorkee, India.
 3. Mishra S. K., **Kumre S. K.**, Singh P. K., Pandey A., (2019). “Structural and Application Inconsistencies Associated with SCS-CN Methodology”, Journal of Hydrologic Engineering, Ms. No.HEENG-4187R1 (**Revised for resubmission**).
 4. Mishra S. K., **Kumre S. K.**, Singh P. K., Pandey A., (2019). “Modification to the Existing SCS-CN Method for Enhanced Applications”. Hydrological Science Journal (Ms. Id. HSJ-2018-0604) (**Revised for resubmission**).
-

Other publications during Ph.D. study

1. Amrit K., **Kumre S. K.**, Mishra S. K., Pandey R. P., (2019). “Assessment of Environmental Flow Condition in Indian River Basin Using SPI”. In World Environmental and Water Resources Congress 2019. <https://ascelibrary.org/doi/abs/10.1061/9780784482339.032>
 2. Amrit K., Mishra S. K., Pandey R. P., **Kumre S. K.**, (2018). “Long-Term Meteorological Drought Characteristics in Southern India”. In World Environmental and Water Resources Congress 2018. <https://ascelibrary.org/doi/abs/10.1061/9780784481417.019>
-

-
3. Singh C. B., Mishra S.K., **Kumre S. K.**, (2018). Effect of land use on runoff curve number in steep slope”. In International Conference on Sustainable Technologies for Intelligent Water Management, 2018, IIT Roorkee, India
 4. Dumrakoti K. P., Mishra S.K., **Kumre S. K.**, (2018). "Effect of watershed characteristics on SCS-CN.”. In International Conference on Sustainable Technologies for Intelligent Water Management, 2018, IIT Roorkee, India.
-

List of Ph.D. manuscript(s) under preparation

1. Kumre S. K., Mishra S. K., Singh P. K., Pandey A., Development of an Improved SCS-CN Based Sediment Yield Model.
 2. Kumre S. K., Amrit K., Mishra S. K. Pandey A., Prediction of environmental flow condition using runoff curve number.
-